Characterisation of an Arabidopsis thaliana mutant purple patch inflorescence: A novel mutant allele of the COP9 Signalsome subunit 5

Saputhanthri, Pradeepika Shaminie

Award date:
2007

Awarding institution:
University of Bath

Characterization of an *Arabidopsis thaliana* mutant *purple patch inflorescence*: a novel mutant allele of the COP9 Signalosome Subunit 5

Pradeepika Shaminie Saputhanthri

A thesis submitted for the Degree of Doctor of Philosophy

University of Bath

Department of Biology and Biochemistry

October 2007

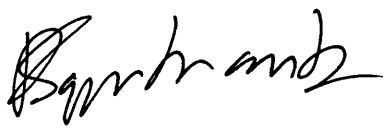

Pradeepika S. Saputhanthri

ProQuest LLC
789 East Eisenhower Parkway
P.O. Box 1346
Ann Arbor, MI 48106-1346

To

Asela

and

Sulakna

Acknowledgements

I would like to thank Richard Hooley, my supervisor, for inspiration, guidance and support throughout my study. Thank you Richard, also for always having time to discuss, to advise and help with my work, especially during the past couple of months in which you helped me with completing the writing-up, however busy you must have been.
Baoxiu, my dear friend, very special thanks to you, not only for the help and company in the lab, but also for being there during times of need and looking after me as one of your own family. Rod Scott, James Doughty, Ben Kemp- thank you very much for helpful ideas and all the help regarding my work. Sushma, Melissa, Pear, Rhiannon, Lucy, Marie, Lihua, Ahlam, thank you for pleasant company in the lab and in the office.
I acknowledge with thanks the initiative work done on the *ppi* mutant by Konstantin Kanyuka. Contributions of all the MRes and undergraduate project students Lihua Zhang, Sharon Casey, Sarah-Marie Gaynor, Kate Beauchamp, Karen Bellenger, Rhiannon Hughes, Kate Downes and Amy Percival to the project are also acknowledged with thanks.
I am grateful to The Centre for Research in Plant Sciences, University of West of England for allowing me to use their superb proteomics facility, to Richard Amey, who instructed and helped with the 2DE and Jenna Hughes who performed the MS.
My thanks to Klaus Harter at University of Tuebingen, Germany, who offered to help us with the light fluence assays and Virtudes Mira-Rodado who did those experiments for us.
My sponsor, the Commonwealth Scholarship Commission, UK and the University of Bath are acknowledged with thanks for financial support.

Abstract

An *Arabidopsis thaliana* Ws-2 mutant *purple patch inflorescence* (*ppi*) was found in the Wisconsin β population of T-DNA insertion lines. The mutation is recessive and is monogenically inherited. The *ppi* mutant has a pleiotropic phenotype with defects in plant hormone and light signal transduction. The phenotype did not segregate with a T-DNA insertion. Map-based cloning and sequence analysis revealed an 11-bp deletion in the 4th exon of the COP9 Signalosome Subunit 5A, *CSN5A* (At1g22920), resulting in a predicted truncated protein. The *ppi* mutant is allelic to T-DNA insertion mutants *csn5a-1* and *csn5a-2*, further confirming the locus identity.

The COP9 Signalosome (CSN) is implicated in diverse cell signalling and developmental processes in eukaryotes, primarily through regulating targeted protein degradation via the 26S proteasome. The metalloprotease activity of the complex resides in CSN5 subunit.

RT-PCR and Western-blot analyses suggest *csn5a-1* to be a null mutant, lacking the gene product and *csn5a-2* to be a partial loss-of-function allele producing residual levels of the protein. The *ppi* mutant could be partially functional as it produces a truncated CSN5A protein.

In general, the three mutants are phenotypically similar, but show allelic differences with the null *csn5a-1* having the most severe phenotype. The *csn5a* mutants showed altered responses to a range of plant hormones, and light. In many aspects of the phenotype and growth responses *ppi* is similar to the other two alleles. However, it showed unique features as well indicating it to be a new information resource on the CSN function. In a comparative proteomic analysis, the three mutants showed accumulation of some stress related proteins compared to the wild-type. In addition to those, *ppi* accumulated two PR proteins (Pathogenesis Related proteins) in the absence of pathogens.

In this thesis I report on the identification and characterization of *ppi* and the new insights gained into the function of the CSN and CSN5 subunit.

List of Abbreviations

AP buffer	Alkaline phosphatase buffer
APS	Ammonium persulfate
BCIP	5-bromo-4-chloro-3-indolyl phosphate
bp (Kbp)	base pair (Kilo base pair)
BSA	bovine serum albumin
CaMV	Cauliflower Mosaic Virus
cDNA	complementary deoxyribonucleic acid
Col	Columbia
CSN	COP9 Signalosome
cTAB	Hexadecyltrimethyl ammonium bromide/ Cetrimide
dATP	deoxy adenosine triphosphate
dCTP	deoxycytidine triphosphate
dH_2O	distilled water
DIG-dUTP	digoxigenin-dUTP
DNA	deoxy ribonucleic acid
DTT	dithiothreitol
EDTA	diaminoethane tetra acetic acid
EST	expressed sequence tags
EtBr	ethidium bromide
EtOH	ethanol
gDNA	genomic DNA
kDa	kilo Dalton
L*er*	Landsberg *erecta*
MES	2-[N-morpholino] ethane sulphonic acid
mRNA	messenger ribonucleic acid
MS medium	Murashige and Skoog medium
NaAc	sodium acetate
NBT	nitro-blue tetrazolium chloride
OD	optical density
o-PT	ortho-phenanthroline
PCR	polymerase chain reaction
pDNA	plasmid DNA
PEG	polyethylene glycol

PMSF	phenylmethylsulfonylfluoride
RNA	ribonucleic acid
RT-PCR	reverse transcriptase polymerase chain reaction
SDS	sodium dodecyl sulphate
SDS-PAGE	SDS-polyacrylamide gel electrophoresis
T-DNA	Transfer DNA
TE buffer	Tris-EDTA buffer
TEMED	NNN'N'-Tetramethylethylenediamine
TGS buffer	Tris-Glycine-SDS buffer
T_{hyb}	hybridization temperature
T_m	melting temperature
Tris	2-amino-2-hydroxymethylpropane-1,3-diol
UV	ultra violet
v/v	volume per unit to volume
w/v	weight per unit to volume
Ws	Wassilewskija
wt	wild-type

Contents

Chapter 1

Introduction

1.1 *Arabidopsis thaliana* as the model flowering plant for genetic and molecular biology research.

Arabidopsis thaliana (Family – Brassicaceae), is a small annual angiosperm weed of central Eurasian origin. Its short life-cycle, simple cultivation requirements, the small genome of 125 Mb in just five chromosomes, and the availability of a large number of mutant lines and genomic resources have made studies with this plant attractive to researchers. According to the *Arabidopsis* Information Resource, TAIR (http://www.*Arabidopsis*.org/), over 750 natural accessions of *A. thaliana* are found world-wide and some of the commonly known ecotypes such as Landsberg *erecta* (L*er*), Columbia (Col) and Wassilewskija (Ws) are used frequently in research.
In 2000, the *Arabidopsis* genomic sequence was published by the *Arabidopsis* Genome Initiative (AGI). This annotation identified 25498 *Arabidopsis* genes (AGI, 2000). Since then, there has been extensive effort to complete the sequence and annotate the genome and this is still continuing. The current version (TAIR7) of the genome lists 27029 protein coding genes, 3889 pseudogenes or transposable elements and 1123 ncRNAs (32041 genes in all, 37019 gene models). To date, 67% of the *Arabidopsis* genome is covered by annotated genes and it has an average density of about one gene per 4.44 kb. (http://www.*Arabidopsis*.org/portals/genAnnotation/genome_snapshot.jsp). Currently, an extensive range of genetic and physical maps of all 5 chromosomes are available for the research community from sites such as MIPS (http://mips.gsf.de/proj/plant/jsf/athal/) and TAIR. The latter currently has 73527 cDNAs and 624151 ESTs mapped to the genome, resulting in 22032 protein coding genes with at least one supporting cDNA and/or EST. However, 4787 protein coding genes are still lacking transcript support. Of those, ~ 4000 loci are uncharacterised proteins including hypothetical, predicted, or unknown proteins (http://www.*Arabidopsis*.org/portals/genAnnotation/gene_structural_annotation/genome_annotation.jsp).

1.2 Functional genomics in *Arabidopsis thaliana*

The ultimate goal of post genome research on this model flowering plant is the identification of all the genes and understanding their functions. Although there has been much progress in *Arabidopsis* genome annotation since AGI 2000, the functions of a significant proportion of the genes are still unknown. The current functional annotation of the *Arabidopsis* genome (excluding pseudogenes) according to the three Gene Ontologies consists of 59% of the *Arabidopsis* genome with known molecular function, 51% with known biological process and 49% known for cellular components (TAIR7). In addition to the fact that many of the annotated genes have no assigned function, many of the functions of the 'characterized' genes are based solely on their sequence similarities to other genes (Parinov and Sundaresan, 2000; Osterlund and Paterson, 2002). The international cooperation network 'The 2010 Project' initiated by the National Science Foundation (NSF), USA, aims to determine the function of all *Arabidopsis* genes by the year 2010 (The 2010 Project - http://www.nsf.gov/pubs/2001/nsf0113/nsf0113.htm).

There are two approaches to determine the function of a novel gene. In the more traditional 'forward genetics' approach, a mutant plant with a desired phenotype is identified and the gene that causes the altered phenotype is searched for. The plant is allowed to reveal what genes are important in the physical process of interest. Sequencing of the genome, availability of molecular markers and new improvements in techniques has made this a popular approach (Jander *et al.*, 2002). In the second 'reverse genetics' approach, a prior knowledge of the gene is required. The gene is mutated and the function of the gene is inferred by the resulting phenotypes. Techniques employed in this approach are gene knock-outs, over expression studies, loss- or gain-of-function studies by T-DNA insertional mutagenesis, antisense mRNA, co-suppression and random large scale insertional mutagenesis. In this way, an available genome sequence can be systematically annotated. In both approaches mutant analysis is fundamental, as a mutant defective in a particular gene product usually mirrors the functional relevance of the gene to the life of the organism.

1.3 The COP9 Signalosome (CSN)

1.3.1 The discovery of the CSN

The CSN is a conserved complex in higher eukaryotes including animals and plants. The complex was originally identified in *Arabidopsis* as a repressor of photomorphogenesis (Wei *et al.*, 1994). Identification of the now collectively known 'pleiotropic *COP/DET/FUS* loci' (*CONSTITUTIVELY PHOTOMORPHOGENIC/ DEETIOLATED/FUSCA*) in *Arabidopsis* led to the discovery of the CSN (Wei and Deng, 1992, Wei *et al*, 1994, Misera *et al*, 1994). Of the *COP/DET/FUS* loci, six encode subunits of the CSN. The others, COP1, DET1 and COP10 are believed to function in connection with the CSN in regulating photomorphogenesis (Wei and Deng, 2003). The CSN was later found from mammalian cells and other organisms indicting the general role of the CSN in developmental regulation, and not only in plant photomorphogenesis (Seeger *et al*, 1998; Wei and Deng, 1998).

1.3.2 The subunit composition and structural relevance of the CSN to other multi-protein complexes.

The complex consists of eight subunits. The identification of CSN subunits from different genetic screens giving unrelated names led to confusion and now a unified nomenclature is being used. In this, the eight subunits of the CSN are now named CSN1 to CSN8, in descending order of molecular weight (Deng *et al*, 2000).

The subunit composition is conserved in *Arabidopsis*, mammals and *Drosophila*. The CSN2 and CSN5 are the most highly conserved, with >60% similarity between animals and plants (Wei and Deng, 2003). The CSN holo-complex is 450-550 kDa and mainly nuclear localized (Chamovitz *et al*, 1996). Smaller complexes containing subsets of CSN subunits have been reported particularly from mammalian cells, however, the function of these are not clear (Tomoda *et al*, 2002).

Of the eight subunits, six are PCI (Proteasome, COP9 Signalosome, Initiation Factor3) domain subunits (CSN1 to CSN4, CSN7 & CSN8) and two are MPN (Mpr1-Pad1-N-terminal) domain subunits (CSN5 and CSN6). PCI domain proteins in the CSN are thought to serve scaffolding function, stabilizing subunit interactions within the complex (Kim *et al,* 2001). Although it was previously thought otherwise (Gusmaroli *et al*, 2004, Dohmann *et al*, 2005), it has recently been shown that the two MPN subunits (CSN5 and CSN6) of *Arabidopsis* are essential for stable subunit assembly of the CSN and that both PCI and

MPN proteins are structurally interdependent on each other for functional CSN complex formation (Gusmaroli *et al,* 2007).

The metalloprotease motif inside the MPN domain called JAMM (Jab1/MPN domain metalloenzyme) is responsible for the cleavage of Nedd8/ Rub1-cullin conjugate by the CSN (see section 1.3.3.1) and of Ub-substrate conjugate by the proteasome (Cope *et al*, 2002). The JAMM motif contains a zinc ion in the catalytic centre (Gusmaroli *et al*, 2004 and references therein).

Two other protein complexes in eukaryotes are known to have PCI and MPN subunits: the lid of the 19S regulatory particle of the 26S proteasome (Lid) and the eukaryotic translation Initiation Factor3 (eIF3) (Glickmann *et al.*, 1998). The three complexes are highly conserved among higher eukaryotes and structurally related. In *Saccharomyces cerevisiae* the Lid and a smaller eIF3 are present, but only the CSN5 subunit of the CSN has been found (Kim *et al*, 2001). Components of the Lid and eIF3 co-purify with the CSN (Seeger *et al,* 1998) and direct interactions between the subunits from the three complexes have been shown (Karniol *et al,* 1998). The CSN is more distantly related to the eIF3 and is more closely related to the Lid. Both the CSN and the Lid have six PCI domain proteins and two MPN domain proteins that show pair-wise homology between the two complexes (Wei and Deng, 2003).

Among its subunits, eIF3 has three PCI subunits and two MPN sub units (Kim *et al,* 2001). The MPN sub units of the eIF3 (eIF3f and eIF3h) do not have the JAMM motif. Only CSN5 and not CSN6 in the CSN, and only RPN11 and not the other MPN protein RPN8 in the Lid have the JAMM motif. The functions of non-JAMM motif MPN sub units are not clear (Wei and Deng, 2003).

There are many lines of evidences suggesting that the CSN evolved parallel to the 26S system: The eight subunits of the Lid and the CSN are paralogous to each other. There are direct interactions of the CSN subunits with the Lid sub units. The CSN and the proteasome associate in coimmunoprecipitation reactions. It has been suggested that the two complexes form a 'CSN-Proteasome' complex to degrade specific substrates (Serino and Deng, 2003). Huang *et al* (2005) demonstrated that purified human CSN directly interacts with the 26S proteasome and the CSN has an impact on the 26S activity. It was suggested that the CSN compete with the Lid for the interaction with the proteasome.

The architecture of the Lid and the CSN are not identical, but share high similarities. (Fig.1.1). They are similar in size, both lack symmetry in the subunit arrangement and both are characterized by a central grove (Kapelari *et al*, 2000, Bech-Otschir *et al*, 2002).

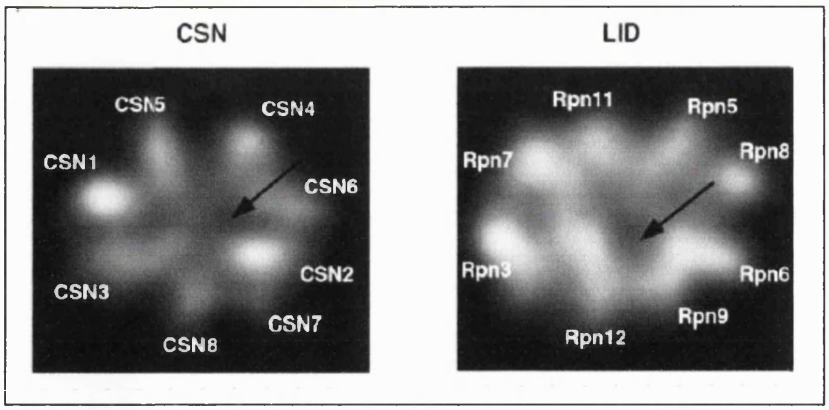

Fig. 1.1: 2D electron microscopic images of the CSN and the 26S proteasome Lid.
The putative subunit arrangement of the CSN on the basis of the subunit-subunit interaction studies (Kapelari *et al.*, 2000) is indicated. Lid subunit-subunit interactions were deduced from CSN data by arranging homologous subunits. The central groove is marked by black arrow.
[The figure and the description taken from Bech-Otschir *et al*, 2002; the original images had been provided by B. Kapelari].

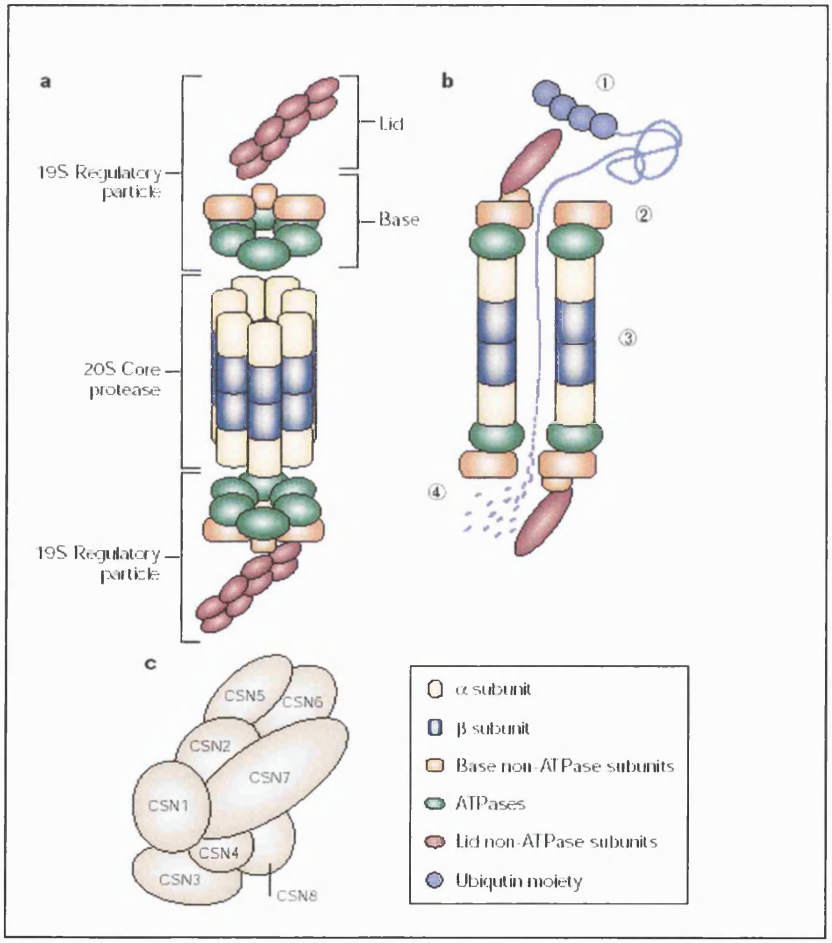

Fig. 1.2: The structural arrangement of the 26S proteasome and the CSN
(a) The subunit arrangement of the 26S proteasome
(b) Steps involved in protein degradation via the 26S proteasome. 1) Polyubiquitinated protein substrate is recognized by the Lid. 2) The substrate is passed through the Base where the protein is unfolded and passed to the Core 3) The substrate is degraded via the protease activity associated with the β subunits. 4) The short peptides released are used by the cell to form new proteins
(c) The CSN with similar structural arrangement to the Lid
[The figure taken from Sullivan *et al*, 2003]

1.3.3 Functions of the CSN

1.3.3.1 Deneddylation/ derubylation of Cullins

The CSN has been implicated in various cellular activities and developmental processes. Many of these are connected with the Ubiquitin-26S proteasome (Ub/26S) pathway of proteolysis.

In a cell, proteins are built up and broken down and are constantly in a dynamic state. One method of protein degradation is non-energy dependent lysosomal proteolysis. In higher eukaryotes, regulated protein degradation plays a key role in mediating various cellular functions and the major pathway responsible is the ubiquitin and ATP dependent proteolysis via the 26S proteasome. Through regulated proteolysis, the Ub/26S pathway governs processes such as cell division, DNA repair and transcription, quality control of newly produced proteins and immune response (Vierstra, 2003). The importance of the mechanism is highlighted in the human diseases such as cervical cancer and cystic fibrosis which are due to defects in it. The significance of the pathway has been acknowledged by awarding the 2004 Nobel Prize for Chemistry to the three scientists Aaron Ciechanover, Avram Hershko and Irwin Rose, who pioneered the work in this field in the early 1980s "for the discovery of ubiquitin-mediated protein degradation" (http://nobelprize.org/nobel_prizes/chemistry/laureates/2004/). Much work has been carried out with regard to the pathway and its many components, especially in mammalian systems because of its importance in human disease.

The 26S proteasome has a catalytic Core, the 20S particle, which consists of a stack of proteolytic α and β subunits surrounding a narrow chamber in which the substrate proteins are degraded into small peptides and later the constituent amino acids are recycled (Moon *et al,* 2004). The cylindrical core is capped on each end by a 19S regulatory particle. The 19S particle forms the gate into the core and confers substrate specificity (Fig.1.2). It is composed of two components- the Lid consisting of 8 subunits, is responsible for recognizing ubiquitinated substrates and removing ubiquitin from the substrate. The Base consists of 6 ATPases that work to unfold the substrate protein (Bech-Otschir, 2002).

In this pathway, the 76-amino acid globular protein ubiquitin (Ub) is activated by the Ub activating enzyme (E1) to form a thioester bond, in an ATP dependent manner. The activated Ub is then transferred to another sulfhydril site in the Ub conjugating enzyme (E2). E2 then transfers the Ub directly to the E3 Ub ligase (E3), in the case of HECT type

E3s, or binds the E3 and transfers Ub to a lysine residue in the substrate protein (Hershko and Ciechanover, 1998; Sullivan *et al*, 2003). The process is repeated several times to polyubiquitinate the substrate. Polyubiquitin chains formed through the K48 residue of Ub are targeted for degradation in the 26S proteasome (Sullivan *et al*, 2003). The target protein is degraded and the Ub monomers are recovered by the action of de-ubiquitinating enzymes. In *Arabidopsis*, only two E1s, about 40 E2s and more than 1200 E3s are known (Vierstra, 2003). E3 determines the substrate specificity.
E3 Ub ligases are a large family of proteins or protein complexes. Depending on the domain type they are grouped in to two. The HECT (Homologous to E6-AP C-terminus) domain E3s are a small group of only 7 members in *Arabidopsis*. The second group is the RING/U-box domain E3s and there are about 400 of those. Single subunit RING/U-box E3s are COP1 (Constitutive Photomorphogenesis1), SINAT5 (Seven In Absentia In *Arabidopsis thaliana*5) and ARC1 (Arm-Repeat-Containing1). Multi subunit RING E3s are SCF (Skp1-Cullin1-F-box) type, BCR (BTB/POZ domain-CUL3-RING) type and APC (Anaphase Promoting Complex).

The SCF type E3s are of particular interest here, as the CSN regulates the action of many SCFs. They have typically four subunits: SKP1 (or ASK in plants for *Arabidopsis* SKP1), CDC53/Cullin, an F-Box protein and a RING finger protein RBX1 (RING-Box1). Cullins serve a scaffolding function by binding to both the RBX1 and the SKP1. SKP1 binds the F-box proteins which determines the substrate specificity for the SCF (Smalle and Vierstra, 2004). In *Arabidopsis* there are five cullins. Only CUL1 and CUL2 have been shown to be in SCFs. Two *RBX* genes, 21 ASKs and about 700 F-Box proteins are in *Arabidopsis* (reviewed in Moon *et al*, 2004)

Cullins can be covalently modified by the Ub-like protein Rub1 (Related to ubiquitn1), also called Nedd8 (for Neural precursor cell expressed, developmentally down regulated gene8) in animal systems (Serino and Deng 2003). In a similar manner to Ub conjugation, the Rub1/Nedd8 is conjugated to the cullin in an enzymatic series of reactions via the Nedd8 activating enzymes APP-BP1 and Uba3 (E1), and Nedd8 conjugating enzyme Ubc12 (E2) (Hershko and Ciechanover, 1998). In *Arabidopsis* Rub1 is attached to AtCUL1 by a heterodimeric AXR1/ECR1 enzyme (Auxin Resistant1/ E1-C-terminus Related1) (Serino and Deng 2003). Rubylation/Neddylation positively regulates the cullin containing Ub ligases by facilitating substrate polyubiquitination and E2 recruitment to the SCF (Gusmaroli *et al*, 2004 and references therein).

Not only neddylation, but active cycles of both neddylation and de-neddylation are essential for the proper activity of SCFs towards their target substrates (Cope *et al* 2002, Schwechheimer *et al* 2001). Cleavage of Nedd8/ Rub1 is catalyzed by the metalloprotease activity residing in the JAMM motif of CSN5 subunit of the CSN (Cope *et al* 2002). CSN binds to CUL1 and Rbx1 via CSN2, CSN6 and CSN1's N-terminal domain (Sullivan *et al*, 2003). Cullin1 and Rbx1 are common to all SCFs. Therefore CSN has the potential to regulate many SCFs, if not all. It has been demonstrated that CSN can interact with multiple cullins in *Arabidopsis* CUL1, CUL3, CUL4 and CUL2, though the exact mechanisms of neddylation/ deneddylation dependent regulation may vary among different cullin based E3s (Serino and Deng 2003, Gusmaroli *et al*, 2007). It is interesting that, in the Lid, RPN11, the CSN5 counterpart of the proteasome, contains the JAMM motif that constitutes the major de-ubiqutinating activity of the proteasome. The CSN5 and RPN11 both show metalloprotease activity only when they are assembled into the complex (Cope *et al,* 2002).

As the derubylation activity is essential for the SCFs to function, the CSN in turn regulates many cellular and developmental processes in connection with the SCFs. Such functions include cell cycle regulation, stress responses, photomorphogenesis in plants, floral development, pathogen resistance, hormone responses and many others (reviewed in Wei and Deng, 2003; Serino and Deng, 2003; Sullivan *et al*, 2003).

1.3.3.2 CSN-associated protein kinase activity

Seeger and co-workers using CSN purified from red-blood cells demonstrated that it was able to phosphorylate various transcription factors including c-Jun, IκBα, NF-κB precursor p105 and the tumour suppressor protein p53 (Seeger *et al,*1998). This kinase activity is now believed not be directly by the CSN but through a CSN-associated kinase or kinases (Sun *et al,* 2002).

The p53 tumour suppressor protein is a transcription factor that promotes genes regulating cell cycle arrest, DNA repair and programmed cell death (apoptosis). The level of p53 in a normal cell is kept low by regulation via the Ub/26S pathway with Mdm2 as the E3 (Xirodimas *et al*, 2004). When DNA damage occurs, p53 is phosphorylated reducing its affinity for Mdm2 and preventing proteolysis. Increase of p53 levels lead initially to arrest the cell cycle allowing DNA repair, and later, if the damage is too extensive, to apoptosis. It has been reported that p53 is mutated in about 50% of all human cancers. The CSN involvement in phosphorylating p53 is implicating its role in regulating the cell cycle.

NF-κB is a transcription factor involved in immune and inflammatory responses. It exists as an inactive complex with an inhibitor protein IκB in the cytoplasm. When exposed to bacterial infections or local signals, IκB is phosphorylated leading to its degradation via the Ub/26S pathway. Once IκB is degraded, NF- κB is translocated to the nucleus where it activates gene expression (Chen *et al,* 1995).

The CSN has been implicated in stress activated MAP kinase pathway in animal cells. The transcription factor AP1 (Activator Protein1) is mainly composed of Jun, Fos and ATF protein dimers, and mediates gene regulation in response to various stress stimuli including cytokines, growth factors, bacterial/viral infections and oncogenic stimuli (Hess *et al*, 2004). The CSN5 activates JNK (c-Jun N-terminal kinase), enhances c-Jun phosphorylation level and stabilizes binding of c-Jun to AP-1 sites (reviewed in Wei and Deng, 2003). CSN5 interacts with many other proteins that are known to regulate AP-1 mediated transcription positively or negatively (reviewed in Chamovitz and Segal, 2001).

The cell cycle inhibitor p27 ($p27^{Kip1}$) is subjected to regulation by the CSN through at least two mechanisms. It is regulated by the CSN-mediated deneddylation leading to its degradation in the Ub/26S pathway via the SCF^{Skp2} (Wei and Deng, 2003). The CSN5 subunit directly binds p27 and facilitate its nuclear export and subsequent proteolysis (Tomoda *et al* 1999, Tomoda *et al*, 2002). It is also potentially phosphorylated by the CSN-associated kinase activity (Wei and Deng, 2003).

1.3.4 The CSN and plants

The PCI subunit mutants (and other *cop/det/fus* mutants as well) of *Arabidopsis* are small, with constitutive photomorphogenic, and deetiolated phenotype in the dark (*cop/det*) and they accumulate anthocyanin in the cotyledons (*fusca*) (Serino and Deng, 2003). These mutants have been shown to display a gene expression profile similar to seedlings under high-light intensity stress (Ma *et al*, 2003). The mutants cannot survive beyond the seedling stage. The MPN subunit mutants (*csn5* and *csn6*) show only a partial *cop/det/fus* phenotype and survive the entire life cycle, because of the functional redundancy of the two homologous genes encoding each subunit (Gusmaroli *et al*, 2004). However, the loss of function mutants (double mutants of the two genes) of *csn5* and *csn6* show the severe phenotype indistinguishable from the other *cop/det/fus* mutants and express similar light

induced gene expression as other *csn* mutants in the dark (Dohmann *et al*, 2005, Gusmaroli *et al,* 2007).

It has been demonstrated that reduction in the levels of any one subunit would lead to a reduction in the level of the CSN complex (reviewed in Wei and Deng, 2003). Mutations resulting in reduction of levels of individual subunits displayed "specific abnormalities in the adult plants with regard to light and auxin signalling, meristem formation, flower development and plant defence responses" (Serino and Deng, 2003). This indicated that the individual subunits have distinct functions even within the complex.

The CSN is involved in regulating a range of signalling and developmental pathways in plants and almost all of those involving CSN-dependent derubylation activity in regulating cullin containing SCFs. The physical interaction between the CSN and a specific SCF has been shown for SCF^{TIR1} for auxin responses (Schwechheimer *et al* 2001), SCF^{COI1} for jasmonate responses (Feng *et al*, 2003) and SCF^{UFO} for flower development (Wang *et al*, 2003) in *Arabidopsis*. Although such interactions are to be established for other SCFs, CSN has been implicated in many other processes regulated by SCFs and will be detailed in Chapters 5 and 6.

As mentioned previously, the CSN was initially identified as a negative regulator of photomorphogenesis. After germination, in the dark, seedlings undergo skotomorphogenesis development, in which they are called 'etiolated' with long hypocotyls, closed and unexpanded cotyledons and an apical hook. In the light, the seedlings undergo photomorphogenesis and show characteristic short hypocotyls, open and expanded cotyledons, absence of apical hook and expression of light induced genes. Photomorphogenic development is triggered by the light absorption of photoreceptors and down stream signalling cascades to express many light induced genes. The expression of those genes are promoted by transcription factors including HY5 (Long hypocotyl5), HYH (HY5 homolog), LFR1 (Long after far-red1). The E3 Ub-ligase COP1 interacts with these transcription factors (and possibly many more) and promotes their degradation via the Ub/26S pathway in the dark and prevent light induced gene expression thereby preventing the photomorphogenic growth (Osterlund *et al*, 1999). The COP1 mediated regulation of the transcription factors involves nuclear-cytoplasmic partitioning of the distribution of COP1. In the dark COP1 resides in the nucleus where it can readily degrade HY5 and related proteins. In light, the COP1 is cytoplasmic resulting accumulation of HY5 and hence transcription of light regulated genes (Osterlund *et al*, 2000). The CSN has been

shown to play a role in nuclear import or retention of COP1 as in the *csn* mutants COP1 remains cytoplasmic (von Arnim and Deng, 1994; Chamovitz *et al*, 1996). The mechanism by which the CSN mediates subcellular distribution of COP1 is yet to be determined and a direct physical link between the CSN and the COP1 is yet to be established (Sullivan *et al*, 2003).

1.3.5 CSN5, the fifth sub unit of CSN

CSN5 is also known as JAB1 (Jun Activation Binding protein1) in animals. It was originally isolated based on its interaction with the activation domain of c-Jun (Claret *et al*, 1996). "CSN5/JAB1 binding stabilizes the c-Jun or JunD complexes at their specific AP-1 binding sites and enhances the specificity of target gene activation" (Chamovitz and Segal, 2001).

CSN5 is a 40 kDa soluble protein which is found as a CSN-holo-complex associated nuclear form and a monomeric, CSN-independent 'free' form which is both nuclear and cytoplasmic in *Arabidopsis* (Kwok *et al*, 1998). CSN5 was also reported to be in association with mini-complexes containing subsets of CSN subunits (Tomoda *et al*, 2002). Within the CSN complex, CSN5 has been shown to interact with at least four other subunits CSN1, CSN2, CSN4 and CSN7 (Kapelari *et al*, 2000). The mutations in other CSN subunits can affect the distribution of CSN-bound or free forms of the CSN5 in *Arabidopsis* and mutations in several other CSN subunits lead to the loss of CSN-bound form but retained the CSN-independent forms (Wei and Deng, 2003). The *cop1* and *det1* mutants show loss of smaller CSN-independent forms, but maintains the larger form (reviewed in Serino and Deng, 2003).

CSN5 has been implicated in many signalling pathways from light signalling in plants to larval development in *Drosophila.* Also, in integrin signalling, cell cycle control and steroid hormone signalling in mammals (reviewed in Chamovitz and Segal, 2001).

CSN5/JAB1 is involved in the control of cell cycle by regulating the Cyclin Dependent Kinase (CDK) inhibitor p27 ($p27^{Kip1}$). p27 induces G1 cell cycle arrest. It was mentioned previously how CSN regulates p27 by phosphorylation and promotes its degradation via the Ub/26S pathway. CSN5 interacts with p27 both *in vitro* and *in vivo* (Tomoda *et al*, 2002). Over expression of CSN5 leads to down regulation of p27 by mediating its nuclear-cytoplasmic partitioning. Phosphorylated p27 is translocated from the nucleus to the cytoplasm where it is degraded. CSN5 acts as an adaptor in binding p27 to bring it to the cytoplasm through a CRM1 (Chromosomal Region Maintenance1) dependent manner.

CRM1 associates with a nuclear export signal (NES) in the C-terminal region of CSN5/JAB1 and mediates its nuclear export (Tomoda *et al*, 2002). Similarly, CSN5 facilitates translocation of Smad7, an inhibitor of the Transforming Growth Factor β (TGF-β) that regulates cell growth (Kim *et al*, 2004).
Many interactions between CSN5 and proteins implicated in regulating AP-1 mediated transcription have been reported and many such interactions involve sequestering of CSN5 (reviewed in Chamovitz and Segal, 2001). Most of the early observations on CSN5 were based on systems with ectopic expression of the protein. Also, the role of CSN in these reactions in these reactions is not clear.

Two JAB1 homologs CSN5A/ AJH1 (for *Arabidopsis* JAB1 Homolog1) and CSN5B/ AJH2 were isolated in *Arabidopsis* (Kwok *et al*, 1998). As mentioned earlier, the products of *CSN5A* and *CSN5B* act redundantly, resulting in only a partial *cop/det/fus* phenotype in their mutants. Recently it was shown that the CSN5 loss of function by depleting both proteins lead to the severe phenotype indistinguishable from the other *cop/det/fus* mutants (Dohmann *et al,* 2005, Gusmaroli *et al*, 2007). CSN5 antisense or co-suppression lines with reduced levels of the protein were used to demonstrate the link between CSN5/CSN and SCF^{TIR1} in mediating auxin responses (Schwechheimer *et al*, 2001). Most studies on the biochemical role of CSN5 in *Arabidopsis* were on its metalloprotease activity in association with the CSN, which is responsible for the derubylation of cullins.
Gusmaroli *et al* (2004) demonstrated that the CSN5A and CSN5B proteins are assembled into distinct CSN complexes in vivo, with differential abundance with CSN^{CSN5A} being the highly abundant one with the dominant role in derubylation of cullins and they also established the CSN5A JAMM motif in derubylation of *Arabidopsis* cullins. The *csn5a* mutants with point mutations in the JAMM motif showed higher accumulation of rubylated CUL1 compared to the wt. However, these were plants mutant in *csn5a*/b and transgenic for constructs expressing point mutations behind a CaMV35S promoter with ectopic over expression, which are clearly different from a point mutation of the endogenous gene in a wild type background.
The physiological importance of CSN5 JAMM motif was previously established only in *Drosophila* where point mutations in JAMM metal binding domain arrest larval development, with abnormalities in photoreceptor neuron deficiencies (Cope *et al*, 2002). Further emphasizing the unequal roles played by the CSN5A and CSN5B, *csn5a* mutants displayed increased photomorphogenesis under constant white-, red-, far-red- and blue

light where as *csn5b* mutants showed increased photomorphogenesis under certain conditions of light only (Dohmann *et al*, 2005, Gusmaroli *et al*, 2007).

Recent work has suggested the existence of a reciprocal regulation between CUL3 and CSN5 accumulation and speculate on a possibility of CUL3 as a component of E3 ligase controlling CSN5 stability by targeting this sub unit for degradation (Gusmaroli *et al*, 2007). The MIF (Macrophage Migration Inhibitory Factor) has been suggested as a regulator or inhibitor of CSN5 (Wei and Deng, 2003). Apart from these, how the CSN or its subunits are regulated is yet to be established.

Since its identification more than 12 years ago, the significance of CSN as a key regulator of multiple cellular processes has been increasingly evident. However, our understanding on the CSN, its functions, and regulation is far from complete.

Still it is not clear how the activities of the CSN are coordinated and regulated according to various requirements of an organism in time and in space. Regulation of CSN-mediated de-neddylation activity and specificity of CSN on E3s need to be addressed. Physical evidence of interactions between the CSN and various E3s are yet to be established.

The involvement of CSN in subcellular localization of proteins, especially of COP1, has to be investigated in order to understand the mechanisms.

Regulation of CSN-associated kinase activity and implications of such activity in plants is yet to be established. The functions of CSN (or of its sub units) other than the CSN-associated derubylaiton of cullins of E3 ligases need to be investigated. Of particular interest would be to investigate the nature of CSN-dependent and CSN-independent functions of individual subunits.

Although the CSN5 subunit is the most extensively studied so far, understanding of its functions other than the metalloprotease activity in plants is not complete. For example, the specific functions of CSN-independent 'free' form of CSN5 need to be addressed carefully. The involvement of CSN5 in nuclear-cytoplasmic partitioning of proteins has been reported from animal systems. This area has not been explored in plants.

Thus, the research into the CSN has a vast potential.

1.4 Aims and Objectives

A mutant of *Arabidopsis thaliana* with a striking pleiotropic phenotype was discovered in a screen for gene knock-outs from the University of Wisconsin β population of T-DNA insertion mutants. Preliminary analyses of the mutant had indicated the mutation to be recessive and monogenic and it was presumably associated with a T-DNA insertion.
The main objective of my PhD research project was to identify the genetic locus of the mutation in this novel mutant which we named as '*purple patch inflorescence*' or *ppi** based on the characteristic pigmented zone in its inflorescence.
In order to isolate the mutant locus, it was necessary to confirm whether the mutation was associated with a T-DNA insertion event and if so, to characterize the insertion to facilitate isolating the gene. Initial work on the mutant proved that the *ppi* phenotype does not segregate with a T-DNA insertion and therefore a map-based approach was taken to isolate the gene locus. It was identified as the gene encoding the fifth subunit of the COP9 Signalosome (*CSN5A*, At1g22920) and this finding was confirmed by molecular studies and allelism tests.
After genetically characterizing the mutation, the next objective was to functionally characterize it. The functional significance of the *CSN5A* gene was analyzed by three approaches.
1) In order to understand the impact of the *csn5a* mutations on the plant morphology a detailed phenotypic analysis of *ppi* and two other mutant alleles of the gene was performed. (The three mutants will be collectively called *csn5a* mutants from here onwards).
2) In order to gain more insight into how the gene product is involved in various signal transduction pathways, the responses of the *csn5a* mutants to a range of growth regulators and stimuli were analysed.
3) Since the *csn5a* mutants are defective in a sub unit of a protein complex that has plays an important role in ubiquitin-mediated protein degradation, a comparative proteomic analysis was performed on the *csn5a* mutants using two–dimensional gel electrophoresis.

**[Note- as ppi is now confirmed to be a mutant allele of the CSN5A (At1g22920) gene, when this work will be published and it will be designated as csn5a-3. There is an already published mutant with the name 'ppi' (= plastid protein import; Bauer et al, 2000). For convenience, through out this thesis I will be using the initial name given to the mutant 'purple patch inflorescence' or ppi, based on its distinct feature].*

Chapter 2

Materials and Methods

2.1 Materials

2.1.1 Reagents, kits and antibodies

Reagents

Complete™ -Protease Inhibitor Cocktail-(Roche # 1697 498)
REDTaq™ ReadyMix™ PCR Reaction Mix with $MgCl_2$ (Sigma)
TriPure Isolation Reagent (Roche # 1667157)
AMV Reverse Transcriptase (Promega # M5101)
ReddyMix PCR Buffer IV containing MgCl2 (ABgene #AB-0815)
Recombinant RNasin Ribonuclease Inhibitor –rRNasin 40U/ul (Promega #N2511)
Taq DNA polymerase, recombinant 5U/ul (Invitrogen #10342-020)
Proteinase K, recombinant, PCR Grade (Roche 3115836)

Kits

2-D Clean Up Kit (Amersham/ GE healthcare #80-6484-51)
2-D Quant Kit (Amersham / GE healthcare # 80-6483-56)
Access RT-PCR System (Promega)
DIG High Prime DNA Labelling and Detection Starter Kit II (Roche)
Expand High Fidelity PCR system (Roche)
Gamborg's B5 medium – micro and macro elements (Duchefa # G 0209)
High Pure PCR Product Purification Kit (Roche)
Immobiline™ DryStrip; pH 3-10 NL, 24 cm (Amersham 17-6002-45)
IPG Buffer -Ampholytes pH 3-10 (Amersham # 17-6000-87)
Nucleon Phytopure kit (Nucleon Biosciences, Galsgow, UK)
TOPO-TA cloning kit with Oneshot TOP10 chemically competent *E.coli* (Invitrogen)
Wizard^{Plus} Miniprep DNA Purification System (Promega)
Wizard^{Plus} Miniprep SV DNA Purification System (Promega)

Antibodies

Anti CSN5 antibody 25 ul (BIOMOL # PW8365)
Anti RPT5 antibody 25 ul (BIOMOL #PW8375)
Anti-Rabbit IgG – Alkaline phosphatase antibody produced in goat (Sigma #A3937)

2.1.2 Plant material

The *ppi* mutant was identified during a screen for gene knock-outs in a seed collection obtained from University of Wisconsin beta population of T-DNA insertion mutants. These mutants have been generated using the activation tag vector pSKI015 in *Arabidopsis thaliana* ecotype Wassilewskija (Ws-2) (Weigel et al, 2000). Amongst the progeny generated in the above screen was *ppi*, a seemingly novel mutant, with a distinctive phenotype and seeds were collected from this plant. The mutant was back-crossed twice to the wild-type in Richard Hooley Lab by Dr Konstantin Kanyuka (Hooley & Kanyuka personal communication) to eliminate any T-DNA insertions that were not associated with the phenotype. Plants originating from these lines were used initially in my project. These original lines had a complex T-DNA insertion event in them which I segregated away. Seeds from the third back-cross to the wild-type were bulked up for assays.
Seeds of the ecotype Columbia-0 (Col-0) used to create crosses for genetics analyses and mapping were also from the Richard Hooley lab. Wild-type seeds of Ws-2 were purchased from the Nottingham Arabidopsis Stock Centre (NASC).
The *CSN5A* T-DNA insertion lines, SALK_063443 (*csn5a-1*) and SALK_027705 (*csn5a-2*) are in the Col-0 background and were identified in the SIGnAL database (http://signal.salk.edu/cgi-bin/tdnaexpress) and the seeds were purchased from the NASC. The T-DNA insertion lines were PCR genotyped to test for the presence or absence of the wild-type *CSN5A* gene the T-DNA insertion and the mutants homozygous for the insertion in the gene were back-crossed once to the wild-type Col-0 and the bulked up seeds were used for subsequent analyses.

2.2 Methods

2.2.1 Growth conditions

2.2.1.1 Growing *Arabidopsis* on compost

For phenotypic characterisation, for generating mapping populations and to obtain mature plant material, seeds were sown on a moist compost mix containing 1:1 volume ratio Levington M2 (medium) and F2 (fine) compost (Levington, Ipswich, UK) supplemented with $2gL^{-1}$ Osmocote, a slow release fertilizer, and 20% v/v Perlite or Vermiculite, also supplied by Levington. A top drench of the insecticide 0.02% w/v Intercept 70 WG solution was applied (100 ml per Litre of compost) before sowing seeds. After 2-5 day incubation at 4°C, the seed trays/ pots were transferred to a controlled environment glasshouse (designed for genetically modified plants) where they were grown under long-day photoperiod (16 h light) at 23 ± 2°C during the day and 17.5 ± 2°C during the night. For the phenotypic characterisation and growth response assays, the plants were grown in SANYO controlled environment (CE) growth rooms where they were grown at 22 °C during the day and 18 °C night temperatures with maximum temperature change allowed 4 °C/h, 60% day humidity & 70% night humidity with allowed change of 10% per hour under. Plants were grown under long-day photoperiod (16h light) unless otherwise stated.

2.2.1.2 Growing *Arabidopsis* on agar medium

Before sowing onto the medium, seeds were surface-sterilized as follows:
Dry seeds were transferred to a 1.5 ml eppendorf tube (50 µl volume ≡ ~1250 seeds) and were incubated for 5 minutes in 1 ml of 70% v/v ethanol, 5 minutes in 1 ml of 50% v/v sodium hypochlorite solution containing 0.1% Tween-20, followed by five rinses using sterile distilled water in a laminar flow cabinet. Then, using a P20 pipette with a cut off yellow tip and a Barky CP100 Ultipette capillary tip, the seeds were transferred on to Murashige and Skoog basal medium containing macro and micro elements, Gamborg's vitamins and MES buffer (DUCHEFA) at a concentration of 4.91g/L, 0.5-1% w/v sucrose and 0.8 % plant agar (DUCHEFA), in 10 x 10 cm square plates (Sterillin). If necessary the plates were air dried in the laminar flow cabinet to remove any drops of water around the seeds. The plates were then sealed with 3M microporous tape. After 2-5 day stratification at 4 °C, the plates were maintained horizontally or near vertically (~5° from vertical) to allow the roots to grow down along the surface, in a SANYO CE growth room under long days (16 h light) . Where seedlings were grown in the dark, seeds sown on agar plates were

pre-treated for 2 hours in white light (approximately 200 $\mu molm^{-2}s^{-1}$) to induce uniform germination and then the plates were wrapped in two layers of aluminium foil immediately prior to stratification.

2.2.2 Growth response assays

2.2.2.1 Analysis of hypocotyl and root responses to growth regulators

Hypocotyl and/or root responses to α-naphthaleneacetic acid (NAA), 2,4-dichlorophenoxyaceticacid (2,4-D), Indole-3-acetic acid (IAA) 2iP, epibrassinolide (EBR), ABA ((±) cis, trans Abscisic Acid), N-1-Naphthylphthalamic acid (NPA), GA_3 and ACC were analysed with seeds germinated and grown on agar media (as in section 2.2.2), supplemented with different concentrations of the growth regulator. In the case of IAA, 10mg/ml of the anti-oxidant butylated hydroxy toluene (BHT) was included in the medium to prevent rapid degradation of IAA in the agar medium. Due to the toxicity of NPA to germinating seeds, the NPA treatment was administered to 3-day-old established seedlings by initially germinating seeds on NPA(-) media and then transferring to NPA(+) media.. To determine the response of root growth to ABA, 3-4 day-old seedlings grown on ABA(-) media were transferred to and grown on ABA(+/-) plates for five more days before the root lengths were measured. The amount of root elongation growth after transferring to the second ABA(+/-) media was measured.

In order to measure the hypocotyl/ root lengths, the agar plates containing the seedlings were scanned using a flat-bed HP Desktop Scanner. A ruler was placed along with the plates to be used as a conversion standard. Hypocotyl or root lengths were measured using the Sigma Scan Pro5 software. The software measures in pixels allowing conversion to mm.

Statistical analyses were performed as described by Townend (2002) using MINITAB version 12 software. Data sets for small samples ($n<10$) were first analyzed by Kolmogorov-Smirnov Test for normal distribution before they were analyzed for statistically significant differences using Two-Sample t-Test with H_0= no significant differences in the measurements between the two data sets compared. When p-value $\leq$ 0.05, the null hypothesis H_0 was rejected and the reverse applied.

2.2.2.2. Analysis of the effects of Paclobutrazol and ABA on seed germination.

To screen for seed sensitivity to the GA biosynthesis inhibitor Paclobutrazol (N-dimethylaminosuccinamic acid), or ABA, 100 seeds (non-surface sterilized) were transferred using a tooth-pick on to 70 mm diameter Whatman GF/A paper, placed on two sheets of 85 mm diameter Whatman No. 1 filter papers in a 9 cm diameter sterile Petri dish, pre-wetted with 5 ml sterile distilled water containing a range of concentrations of Paclobutrazol (DUCHEFA) or ABA. The plates were sealed with 3M microporous tape and after 2-5 days stratification, they were kept horizontally in a SANYO CE room under long days (16-h light). Percentage germination was scored after 5-7 days.

2.2.2.3. Analysis of lateral root response to localized $NO3^-$ treatment

To assess the effects of localized $NO3^-$ treatment on lateral roots, segmented agar plate (SAP) method described by Zhang and Forde (1998) was used. Seeds of the wt and mutant lines were surface sterilized (section 2.2.1.2) and sown into 10x 10 cm Petri-dishes (Sterillin) containing agar medium with Gamborg's B5 salts*(see below) where $(NH_4)_2SO_4$ and KNO_3 were substituted with NH_4NO_3 and KCl, at a final dilution of 1:50, 23 mM MES Buffer (SIGMA), 0.5% w/v sucrose (DUCHEFA) and 0.8% plant agar (DUCHEFA), pH 5.7.

Once the primary roots had developed to ~2 cm in these plates, seedlings were transferred (three per plate) to a fresh, second set of plates. This second set of plates had the same agar medium which was segmented by removing 4mm strips to provide three separate sections, the middle section measuring 15mm. The middle section was supplemented with 1mM KNO_3 (N+) or 1mM KCl (designated control). Seedlings were transferred to these plates when root length reached 2 cm, with the root tip just touching the second section. Plates were scanned 12 days later and measurements were taken and analysed as described in 2.2.2.1.

*In this experiment, the KNO_3 and $(NH_4)_2SO_4$ in the original recipe (DUCHEFA Catalogue 2000-2002: Plant Cell and Tissue Culture Media) of Gamborg's B5 salt were replaced with 1mM KCl and 10μM NH_4NO_3 to produce a $NO3^-$poor medium.

Micro Elements (final concentration)		Macro Elements (Final concentration)	
$CoCl_2.6H_2O$	0.025 mg/L	$CaCl_2$	113.23 mg/L
$CuSO_4.5H_2O$	0.025 mg/L	KCl	47.55 mg/L (replaces KNO_3 2500 mg/L)
FeNaEDTA	36.7 mg/L	$MgSO_4$	121.56 mg/L
H_3BO_3	3 mg/L	NaH_2PO_4	130.44 mg/L
KI	0.75 mg/L	NH_4NO_3	0.8 mg/L (replaces $(NH_4)_2SO_4$ 134 mg/L)
$MnSO_4.H_2O$	10 mg/L		
$Na_2MoO_4.2H_2O$	0.25 mg/L		
$ZnSO_4.7H_20$	2 mg/L		

Stock solutions of micro- and macro-elements were prepared separately by dissolving the salts in sterile MilliQ water, and the stock aliquots were stored at -20 C until required.

2.2.2.4 Fluence rate response experiments.

These experiments were performed by Dr. Virtudes Mira-Rodado in Professor Klaus Harter's lab at the University of Tuebingen, Germany. The experimental procedure has been provided by her and presented here with her permission. The method has been detailed in Kircher et al, 1999 and Sweere et al, 2001.

To study the effect of different light quantities in the photomorphogenesis of the plant, responses of hypocotyl growth was measured after irradiation treatments in different light intensities. To avoid any influence of carbohydrates and growth media components on the photomorphogenic response, the seeds were sown on four layers of filter paper and allowed to imbibe on sterile water in the dark for 24 h at 4°C. After stratification and germination induction, seedlings were grown at 23°C for three days in the dark or in constant red, far-red or blue light under different fluence rates achieved as described below. After three days the hypocotyl lengths were measured.

To achieve the different light intensities, Petri dishes (each containing >30 germinating seeds) were piled up in a column which was subsequently wrapped with black paper to avoid light coming through the sides of the column. By this way, light can only penetrate through the first plate in the column.

The light intensity that reaches the subsequent plates can be calculated with the following formula:

F1= light intensity in the first plate (μmol/m^2s).

F2= 0.256 x F1

F3= 0.418 x F2

F4= $(0.418)^2$ x F2

Fn= $(0.418)^{n-2}$ x F2 Where n is the position number of the plate in the column.

For this experiment F1 first plate for red: 24 μmol/m^2s; far-red: 18 μmol/m^2s and blue: 7 μmol/m^2s

.

2.2.3 Crossing *Arabidopsis* for genetic analyses and mapping

Healthy plants were selected and "female parents" were prepared trimming to remove immature buds, already fertilized flowers, siliques and secondary and tertiary flowering stems, leaving 3-5 flowers to be emasculated. Flowers with the stigma just protruding from the unopened white petals and with un-dehisced anthers were chosen for the crossing. Emasculation was carried out 48 hours prior to crossing, by removing the stamens under the microscope, but leaving the rest of the floral parts intact. Two days later, fully opened flowers were taken with forceps from a 'male parent', mature, dehisced anthers were separated from the flower and they were used to spread pollen over the emasculated female parent flower by dabbing pollen onto the stigma. Flowers thus hand pollinated were marked with coloured tape. The plants were kept in the controlled environment glasshouse until the mature seeds were harvested.

2.2.4 Phenotypic analysis

2.2.4.1 Seed weight measurements

Mature pods were collected and dried in paper bags until the seeds were released from the dried pods. After removing the plant debris, the seeds were stored in 1.5 ml eppendorf tubes. Seed weights were obtained using a UMT 2 Micro balance (Mettler-Toledo, Leicester, UK). For each genotype three batches of seeds with 50 seeds per batch were weighed to get an average weight which in turn was used to calculate the weight per seed. A fine paint brush was used to manipulate the seeds.

2.2.4.2 Photography and image processing

Root hairs - Primary roots were dissected from 5-d old seedlings grown on agar medium (section 2.2.1.2). These were mounted on 50% (v/v) glycerol on a glass slide, covered with a fine glass cover slip and sealed with nail varnish. The roots were photographed under Nikon Eclipse E800 microscope using a phase contrast green filter (Cokn A.004) with a lens magnification of x4 x 1.25 x10

Whole plants, inflorescences, flowers and seeds- Whole plants were photographed using a Nikon Coolpix 4500 digital camera directly. Photographs of inflorescences and flowers were obtained as above under a Leica MZ6 dissecting microscope and of seeds, under an Olympus BH-2 microscope.

Digital images were processed using Adobe Photoshop software.

2.2.4.3 Anthocyanin extraction and spectrophotometric analysis

A method described by Lange *et al* (1971) was adapted to extract anthocyanin from plant tissue (pigmented zones from the *ppi* inflorescences, equivalent regions from the wt plants or wt and *ppi* seedlings). Plant tissue was placed in ~ 500 µl extraction solution (propanol-HCl-H_2O 18:1:81 vol%) in eppendorf tubes. Then they were boiled at 100 °C using a heat block, for 3 minutes. The tubes were then covered with foil, and left at 25 °C in the dark for 3 hours for the full extraction of the pigment. The tubes were then centrifuged for 12 minutes at 13000 rpm. The supernatant containing anthocyanin was made up to 1 ml with the extraction solution and using a Unicam Heλios λ Spectrophotometer the absorbance (A) was measured at 535 nm and 650 nm.

The A values at 535 nm were corrected for scattering using the A value at 650 nm (A_{650}) and Rayleigh's formula. Since there is no absorbance by anthocyanin at 650 nm,

corrected $A_{535} = A_{535} - 2.2\ A_{650}$ (Lange *et al*, 1971).

2.2.5 Southern hybridisation analysis of the T-DNA insertion

2.2.5.1 Isolation of plant genomic DNA for Southern hybridisation analysis

Approximately 1 g of plant tissue (pooled from about 50 young plants in the case of the *csn5a* mutant lines) was harvested and genomic DNA (gDNA) was extracted using the DNA extraction kit Nucleon® Phytopure (Nucleon Biosciences) as described in the manufacturer's hand book. Extracted DNA was resuspended in 300 µl of 0.1x TE buffer (1mM Tris-HCl pH 8.0, 0.1 mM EDTA, pH 8.0), treated with RNaseA (Sigma, Poole, UK) ~25 µg/ml and by incubating for 30 minutes at 37 °C.

2.2.5.2 Purification of DNA by phenol-choloroform extraction and subsequent precipitation with EtOH.

The DNA sample was brought to 300 µl and mixed with an equal volume of 1:1 v/v phenol:chloroform by vortexing until an emulsion formed. The mixture was then centrifuged at 13000 g for 1 minute at room temperature. The aqueous upper phase containing the DNA was transferred to a fresh microfuge tube and the DNA was recovered by ethanol precipitation by adding 1/10 volumes of 3M NaAcetate (pH 5.2) mixing, then adding 2 ½ volumes of 100 % (v/v) EtOH. After 2 hours incubation at -20 °C to facilitate DNA precipitation, tubes were centrifuged at 13000 g for 15 minutes.
The DNA pellet was rinsed with 1 ml of 70% (v/v) EtOH and then air dried for 5 minutes. The DNA was resuspended in 300 µl sterile MilliQ H_2O.

2.2.5.3 Quantification of DNA yield

Purity of DNA samples was determined and the DNA yield was quantified using spectrophotometric measurements of absorbance at 260 nm (A_{260}) and 280 nm (A_{280}).
To assess the purity of the sample the A_{260} /A_{280} ratio was determined. If the ratio was out of the range between 1.8 -2.0, the sample was purified by phenol:chloroform extraction and ethanol precipitation.

The DNA yield was calculated with the formula:

[DNA] µg/ml = A_{260} x dilution factor x 50 µg/ml double strand (ds) DNA.

Extracted DNA was stored at -20 °C until further use.

2.2.5.4 Restriction endonuclease digestion of gDNA for Southern hybridisation analysis

Restriction endonuclease digestion of 5 µg of RNaseA-treated DNA was performed in a 60 µl reaction containing 5 µl of 10x restriction enzyme buffer, 20 units of restriction enzyme containing 0.1 mg/ml BSA. Reactions were incubated on ice for 30 minutes to allow the enzyme to penetrate the DNA before transferring to 37 °C for 2 hours. Another 20 units of restriction enzyme was added and the reactions were incubated at 37 °C overnight. Digestion was terminated by EtOH precipitation, and the digested DNA was then resuspended in 20 µl 1x TE (10 mM Tris-HCl pH 8.0 & 1 mM EDTA, pH 8.0).

2.2.5.5 Agarose gel electrophoresis

The DNA samples and Digoxigenin-labelled length markers were mixed with 3 µl 10xDNA dye (0.25% w/v Bromophenol Blue, 0.25% w/v Xylene Cyanol, 30% v/v Glycerol & 0.1M EDTA pH 8.0) and were run overnight at 25 V, on a submerged 0.8% (w/v) agarose gel (15 cm x 20 cm) in 1x NEB buffer (0.1M Tris, 1mM EDTA disodium salt and 12.5mM sodium acetate, pH 8.1). The gel was stained with 0.5 µg/ml ethidium bromide in water for 15 minutes and photographed under UV light.

2.2.5.6 Southern blotting

The gel was treated with 500ml of 0.25 M HCl for 10 minutes with gentle shaking to de-purinate, then rinsed once with ddH2O followed by treating with 500 ml of solution denaturating solution 0.5M NaOH,1.5M NaCl for 30 minutes with gentle shaking, rinsed with ddH2O and finally treated with 500 ml of neutralising solution (0.5M Tris-HCl pH 7.5, 1.5M NaCl).

The DNA fragments were capillary blotted onto a Sigma BIOBOND^{TM} nylon membrane using 20xSSC (3M NaCl, 0.3 M Sodium citrate) as the transfer buffer. The blot was set up as follows: a glass plate/ support was placed on the bottom of a tray (500-1000 ml capacity) and 3 MM paper soaked in 20xSSC was wrapped around it so that the paper can act as a wick with the ends of the paper lying on the bottom of the tray. The upper left corner of the gel was marked by cutting off a small piece of the gel and the gel was placed up side down on the 3MM paper, any air bubbles were removed by rolling a sterile glass tube over the gel carefully. The upper left corner of the Sigma BIOBOND^{TM} nylon membrane cut to exactly the same size of the gel was marked as the gel. The membrane was soaked in 2xSSC and was placed on the gel with the corner maker correctly orientated. Air bubbles were avoided or removed carefully. Strips of parafilm were used to isolate the

blotting buffer. Three sheets of 3 MM paper were soaked in 2x SSC and were placed on top of the membrane. A stack of (~6 cm) paper towels was placed on the blot and topped with a sheet of glass and a 250g weight. The tray was then topped up with 500 ml 20xSSC and blotted overnight.

The membrane was removed from the gel and rinsed in 2xSSC for 5 minutes. It was air-dried on clean sheets of filter paper. DNA was cross-linked to the membrane by exposing twice to UV in a StrataLinker at 120 energy level (2x 5s) or by baking at 80 °C for 30 to 120 minutes. Membranes were stored at 4 °C in a sealed polythene bag until detection.

2.2.5.7. Preparation of digoxigenin-dUTP labelled probes

Digoxigenin-dUTP (DIG-dUTP) labelled probes were prepared from pSKI015 DNA by PCR using the DIG High Prime DNA Labelling and Detection Starter Kit II (Roche Molecular Biochemicals, Germany) as described in the manufacturer's hand book. Labelled PCR products were examined by electrophoresis of a 5 µl portion of the product on a 1.1 % (w/v) agarose gel. Probes were denatured by boiling for 5 minutes prior to use. DIG-labelled Basta and 35S probes were prepared using the pSKI015 vector DNA as the template and the GCR1 probe was prepared using the genomic DNA from the Ws-2 wild-type plats. The primer details are given in Chapter 3.

Hybridization temperature (T_{hyb}) for the Basta probe was 47 °C, for the 35S probe it was 42 °C and for the GCR1 probe it was 42 °C. T_{hyb} determined according to the following equation:

$T_{hyb} = T_m - 20$ to 25 °C

$T_m = 49.28+0.41(\%G+C) - (600/l)$ where l is the length of hybrid in base pairs.

The % GC content was calculated using online software http://www.artsci.wustl.edu/~twest/molbio/gccontent.php in calculating the % GC content].

2.2.5.8. Hybridization of nucleic acids on membranes with probes and immunological detection

Membrane filters were pre-hybridized at the hybridization temperature (T_{hyb})* in 10ml/100 cm^2 of DIG Easy Hyb hybridization buffer (Roche) and hybridized at T_{hyb} for 16-20 hours in 3.5ml/100cm^2 membrane using fresh hybridization buffer containing denatured DIG-labelled probe (3.5 µl/ml hybridization buffer). Pre-hybridization and hybridization were performed in rotating glass tubes in a hybridization oven. Membranes were then washed 2x 5 minutes in ample 2x SSC, 0.1% (w/v) SDS at room temperature, followed by 2x15 min

washes in 0.5 x SSC, 0.1% (w/v) SDS at 68 °C. Immunological detection was carried out as described in DIG High Prime DNA Labelling and Detection Starter Kit II (Roche Molecular Biochemicals, Germany). The membrane filter was treated with chemiluminiscent CSPD ready–to-use and the luminescence was detected by exposing to Lumi-Imager (Fuji) for 20-60 minutes or by exposing to X-ray film (Kodak) for 3-5 hours or by exposing to high performance autoradiography film (18x24 cm, HyperfilmTM MP, Amersham Biosciences) for 0.5 – 1 h. Films were scanned on a flat bed scanner filled with a transparency adaptor and images preserved and processed using Adobe Photoshop software. .

2.2.5.9. Stripping probes from membrane filters

DIG-labelled probes were removed from membrane filters by washing twice in 0.2 M NaOH, 0.1% (w/v) SDS for 15 minutes at 37 °C . After rinsing thoroughly with 2x SSC, the membrane could then be hybridized to another probe. Stripped membrane filters were stored in 2xSSC at 4 °C, until further use.

2.2.6. Plasmid Rescue of DNA flanking T-DNA insertion.

The plasmid sequences in pSKI015 are flanked by several restriction enzyme sites (Weigel et al, 2000) that can be used for rescue of T-DNA and adjacent plant sequences from transformed plants. Restriction enzymes BamHI, SpeI and NotI were used for rescue of sequences adjacent to the left T-DNA border.

2.2.6.1 Restriction endonuclease digestion of DNA, ligation and transformation of competent *E.coli* cells with ligated DNA

For plasmid rescue, 1g of plant tissue was harvested and genomic DNA was extracted with Nucleon Phytopure DNA extraction kit (section 2.2.5.1). The extracted DNA was resuspended in 300 µl 1x TE buffer and purified further by extracting twice with phenol-chloroform followed by EtOH precipitation (2.2.5.2). The DNA was resuspended in 300 µl sterile MilliQ H_2O and quantified as in section 2.2.5.3

A 15 µg sample of DNA from *ppi* and Ws-2 was digested with either *Bam*HI, *Spe*I or *Not*I at 37 °C overnight in a 50 µl reaction. Digested DNA was extracted with phenol-chloroform followed by EtOH precipitation and then washed with 70% EtOH before resuspending in 50 µl of sterile dH_2O.

Samples (50 µl) were ligated overnight at 16 °C in a total volume of 250 µl containing 1x T4 DNA Ligase buffer with ATP (New England Biolabs NEB) and 1.5 µl of high concentration T4 DNA Ligase (2,000 U/ µl ; NEB).

Ligated DNA was precipitated with EtOH and resuspended in 10 µl of 1x TE. 2 µl of the ligated DNA was used to transform 50 µl of electroporation-competent and recombination-deficient *E. coli* SURE® cells (Stratagene), by electroporation in a BIO-RAD Micropulser™ (BIO-RAD) according to the protocol given in the Micropulser handbook. After electroporation, the cells were gently and quickly resuspended in 960 µl of SOC medium (2% w/v tryptone, 0.5% w/v yeast extract, 0.05% w/v NaCl, 10 mM $MgCl_2.6H_2O$, 10 mM $MgSO_4$ & 0.4 % w/v glucose) and incubated at 37 ^{0}C for 1 hour with shaking at 225 rpm. 100 µl of the cell suspension was plated on LB-Agar selective medium (1% w/v NaCl, 1% w/v tryptone, 0.5% w/v yeast extract pH 7.0, and 2% w/v Bacto Agar) containing 100 µg/ml Ampicillin. The rest of the cell suspension was centrifuged at 5000 rpm for 3 minutes, 700 µl of the supernatant was discarded and then the pellet formed was resuspended in the remaining 200 µl liquid. 100 µl portions of the concentrated cell suspension were plated on two more selective media (LB-ampicillin-agar) plates. Plates were incubated at 37 °C for 16 hours, and each transformed colony resistant to ampicillin were re-cultured in 10 ml of selective LB-liquid media containing 100 µg/ ml Ampicillin, and incubated for 16 hours at 37 °C. 750 µl of each overnight culture were mixed with 750 µl of 50% glycerol and stored at -80 °C until further use.

2.2.6.2. Purification of Plasmid DNA

Plasmid DNA was prepared from 10 ml of the cultures, extracted and purified using Wizard® Plus Miniprep DNA Purification System (Promega) according to the manufacturers protocol. Purified plasmid DNA (in 50 µl sterile dH_2O) was stored at -20 ^{0}C until further use.

2.2.6.3. Restriction enzyme digestion of plasmid DNA

Either single enzyme (the relevant restriction enzyme that was used to rescue plasmids-*BamH*I, *Spe*I or *Not*1) digestions or double digestions with the relevant enzyme and *Hind*III were performed in 15 µl reactions containing 1x restriction enzyme buffer, 5 units of enzyme(s) (NEB or Promega), 0.1 mg/ml BSA and 1 µl of plasmid DNA. The reactions were incubated at 37 ^{0}C for 2 hours.

The DNA fragments were separated by electrophoresis in a 0.8 % (w/v) agarose gel containing 0.5 µg/ml ethidium bromide and photographed on a transilluminator.

2.2.6.4. Sequence analysis of plasmid DNA

Plasmid DNA from step 2.2.6.2 was precipitated with EtOH and was resuspended in 50 µl of sterile dH_2O. DNA was sequenced at the sequencing facility, Department of Biology and Biochemistry, University of Bath, in a 6 µl reaction containing 300-500 ng of pDNA (5 µl of sample) and 5 pmoles of sequencing primer. Two primers were used so that genomic DNA adjacent to the LB was sequenced on both strands (see Chapter 3 for details). Sequence homology searches were performed using the BLAST algorithm facility available on the National Centre for Biotechnology Information (NCBI) server (www.ncbi.nlm.nih.gov/BLAST/) and The Arabidopsis Information Resource (TAIR) server (www.arabidopsis.org/)

2.2.7. Detection of possible location of the T-DNA in *ppi* mutants by PCR

2.2.7.1 Genomic DNA extraction from *Arabidopsis*

Plant DNA for PCR analysis was extracted and isolated as described by Bendahmane *et al.*, (1997).

Approximately 0.5 cm^2 leaf tissue was placed in a microfuge tube containing a pinch of acid washed sand and 100µl of extraction buffer (0.14M d-Sorbitol, 0.22M Tris-HCl pH 8.0, 0.022 M EDTA pH 8.0, 0.8M NaCl, 0.8% w/v cTAB, 0.1% w/v n-Lauroylsarcosine) and ground using a heat-sealed 1 ml pipette tip or with a disposable pestle and a bench drill. The ground tissue was heated at 65°C for five minutes before extracting the DNA in 100µl of chloroform. After centrifugation at 13,000 rpm for 5 minutes, the aqueous fraction was transferred to a clean microfuge tube and DNA was precipitated with 100µl iso-propanol at room temperature for 15 minutes and collected by centrifugation at 13000 rpm for 5 minutes. The pellet was washed with 70% (v/v) ethanol by vortexing and recovered by centrifuging at 13000 rpm for 10 minutes. It was then air-dried on the bench for 10 minutes or in a SpeediVac for 2 minutes, before resuspending in 50µl of sterile ddH_2O and stored at 20 ^0C. For each 20 µl PCR, 2 µl of the DNA sample was used.

2. 2.7.2 Polymerase Chain Reactions (PCRs)

Each 50µl PCR reaction contained 25 µl of REDTaq™ReadyMix™ PCR Reaction Mix with $MgCl_2$ (SIGMA), 2x 2.5 µl of 10 µM primer stocks, 15 µl ddH_2O and 5µl of DNA template.

PCR conditions consisted of an initial incubation period of 94°C for 3 minutes, followed by 35 cycles at a denaturing temperature of 94°C for 45 seconds, at the annealing temperature for 30 seconds and at the extension temperature of 72°C for 1.5 minutes. A final polishing step of 72 °C for 10 minutes was also included before reaching a holding temperature of 4 °C. Primer details are given in Chapter 3.

2.2.7.3 Agarose Gel Electrophoresis

PCR samples were analysed by electrophoresis through 1.1% (w/v) agarose gels in 1x TBE (90 mM Tris-borate, 2 mM EDTA, pH 8.0), and the size of amplified fragments determined by comparison with 0.1 µg/mm lane width 1Kb Plus DNA Ladder (Invitrogen) or with 50 bp DNA Ladder (Invitrogen).

2.2.8 Mapping the *ppi* gene

2.2.8.1. Generating Mapping Populations

Generation of mapping populations were described in section 2.2.3.

2.2.8.2. Crude plant DNA extraction for PCRs

Plant DNA for PCR analysis was extracted and isolated as described by Edwards et al., (1991). Approximately 0.5 cm^2 leaf tissue was placed in a microfuge tube containing a pinch of acid washed sand and 400µl of extraction buffer (200mM Tris-HCl pH 7.5, 250 mM NaCl, 25 mM EDTA and 0.5% w/v SDS) and macerated using a bench drill and disposable pestle (Sigma) for 15s. The extract was then centrifuged at 13000 rpm for 6 minutes and 300 µl of the supernatant transferred to a clean microfuge tube. An equal volume of iso-propanol was added and left at room temperature for 2 minutes. Following centrifugation at 13000 rpm for 6 minutes, the supernatant was discarded and the pellet was washed with 70%)v/v) EtOH by vortexing for 1 minute. After centrifuging at 13000 rpm for 10 minutes, the pellet obtained was air/ vacuum dried before resuspending in 80 µl

of sterile ddH2O or 1x TE. Extracted DNA was stored at -20 ^{0}C until further use. For each 20 µl PCR, 2 µl of the DNA extraction was used.

2.2.8.3. Polymerase Chain Reactions (PCR) for mapping

Each 20µl PCR reaction contained 0.025U/µl Taq DNA polymerase (Invitrogen), 1.5 mM $MgCl_2.6H_2O$ (Invitrogen), 0.2 mM each dNTPs (Invitrogen), 1x PCR buffer (20 mM Tris-HCl pH 8.4, 50 mM KCl; Invitrogen) 0.5 µM each of forward and reverse primers and 2 µl of DNA template from methods above.

PCR conditions consisted of an initial incubation period of 94 ^{0}C for 3 minutes, followed by 30 to 35 cycles at a denaturing temperature of 94 °C for 45 seconds, a relevant annealing temperature for 30 seconds and an extension temperature of 72°C for 40 s to 1 minute and 30s depending on the size of the amplified fragment (40s per 1 kb length). A final polishing step of 72°C for 10 minutes was also included before reaching a holding temperature of 4 °C.

Primer details for molecular markers are given in Chapter 4.

2.2.8.4. Designing new SSLPs or CAPs molecular markers

A. thaliana Col-0 genomic sequence from TAIR was used to design primer pairs in order to find polymorphisms that can be used as potential SSLP or CAPs markers. Primers were designed with the help of Web-Primer software available on the internet (http://seq.yeastgenome.org/cgi-bin/web-primer).Amplified regions were subjected to restriction enzyme digestion with the help of Web-Cutter software available on the internet (http://rna.lundberg.gu.se/cutter2/) using a range of restriction enzymes. When restriction patterns with differences were obtained the primer pair was taken as a potential new molecular marker. These were confirmed by actually restricting the DNA by the relevant enzymes to produce different band patterns.

2.2.9 TOPO® TA cloning of PCR products and subsequent sequencing

TOPO® TA Cloning is a one-step cloning strategy for the direct insertion of *Taq* polymerase amplified PCR products into a plasmid vector.

2.2.9.1 Amplification of DNA fragments by PCR for TOPO Cloning

DNA fragments were amplified using Expand High FidelityPlus PCR system (Roche) according to the manufacturer's protocol.

2.2.9.2 Purification of PCR products

The PCR fragments were gel-purified using High Pure PCR Product Purification Kit (Roche). Total PCR was electrophoresed on a 1xTBE Agarose gel (0.8 – 1.2% w/v). The desired bands were visualized under UV and the gel areas were excised with a clean blade and the DNA fragments were purified using the above kit as directed.

2.2.9.3 Cloning the purified PCR Products into the pCR2.1-TOPO vector

Once the desired PCR product was produced and purified it was TOPO Cloned into the pCR2.1-TOPO vector using the TOPO-TA Cloning Kit (Invitrogen # K4500-01).
The TOPO Cloning reaction was set up by mixing 2 µl fresh, purified PCR product, 0.5 µl Salt solution (1.2 M NaCl, 0.06 M MgCl2.6H2O) and 0.5 pCR2.1-TOPO vector (10 ng/µl pDNA in 50% v/v glycerol, 50 mM Tris-HCl pH 7.4, 1mM EDTA, 1 mM DTT, 0.1% v/v Triton x-100, 100 µg/ ml BSA and phenol red). The reaction was incubated for 15 minutes at room temperature (22-23 °C). The TOPO Cloning reaction was placed on ice until transformation or stored at -20 °C overnight.

2.2.9.4 Transforming the recombinant vector into competent *E. coli* cells:

Once the TOPO-Cloning reaction was performed, the pCR2.1-TOPO construct was transformed into the One Shot® TOP10 Chemically Competent *E. coli* cells provided with the Kit.
25 µl of competent cells was added to the tube containing 3 µl TOPO Cloning reaction, mixed gently and incubated on ice for 15 minutes. The cells were then given a heat-shock at 42 °C for 1 minute without shaking and were transferred immediately onto ice. 125 µl S.O.C. medium was added, gently mixed and then incubated at 37 °C for 1 h.

The transformation mixture was spread on selective LB-Agar (1% w/v Tryptone, 0.5% w/v Yeast extract, 1.0 % w/v NaCl, pH 7.0 ; 1.5% to 2% w/v Bacto agar) plates containing Kanamycin (50 µg/ml) and X-gal (40mg/ml in DMF), prewarmed to 37 °C. The plates were then incubated overnight at 37 °C for blue/white selection. White colonies were analyzed for positive clones.

2.2.9.5 Analyzing transformants by 'colony PCR':

'Colony PCR' was performed to analyze positive transformants. Either M13 forward (-20) (5'-GTAAAACGACGGCCAG-3') or M13 reverse (5'-CAGGAAACAGCTATGAC-3') primer that hybridizes with the vector and a primer that hybridizes within the insert were used to test for positive clones.

After making a patch plate to preserve the colonies for further analysis, selected white colonies were resuspended individually in 15 µl of 1xTE buffer containing 0.6 µl of Proteinase K (Promega.) and the reaction was incubated at 55 °C for 15 minutes and then at 80 °C for 15 minutes in a thermocycler to lyse the cells and inactivate nucleases. A 15 µl PCR was set up with 1.5 µl of the above Colony PCR mix, 10 pmoles each forward and reverse primers and 1x PCR premix (AB Gene) PCR programme was as in section 2.2.7.2. The PCR products were checked for the presence of correctly sized bands by electrophoresis in a 1 % (w/v) Agarose gel.

2.2.9.6 Purification of Plasmid DNA

Plasmid DNA was prepared from selected clones. These were streaked onto LB+Kanamycin+X-gal selective plates (section 2.2.9.4.) and incubated at 37 °C overnight. The cultures were scraped out into microfuge tubes and the plasmid constructs were extracted and purified using Wizard Promega WizardPlus SV Miniprep DNA Purification Kit (Promega # A1330) according to the manufacturer's protocol. Purified pDNA was resuspended in 100 µl sterile MilliQ water and stored at -20 °C until further use.

2. 2.9.7 Purification of pDNA constructs by phenol/chloroform extraction

The plasmid DNA sample was brought to 300 µl and purified using phenol:chloroform extraction and recovered by EtOH precipitation as 2.2.5.2 and DNA yield was quantified as in 2.2.5.3.

2.2.9.8 Confirmation of the presence of inserts by restriction endonuclease digestion

To confirm if the desired inserts were truly present in the clones, pDNA constructs extracted above were digested with restriction endonuclease *EcoR* I because two *EcoR* I sites are present on either side of the cloning site of pCR2.1-TOPO vector. 2 µl plasmid miniprep was digested with 0.5 µl *EcoR* I (NEB) with 1x buffer and 0.1mg/ml BSA in a total 10 µl reaction incubated at 37 ^{0}C for 1 h. The products were visualized by electrophoresis on 1 % (w/v) Agarose gels.

2.2.9.9 Sequencing and deriving a consensus

The clone containing the entire gene (2.3 kb) was sequenced as described in section 2.2.6.4 with 5 primers at approximately 480 bp intervals across the gene on the forward strand and 5 primers on the reverse strand (primer details and positions are given in Chapter 4).

For each of the mutant and wild type, three independent clones were selected, and each of these was sequenced fully on both strands by obtaining three replicate sequencing reads from each of the primers. The quality of sequence traces was confirmed using 'CHORMAS' software and where necessary samples were re-sequenced until all replicates had been obtained. Sequence reads of between 500-600 nt were obtained. The sequence files loaded into SeqMan (LaserGene) software and the sequences were edited by removing vector sequences and trimmed to remove unreadable or poor quality regions. Then the edited sequences were aligned and compared to derive a consensus. When a nucleotide (nt) reading was different only in one out of the three sequences, the nt that was similar in two readings were taken as the consensus. Where a consensus could not be derived as all three reads were different, sequence reads from other primers were considered as there were often more than 3 reads available at sites because of extensive overlap of sequences.

2.2.10 Transcript analysis by RT-PCR

2.2.10.1 Isolation of total RNA from *A. thaliana*

Total RNA was isolated from 15-day old whole plants grown on nutrient agar. 100 mg plant tissue was frozen by plunging into liquid nitrogen immediately after harvesting and ground to a powder in liquid nitrogen. The powdered material was warmed at -20 °C for 10 minutes and mixed with 1 ml of Roche TriPure Isolation Reagent (Roche) pre-warmed

to 50 °C and the RNA was extracted according to the manufacturer's protocol. Isolated RNA was resuspended in 100 µl sterile RNase-free water. 1 µl (40U) of Recombinant RNasin Ribonuclease Inhibitor (rRNasin, Promega Cat. # N2511) was added to each RNA sample for long-term storage at -80 °C.

The quality of the RNA was checked as in section 2.2.5.3 and the RNA yield was evaluated using spectrophotometric measurements at 260 nm and 280nm.

The RNA yield was calculated with the formula:

[RNA] µg/ml = A_{260} x dilution factor x 40 µg/ml

2.2.10.2 Reverse Transcriptase-PCR (RT-PCR)

To provide semi-quantitative analysis of transcript levels, reverse transcription analyses were performed using the Access RT-PCR System (Promega).

Fragments of DNA were amplified from total RNA templates using gene specific oligonucleotide primers. 50 µl reactions were set up in 0.2 ml thin walled PCR tubes. Each reaction contained 1x *AMV/ Tfl* Reaction buffer, 1 mM $MgSO_4$, 0.2mM dNTPs, 10U AMV Reverse Transcriptase, 5U *Tfl* DNA polymerase and 50 ng total RNA sample. 40 U of rRNasin was also added to inhibit any RNase activity. 50 pmoles each of reverse and forward primers were used. Before adding the enzymes, the reaction mix containing the RNA was heated at 65 °C for 5 minutes to denature the RNA and cooled to 45 °C. 1st strand cDNA was synthesized by incubating the reverse transcriptase reaction at 45 °C for 45 minutes in a thermocycler . The reaction was then incubated at 94 °C for 2 minutes for the AMV reverse transcriptase inactivation and RNA/ cDNA primer denaturation. Second strand cDNA synthesis and PCR amplification was carried out using 40 cycles of incubation at a denaturating temperature, 94 °C for 30 seconds, annealing 60 °C for 1 minute, extension at 68 °C for 2 minutes followed by a final extension at 68 °C for 7 minutes. A 10 µl sample of the total reaction was analyzed by agarose (1% w/v) gel-electrophoresis.

2.2.11. Protein expression analysis by immunoblotting

2.2.11.1. Extraction of total proteins

To extract the total proteins from *csn5a* mutants and wt plants, the method described by Gusmaroli *et al.* (2004) was used.

Plants were grown on agar as in section 2.2.1.2. From 15-20 day old plantlets 0.3g plant material (whole plants-pooled) was obtained and homogenized in liquid N_2 in 300 ul Extraction Buffer [50 mM Tris-HCl, pH 7.5, 150 mM NaCl, 10mM $MgCl_2.6H_2O$, 2.5 mM EDTA, 1mM DTT, 10% v/v Glycerol, 0.1% v/v Nonidet-P-40, Freshly added protease inhibitors PMSF (1mM), 1X Complete^{TM} Cocktail (Roche), phosphatase inhibitors β-glycerophosphate (60 mM), Na_3VO_4 (50 mM), NaF (10 mM) and the metalloprotease inhibitor o-PT (2mM)]

The homogenate was centrifuged at 20 000g for 1h at 4 °C and the supernatant enriched in soluble proteins was filtered through a 0.2 μm filter before determining the protein concentration using the 2-D Quant Kit (Amersham BioSciences) according to the manufacturer's protocol. Proteins were purified precipitated and concentrated using the 2-D Clean-Up Kit (Amersham BioSciences) as directed. The pellet of proteins obtained was resuspended in 100 μl Protein Sample Buffer (0.06M Tris, 5% v/v glycerol, 4% w/v SDS 0.0025% w/v bromophenol blue) containing freshly added 5% v/v 2-mercaptoethanol)

2.2.11.2 SDS-PAGE of proteins

20 μg of total protein sample extracted as above was brought up to about 8 μl with Protein Sample Buffer containing freshly added 5% v/v 2-mercaptoethanol, and then boiled for 5 minutes. The sample was spun for 5 minutes at 13000g and the supernatant was loaded SDS-PAGE gels. Polypeptides were separated by vertical electrophoresis on a 12.5% (w/v) polyacrylamide gel (12.5% resolving gel; 4% stacking gel) in TGS buffer (25 mM Tris, 192 mM glycine, 0.1% w/v SDS pH 8.3) initially at 60V for 30 minutes until the dye front bands passed into the resolving gel and then at 80 V for approximately 2 hours until the dye front reaches the bottom of the gel. 5 μl Precision Plus Protein Standard stained/ unstained (Biorad) were run along with the protein samples.

The gel was removed carefully from the gel cassette. After rinsing with dH2O the gel was stained with Coomassie Brilliant Blue Stain [0.3% w/v Coomassie Brilliant Blue R-250 (Biorad # 161-0400), 25% v/v methanol, 10% v/v acetic acid] for 2 hours to over night and then de-stained in 25% v/v methanol, 10% v/v acetic acid for <1 hour.

2.2.11.3 Immunoblotting

Polypeptides were electrophoretically separated as described above in section 2.2.11.2 and then electrophoretically blotted onto a Immobilin membrane (Sigma) using Transfer Buffer (25 mM Tris, 192 mM Glycine, 15 % v/v methanol) in a vertical electrophoresis unit (Biorad) as follows:

TGS buffer was poured off from the electrophoresis unit and the gel cassettes were rinsed with water. The gel was removed from the cassette and equilibrated in the Transfer Buffer for 15 minutes. Immobilin membrane and 3MM filter papers were cut to the dimensions of the gel and were soaked first in methanol and then in H_2O before soaking in the transfer buffer for approximately 15 minutes. The blot (gel cassette) was prepared as directed and the protein bands were electrophoretically transferred to the membrane by running at 100 V for 1 hour. After discarding the Transfer buffer, the membrane was removed from the gel cassette and air dried between two pieces of 3MM filter paper if not immediately used in hybridization.

2.2.11.4 Hybridization and immunodetection

The membrane was soaked in methanol and rinsed with H_2O for 2 minutes and placed in 50 ml of Blocking buffer (0.3% Casein, 500 mM NaCl, 20mM Tris pH 7.4, 0.1% Tween-20) with gentle shaking for 1 hour. The membrane was the incubated with either 1:2000 CSN5 rabbit polyclonal antibody (α-CSN5) (BIOMOL) or with 1:1000 RPT5 rabbit polyclonal antibody (α-RPT5) (BIOMOL) sealed in a plastic bag with gentle shaking over night. The α-RPT5 antibody was used to ensure equal loading of the samples. The same amounts of total proteins were loaded and were run alongside the other samples and immunoblotted with the antibody.

The membrane was then washed 3 times in 50 ml Blocking buffer and incubated in 1: 30000 goat anti rabbit IgG antibody (Sigma)for 1.5 hours and washed 3 times in 50 ml blocking buffer. After washing 3 times in AP buffer (0.2 M Tris, 0.1M NaCl pH 9.5) with 0.05M $MgCl_2.6H_2O$, detected with 20 ml of BCIP/NBT premixed solution (0.48 mM NBT, 0.56 mM BCIP, 10 mM Tris, 59.3 mM $MgCl_2.6H_2O$; Sigma # B6404) by keeping the membrane in the solution for 1-15 minutes. The membrane was photographed after washing in dH_2O.

2. 2.12 Two Dimensional Electrophoresis (2 DE) of Soluble Proteins

Two DE of soluble proteins extracted from mutants and wt plants was performed at the Centre for Research in Plant Sciences (CRIPS), University of West of England (UWE).

2. 2.12.1. Sample preparation

The fractionated protein extraction procedure for plant tissue described by Giavalisco et al. (2003), was used to isolate mainly cytosolic protein fraction from mutant and wild-type *Arabidopsis* plants.

Shoot tissues ('above ground' vegetative tissue) were harvested from 21 days old plants grown on 1x MS as described in section 2.2.1.2, weighed to obtain 300 mg samples, washed with de-ionized water and dried with filter paper to remove residual water and then frozen in liquid N_2 and stored at -80 °C prior to protein extraction.

The frozen plant material (300 mg) was mixed with 0.125 parts (weight solution per weight plant material, w/w) of Protease Inhibitor Mixture I (one CompleteTM tablet dissolved in 2 mL of 100 mM KCl, 20% v/v Glycerol and 50 mM Tris; pH 7.1) and 0.05 parts w/w protease inhibitor mixture II (1 mM Pepstatin A and 1.4 µM PMSF dissolved in 100% ethanol). Plant tissue was ground to a fine powder in liquid N_2 in a mortar placed kept in a ice bucket that was further cooled by pouring liquid N_2 over ice. The homogenate obtained was then ultra-centrifuged at 22000 g for 60 minutes at 4 °C. The resulting supernatant containing the soluble protein fraction was transferred to a new container.

In order to remove substances likely to interfere with the subsequent first dimension isoelectric focusing (IEF), and also to concentrate proteins in dilute samples, the extract was purified with the 2-D Clean Up Kit , according to the manufacturer's instructions(Amersham Biosciences).

The proteins were then resolubilized in 100 µl Sample Solution (7M Urea, 2M Thiourea, 30 mM Tris-base, 4% w/v CHAPS) at room temperature for 1 hour. The protein yield in the sample was determined using the 2-D Quant Kit (Amersham Biosciences) as described in the manufacturer's protocol.

2.2.12.2. IPG Dry Strip rehydration and first dimension IEF

Ready-made immobilized pH gradient (IPG) strips Immobiline Dry Strip pH 3-10 NL (non linear), 24 cm were used to obtain increased resolution between pH 5 & 7. IPG Dry Strips were rehydrated prior to IEF in Strip Holders. Cleaning and preparation of strip holders for strip rehydration/IEF were done according to the manufacturer's instructions.

Protein samples were applied by in-gel rehydration method by including it in the rehydration solution (rehydration loading). 200µg protein sample in approximately 10-20 µl Sample Solution was brought to 450 µl with the Rehydration Stock Solution (8M Urea, 2% CHAPS, 0.002% w/v Bromophenol Blue, without IPG Buffer). Prior to loading, DTT and IPG Buffer (carrier ampholyte mixture- pH 3-10 non linear- Amersham BioSciences, Cat. # 17-6000-87) were added to the Rehydration Stock Solution to final concentrations of 0.2 % w/v and 0.5% v/v respectively.

After pipetting the 450 µl solution containing the proteins into the Strip Holder, the IPG Dry Strip was positioned gel side down in the groove without trapping air bubbles and overlaid with IPG Dry Strip Cover Fluid (Amersham Biosciences) as directed by the manufacturer. The Strip Holder was covered with its lid and the IPG Strip was allowed to rehydrate on the Ettan IPGPhor platform for 10 hours and IEF was followed directly after rehydration. Rehydration and IEF was carried out automatically according to the programmed settings given below, overnight.

Rehydration time 10 h at low voltage 20-50 V and then,

First voltage step and hold at	500 V for 1 h	(0.5 kVh)
Second voltage step and hold at	1000 V for 1 h	(1.0 kVh)
Third voltage step and hold at	8000 V for 8 h 20 min.	(62.5 kVh)

With a total isoelectric focussing duration of 10 h 20 minutes and 64.0 kilo-Volt-hours (50 µA per IPG Strip, 0.5 % v/v IPG Buffer, 20 °C for both rehydration and IEF).

After IEF, the IPG Strips were either stored at -80 °C in Equilibration Tubes (Amersham BioSciences), or immediately transferred to second dimension SDS-PAGE.

2.2.12.3. IPG Strip Equilibration and Second Dimension SDS-PAGE

2.2.12.3.1 Equilibration

Prior to the second dimension, the IPG strips were equilibrated for 15 minutes with gentle shaking in 10 ml of SDS-Equilibration Buffer (50 mM Tris-HCl pH 8.8, 6M Urea, 30% v/v Glycerol, 2% w/v SDS, 0.002% w/v bromophenol blue in ddH_2O) with DTT (1% w/v) was added to the equilibration solution. A second equilibration step was performed for 15 min with iodoacetamide (2.5 % w/v) instead of DTT.

2.2.12.3.2 Preparation of SDS slab gels for EttanDALT*six* vertical system

After IEF, the second dimension separation was performed in an EttanDALT*six* vertical system, in which parallel multiple runs can be performed.

Multiple SDS slab gel casting and vertical SDS electrophoresis were performed as described. EttanDALT*six* Multiple Gel Caster (Amersham BioSciences) and Tris-Glycine buffer system.

A homogenous resolving gel containing 12.5 % (w/v) total acrylamide having a separation range 14-100 (M_r x 10^{-3}) was used. A 450 ml total of gel solution was required to pour 6 gels with dimensions 25.5cm x 20.5 cm and a 1 mm thickness:

Acrylamide-bis- ready to use solution 40% w/v (19:1)	140.6 ml
4 x resolving buffer (1.5 M Tris, pH 8.8)	112.5 ml (final conc. 1x)
10% w/v SDS	4.5 ml (final conc. 0.1%)
Amonium persulfate (APS)	0.23 g (final conc. 0.05 % w/v or 2.2 mM)
TEMED	48.0 µl (final conc. 0.033% v/v or 2.8 mM)

Preparation of the EttanDALT*six* system for electrophoresis, insertion of the already prepared polyacrylamide gels and the blank cassette inserts into the unit, placing the equilibrated IPG Strip touching the gel in the gel cassette etc. were performed as manufacturer's instructions. A 5 µl sample of protein molecular weight marker (Promega Broad Range Protein Molecular Weight Marker, V8491A; 10-225 kDa) was applied to a small piece of IEF Sample Application Paper. The piece of paper was then placed on the top surface of the gel at the acidic / + end of the IPG strip. A 1.5 ml aliquot of Agarose Sealing Solution (0.5 % w/v Agarose, 0.002% w/v Bromophenol Blue in SDS Electrophoresis buffer (25 mM Tris-HCl, pH 8.3, 192 mM Glycine, 0.1% w/v SDS) was melted in a 100 °C dry heating block, cooled to approximately 60 °C, and slowly pipetted on to the IPG strip that had been inserted into the gel cassette and was allowed to solidify.

After the agarose had set, the six gels were run simultaneously in the EttanDALT*six* electrophoresis unit.

2.2.12.3.3 Electrophoresis

EttanDALT*six* electrophoresis unit was assembled as directed by the manufacturer for electrophoresis with approximately 4 L of 1x SDS Electrophoresis buffer in the Lower Buffer chamber (anode assembly) and approximately 0.8 L of 2x SDS Electrophoresis Buffer in the Upper Buffer Chamber (cathode assembly).

Electrophoresis was performed at constant power at 25 °C in two steps: initial migration and stacking at 2.5W per gel for 30 minutes and then at a maximum of 100 W until the dye front had completely migrated out of the gel (approximately 3 ½ h). Up to 6 gels were run in parallel.

After electrophoresis, the gels were removed from the gel cassettes in preparation for visualization by staining.

2.2.12.4 Staining and image analysis

Gels were removed from the cassettes and fixed in 200 ml per gel fixing solution (40 % v/v methanol, 7% v/v acetic acid) by gently agitating in an orbital shaker for 3 h. After fixing, the gels were rinsed with ddH2O three times before staining with the fluorescent dye SYPRO™ Ruby Protein Gel Stain (Molecular Probes™ # S12000) . A 150 ml aliquot of the undiluted stain was used per gel and the staining was performed by gently agitating on an orbital shaker over night. After staining, the gels were washed in ~200 ml wash solution (10% v/v methanol, 7% v/v acetic acid) for 30 minutes (x 2). Before imaging, the gels were rinsed in ddH_2O two times for 5 minutes to prevent corrosive damage to the imager.

The gels were scanned using a Typhoon™ 9400 Series Variable Mode Image Scanner (Amersham Biosciences) with the green 532 nm excitation source for fluorescence imaging. The images were used for comparative analysis of the spot arrays of different samples.

In order to visualize the spots for subsequent picking for MS, the gels had to be counter stained with Colloidal Coomassie stain (Coomassie Brilliant Blue G-Colloidal Concentrate, Sigma #B2025). The stain was prepared according to the manufacturer's instructions and gels were stained by immersing in Coomassie stain over night. The gels were then destained in 25% v/v methanol, 10% v/v acetic acid for 1 minute with gentle agitation and rinsed with and further destained for 24 h in 25% v/v methanol. After rinsing

with deionized water, the gels could be scanned with an ImageScanner™ at 600 nm (Amersham Biosciences) which is required when the spots are to be picked up by the robotic system Ettan Spot Picker (Amersham Biosciences) for MS.

2.2.12.5 Identifying the protein spots by MALDI-ToF-MS peptide mass fingerprints (PMFs)

The digital images of the SYPRO Ruby stained gels obtained using the Typhoon scanner were analysed manually to identify protein spots that differ in abundance between the samples.

When such an 'interesting spot' was seen, it was excised either by manually or by using a robotic system, the Ettan Spot Picker that automatically picks selected protein spots in a particular gel using a pick list from the ImageScanner™ image analysis and transfers them into micro-titre plates. Individual spots from at least three replicate gels were picked up separately for MS. Trypsin digestion of the gel plugs containing the protein spots and the subsequent MALDI-ToF-MS to obtain the PMF data were performed by Jenna Hughes at CRIPS, UWE.

The software associated with the MALDI-ToF-MS is equipped to search SwissProt with the PMF data to identify the protein. In addition, the PMF data were used to search protein data bases using the MASCOT search engine to extend the search to hypothetical proteins as well.

After the database search, if a majority of the replicate PMF data for a particular spot gave the came up with the same protein match, the identity was accepted confidently. If only one PMF out of all the replicates for a spot gave a good match (with a reasonably high probability score and with reasonably long matching peptide fragments) the estimated and theoretical pI and M_r values were compared and if they were close the protein identity was accepted. For some spots, although they came up with good peptide matches if the estimated pI and M_r were not close to the theoretical values those identities were not accepted, though they have to be analyzed further before rejecting entirely.

2.2.12.6 Estimating pI and M_r after 2DE

The reliability of the first dimension separation with the IPG-dry strips is said to be high and the pI of a protein can be estimated by relating the position of the protein in the second dimension gel to its original position in the Immobiline DryStrip gel.

The first dimension position was determined by measuring the length of the plastic backed Immobiline DryStrip gel, and the position of the strip on the second dimension gel. The spot position was plotted (as a per cent of gel length) versus pH and the pI was read off from the graph of the pH gradient in the manufacturer's hand book 'Immobiline DryStrip Visualization of pH gradients' (Amersham Biosciences # 18-140-60) which is available at http://proteomics.apbiotech.com .

The M_r was estimated based on the protein molecular weight standards run along with the sample in the second dimension SDS-PAGE.

Chapter 3

The pleiotropic phenotype of *ppi* does not segregate with a T-DNA insertion.

3.1. Introduction

3.1.1 *ppi* – a novel mutant of *Arabidopsis thaliana*

An *Arabidopsis thaliana* Ws-2 mutant *purple patch inflorescence* (*ppi*) was found in the University of Wisconsin-Madison Biocentre beta population of T-DNA insertion mutants in the Ws-2 ecotype. The mutant displayed a striking phenotype with reduced apical dominance, pale green colour, semi-dwarfed stature, reduced number of flowers compared to the wild-type and also a distinctive purple pigmented zone below the terminal flower of each inflorescence (Fig.3.1). Some aspects of the phenotype such as the reduced apical dominance and fewer root hairs indicated possible defects in plant hormone responses. Although *ppi* phenotype showed some similarities with hormonal and light signalling mutants, the overall phenotype did not closely resemble any recorded in literature at the time the project was initiated. Working along with the *Arabidopsis* research community to identify the function of every *Arabidopsis* gene and to saturate the genome with informative mutants, my PhD research project set out to isolate and characterize the gene responsible for the *ppi* mutation.

Dr. Konstantin Kanyuka discovered and initiated the work on the *ppi* mutant at the Richard Hooley lab, some time before the commencement of my PhD project. His preliminary studies had shown the mutation is monogenic and recessive and also the presence of a complex T-DNA insertion that could be the cause of the mutation. The mutant had been back-crossed to the wild-type twice to remove any additional insertion events and my work reported in this chapter was performed with the *ppi* mutant plants originating from this twice back-crossed line.

3.1.2 T-DNA insertional mutagenesis and activation tagging as tools for functional genomics in *Arabidopsis*

Screening for loss of function mutations in a genetic pathway is fundamental in dissecting the pathway. Some strategies like antisense and co-suppression that have been used in this respect are not efficient enough to be used on a large scale, and are mostly limited to the study of single genes (Parinov and Sundaresan, 2000). An effective alternative strategy is random large-scale insertional mutagenesis. The high gene density in the *Arabidopsis* genome is particularly favourable for random mutagenesis, as theoretically every second insertion will disrupt a gene sequence (Azpiroz-Leehan and Feldmann, 1997; Parinov and Sundaresan, 2000). The insertion of large T-DNA (Transfer DNA) or transposon constructs will most likely lead to partial or complete inactivation of a gene. The foreign DNA disrupts the expression of the gene into which it is inserted and also acts as a marker for subsequent identification of the mutation (Krysan et al, 1999). Because the sequence of the insertion is known, primers complementary to the end of the insertion and to the gene of interest can be used for PCR screening of insertion collections to identify the plants carrying an insertion within the gene of interest. Alternatively, the disrupted gene can be identified directly by sequencing of the DNA flanking each insertion. (Parinov and Sundaresan, 2000). Alonso *et al* (2003) report on a large scale insertional mutagenesis of *Arabidopsis* creating "over 225000 independent T-DNA insertion events that represent near saturation of the gene space, which resulted in the identification of mutations in more than 21700 of the 29454 predicted *Arabidopsis* genes".

Loss-of-function screens can rarely be used to identify genes that act redundantly, or in situations such as where the loss of function results in early lethality of the mutant. Both loss-of-function mutations and gain-of-function mutations can be created by T-DNA insertions. The latter is a means to identify genes that act redundantly, or genes whose inactivation may be lethal to the plant. Gain-of-function phenotypes can either be caused by mutations in the coding region that lead to constitutive activation of the resulting protein, or by mutations that alter levels or patterns of gene expression. The traditional way to induce the latter type of mutation has been through chromosomal rearrangements or transposons that bring genes under the control of new promoters or enhancers (Weigel *et al*, 2000 and references therein). A more directed way to induce such mutations was developed by constructing T-DNA vectors with four copies of an enhancer element from the constitutively active promoter of the cauliflower mosaic virus (CaMV) 35S gene

(Hayashi *et al*, 1992). These enhancers can cause transcriptional activation of nearby genes and, because activated genes will be associated with the T-DNA insertion, this approach has become known as 'activation tagging'. If the insertion event is into a gene then these activation tagging T-DNAs may also cause gene knock-outs or partial knock-outs. Recently Weigel and colleagues of the Salk Institute for Biological Studies, California, have generated several large sets of *Arabidopsis* plants transformed with activation-tagging vectors containing CaMV 35S enhancers (Weigel *et al*, 2000) and these are available for the research community to search for the presence of T-DNA inserts within specific genes of interest.

3.1.3 Objectives and experimental approach

The primary aim of my PhD project was to isolate and characterize the gene responsible for the *ppi* mutation. As mentioned earlier, research on the *ppi* mutant had been initiated in the Richard Hooley lab sometime before I joined it. The *ppi* mutant had been back-crossed twice to the wild-type (Ws-2) in order to remove any possible additional T-DNA insertions from the background. At this stage, PCR-based analyses had indicated the presence of T-DNA in *ppi* genome. This T-DNA insertion event was assumed to be the cause of the mutation.

From the preliminary genetics analyses it was observed that the mutation is recessive and is inherited as a monogenic character. This suggested that the activation-tagging vector had probably inserted within a gene creating a recessive mutation. The obvious strategy for determining the mutant locus was by plasmid rescue of genomic DNA (gDNA) flanking the insertion. For this, some understanding of T-DNA insertion presumably causing the mutation was required. Therefore, the initial step in my research was to characterize the T-DNA insertion event by Southern hybridization analyses. Once this was achieved, left border regions of the T-DNA insertion would be recovered by plasmid rescue to identify the gene locus.

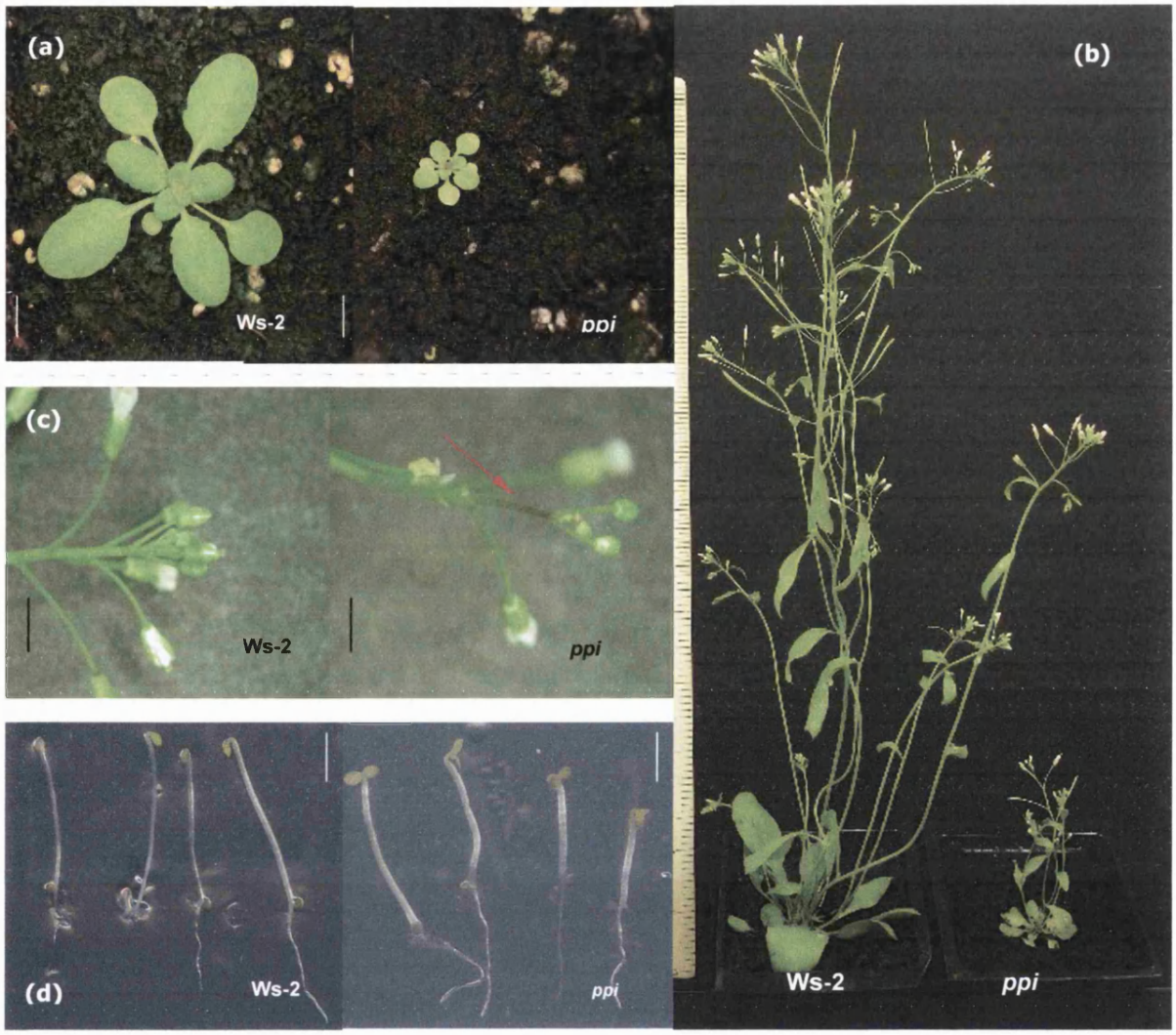

Fig.3.1: Pleiotropic phenotype of *ppi*

(a) to (c) Plants grown in controlled environment room (SANYO) on compost under long-day photoperiod (16 h light), at 23 ± 2 ^{0}C day- and 17.5 ± 2^{0}C night temperatures : (a) 12-day old plants (b) 35-day old plants (c) primary inflorescences of 35-day old plants. Pigmented zone in *ppi* inflorescence marked with the red arrow.
(d) 3-day old seedlings grown on nutrient agar in the dark. *ppi* seedlings are partially de-etiolated.
bars= 1 cm

3.2 Results

All studies reported in this chapter were done on two lines, namely, *p9* and *p11* which are siblings from a single mutant *ppi* parent, originated from the twice back-crossed line obtained from the Richard Hooley lab.

3.2.1. Characterization of the T-DNA insertion by Southern hybridisation analysis revealed a complex insertion event of ~ 30 kb, with several T-DNAs together with regions of vector DNA in between.

The Wisconsin β population of mutants was generated using the activation tag vector pSKI015 (Fig.3.2a & Fig.3.2b). The vector is 10138 bp in total and it confers resistance to the herbicide Basta (glufosinate ammonium, also called phosphoinothricin) because it contains the *BAR* gene. This allows herbicide selection in soil or agar medium PCR analysis of the *ppi* genome by Dr. Kanyuka had indicated the presence of a T-DNA insertion event. The first part of my research was to characterize the T-DNA.

T-DNA insertion was partially characterized by Southern hybridisation analysis. DNA extracted from *p9* or *p11* (from pooled plant material obtained from seedlings grown on nutrient agar) were subjected to either single digestions with *Eco*RI, *Bam*HI, *Hin*dIII or double digestions with *Eco*RI/*Bam*HI, *Eco*RI/*Hin*dIII and *Hin*dIII/*Bam*HI, and were capillary blotted on to nylon membrane. Two T-DNA specific, digoxigenin(DIG)-dUTP-labelled probes, Basta and 35S, that binds to the Basta and CaMV 35S promoter enhancer regions of the vector were used to detect the DNA fragments containing one or both of the regions. See Table 3.1 for primer details and Fig. 3.2b for primer positions in the T-DNA sequence.

Analysis of several Southern blots (Fig.3.3a) and by determining possible combinations of fragment lengths hybridizing with the probes suggested a complex insertion event of about 30 kb. It was possible to predict the structure of the insertion to consist of at least four T-DNA left border (LB) to right border (RB) regions integrated with tandem and inverted repeats and also a ~ 3.5 kb region of plant genomic or vector (V) DNA between one RB-LB junction (Fig.3.3b). The fragments observed particularly with the single or double digests including *Hin*dIII indicated the presence of a *Hin*dIII site in this non-T-DNA region. In fact, the pSKI015 vector sequence (that is, excluding the 6742 bp T-DNA) is

3396 bp in length and has a *Hin*dIII site at 2838 bp from the RB. Therefore it is most likely the vector sequence of ~2.8 to3.4 kb is in the RB-BL junction. It was possible to identify most of the fragments of DNA hybridizing with Basta and/or 35S probes with the proposed structure –LB--RB[V]LB--RBRB--LBLB--RB- (Fig.3.3c & d). The few fragments in the Southern blots that could not be assigned to a specific location in the proposed structure could be fragments cutting into the flanking plant genomic DNA from either side of the insertion. Depending on the number of restriction sites present in the region of the genome we could obtain more than one such fragment for a particular digestion.

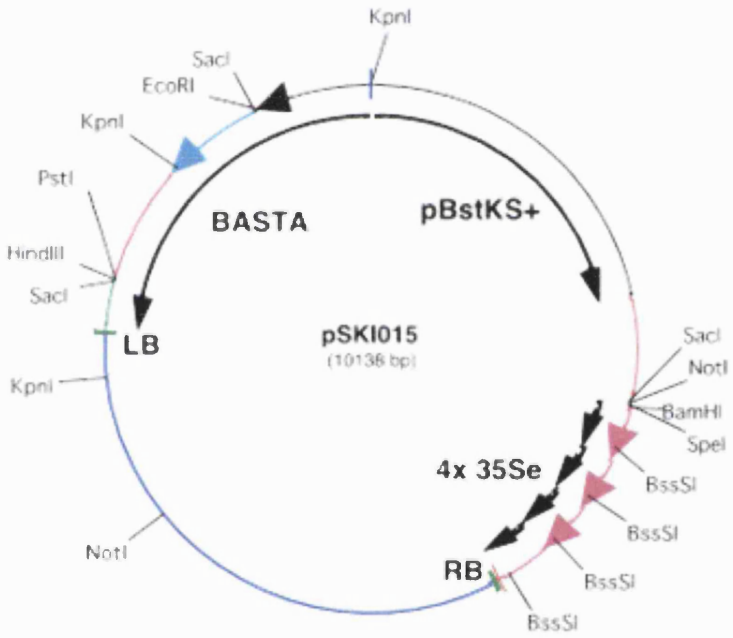

Fig.3.2a: Activation tagging vector pSKI015 map

The pSKI0115 vector (GenBank accession AF187951) constructed at the Weigel lab. The vector contains four repeats of CaMV 35S promoter enhancer regions. Herbicide Basta resistance is conferred by the BAR gene. Sites leaving the pBstKS+ sequences intact cutting only on one side between the pBstKS+ and either the left or right border can be used for plasmid rescue. Plasmid rescue in *E.coli* is ampicillin resistance.
(Figure taken from Weigel *et al*, 2000)

pSKI015 LB to RB integrated DNA

```
LB      1  GGGGCAGCGG CGGCAGGATA TATTCAATTG TAAATGGCTT CATGTCCGGG
      51  AAATCTACAT GGATCAGCAA TGAGTATGAT GGTCAATATG GAGGAAAAGA
     101  AAGAGTAATT ACCAATTTTT TTTCAATTCA AAAATGTAGA TGTCCGCAGC
     151  GTTATTATAA AATGAAAGTA CATTTTGATA AAACGACAAA TTACGATCCG
     201  TCGTATTTAT AGGCGAAAGC AATAAACAAA TTATTCTAAT TCGGAAATCT
     251  TTATTTCGAC GTGTCTACAT TCACGTCCAA ATGGGGGCTT AGATGAGAAA
     301  CTTCACGATC GATATCTAGA TCTCGAGCTC GAGATCTAGA TATCGATAAG
     351  CTTGCATGCC TGCAGGTCCT GCTGAGCCTC GACATGTTGT CGCAAAATTC
     401  GCCCTGGACC CGCCCAACGA TTTGTCGTCA CTGTCAAGGT TTGACCTGCA  SKC12
     451  CTTCATTTGG GGCCCACATA CACCAAAAAA ATGCTGCATA ATTCTCGGGG
     501  CAGCAAGTCG GTTACCCGGC CGCCGTGCTG GACCGGGTTG AATGGTGCCC
     551  GTAACTTTCG GTAGAGCGGA CGGCCAATAC TCAACTTCAA GGAATCTCAC
     601  CCATGCGCGC CGGCGGGGAA CCGGAGTTCC CTTCAGTGAA CGTTATTAGT
     651  TCGCCGCTCG GTGTGTCGTA GATACTAGCC CCTGGGGCCT TTTGAAATTT
     701  GAATAAGATT TATGTAATCA GTCTTTTAGG TTTGACCGGT TCTGCCGCTT
     751  TTTTTAAAAT TGGATTTGTA ATAATAAAAC GCAATTGTTT GTTATTGTGG
     801  CGCTCTATCA TAGATGTCGC TATAAACCTA TTCAGCACAA TATATTGTTT
     851  TCATTTTAAT ATTGTACATA TAAGTAGTAG GGTACAATCA GTAAATTGAA
     901  CGGAGAATAT TATTCATAAA AATACGATAG TAACGGGTGA TATATTCATT
     951  AGAATGAACC GAAACCGGCG GTAAGGATCT GAGCTACACA TGCTCAGGTT  Basta F
    1001  TTTTACAACG TGCACAACAG AATTGAAAGC AAATATCATG CGATCATAGG
    1051  CGTCTCGCAT ATCTCATTAA AGCAGGACTC TAGGATCGAT CCCCCGGGTC  Basta TGA
    1101  ATCACATCTC GGTGACGGGC AGGACCGGAC GGGGCGGTAC CGGCAGGCTG
    1151  AAGTCCAGCT GCCAGAAACC CACGTCATGC CAGTTCCCGT GCTTGAAGCC
    1201  GGCCGCCCGC AGCATGCCGC GGGGGGCATA TCCGAGCGCC TCGTGCATGC
    1251  GCACGCTCGG GTCGTTGGGC AGCCCGATGA CAGCGACCAC GCTCTTGAAG
    1301  CCCTGTGCCT CCAGGGACTT CAGCAGGTGG GTGTAGAGCG TGGAGCCCAG
    1351  TCCCGTCCGC TGGTGGCGGG GGGAGACGTA CACGGTTGAC TCGGCCGTCC
    1401  AGTCGTAGGC GTTGCGTGCC TTCCAGGGGC CCGCGTAGGC GATGCCGGCG
    1451  ACCTCGCCGT CCACCTCGGC GACGAGCCAG GGATAGCGCT CCCGCAGACG
    1501  GACGAGGTCG TCCGTCCACT CCTGCGGTTC CTGCGGCTCG GTACGGAAGT
    1551  TGACCGTGCT TGTCTCGATG TAGTGGTTGA CGATGGTGCA GACCGCCGGC
    1601  ATGTCCGCCT CGGTGGCACG GCGGATGTCG GCCGGGCGTC GTTCTGGGCT
    1651  CATGGTAATT GTAAATAGTA ATTGTAATGT TGTTGTTGTT TGTTGTTGTT  Basta ATG
    1701  GGTAATTGTT GTAAAAATAG AGCTCTTATA CTCGAGGAAT TCGCTAGAGT
    1751  CGATTTGGTG TATCGAGATT GGTTATGAAA TTCAGATGCT AGTGTAATGT
    1801  ATTGGTAATT TGGGAAGATA TAATAGGAAG CAAGGCTATT TATCCATTTC
    1851  TGAAAAGGCG AAATGGCGTC ACCGCGAGCG TCACGCGCAT TCCGTTCTTG  Basta R
    1901  CTGTAAAGCG TTGTTTGGTA CACTTTTGAC TAGCGAGGCT TGGCGTGTCA
    1951  GCGTATCTAT TCAAAAGTCG TTAATGGCTG CGGATCAAGA AAAAGTTGGA
    2001  ATAGAAACAG AATACCCGCG AAATTCAGGC CCGGTTGCCA TGTCCTACAC
    2051  GCCGAAATAA ACGACCAAAT TAGTAGAAAA ATAAAAACTG ACTCGGATAC
    2101  TTACGTCACG TCTTGCGCAC TGATTTGAAA AATCTCAATA TAAACAAAGA
    2151  CGGCCACAAG AAAAAACCAA AACACCGATA TTCATTAATC TTATCTAGTT
    2201  TCTCAAAAAA ATTCATATCT TCCACACGTG AAAATGCCAA TTTCTCAGAC
    2251  CTACCTCGGC TCTGCGAAGG CCCCCGCTGG TATCAAAAGT TTTTATTTCA
    2301  TCCGACATGG CGCGACCGAC CTCAACGAGA AGGAAATTGT CGTGAACGGT
    2351  GAGAAGCTCT GGGGCGTGCA AGGTTCCGGA ACGAACATCG GTCTCAATGC
    2401  AAAAGGGGAA CGCCAGGCTC TGTTGGCCCC TCGAGGGGGG GCCCGGTACC
    2451  AGCTTTTGTT CCCTTTAGTG AGGGTTAATT CCGAGCTTGG CGTAATCATG
    2501  GTCATAGCTG TTTCCTGTGT GAAATTGTTA TCCGCTCACA ATTCCACACA
    2551  ACATACGAGC CGGAAGCATA AAGTGTAAAG CCTGGGGTGC CTAATGAGTG
    2601  AGCTAACTCA CATTAATTGC GTTGCGCTCA CTGCCCGCTT TCCAGTCGGG
    2651  AAACCTGTCG TGCCAGCTGC ATTAATGAAT CGGCCAACGC GCGGGGAGAG
    2701  GCGGTTTGCG TATTGGGCGC TCTTCCGCTT CCTCGCTCAC TGACTCGCTG
    2751  CGCTCGGTCG TTCGGCTGCG GCGAGCGGTA TCAGCTCACT CAAAGGCGGT
    2801  AATACGGTTA TCCACAGAAT CAGGGGATAA CGCAGGAAAG AACATGTGAG
    2851  CAAAAGGCCA GCAAAAGGCC AGGAACCGTA AAAAGGCCGC GTTGCTGGCG
    2901  TTTTTCCATA GGCTCCGCCC CCCTGACGAG CATCACAAAA ATCGACGCTC
    2951  AAGTCAGAGG TGGCGAAACC CGACAGGACT ATAAAGATAC CAGGCGTTTC
    3001  CCCCTGGAAG CTCCCTCGTG CGCTCTCCTG TTCCGACCCT GCCGCTTACC
    3051  GGATACCTGT CCGCCTTTCT CCCTTCGGGA AGCGTGGCGC TTTCTCATAG
    3101  CTCACGCTGT AGGTATCTCA GTTCGGTGTA GGTCGTTCGC TCCAAGCTGG
    3151  GCTGTGTGCA CGAACCCCCC GTTCAGCCCG ACCGCTGCGC CTTATCCGGT
    3201  AACTATCGTC TTGAGTCCAA CCCGGTAAGA CACGACTTAT CGCCACTGGC
    3251  AGCAGCCACT GGTAACAGGA TTAGCAGAGC GAGGTATGTA GGCGGTGCTA
    3301  CAGAGTTCTT GAAGTGGTGG CCTAACTACG GCTACACTAG AAGGACAGTA
    3351  TTTGGTATCT GCGCTCTGCT GAAGCCAGTT ACCTTCGGAA AAAGAGTTGG
    3401  TAGCTCTTGA TCCGGCAAAC AAACCACCGC TGGTAGCGGT GGTTTTTTTG
    3451  TTTGCAAGCA GCAGATTACG CGCAGAAAAA AAGGATCTCA AGAAGATCCT
    3501  TTGATCTTTT CTACGGGGTC TGACGCTCAG TGGAACGAAA ACTCACGTTA
    3551  AGGGATTTTG GTCATGAGAT TATCAAAAAG GATCTTCACC TAGATCCTTT
    3601  TAAATTAAAA ATGAAGTTTT AAATCAATCT AAAGTATATA TGAGTAAACT
    3651  TGGTCTGACA GTTACCAATG CTTAATCAGT GAGGCACCTA TCTCAGCGAT
    3701  CTGTCTATTT CGTTCATCCA TAGTTGCCTG ACTCCCCGTC GTGTAGATAA
    3751  CTACGATACG GGAGGGCTTA CCATCTGGCC CCAGTGCTGC AATGATACCG
    3801  CGAGACCCAC GCTCACCGGC TCCAGATTTA TCAGCAATAA ACCAGCCAGC
    3851  CGGAAGGGCC GAGCGCAGAA GTGGTCCTGC AACTTTATCC GCCTCCATCC
```

Fig.3.2b: Activation tagging vector pSKI015 LB to RB integrated sequence.

The Basta and CaMV 35S regions and primer positions are indicated. The pSKI0115 vector (GenBank accession AF187951) sequence obtained from MIPS data base.

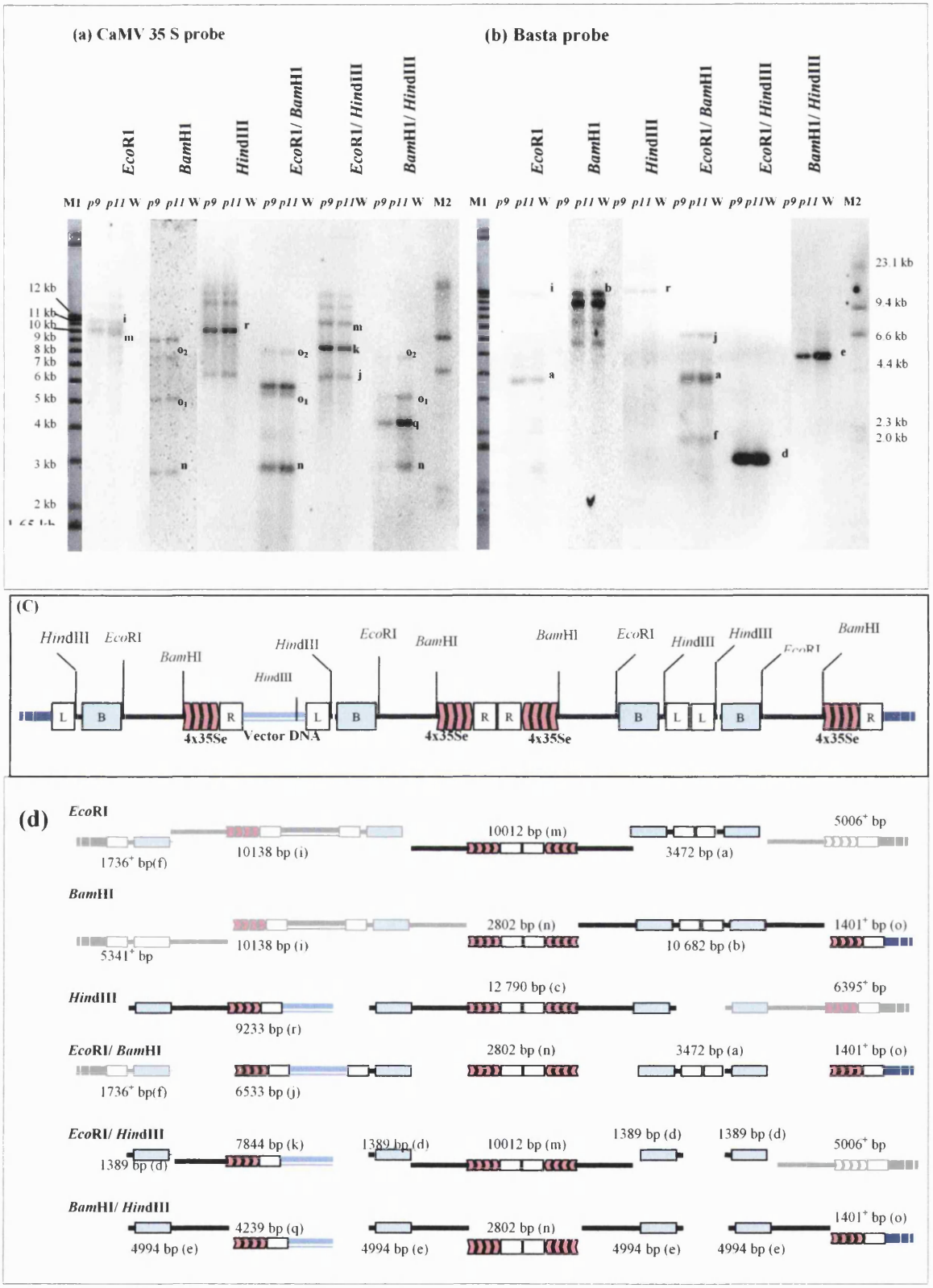

Fig.3.3: Southern hybridization analysis and the proposed structure of the complex T-DNA insertion event.

(a) & (b) are composite images from 3 Southern blots showing bands hybridising to 35S (a) and Basta (b) probes. The identified bands are given a letter a-o. The proposed complex insertion with 4 x T-DNA regions is given in (c). The identified and the predicted bands from each restriction in relation to the proposed structure is given in (d). Fragments in full colour are the ones that could be identified and confirmed by the size in the blots. The fragments shown in pale colour could be observed only in some blots, probably due to sensitivity of the detection method. Some predicted fragments (in grey) could not be identified based on their size as these could probably be the bands cutting into the genomic DNA.

M1 and M2 are DNA molecular length markers.

Table 3.1 Primers used in the experiments reported in this chapter.

Primer name	Primer sequence	T_m °C
Primers used to prepare DIG-labelled BASTA probe		
Basta R	5' AAACCGGCGGTAAGGATCT 3'	60.9
Basta F	5' AAGAACGGAATGCGCGTGA 3'	65.3
Primers used to prepare DIG-labelled CaMV 35S probe		
35S R	5' TCCATCTTTGGGACCACTGT 3'	60.4
35S F	5' CGAGGAACATCGTGGAAAAA 3'	61.1
Primers used to prepare DIG-labelled GCR1 probe		61.4
GCR1-ATG	5' ATGTCGGCGGTTCTCACA 3'	54.5
GCR1-TGA	5' TCATTGCTGGTCCTCGGTCTT 3'	
Primers used for PCR analysis of the location of T-DNA insertion		
For *GCR1* gene promoter region		
401_ up	5' TATACAAAGAGTGAGGACACGAGAAGCAATATGT 3'	68.1
401_ down	5' GAATAAGTCTAAGTGGCATTGCTATCTTGTTGAG 3'	67.3
For *GCR1* gene coding region		
1142_ up	5' GGTTCTGGTGAATCTTGTTGAGATTATTTTGATA 3'	67.3
1142 _down	5' TCAGTAACGTTTGTGAACTACTTTCAGAAGACAA 3'	67.5
pSKI015 vector specific primers		
SKC12	5' TTGACAGTGACGACAAATCG 3'	58.2
T7	5' TAATACGACTCACTATAGGG 3'	46.7

Primers were designed with the help of online primer design software, Primer3 (http://www.genome.wi.mit.edu/cgi-bin/primer/primer3.cgi/primer3_www.cgi).

T_ms were determined at http://alces.med.umn.edu/rawtm.html using primer concentrations 50nM and 52mM salt.

3.2.2. Plasmid rescue of DNA flanking the T-DNA insertion identified an insertion event in the second intron of the gene At1g48270, *GCR1*.

With the proposed ~30 kb complex insertion, it was feared that the complexity of the insertion might affect the success of plasmid rescue of flanking plant genomic DNA. However, provided that at least one anchoring T-DNA sequence exists near a genomic DNA junction, it could be possible to obtain insertion flanking sequences for cloning tagged genes, no matter whether the insertions are single or concatameric (Liu *et al*, 1995). Therefore, it was decided at this point not to follow up the characterisation of the T-DNA insertion, but to proceed with plasmid rescue of adjacent plant DNA, because the proposed T-DNA insertion had at least one left or right border near plant genomic DNA.

The plasmid sequences in pSKI015 are flanked by several restriction sites that can be used for the rescue of T-DNA and adjacent plant sequences from transformed plants. Restriction enzyme sites that leave the pBstKS+ sequences intact and cut only on one side between pBstKS+ and either left or right border can be used for plasmid rescue. Plasmid selection in *E. coli* and in *A. tumefaciens* is through Ampicillin resistance (Weigel *et al*, 2000). Fig.3.4 illustrates the steps involved in a plasmid rescue experiment.

The restriction enzymes *Bam*HI, *Spe*I and *Not*I were used for rescue of plasmids across the left T-DNA border containing plant genomic sequences adjacent to it.
Genomic DNA from *p9* and *p11* plants were separately digested with restriction enzymes *Bam*HI, *Spe*I and *Not*I, re-ligated using T4 DNA ligase (NEB) and used to transform *E.coli* SURE® electroporation competent cells. In a single transformation experiment, ten ampicillin resistant colonies were recovered. *Not*1 digests of *p9* and *p11* gDNA yielded three and five colonies respectively. A single colony was obtained for each of the *Spe*1 and *Bam*H1 digests of *p11* gDNA.
Plasmid DNA was purified from the overnight cultures from each of the 10 colonies. Restriction of the purified plasmid DNA with *Not*1, *Spe*1 and *Bam*H1 or combinations *Not*1/ *Hin*dIII, *Spe*1/ *Hin*dIII and *Bam*H1/ *Hin*dIII double digests of purified plasmid DNA, it was indicated that the 10 colonies consisted of only three types of plasmid clones depending on the endonuclease used in the digestion (Fig.3.5).

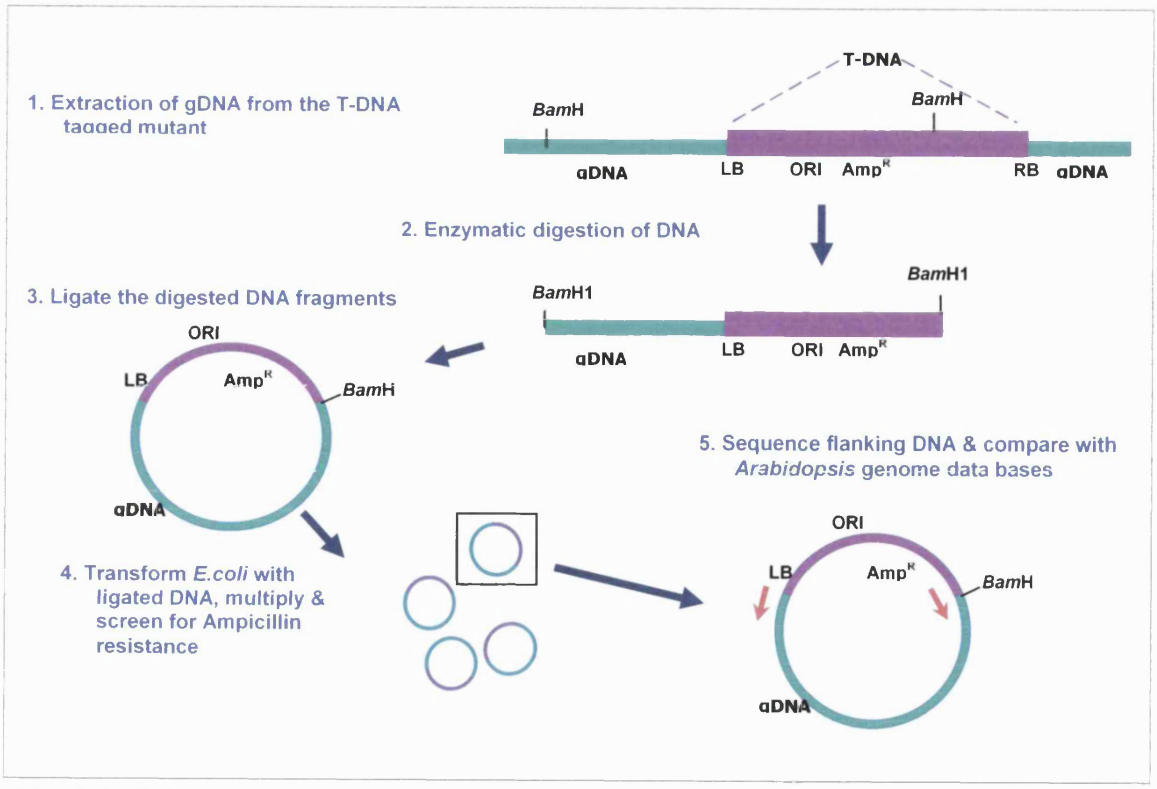

Fig. 3.4: Schematic representation of steps involved in a plasmid rescue experiment and sequencing flanking DNA

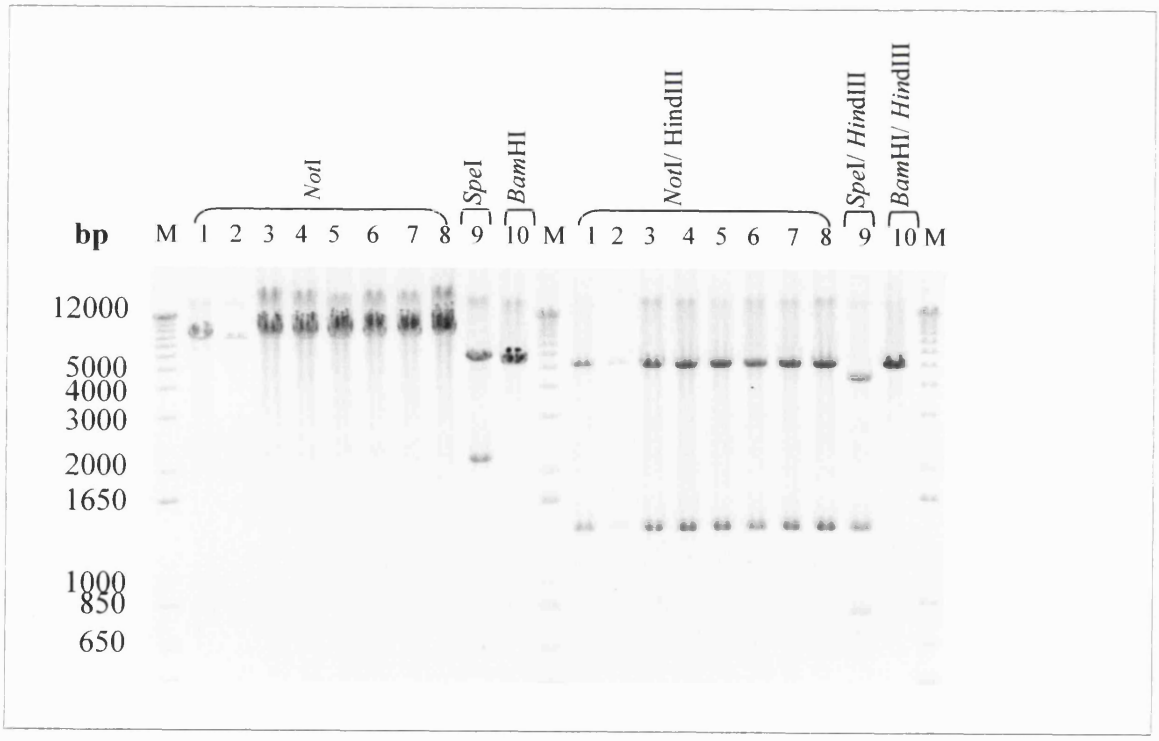

Fig.3.5: Restriction endonuclease digestion of rescued plasmids

Plasmids purified from overnight cultures of ampicillin resistant *E.coli* transformants were restricted with the enzymes used in the plasmid rescue or their combinations. # 1-10 are the ten colonies; M= DNA length marker.

Ten plasmid DNA samples representing the three types of the clones were sequenced in 6 ul reactions containing 300 ng pDNA and 5 pmoles of primer. Two vector specific primers, namely SKC12 and T7 were used to sequence the plasmids on both strands. Sequences obtained with SKC12 primer for the plasmids of the *Not*I (named S1 to S3) digests and *Spe*I (S4) digests were repeatedly unreadable. But, the SKC12 on the plasmid *Bam*HI digest (S5) gave a high quality, readable sequence . With the T7 primer, all *Not*I (S6 to S8), *Spe*I (S9) and *Bam*HI (S10) digests also gave high quality sequences. All the sequences were analysed by homology searching with Blastn for potential plant genomic DNA.

S6 sequence was 973 nt in length. Region 476 nt to 503 nt had high homology to pSKI015 vector sequences just upstream of the *Bam*HI site in the vector. Sequences S7 to S9 all had this short homology to the vector and nothing else that is clearly vector sequence. Blastn searches of these sequences did not reveal any homologies better than 60-70% against *Arabidopsis* genome.

S5 (i.e, the sequence obtained with the SKC12 primer for the plasmid from *Bam*H1 digest) gave a 1001 nt sequence. In this, region 16nt to 404nt is just upstream of the SKC12 primer site to the point of the left border sequence in the vector. Region 475 nt to 674 nt and beyond run from *Bam*HI site into the vector.

VecScreen (http://www.ncbi.nlm.nih.gov/VecScreen/VecScreen.html) of sequence showed the region from 404 nt to 474 nt did not contain vector sequences while the other parts did and could be plant genomic DNA. This region is identical to a region of the same size in the sequence S10 (i.e the T7 sequence of *Bam*H1 digest).

Blastn search of AGI TAIR sequences including introns did not match to any with high (>90%) identity to any one *Arabidopsis* sequence indicating the possibility that the sequence is chimeric. Searching for short near identical matches from the NCBI Blast server yielded two sequences: the first, region from nt 21 to 42 was identified to be re-arranged vector sequence. The second, the region nt 53 to 70 is 100% identical to *GCR1 (G-PROTEIN COUPLED RECEPTOR 1)*, At1g48270. This region is in intron 2 near to the exon 3 boundary of *GCR1*.

The LB region is at the 53rd nt position on the S5 sequence and pointing in the right direction to be rescued as observed. Also, just beyond the nt70 of S5 is a *Bam*H1 site in the *GCR1* sequence that would have produced the fragment and the S5 sequence was identical to *GCR1* through this region should be extended to 77 nt.The origin of the remaining nts 1 to 52 that are between the LB region and the area of identity to *GCR1* was not clear.

VecScreen was repeated by searching with just the 70nt region in case it contains any re-arranged vector sequence. A portion of the sequence did contain vector like sequence. This motif is present in the pSK1015 sequence just upstream from the LB region Visual search for potential re-arranged vector sequences confirmed that part of the 77nt region of S5 may be re-arranged vector sequence.

The 77nt sequence of S5 that could contain gDNA:

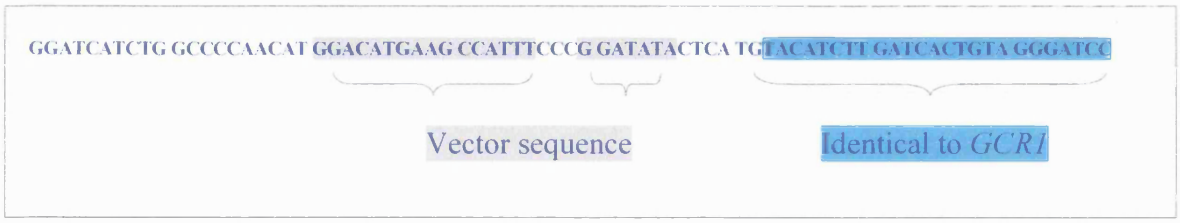

In conclusion, sequence analysis of the LB regions rescued by *Not*1 and *Spe*1 digests did not reveal any significant sequence similarity to *Arabidopsis* genome sequences. However, the plasmids rescued by *Bam*H1 revealed a 24 nt region that is 100% identical to *Arabidopsis* genomic DNA. This identified an insertion event in the second intron of the gene At1g48270, *GCR1* (Fig.3.6).

```
   1  ccataaaatt tcaatgtatg aagataattc ataattgctg tactaattaa
  51  atttatgtat ttttgtgtgg attgacaaat tcgtctgttt ggtttttgta
 101  cgtttgttgc catttagtag atgatatgtc attgggtaaa ttagcacacg
 151  aaaatcattt aatatatata ataaacagtc attataacat gtatacgtaa
 201  attatattac gaattgtgat aagtctagcc acggggttta cgaccaaaag
 251  caatacataa ataataatca gggagatcca tgaacttata tatacaaaga
 301  gtgaggacac>gagaagcaat>atgtgtcaat gtgtggaaga atgtctccat
 351  cattaaccta attatattat attttatgtt ttataatttt tatggtcttc
 401  tccgcttggt agttttagcc ttacagccat taactatcgt aaattagggt
 451  actaatactt gttatttttt ttggtaaaag gtgaaatttt atactatttt
 501  tagtttgtga tagaattaca gagaaaacta gaaacagatt aaagcaatct
 551  acgtaaatat aaaaacaaca ttacaactca agatgcaaag gatcactact
 601  aagtggtcaa agccaaattg caaaaagaaa caccgattcc gaacccgcga
 651  agctcagaaa attgtgtggt tgccacaaaa accgaagaac tggaatcatc
 701  atcttaattg caccgagcaa actatccaag atccgtccac aaaacttcaa
 751  gatagaagtc tacaacttct ctgagaacta acgcaaaaac gtaaaagcaa
 801  tcgtggactt ctatactaac<tcaacaagat<agcaatgcca<cttagactta
 851  ttcgccgcct ctattcaaca ttctgacaac ctagccaatg ctcgttattt
 901  gcttattatt agttcttacg tacgtgtttt atattcgttt tgaaaaacaa
 951  ataattgtcg ttaataatca gctaataaat gacgtataaa tttatgactt
1001  gcaagtacaa gcttgttata tatattactt gcttatatat aacttatttt
1051  tatttgaatg ttttgtgctt aggatgcttg aaactttgaa tgttttgtaa
1101  tttctattgt atatgagatt ttttttcgat tcaagttgca attattttac
1151  aagtaacaag caatatcaaa ttatttagca agtaataagc caaatcaagt
1201  tatttagcaa ataatcatat tttatatgtt ataacaagtc caaaattcat
1251  ttacttgaaa ggggcaaaac gggtcagaag gccatgctag gtatttttgt
1301  gctcggtgat tgatagtata gtcgtgtaga taatttattt aaaaacaata
1351  gtatacataa tttgttataa tattatatat atatatatat atatatatat
1401  ttatttttat atagagtata ctataaataa gattaattat aaaattaaat
1451  agtataatat ttacatgtgc ataacataag ttattaccta gtataattta
1501  aatattcata catgtataaa attaaaattt tccaaaaata tgtgataact
1551  tgacatgtaa ataacatcat ataaatgttt ttaataatta atatagcata
1601  tatgaattaa tgcttaacaa aatcattggg ctgggcctaa agaagtgcac
1651  tacgaggagt ccggttcaaa agacacgact tgacccgacc gatccgaccc
1701  gggtaagagg ttagcccacc acgcaacgtc cgtcggggaa gataccacgc
```

401_up primer

401_down primer

Fig.3.6: *GCR1* gene sequence showing the position of the T-DNA insertion

The S5 sequence is highlighted. The matching regions of the two sequences are aligned inside the smaller rectangle. Initiating ATG codon is at nucleotide 1826. Exons are in capitals, introns in lower case.

The positions of the 401_up/down primers in the *GCR1* promoter region and 1142_up/down primers in the coding region, are also marked.

3.2.3 The approximate location of the T-DNA in *GCR1* was confirmed by PCR

Parallel to the plasmid rescue experiments, a series of PCRs and Southern blots were performed by the MRes student Lihua Zhang as her research project, under my day-to-day supervision, to find the approximate location of the insertion.
The PCRs were performed with DNA extracted from 22 individual *ppi* mutants from the *p9* line and 24 from the *p11* line.
Initially, Basta F and Basta R primers (Table 3.1) were used to amplify a 938 bp fragment from Basta region in the T-DNA. It was expected all the *ppi* plants to test positive as the mutation was assumed to be due a T-DNA insertion. Although most of the plants resulted positive, to my surprise, some samples did not give a band. As a positive control, another PCR using 401_up and 401_down primers (Table 3.1 for primer details) was performed to amplify a 568 bp fragment from the promoter region of the *GCR1*, where there is no predicted insertion event. All *ppi* plants tested positive, suggesting that some *ppi* may not contain a T-DNA or, at least, the part of T-DNA containing the Basta region. Since the *ppi* mutant has been originally identified in a pool of plants containing a T-DNA insertion event in the *GCR1*, a pair of *GCR1* specific primers, 1142_up and 1142_down, were used to amplify a 735 bp region from the gene. Absence of the PCR product would indicate the gene has been disrupted probably due to a large insertion event. All the samples tested negative for this had been positive for the Basta region in the previous PCR. However, a few other were positive for both the *GCR1* specific 1142 up and 1142 down primers and T-DNA specific Basta primers, indicating two possibilities: either these plants are heterozygous for the T-DNA (as judged by the presence of Basta region) in *GCR1*, or there could be a T-DNA elsewhere in the genome. The location of the insertion to be the *GCR1* was confirmed by a PCR with a *GCR1* specific 1142_down primer and T-DNA LB specific SKC12 primer combination. All the plants that were positive for the Basta region gave the expected 1.1 kb product suggesting T-DNA LB region to be in the second intron of *GCR1*, near to the exon 3 boundary. This observation was in agreement with the plasmid rescue results mentioned in section 3.2.1.

From combined results of the PCRs (Fig.3.7a), it was shown that there were three groups of *ppi* population used in this studies reported here: group A (7 out of total 46) did not contain a T-DNA insertion in *GCR1* as judged by the PCR amplification of fragments from the T-DNA Basta region and the presence of LB region in the *GCR1* second intron. Negative results obtained for the plants of this group with PCR primers specific to the CaMV 35S region

(Fig.3.7b) in the T-DNA confirmed those plants do not have T-DNA insertion anywhere in the genome as judged by PCR amplification of fragments from Basta or 35S regions. Second group (B) of plants (30/46) are homozygous for a T-DNA insertion in the *GCR1* gene. The third group (C) of plants (9/46) are heterozygous for the T-DNA insertion in the *GCR1* gene.

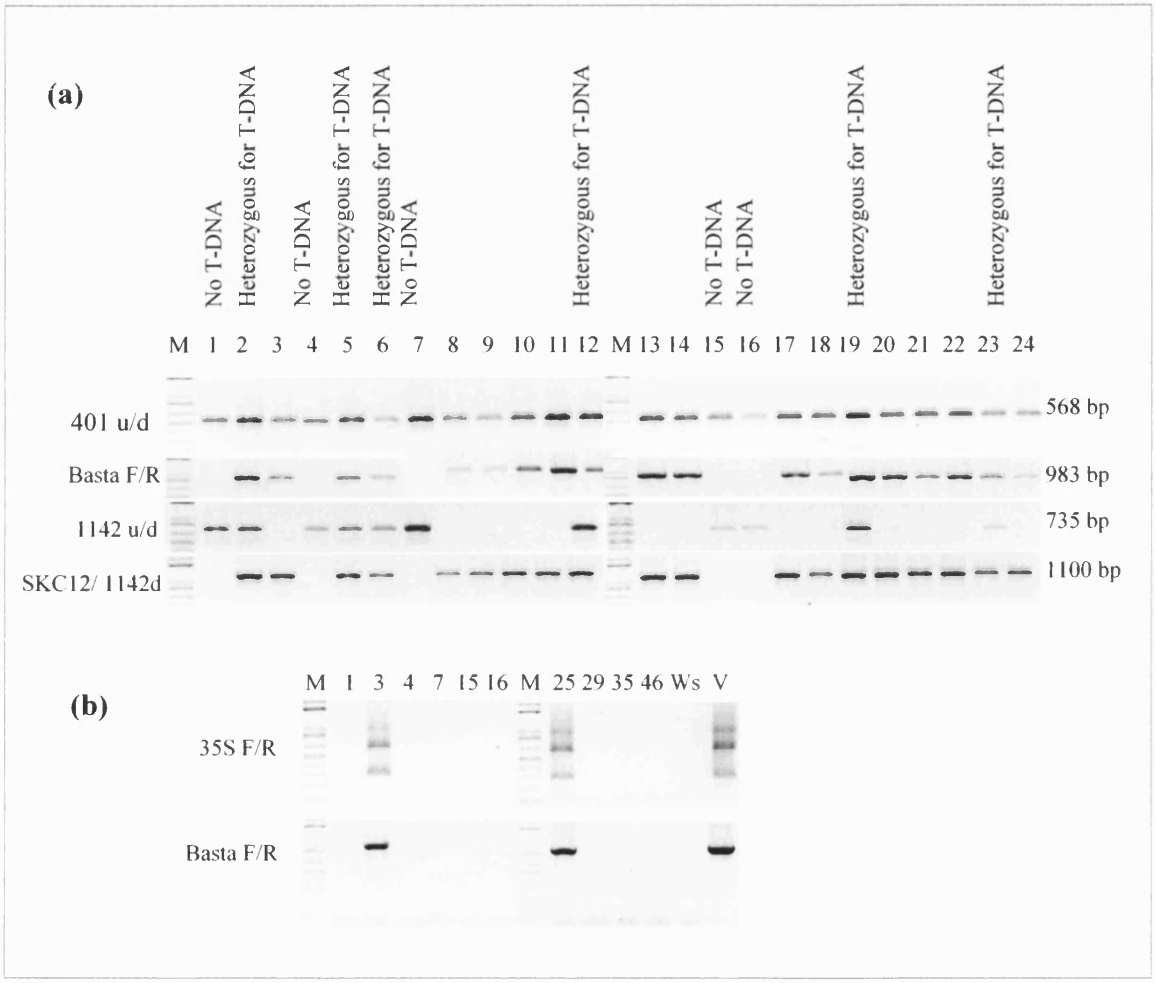

Fig.3.7: The *ppi* population was not homogenous with respect to the presence of a T-DNA insertion.
Agarose gel-electrophoresis of PCR amplified DNA fragments from individual *ppi* plants (#1-25, 29, 35 & 46) and Ws-2 using gene specific and/or T-DNA specific primers.
401_up & 401_down primer pair amplifies a 568 bp region in the *GCR1* promoter region. 1142_up and 1142_down primer pair amplifies a region of 735 bp between intron 1 and intron 6 of *GCR1*. Basta F and Basta R primer pair amplifies a 983 bp fragments from the T-DNA Basta region. SKC12 T-DNA LB specific primer and 1142_down primer would amplify a 1.1 kb fragment if a T-DNA LB is present in *GCR1*.
(a) Combined results of the PCRs indicated three groups of plants in the *ppi* population studied, with respect to presence or absence of a T-DNA in *GCR1*. Plants #1,4,7,15,16,29,35 & 46 did not have a T-DNA in *GCR1* (Group A). Plants #3,8-11, 13, 14,17,18, 20-22 & 24 were homozygous for a T-DNA in the *GCR1* (Group B). Plants # 2,5,6,12,19 & 23 were heterozygous for a T-DNA in *GCR1* (Group C).
(b) Group A *ppi* plants did not have a T-DNA insertion anywhere in the genome as judged by the negative results for PCR amplification of both CaMV 35S and Basta regions from T-DNA.
M= DNA molecular weight markers; V= Vector

3.2.4 Southern hybridization analyses confirmed some *ppi* plants lacking a T-DNA insertion anywhere in the genome.

To confirm the findings reported in the previous section, a series of Southern hybridizations were performed on gDNA extracted from individual *ppi* plants representing the three groups. Initially, the DNA was digested with either *Eco*RI or *Bam*HI and Southern hybridized with DIG-labelled Basta and 35S probes to detect DNA fragments containing regions from the T-DNA insertion (Fig.3.8a & b) Group A plants as well as the wild-type (Ws-2) did not give any band hybridizing with either the Basta or the 35S probe. Group B and C gave similar band patterns indicating group B and C individuals to contain the same or very much similar T-DNA insertions. The results re-confirmed the absence of a T-DNA insertion in the genome of the group A plants as judged by the absence of Basta and 35S hybridizing DNA fragments.

GCR1 gene specific GCR1 probe was used to check the presence of a T-DNA in the gene. The genomic DNA was digested with *Eco*RI. In the group A *ppi* plants as well as in the wild-type (Ws-2), the probe hybridized with a ~8000 bp fragment indicating an intact *GCR1* (Fig. 3.8c), which is in agreement with a previous research on *GCR1* (Couch, D.,PhD thesis, 2001). For Group B, only two bands appeared, both were less than ~7000bp.
In the third group C, there were two bands hybridising with the probe, one ~8000 bp, of the same size as the band observed for group A and the other one as similar to the smaller band seen for Group B. This suggested that the group B homozygous for the T-DNA insertion event, and group C heterozygous for the same.

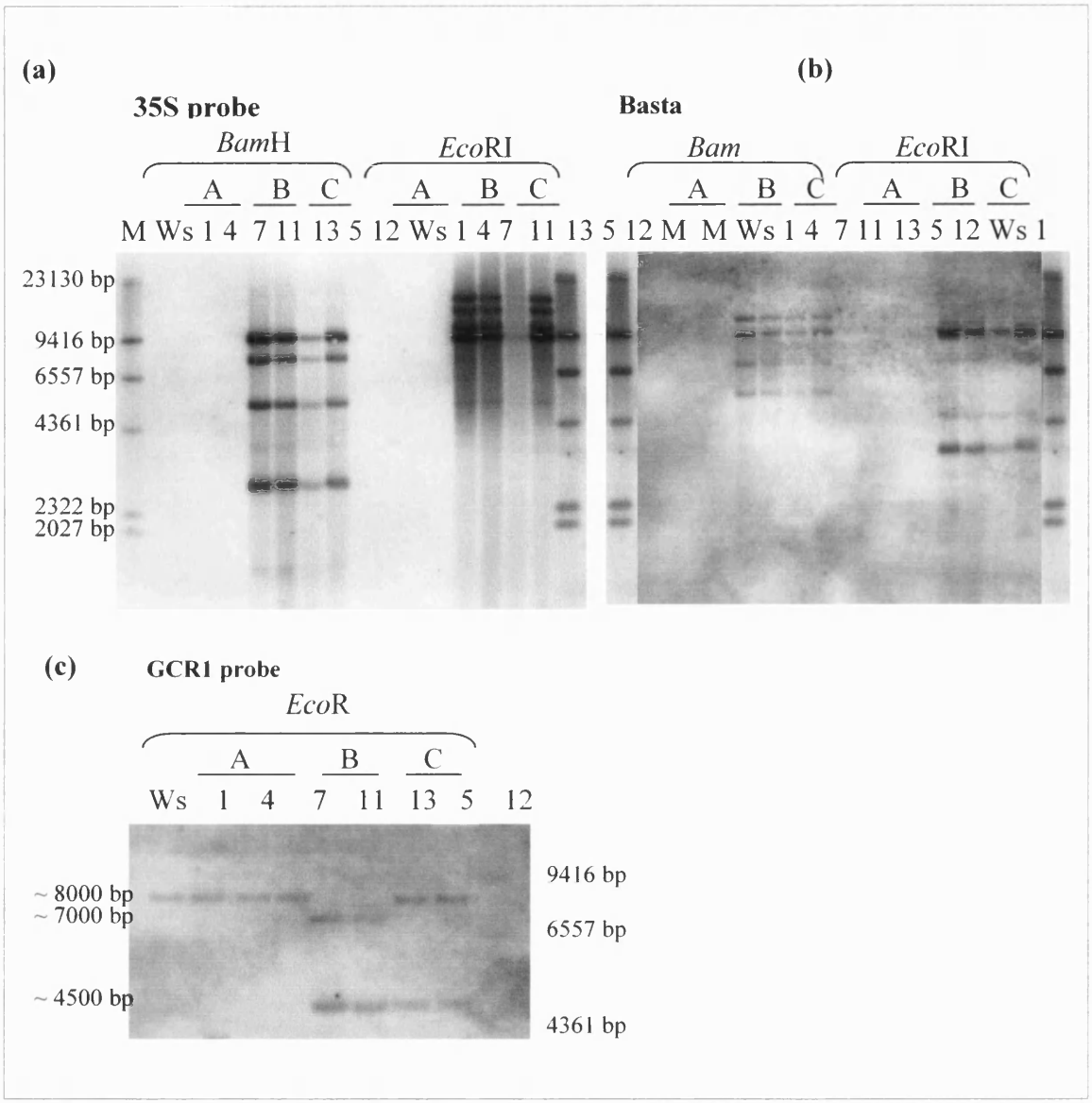

Fig.38: Southern hybridization analysis of DNA from individual *ppi* plants representing the three groups with respect to presence or absence of a T-DNA

Southern hybridization with T-DNA specific 35S (a) and Basta (b) probes and with *GCR1* gene specific GCR1 probe (c).

(a) & (b) The wild-type and Group A did not hybridize with either the 35S or the Basta probe indicating the absence of a T-DNA insertion in the genome.
Group B & C hybridized to both these probes indicating the same or very similar T-DNA insertion in the genome.
(c) The GCR1 probe hybridized to both wt and *ppi* group A DNA to give a single band at ~8 kb indicating an intact *GCR1* in *ppi* Group A. It gave 2 bands for Group B at ~7 kb and ~4.5 kb. With Group C it gave two bands, one similar in size to the 7 kb band of Group B, and the another band of ~8 kb similar to that of wt and Group A, indicating that the group C was heterozygous for a T-DNA in the *GCR1*

3.3 Discussion

3.3.1 The *ppi* mutation did not segregate with a T-DNA insertion

Characterization of the T-DNA insertion presumably causing the *ppi* mutation revealed a complex insertion event of approximately 30 kb. The proposed structure of the insert consisted of four tandem and some possibly inverted T-DNAs and an integrated vector DNA within. Successful cloning of mutant genes from complex T-DNA insertion events by plasmid rescue or other similar methods have been reported previously (McElver et al., 2000, Sanders et al., 2000, Stintzi and Browse, 2000). With the anticipated difficulties associated with complex insertion events, it was decided to proceed with plasmid rescue, mainly because the proposed structure predicted at least one anchoring T-DNA adjacent to plant genomic DNA. I identified a T-DNA insertion event by isolating LB flanking genomic DNA from the second intron of the *GCR1* (At1g48270).

The complex insertion detected by Southern blot analysis is in contrast to what has been reported on activation-tagging lines. Weigel et al., 2000 reports that "T-DNA insertions in activation-tagged mutants were never rearranged in such a way it was difficult to recover adjacent plant DNA by plasmid rescue or to determine structure of T-DNA, reflecting the fact that activation tagged phenotype requires productive interaction of enhancer sequences in the T-DNA with the adjacent plant sequences". However, such rearranged complex T-DNA insertions have been observed for many loss-of-function mutants T-DNA integrations often induces base substitutions, insertions, and small(<500bp) rearrangements, deletions or duplications at the insertions site, and chromosomal rearrangements, too, could be a common feature of T-DNA transformed plants (Nacry *et al*, 1998). Complex patterns of T-DNA integration, including transfer of vector sequences adjacent to T-DNA borders and the large frequency of concatemeric T-DNA insertions has shown to complicate further research on the T-DNA insertion event. In addition to those, small or major chromosomal rearrangements induced by T-DNA integration could influence genetic analysis of the insertion, such as mutant phenotypes that are not correlated with the T-DNA insertion (Parinov and Sundaresan, 2000).

The approximate location of the T-DNA left border region in the second intron of *GCR1* was indicated by the plasmid rescue results and this was confirmed by PCR with DNA prepared from 46 individual *ppi* mutants. However, it was not possible to conclude this insertion in the *GCR1* is causing the *ppi* phenotype. The *gcr1-1* and *gcr1-2* mutants, too, contain T-DNA

insertions at different locations in *GCR1* and do not produce the transcript (Kanyuka and Hooley, personal communication.); the phenotype of these mutants is not different from the wild-type. But, this is not sufficient to conclude the insertion in *GCR1* is not responsible for the *ppi* phenotype, either.

There could there be something unusual or different about the *ppi* mutation that somehow generates the phenotype, even though it was not seen in other mutant alleles. It could be possible that this insertion in the *GCR1* may be giving a partial phenotype, whereas the previously reported ones were having no effect on the phenotypes. The activation-tagged insertion in *GCR1* might be switching on a neighbouring gene to give the *ppi* phenotype. Another possibility is that the plasmid rescue failed to recover genomic DNA flanking the complex insertion described in section 3.2.1, but instead recovered sequences adjoining another possibly simple insertion event in *GCR1* or alternatively, a separate insertion event which may be close to *GCR1* could be responsible for the *ppi* mutation.

Answers to these questions were found in the series of PCRs and Southern blots performed to confirm the approximate location of the insertion.

These PCRs and the Southerns proved that the population of *ppi* studied was not genetically homogenous in terms of presence or absence of a T-DNA insertion. Many *ppi* mutants had a T-DNA insertion in the *GCR1* second intron as judged by the presence of T-DNA left border within the gene. Some were heterozygous for the insertion. Most importantly, some *ppi* plants did not co-segregate with a T-DNA insertion as judged by the absence of T-DNA Basta or CaMV 35S enhancer regions in their genome by PCR and Southern hybridization analyses.

While the characterization of the T-DNA was in progress, I attempted to examine the Basta resistance of the *ppi* mutants. The mutant phenotype and the Basta resistance conferred by the vector would co-segregate only if the mutation is due to a T-DNA insertion. However, experiments done on both soil and agar medium to determine if the Basta resistance co-segregates with the phenotype did not support this. It was not possible to select Basta resistant *ppi* mutants because the *ppi* mutants did not grow and establish very well in the presence of Basta (data not shown). This indicated two possibilities: 1) that the T-DNA insertion could be a large insertion event with several T-DNAs silencing the *BAR* gene expression and 2) that the *ppi* phenotype is not due to a T-DNA insertion event that could be detected by Basta resistance.

Later, as reported in this chapter, it was proved that the studied population of *ppi* had plants matching both these possibilities. The ones that did not have a T-DNA (i.e. group A) would not be resistant to Basta. Those with the large complex T-DNA insertion are most

likely to have silenced *BAR* gene expression and therefore again would not be resistant to Basta.

It has been reported on rare occasions that, when there are repeats of T-DNAs in the same location with CaMV 35S enhancers pointing to different directions, over expressed genes were observed next to only one CaMV 35S enhancer tetramer (Weigel *et al,* 2000). This correlates with the requirement of productive interactions between the enhancer sequences and the plant gene sequences (Weigel *et al*, 2000). Thus, the presence of a number of copies of the enhancer tetramer does not always result in highly expressed genes.

From the results and observations described in this chapter it was most likely that the *ppi* mutation does not segregate with a T-DNA insertion. Hence, it was decided to take a map-based cloning approach to isolate the gene. Even if the mutation is not due to a T-DNA insertion it is possible to map the gene. Although any additional insertion event(s)-if present- can be eliminated by back crossing several times with the wild-type, such 'cleaning up' is not usually essential in map-based cloning. In fact, *ppi* plants from group A (i.e. those without a T-DNA) were back-crossed to the wild-type and the plants having *ppi* phenotype in the F2 segregating population were confirmed for the absence of T-DNA by Basta and 35S specific PCRs. Mutants originating from one such line were used in the studies reported in the subsequent chapters.

Chapter 4

Mapping the *ppi* locus and confirming the gene identification by DNA sequencing, allelism tests, RT-PCR and Western Blotting

4.1 Introduction

4.1.1 Map-based cloning of novel *Arabidopsis* mutants in the post-genome era

Map-based Cloning or Positional Cloning is a forward genetic approach widely used to identify the underlying genetic cause of a mutant phenotype. In this technique, starting with a mutant, all the genes in a genome are analysed without prior assumptions about the gene and eventually the gene responsible for the altered phenotype is identified (Lukovitz *et al*, 2000). This is in contrast to the reverse genetics approaches such as insertion mutagenesis that tend to rely on a prior knowledge about the gene (Jander *et al*, 2002).
In map-based cloning, the gene responsible for a mutant phenotype is isolated by locating the mutation on the chromosome relative to previously known markers. This is done by looking for linkage to markers whose physical location in the genome is already known. Two types of markers are used in mapping studies: morphological markers with easily scorable phenotypes that are caused by mutations in other genes and with a defined map-position and molecular markers that reveal polymorphism between the DNA of different ecotypes (Wilson, 2000).
When using a morphological marker, the mutant of interest is crossed to another mutant used as a phenotypic marker, the resulting F_1 double heterozygote is allowed to self, and the segregation of the two phenotypes is analysed in the F_2 population.
When loci are sufficiently far apart on a chromosome or on different chromosomes, they assort independently at meiosis. If the loci are close enough on the same chromosome, they do not assort independently and are linked. The genetic distance is measured by determining the number of meiotic recombination events that occur between the two loci in 100 chromosomes. The genetic distance is expressed in centiMorgans (cM) or map units. 1cM is equal to recombination frequencies of 0.01 (or 1 recombination event in 100 meioses). The genetic distance can range from 0 cM (absolute linkage) to 50 cM (non-linked loci). Once linkage is detected, it is necessary to convert the recombination frequency to map distance to account for two facts: i) the chromosomes where double cross-overs had taken place between the marker and the locus of interest are scored as

having no recombination event; and ii) recombination events can influence the probability of a second recombination event happening in the vicinity by a phenomenon named interference (Giraudat *et al*, 1999). In *Arabidopsis*, these errors are reasonably corrected by applying the Kosambi function in estimating the map distance: $D = 25 \times \ln [(100 + 2r) / (100 - 2r)]$, where r is the recombination frequency expressed as a percentage, and D is the map distance in cM (Kosambi, 1944). Map distances over adjacent intervals are additive whereas recombination frequencies are not.

Tester lines recessive for several morphological markers have been generated and are available from the Nottingham *Arabidopsis* Stock Centre (NASC). The use of morphological markers is relatively inexpensive and relatively quick to score. However, it is difficult to score many different phenotypes in a single population and therefore detailed mapping using such markers becomes tedious because it requires a number of crosses. Moreover, sometimes it may be difficult to detect the phenotype under certain growth conditions.

When using molecular markers, a single cross can be used to analyse linkage with an unlimited number of markers. In *Arabidopsis*, molecular markers are based on the natural differences in the DNA sequence between distinct ecotypes. Such local differences or polymorphisms of the DNA sequence are due to point mutations, insertions or deletions that randomly occurred in one ecotype and not in the other (Bell and Ecker, 1994).

To map a novel mutation in the *Arabidopsis* ecotype Ws using molecular markers, the mutant can be crossed to a wild-type plant of a polymorphic ecotype such as Col or L*er*, and the F_1 progeny is allowed to self. The resulting F_2 population is then used to analyse the linkage between the mutation of interest and any DNA marker that distinguishes between the two ecotypes (Giraudat *et al*, 1999). An advantage of molecular markers is that because they are co-dominant, in most cases, homozygous and heterozygous individuals can be readily distinguished. The availability of a vast number of molecular markers (since they do not necessarily correspond to expressed genes) also makes their use attractive and allows finer mapping.

The DNA polymorphisms can be visualized by several methods using different molecular markers such as Restriction Fragment Length Polymorphisms (RFLPs), Cleaved Amplified Polymorphic Sequences (CAPS), Simple Sequence Length Polymorphisms (SSLPs), RAPD (Random Amplified polymorphic DNA), Amplified Restriction Fragment length Polymorphisms (AFLP) and Single Nucleotide Polymorphisms (SNPs).

PCR-based markers like CAPS and SSLPs are widely used in *Arabidopsis* genome research now because they require only a small sample of DNA and avoid the time requirement for DNA blotting and hybridisation and other lengthy procedures.
SSLPs are tandem repeats of one-, two- or three-nucleotide motifs found in a genome. These microsatellite repeat sequences are usually polymorphic in different ecotypes because of variations in the number of repeat units (Bell and Ecker, 1994). Specific primers are used to PCR amplify a small genomic region (150 -250 bp) that contains a polymorphic microsatellite sequence. The size of the amplified fragment will vary depending on the number of repeats present in a given ecotype. These polymorphic fragments can be separated and visualized by gel electrophoresis (Fig 4.1a). In CAPS, a genomic DNA region is amplified by PCR using specific primers and the amplified fragments are then digested with a diagnostic restriction enzyme to reveal polymorphisms between different ecotypes (Fig 4.1b).
When molecular markers are used, mutants are localized relative to other molecular markers already placed on the Recombinant Inbred (RI) map prepared by Lister and Dean (1993) which continues to be updated and maintained by the NASC. When visible markers are used, mutants are localized on the classical genetic map. These two maps do not correspond exactly in chromosome length (Wilson, 2000). An update to the classical genetic map contains 462 loci distributed over 5 chromosomes and 469 total centiMorgans based on the recombination frequencies with visible and molecular markers (Meinke *et al*, 1998; Meinke *et al*, 2003).
A comprehensive list and sequence-based map of 620 cloned genes with mutant phenotypes has been provided by Meinke *et al*, (2003). This map documents for the first time the exact location of large numbers of *Arabidopsis* genes that give a phenotype when disrupted by mutation.

4.2 Results

Since the *ppi* mutation was found not to be associated with a T-DNA insertion (Chapter 3), map-based cloning approach was taken to identify the gene. The time-efficient mapping procedure described by Jander and co-workers (Jander *et al*, 2002) was used in the research. The mapping procedure is described in section 2.2.8. Steps in a typical 1-year mapping process are illustrated in Fig 4.2.

The mutant *ppi* which is in Ws-2 background was out-crossed to the polymorphic ecotype Col-0. F_1 plants were allowed to self pollinate and F_2 seeds were grown. About 150 individual homozygous F_2 *ppi* plants were selected for first–pass mapping. DNA was extracted from leaves according to the quick extraction method described by Edwards *et al* 1991 (section 2.2.8.2), and initially the 150 plants were genotyped with 25 published SSLP or CAPS markers (Fig 4.1), spaced roughly every ~5000 kb (roughly 20 cM) apart on the five *Arabidopsis* chromosomes. Information on markers was obtained from the TAIR data base (http://*Arabidopsis*.org/).

After observing genetic linkage to several of the markers, a larger F_2 population (~ 3000-4000 including the initial 600) was planted and ~ 1000 homozygous mutants were used to identify ~200 recombinants that have genetic recombination events in a ~4-cM (1000 kb) region of interest determined by the first-pass mapping. This was achieved by genotyping the mutant plants with the two flanking markers closest to the mutation on either side. When necessary, i.e. when no more published molecular markers were available for the chromosomal region of interest, new markers were designed with the help of Web-Primer software to design primer pairs (http://seq.yeastgenome.org/cgi-bin/web-primer), using the *Arabidopsis thaliana* Col-0 sequence data available on the TAIR data base. Mutants with recombination events in the region of interest were used in fine resolution mapping, targeting to narrow down the region containing the gene of interest to ~ 0.16 cM (40 kb) or less, by using additional markers in the 4 cM interval to look for increasingly tight linkage to the mutation. Once the region of interest was narrowed down as much as possible, candidate genes in the region of interest were considered. Most likely candidate gene was identified by a bioinformatics search combined with a literature survey.

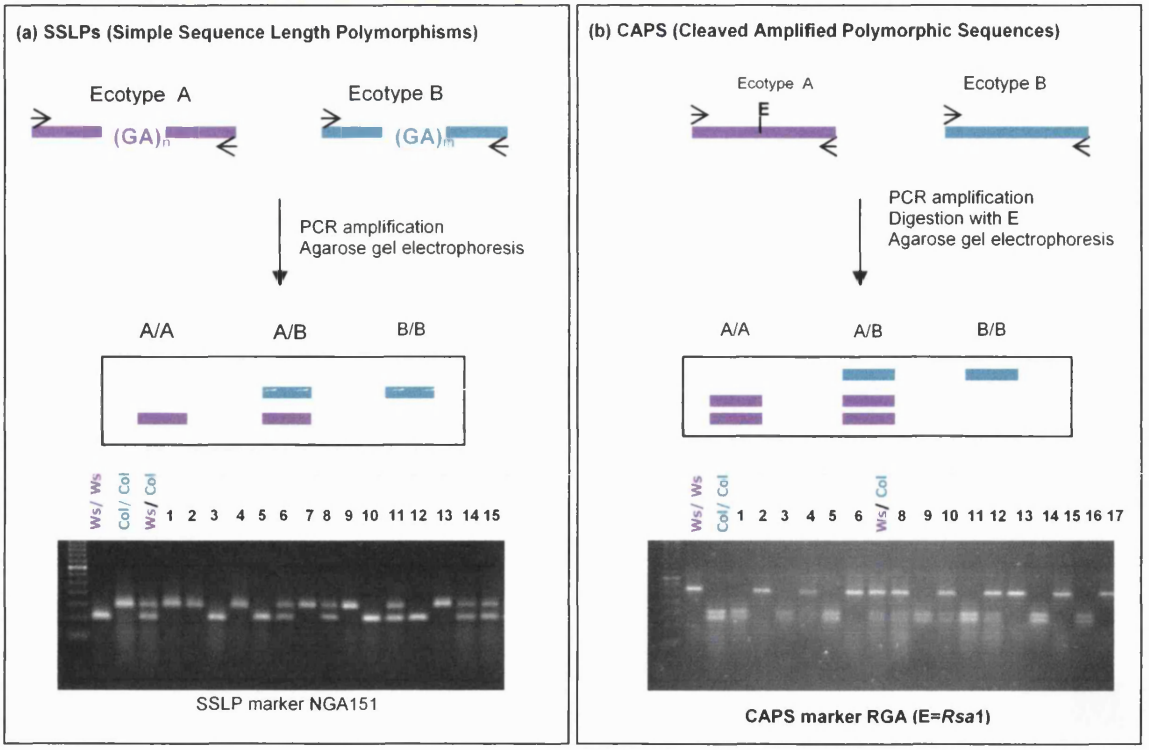

Fig 4.1: The use of Cleaved Amplified Polymorphic Sequences (CAPS) and Simple Sequence Length Polymorphisms (SSLPs) in mapping.

(a) **SSLP markers**: Genomic DNA containing a tandem repeat of a two nucleotide microsatallite motif (GA). In the ecotype A, there is 'n' number of tandem repeats of GA and in the ecotype B, there is 'm' number of GA repeats. The microsatallite polymorphism is revealed by PCR amplification of the genomic DNA region and agarose gel electrophoresis.
NGA151 is a published SSLP marker. PCR amplification revealed 102 bp fragment for Ws-2 DNA and a 150 bp fragment for Col-0. No.1-15 are PCR amplified DNA for F_2 plants homozygous for the recessive *ppi* mutation. Plants 1, 2, 4, 7, 9 & 13 were homozygous Col-0/Col-0 at the NGA 151 locus. Plants 3, 5, 10 & 12 are homozygous Ws-2 /Ws-2 for NGA 151. Plants 6, 8, 11, 14, 15 were heterozygous Ws-2/ Col-0 for the NGA 151 and therefore were recombinants for the locus.

(b) **CAPS markers**: PCR amplified genomic DNA is digested with a diagnostic restriction enzyme. Agarose gel electrophoresis reveals polymorphism in different ecotypes having a different number of fragments.
RGA is a published CAPS marker. When digested with the restriction endonuclease (E) *Rsa*I, Ws-2/Ws-2 gave a 275 bp single fragment whereas Col-0/ Col-0 gave two fragments (~150 bp and 125 bp) due to a polymorphic restriction site. No.1-17 were F_2 plants homozygous for the *ppi* mutation. Plants 2,6,13,15,17 were homozygous Ws-2/WS-2 for the RGA locus and plants 1,3,5,9,11,14,16 homozygous Col-0/Col-0. Plants 4,7,8,10 & 12 are heterozygous Ws-2/Col-0 and therefore, were recombinants for the RGA locus.

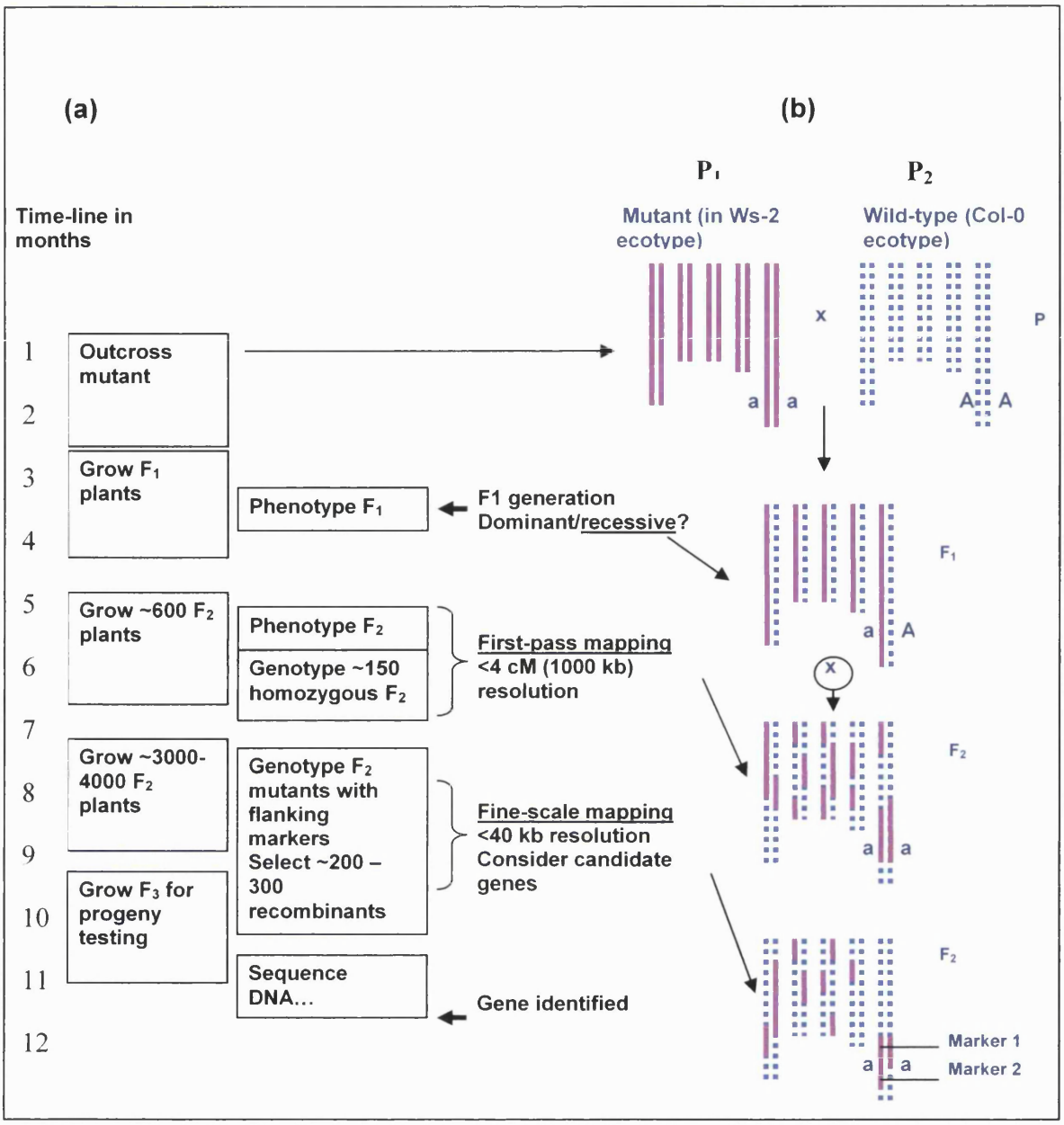

Fig 4.2: Map-based cloning process for *Arabidopsis* genes using molecular markers

(a) One-year mapping time-line for a mutation whose phenotype can be scored as the plants are growing. Five cycles of planting is involved, assuming 2 months per cycle.
(b) Illustration of a mapping cross. The five pairs of *Arabidopsis* chromosomes during critical stages of a sample mapping of a recessive mutation on Chromosome 5 in the Ws-2 background.
Parental lines P_1 & P_2 are homozygous for the mutant allele in Ws-2 ecotype and the wild-type (Col-0) allele respectively. F_1, the first filial generation is heterozygous for the mutant allele. F_2 is the segregating second filial generation. Homozygous mutants (a/a) in the F_2 are scored for the recombination events with respect to different molecular markers and mutant locus is identified based on the linkage to those markers.
'x' indicates cross fertilization and ⊗ indicates selfing.

(Taken from Jander *et al*, 2002)

4.2.1 The *ppi* mutation mapped to At1g22920, *CSN5A* (*COP9 signalosome subunit 5A*).

4.2.1.1 First-pass mapping revealed linkage to markers in the upper arm of *Arabidopsis* chromosome 1

From the first-pass mapping, linkage to several markers in the upper arm of *Arabidopsis* chromosome 1 was detected (Table 4.1). The region of interest was between the markers M59 (r = 8%) and CIW12 (r=9%) which are ~ 3766 kb apart on chromosome. There was not much information for polymorphisms and not many published markers within this region of the *Arabidopsis* sequence and therefore new markers had to be generated (section 2.2.8.4) to obtain a precise location of the *ppi* mutation (Fig 4.3). A total of 43 DNA sequence fragments were analysed and 8 new markers were identified for the region between markers M59 at 5855 kb and CIW12 at 9621 kb on chromosome 1 (Table 4.2). With the help of newly designed markers, the region was narrowed down to 1170 kb between the new markers R1.2 (r= 3.8%) and R2.4 (r=1.73%) that were subsequently used as flanking markers for fine mapping (Figure 4.4a).

4.2.1.2 The *ppi* mutation fine-mapped to a 167 kb region in the upper arm of *Arabidopsis* chromosome 1

About 1000 homozygous mutant plants (951 to be precise) were genotyped with R1.2 and R2.4 flanking markers and identified 102 recombinants in the region of interest. These recombinants were used in fine mapping. Fine mapping identified markers R2.8 (CAPS) at 8108 kb and R4.17 (SSLP) at 8242 kb on chromosome 1 which are 134 kb apart and gave recombination frequencies of 0 & 1.2% respectively, indicating the mutation to be very much closer to R2.8 (Fig 4.4b). However it was not clear how far the mutant gene was from R2.8 or which side relative to the marker. It was extremely difficult to find polymorphisms to be used as new markers within this region.

The chance of getting a recombinant is very low when the genetic distance decreases and could result in inaccuracies in recombination frequencies (Jander *et al*, 2002). To obtain more recombinants in the region, it would have been necessary to plant and screen a larger F_2 population and this could increase the mapping time unnecessarily. Because of those reasons and since the genome of *Arabidopsis thaliana* has been sequenced, we decided to do a database search to see what known genes are in the region and their potential to cause this phenotype through mutation was considered.

Table 4.1: First-pass mapping results for all 5 *Arabidopsis* chromosomes

Markers to which linkage was detected are given in bold. * indicates self-made markers. The others are published markers with information available in TAIR.

Markers used for each chromosome	Type of marker and diagnostic restriction enzyme	Start point in the *Arabidopsis* genome (Col-0 forward strand) kb	Recombination frequency (r%)
Chromosome 1 (30621 kb)			
NF21M12	**SSLP**	**3212**	**15%**
JV18/19	**SSLP**	**5160**	**11%**
M59	**CAPS; *Bst*U1**	**5855**	**8%**
R1.2*	**CAPS; *Alu*I**	**7129**	**3.8%**
R2.4*	**CAPS; *Hin*fI**	**8299**	**1.7%**
R3.1*	**CAPS; *Mnl*I**	**8522**	**3.2%**
CIW12	**SSLP**	**9621**	**9%**
T27K12-SP6	SSLP	15926	36%
NGA128	SSLP	20695	52%
NGA111	SSLP	27418	59%
Chromosome 2 (19787 kb)			
RGA	CAPS; *Rsa*I	255	59%
ER	CAPS; *Dde*I	11219	60%
NGA168	SSLP	16298	68%
Chromosome 3 (23470kb)			
NGA172	SSLP	786	40%
NGA162	SSLP	4608	34%
CIW11	SSLP	9775	43%
ALS	CAPS; *Rsa*I	18012	52%
NGA6	SSLP	23042	52%
Chromosome 4 (18662 kb)			
CIW5	SSLP	737	42%
NGA8	SSLP	5628	47%
CIW6	SSLP	7892	56%
CIW7	SSLP	11524	38%
NGA1107	SSLP	18096	50%
Chromosome 5 (27105 kb)			
NGA158	SSLP	1698	56%
NGA151	SSLP	4669	55%
NGA76	SSLP	10418	61%
SO191	SSLP	15021	60%
CIW9	SSLP	17061	56%
CIW10	SSLP	24548	55%

Table 4.2: List of new markers to distinguish Ws-2 and Col-0 between the region of 7000 kb to 9621 kb on the upper arm of *Arabidopsis* chromosome 1.

Sequence data and BAC annotation unit details are from TAIR (as of August 2004)

Marker name	Primer sequences (Forward/Reverse) 5'-3'	Tm °C	Prod--uct size (bp)	Marker type/ Enzyme	BAC position (AGI whole genome map)	Starting point in Col-0 forward sequence (bp)
R1.2	GAACCATAGGTTTCGTTTCAATTTC CCATTAGTAGTGACAAAGAAGAAACA	56	1083	CAPS/ *Alu*I	F2D10 & F5M15 (overlaps)	7129128
R1.8	ACGCAAGTACTCCTATCACAAT TTATCGAGTACATGCATTTCA	56	1278	CAPS/ *Mbo*II or *Nde*II	F24J8	7473512
R2.1	TAAGCACATAACCCCAAAGTC TGGTAATTCCATGTTTGCGA	52	1373	CAPS/ *Dra*I	F12K8	7910515
R2.4	GCATTGACTGCTTTGAAAATAGG CAGCTTTGCAGGAGTTTTCCAT	56	1090	CAPS/ *Hinf*I	F28C11 & F26F24	8299007
R2.8	CTTTGGGGAGTAACATCTCA GTTTGAACAGCATTTCTTTTG	52	1185	CAPS/ *Mnl*I	F19G10	8108305
R3.1	CGGTTAGACAACCTAGTCTCCTCTT CAACAATTCAACCTAGAAACACA	56	1379	CAPS/ *Mnl*I	T23E23/F3I6	8522610
R4.10	AAGAATGAGAATGAAGTTGACC GGACGAAGCGAAAGTAGGAGTA	56	1486	CAPS/ *Nla*III	T22J18	8075114
R4.17	GTTAGATCTTTTGTATCTCTCTCAT GACAGATGGAAAACTGTTTCGTG	52	1122	SSLP	T26J12/F26F24	8242834

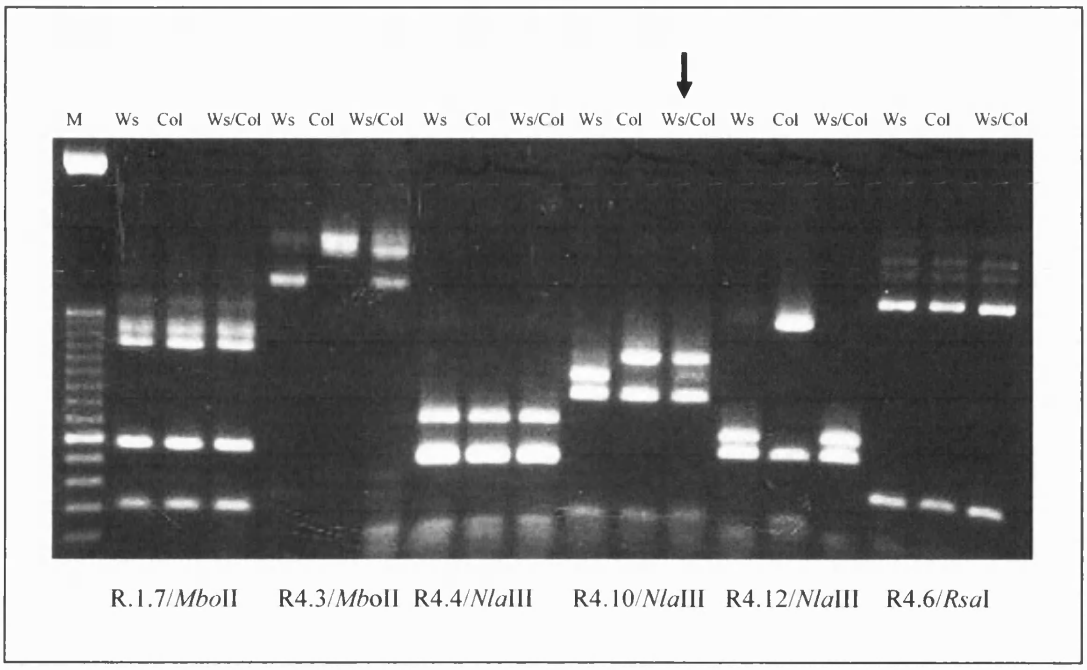

Fig 4.3: Restriction analysis of PCR amplified DNA in searching for potential CAPS markers

PCR-amplified fragments for the new, potential markers R1.7, R4.3, R4.4, R4.10, R4.12 and R4.6 were restricted with the enzymes indicated in the figure. The 1486 bp fragment for R4.10 revealed a restriction site polymorphism with *Nla*III and was subsequently used in fine mapping. The arrow points to the polymorphic bands in the Ws-2/ Col-0 heterozygous DNA.

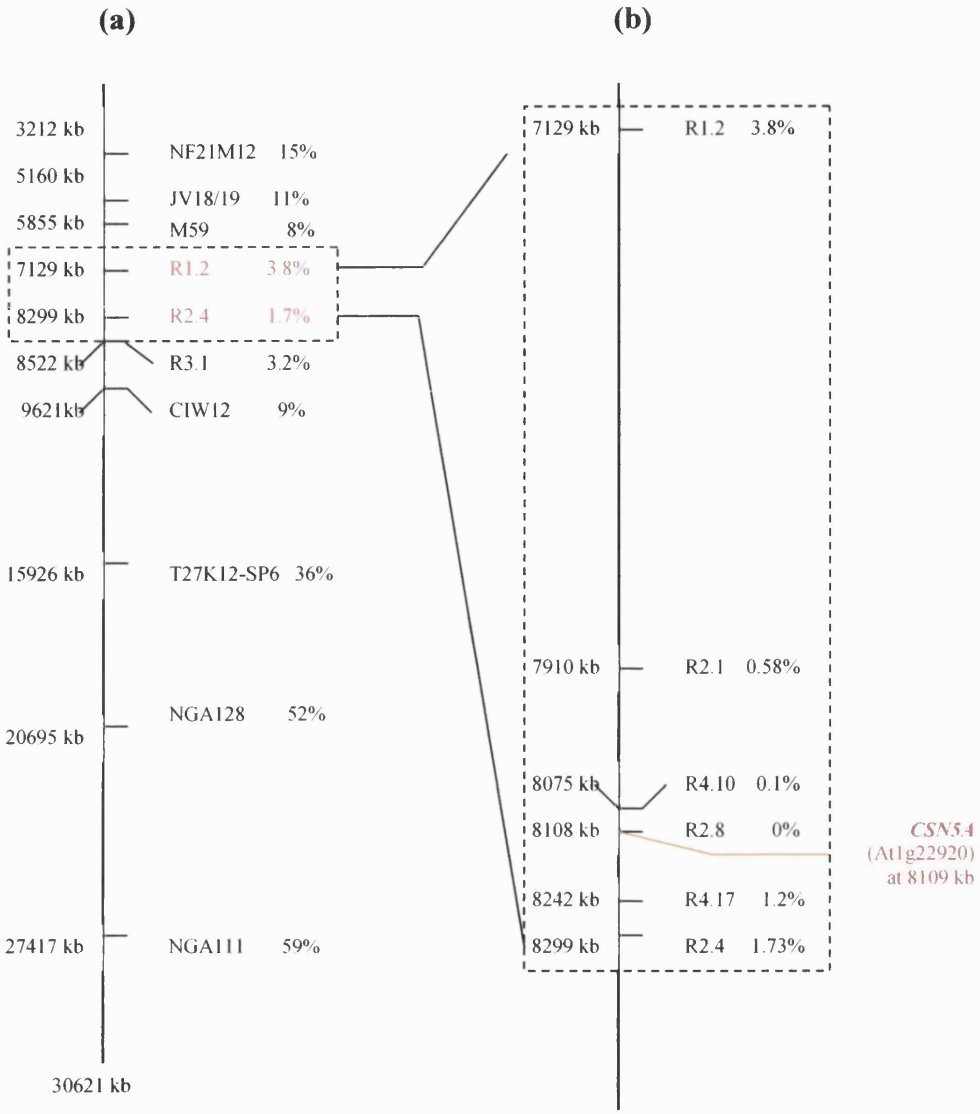

Figure 4.4: **Mapping the *ppi* mutation.**

Relative position of the markers on *Arabidopsis* chromosome 1 and Recombination Frequencies (r%) are indicated.

(a) First-pass mapping identified flanking markers R1.2 and R2.4 that are 1170 kb apart on the upper arm of chromosome 1.
(b) Fine mapping identified R4.10 and R4.17 which are 167 kb apart as the closest flanking markers to the mutation based on the available recombinants. There are 44 genes listed for this region.
CSN5A (At1g22920 on the BAC annotation unit F19G10.12) was recognized and later confirmed as the most suitable candidate gene.
R2.8 at 8108 kb gave a zero recombination frequency indicating the mutation to be very close. Later, it was found that the locus is *CSN5A* which is at 8109 kb- just 1kb south to the R2.8 marker.

4.2.1.3 The most likely candidate gene to contain the *ppi* mutation was At1g22920 (*CSN5A*) at 8109703 – 8112041 bp on *Arabidopsis* chromosome 1

A detailed bioinformatics search of the 167 kb region between markers R4.10 (r=0.58%) and R4.17 (r=1.2%) between the chromosome 1 region 8075 kb and 8242 kb for candidate genes (Fig 4.4b), using the TAIR data base yielded 44 genes in the region bp on chromosome 1.

The list of 44 genes obtained from the TAIR data base was analysed carefully. First each gene annotation in TAIR was searched for mutant phenotypes. Already characterized mutants as judged by a named mutation were searched to see if any one of those has a phenotype similar to *ppi*. None appeared to closely resemble *ppi*. But then there was the risk that gene annotation in TAIR may not be updated and that there could be a time gap between an actual paper being published and the information is added to the data base. Thus a literature survey was also performed to accompany data base search.

First we tried to eliminate as many as possible genes in the list with criteria being it is unlikely to cause characteristics of *ppi* as it could either be an unrelated part of plant metabolism or the mutation would be lethal to the plant. Some could be eliminated with a high degree of certainty, and others with only a moderate degree of certainty. This seemed to be the appropriate strategy to home in on the mutant gene.

There were some genes that could not be eliminated as they were only hypothetical proteins based on the genome annotation but no information was available about them. Similarly we could not eliminate the 'expressed protein' category as those too did not have much information about them.

In the third group a mutation in the gene could cause one or more of the phenotypic characteristics of *ppi* through hormone signalling or through regulating other cellular pathways and therefore could be possible candidates. After eliminating some genes as described above and leaving the genes with no information to be dealt with afterwards, I ended up with a list of 12 genes that could contain the candidate for the *ppi* locus (Table 4.3). However, none of the 12 genes were particularly convincing except for the *CSN5A* (At1g22920) which encode a subunit of the COP9 Signalosome complex which was originally identified as a negative regulator of photomorphogenesis in *Arabidopsis* (Wei *et al,* 1994). In an initial characterization of *ppi*, it had shown a partial photomorphogenic phenotype in the dark. Moreover, the *CSN5A* gene was quite close (at 8109 kb) to the R2.8 marker (at 8108 kb) that gave a zero recombination frequency indicating the mutation is at very close proximity. For those two reasons, we therefore concentrated more on this gene.

Table 4.3 : List of genes from 8075000-8242000 bp on *Arabidopsis* chromosome 1 in which a mutation could cause one or more of the phenotypic characteristics of *ppi*

	Gene description from TAIR (as of August 2004)
1	**8079279-8080563** **AT1G22840.1** AT1G22840.1:cytochrome c, putative, similar to cytochrome c (Pumpkin, Winter squash) SWISS-PROT:P00051
2	**8089490-8094162** **AT1G22870.1** AT1G22870.1:protein kinase family protein, contains protein kinase domain, Pfam:PF00069
3	**8095491-8097698** **AT1G22880.1** AT1G22880.1:glycosyl hydrolase family 9 protein, similar to GB:AAB65156 and GB:AAA96135
4	**8109703-8112040** **AT1G22920.1** AJH1:AJH1 encodes a protein similar to JAB1, a specific mammalian coactivator of AP-1 transcription. It is a part of the COP9 complex.; AT1G22920.1:COP9 signalosome subunit 5A / CSN subunit 5A (CSN5A) / c-JUN coactivator protein AJH1, putative (AJH1), COP9 complex subunit CSN5-1; identical to *Arabidopsis* homologs of a c-Jun coactivator AJH1 GI:3641314 from (*Arabidopsis* thaliana); identical to cDNA CSN complex subunit 5A (CSN5A) GI:18056662; contains Pfam profile PF01398: Mov34/MPN/PAD-1 family
5	**8122340-8125057** AT1G22940.1 TH1:Thiamine requiring 1; AT1G22940.1:thiamin biosynthesis protein, putative, strong similarity to hydroxymethylpyrimidine kinase/thiamin-phosphate pyrophosphorylase (BTH1) GI:7488455 from (Brassica napus)
6	**8139154-8140191** AT1G22990.1 AT1G22990.1:heavy-metal-associated domain-containing protein / copper chaperone (CCH)-related, low similarity to copper homeostasis factor (GI:3168840)(PMID:9701579); strong similarity to farnesylated protein ATFP7 (GI:4097555); contains heavy-metal-associated domain PF00403
7	**8143393-8145059** AT1G23000.1 AT1G23000.1:heavy-metal-associated domain-containing protein, similar to farnesylated protein ATFP3 (GI:4097547); contains PF00403 Heavy-metal-associated domain
8	**8180566-8183559** AT1G23080.1 PIN7:auxin transport protein (PIN7) mRNA, complete cds; AT1G23080.1:auxin efflux carrier protein, putative, similar to efflux carrier of polar auxin transport (Brassica juncea) gi|12331173|emb|CAC24691
9	**8184941-8189020** AT1G23090.1 AST91:AST91 mRNA for sulfate transporter, complete cds; AT1G23090.1:sulfate transporter, putative, similar to sulfate transporter (*Arabidopsis* thaliana) GI:2285885; contains Pfam profiles PF00916: Sulfate transporter family, PF01740: STAS domain
10	8209221-**8211314** AT1G23160.1 AT1G23160.1:auxin-responsive GH3 family protein, similar to auxin-responsive GH3 product (Glycine max) GI:18591, auxin-responsive GH3 homologue (*Arabidopsis* thaliana) GI:11041726; contains Pfam profile PF03321: GH3 auxin-responsive promoter
11	**8215710-8219573** AT1G23180.1 AT1G23180.1:armadillo/beta-catenin repeat family protein, contains Pfam profile: PF00514 armadillo/beta-catenin-like repeat
12	**8219879-8224458** AT1G23190.1 AT1G23190.1:phosphoglucomutase, cytoplasmic, putative / glucose phosphomutase, putative, strong similarity to SP|P93805 Phosphoglucomutase, cytoplasmic 2 (EC 5.4.2.2) (Glucose phosphomutase 2) (PGM 2) {Zea mays}; contains InterPro accession IPR006352: Phosphoglucosamine mutase

While searching the literature for individual genes, we came across a published report (Schwechheimer *et al*, 2001) on *Arabidopsis* transgenic plants with anti-sense *CSN5A* having a pleiotropic phenotype very much similar to *ppi.* In addition, a partial de-etiolation phenotype and a reduced number of root hairs phenotype were common to both mutants. Although we had gone through the then available lists of *Arabidopsis* mutant lines for phenotypic comparison in the beginning of this research, this being an anti-sense transgenic mutant, was not in those lists. With this lead, we decided to examine the *CSN5A* sequence in *ppi* for a possible mutation.

4.2.2 The molecular basis of *ppi* mutation is an 11-basepair deletion in the 4th exon of *CSN5A* gene, predicting to result in the production of a truncated polypeptide

The un-spliced *CSN5A* is 2.3 kb. The full length ORF was PCR amplified from wild-type and *ppi* with gene specific primers 6F and 7R (see Table 4.4 for details of primers), and sub cloned into the pCR2.1-TOPO vector (Invitrogen.) (section 2.2.9). The construct was transformed into TOP10 chemically competent *E.coli* cells and plasmid DNA was prepared from selected clones. To confirm if the desired inserts were truly present in the clones, pDNA constructs extracted above were digested with restriction endonuclease *EcoR* I because two *EcoR* I sites are present on either side of the cloning site of pCR2.1-TOPO vector.

The clones carrying the 2.3 kb insert were sequenced on the forward strand with M13 Reverse vector specific primer and 4 gene specific primers 2F, 3F, 7F and 5F (Table 4.4) that were designed to amplify 480 bp overlapping segments of the DNA, spanning the entire 2.3 kb region. Similarly, the clones was sequenced on the reverse strand with the T7 vector specific primer and 4 gene specific primers 1R, 2R, 3R and 4R (Table 4.4).

Three clones for each wild-type and *ppi* were sequenced completely on both strands with above primers and altogether 30 overlapping sequence reads were obtained for each *ppi* and Ws-2 spanning the entire gene. Analysis of sequences was done with the help of 'CHROMAS' software and with Lasergene SeqMan (http://www.dnastar.com/products/lasergene.php) software to which we obtained a temporary free trial licence. The process by which the consensus sequences were obtained is given in section 2.2.9.9.

Consensus derived from analysing three clones from Ws-2 was compared with the TAIR accession (Col-0) and found it to be identical to this. The consensus derived for analysing

three clones from *ppi* (Ws-2 back ground) was found to be identical to the wild-type (Col-0 and Ws-2) except for an 11-base pair deletion in the 4th exon of *CSN5A* in *ppi* (Fig 4.5). When translated, it is predicted to give a premature stop codon in *ppi* that may result in a truncated protein (Fig 4.6). The theoretical isoelectric point (pI) and molecular weight (M_r) for the wild-type protein are 5.11and 39731.48 Da respectively and for the predicted truncated protein those were calculated (http://www.expasy.org/cgi-bin/pi_tool) to be 4.86 and 33271.18 Da .

Table 4.4 Primers for used in *CSN5A* molecular analyses.

Primer name	Primer sequences 5'-3'	T_m °C
1R	GCTGGTCTGAGAGTATTCAACCA	55
1F	TGTTTTGGATTAGCATTAGTCC	50
2F	TGCTTTTGCTTTGCCTGTTG	56
2R	GCCACATACAAAAAAAATGAATC	52
3F	CATTGCAAACAGGTATGTATAATTC	51
3R	GCAGTTAATTAGCCAAATGAAAAG	53
4F	ACTGGACCATGATCTTGAGCT	52
4R	TTATCTTCGCGAGTTGAGGCT	55
5F	CATTTGTTTTGGAGATTACATTACC	53
5R	CGCAAAAACATAATGATCGA	51
6F	GCATTAGTCCCCAAATCCCATA	56
6R	GTTTCTACACAGGAACAAGCTTGA	54
7F	GGTTGCTTTAGCAAAATTATTTG	54
7R	AGAGATATAGGGAACAATGGGC	53
CSN5A-ATG (with a *Bam*H1 linker sequence.)	CGCGGATCCATGGAAGGTTCCTCGTCAGC	56
LBaI	TGGTTCACGTAGTGGGCCATCG	56
M13 Reverse	CAGGAAACAGCTATGAC	56
T7	ATTATGCTGAGTGATATCCC	56
FUS6-F	AATGGAGCGAGACGAAGAA	52
FUS6-R (CDS)	TCAAAGTTTCCTTGCCGATCT	55

Primer positions in the *CSN5A* gene are shown in Fig 4.7.

CLUSTAL W (1.82) multiple sequence alignment

```
Ws-2            GCATTAGTCCCCAAATCCCATATTAAGTAAATCCATTTTGAGTTTTGTTCTCGCAAACCG 60
ppi             GCATTAGTCCCCAAATCCCATATTAAGTAAATCCATTTTGAGTTTTGTTCTCGCAAACCG 60
                ************************************************************

Ws-2            GTTTAACCCAAGAACCCAAAGATCTCTCTCTATTTGTTTGCCTTCTTCTTTCTTTCTGAC 120
ppi             GTTTAACCCAAGAACCCAAAGATCTCTCTCTATTTGTTTGCCTTCTTCTTTCTTTCTGAC 120
                ************************************************************

Ws-2            TCAAACCCTTAAATCAATTCTCGCGATTAAGCAAAACCCTAGATTTATTCTACTCTTCGA 180
ppi             TCAAACCCTTAAATCAATTCTCGCGATTAAGCAAAACCCTAGATTTATTCTACTCTTCGA 180
                ************************************************************

Ws-2            AGTCGATTTCAATGGAAGGTTCCTCGTCAGCCATCGCGAGGAAGACATGGGAGCTAGAGA 240
ppi             AGTCGATTTCAATGGAAGGTTCCTCGTCAGCCATCGCGAGGAAGACATGGGAGCTAGAGA 240
                ************************************************************

Ws-2            ACAACATTCTCCCAGTGGAACCAACCGATTCAGCCTCCGACAGTATATTCCACTACGACG 300
ppi             ACAACATTCTCCCAGTGGAACCAACCGATTCAGCCTCCGACAGTATATTCCACTACGACG 300
                ************************************************************

Ws-2            ACGCTTCACAAGCCAAAATCCAGCAGGAGAAGCCATGGGCCTCCGATCCTAACTACTTCA 360
ppi             ACGCTTCACAAGCCAAAATCCAGCAGGAGAAGCCATGGGCCTCCGATCCTAACTACTTCA 360
                ************************************************************

Ws-2            AGCGCGTTCACATCTCAGCCCTTGCTCTTCTCAAGATGGTGGTTCACGCTCGCTCCGGTG 420
ppi             AGCGCGTTCACATCTCAGCCCTTGCTCTTCTCAAGATGGTGGTTCACGCTCGCTCCGGTG 420
                ************************************************************

Ws-2            GCACAATCGAGATCATGGGTCTTATGCAGGGTAAAACCGAGGGTGATACAATCATCGTTA 480
ppi             GCACAATCGAGATCATGGGTCTTATGCAGGGTAAAACCGAGGGTGATACAATCATCGTTA 480
                ************************************************************

Ws-2            TGGATGCTTTTGCTTTGCCTGTTGAAGGTACTGAGACTAGGGTTAATGCTCAGTCTGATG 540
ppi             TGGATGCTTTTGCTTTGCCTGTTGAAGGTACTGAGACTAGGGTTAATGCTCAGTCTGATG 540
                ************************************************************

Ws-2            CCTATGAGTATATGGTTGAATACTCTCAGACCAGCAAGCTGGTAAGATATCTCTTATTCA 600
ppi             CCTATGAGTATATGGTTGAATACTCTCAGACCAGCAAGCTGGTAAGATATCTCTTATTCA 600
                ************************************************************

Ws-2            TCTCTCGCTGTAGCTCCTTGTTTAATTAGCTAGTTGCTACTTGGATCCTTTATGCAAGAT 660
ppi             TCTCTCGCTGTAGCTCCTTGTTTAATTAGCTAGTTGCTACTTGGATCCTTTATGCAAGAT 660
                ************************************************************

Ws-2            TTTGCGAGTGTTTGATTGATTGGTTATGACTGTAACTTTGAACTATAGGCTGGGAGGTTG 720
ppi             TTTGCGAGTGTTTGATTGATTGGTTATGACTGTAACTTTGAACTATAGGCTGGGAGGTTG 720
                ************************************************************

Ws-2            GAGAACGTTGTTGGATGGTATCACTCTCACCCTGGGTATGGATGTTGGCTCTCGGGTATT 780
ppi             GAGAACGTTGTTGGATGGTATCACTCTCACCCTGGGTATGGATGTTGGCTCTCGGGTATT 780
                ************************************************************

Ws-2            GATGTTTCGACACAGATGCTTAACCAACAGTATCAGGAGCCATTCTTAGCTGTTGTTATT 840
ppi             GATGTTTCGACACAGATGCTTAACCAACAGTATCAGGAGCCATTCTTAGCTGTTGTTATT 840
                ************************************************************

Ws-2            GATCCAACAAGGACTGTTTCGGCTGGTAAGGTTGAGATTGGGGCATTCAGAACATATCCA 900
ppi             GATCCAACAAGGACTGTTTCGGCTGGTAAGGTTGAGATTGGGGCATTCAGAACATATCCA 900
                ************************************************************

Ws-2            GAGGGACATAAGATCTCGGATGATCATGTTTCTGAGTATCAGACTATCCCTCTTAACAAG 960
ppi             GAGGGACATAAGATCTCGGATGATCATGTTTCTGAGTATCAGACTATCCCTCTTAACAAG 960
                ************************************************************

Ws-2            ATTGAGGACTTTGGTGTACATTGCAAACAGGTATGTATAATTCTTATTTATCGATTTTAA 1020
ppi             ATTGAGGACTTTGGTGTACATTGCAAACAGGTATGTATAATTCTTATTTATCGATTTTAA 1020
                ************************************************************
```

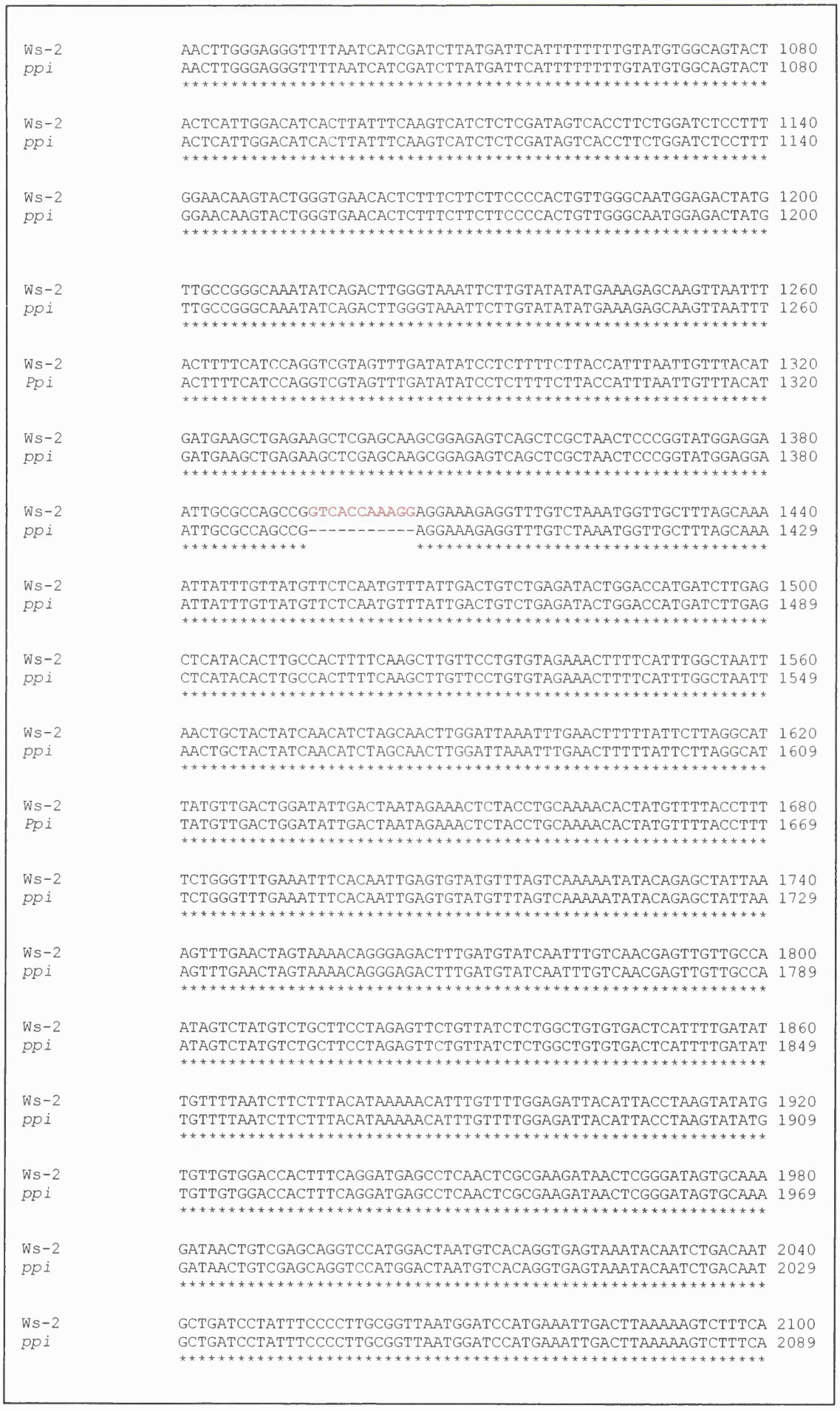
Ws-2 AACTTGGGAGGGTTTTAATCATCGATCTTATGATTCATTTTTTTTGTATGTGGCAGTACT 1080
ppi AACTTGGGAGGGTTTTAATCATCGATCTTATGATTCATTTTTTTTGTATGTGGCAGTACT 1080
Ws-2 ACTCATTGGACATCACTTATTTCAAGTCATCTCTCGATAGTCACCTTCTGGATCTCCTTT 1140
ppi ACTCATTGGACATCACTTATTTCAAGTCATCTCTCGATAGTCACCTTCTGGATCTCCTTT 1140
Ws-2 GGAACAAGTACTGGGTGAACACTCTTTCTTCTTCCCCACTGTTGGGCAATGGAGACTATG 1200
ppi GGAACAAGTACTGGGTGAACACTCTTTCTTCTTCCCCACTGTTGGGCAATGGAGACTATG 1200
Ws-2 TTGCCGGGCAAATATCAGACTTGGGTAAATTCTTGTATATATGAAAGAGCAAGTTAATTT 1260
ppi TTGCCGGGCAAATATCAGACTTGGGTAAATTCTTGTATATATGAAAGAGCAAGTTAATTT 1260
Ws-2 ACTTTTCATCCAGGTCGTAGTTTGATATATCCTCTTTTCTTACCATTTAATTGTTTACAT 1320
Ppi ACTTTTCATCCAGGTCGTAGTTTGATATATCCTCTTTTCTTACCATTTAATTGTTTACAT 1320
Ws-2 GATGAAGCTGAGAAGCTCGAGCAAGCGGAGAGTCAGCTCGCTAACTCCCGGTATGGAGGA 1380
ppi GATGAAGCTGAGAAGCTCGAGCAAGCGGAGAGTCAGCTCGCTAACTCCCGGTATGGAGGA 1380
Ws-2 ATTGCGCCAGCCGGTCACCAAAGGAGGAAAGAGGTTTGTCTAAATGGTTGCTTTAGCAAA 1440
ppi ATTGCGCCAGCCG----------AGGAAAGAGGTTTGTCTAAATGGTTGCTTTAGCAAA 1429
Ws-2 ATTATTTGTTATGTTCTCAATGTTTATTGACTGTCTGAGATACTGGACCATGATCTTGAG 1500
ppi ATTATTTGTTATGTTCTCAATGTTTATTGACTGTCTGAGATACTGGACCATGATCTTGAG 1489
Ws-2 CTCATACACTTGCCACTTTTCAAGCTTGTTCCTGTGTAGAAACTTTTCATTTGGCTAATT 1560
ppi CTCATACACTTGCCACTTTTCAAGCTTGTTCCTGTGTAGAAACTTTTCATTTGGCTAATT 1549
Ws-2 AACTGCTACTATCAACATCTAGCAACTTGGATTAAATTTGAACTTTTTATTCTTAGGCAT 1620
ppi AACTGCTACTATCAACATCTAGCAACTTGGATTAAATTTGAACTTTTTATTCTTAGGCAT 1609
Ws-2 TATGTTGACTGGATATTGACTAATAGAAACTCTACCTGCAAAACACTATGTTTTACCTTT 1680
Ppi TATGTTGACTGGATATTGACTAATAGAAACTCTACCTGCAAAACACTATGTTTTACCTTT 1669
Ws-2 TCTGGGTTTGAAATTTCACAATTGAGTGTATGTTTAGTCAAAAATATACAGAGCTATTAA 1740
ppi TCTGGGTTTGAAATTTCACAATTGAGTGTATGTTTAGTCAAAAATATACAGAGCTATTAA 1729
Ws-2 AGTTTGAACTAGTAAAACAGGGAGACTTTGATGTATCAATTTGTCAACGAGTTGTTGCCA 1800
ppi AGTTTGAACTAGTAAAACAGGGAGACTTTGATGTATCAATTTGTCAACGAGTTGTTGCCA 1789
Ws-2 ATAGTCTATGTCTGCTTCCTAGAGTTCTGTTATCTCTGGCTGTGTGACTCATTTTGATAT 1860
ppi ATAGTCTATGTCTGCTTCCTAGAGTTCTGTTATCTCTGGCTGTGTGACTCATTTTGATAT 1849
Ws-2 TGTTTTAATCTTCTTTACATAAAAACATTTGTTTTGGAGATTACATTACCTAAGTATATG 1920
ppi TGTTTTAATCTTCTTTACATAAAAACATTTGTTTTGGAGATTACATTACCTAAGTATATG 1909
Ws-2 TGTTGTGGACCACTTTCAGGATGAGCCTCAACTCGCGAAGATAACTCGGGATAGTGCAAA 1980
ppi TGTTGTGGACCACTTTCAGGATGAGCCTCAACTCGCGAAGATAACTCGGGATAGTGCAAA 1969
Ws-2 GATAACTGTCGAGCAGGTCCATGGACTAATGTCACAGGTGAGTAAATACAATCTGACAAT 2040
ppi GATAACTGTCGAGCAGGTCCATGGACTAATGTCACAGGTGAGTAAATACAATCTGACAAT 2029
Ws-2 GCTGATCCTATTTCCCCTTGCGGTTAATGGATCCATGAAATTGACTTAAAAAGTCTTTCA 2100
ppi GCTGATCCTATTTCCCCTTGCGGTTAATGGATCCATGAAATTGACTTAAAAAGTCTTTCA 2089

Fig 4.5 *CSN5A* gene sequence comparison between Ws-2 (wild-type) and *ppi*

The 2.3 kb un-spliced *CSN5A* genomic regions from both Ws-2 and *ppi* were PCR amplified with gene specific primers, cloned and sequenced. ClustalW (version 1.82) multiple sequence alignment of the consensus sequences were identical except for an 11-bp deletion (highlighted in red) in the 4th exon of the gene in *ppi*.

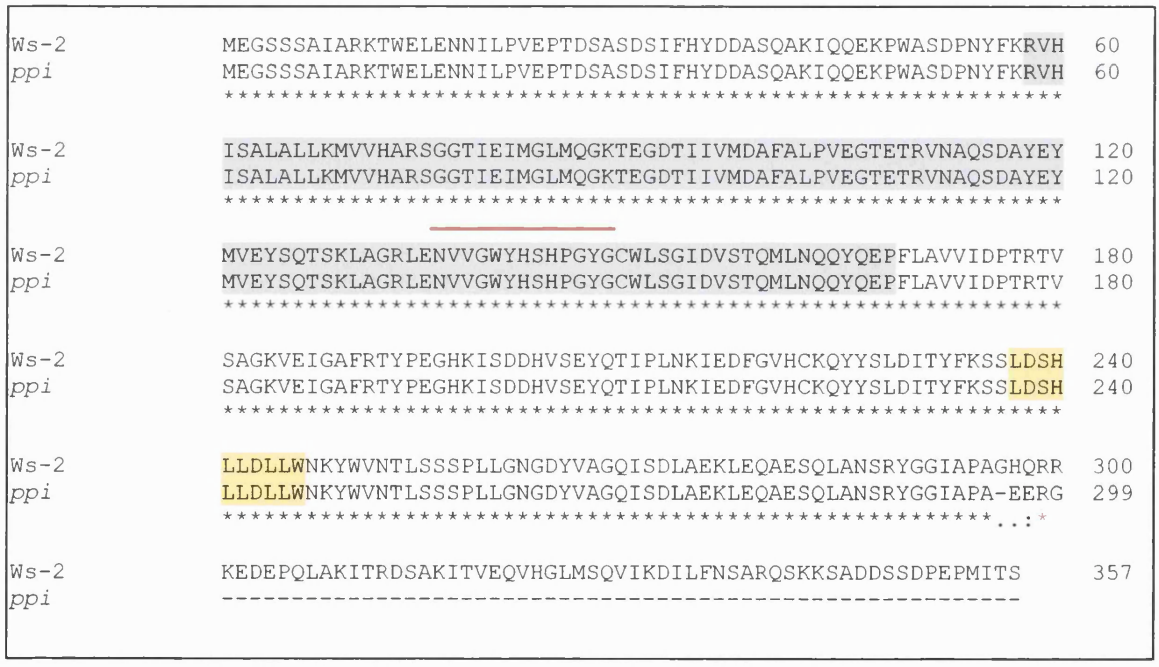

Figure 4.6. CSN5A protein sequence comparison of Ws-2 and *ppi.*

CulstalW (1.82) multiple sequence alignment of the amino acid sequences of Ws-2 and the predicted *ppi* truncated polypeptide.
The MPN domain is highlighted in grey. The JAMM motif in the MPN domain is marked by a red line on the top. Positions of the MPN domain and JAMM motif are based on UniProtKB/SwissProt data as of 15/06/2007). The nuclear export signal NES (Tomoda *et al*, 2002) is highlighted in yellow.

The COP9 Signalosome subunit 5 (CSN5)

The *Arabidopsis* COP9 Signalosome Subunit 5 (*CSN5*) encodes a subunit of the COP9 Signalosome complex that is involved in protein de-neddylation and degradation of proteins (Chapter 1). A known biochemical activity of the CSN is the removal of the ubiquitin-like protein RUB/NEDD8 from the cullin subunit of the Cullin-RING ligase (CRL) family of E3 complexes (Gusmaroli *et al.*, 2007). The CSN de-neddylation activity is located within the JAMM motif of CSN5 which is embedded within its MPN domain. In *Arabidopsis* the subunit 5 is encoded by a small gene family comprised of two conserved genes, namely, *CSN5A* (At1g22920; annotated BAC unit F19G10.12) and *CSN5B* (At1g71230; annotated BAC unit F3I17.12). The two genes are located in the opposite arms of *Arabidopsis* chromosome 1. Sequence analyses indicated that *CSN5A* and *CSN5B* share 86% and 88% similarity at the cDNA and protein revels respectively (Kwok *et al.*, 1998). CSN5 was first identified as a c-Jun activation domain binding protein in humans (Claret *et al*, 1996). Two homologs of CSN5 were identified from *Arabidopsis* based on peptides sequenced from the p42 protein band co-purifying with the CSN complex (Kwok *et al.*, 1998). The two cDNAs were designated as p42A and p42B. The two genes defined by the p42A and p42B cDNA clones were designated as *AJH1* and *AJH2* (*Arabidopsis* JAB1 homolog 1 and 2) respectively. GenBank accession numbers for the nucleotide sequence of AJH1 is AF087413 and for AJH2 it is AF087412.
With the standardising of names for CSN subunits, the *AJH1* and *AJH2* have the gene aliases *CSN5A* and *CSN5B* respectively (Deng *et al*, 2000).
The CSN5A protein is 357 aa in length with a pI/M_r of 5.05/39732 Da and AJH2 is 358 aa with a pI/M_r of 5.11/ 40318 Da (UniProtKB/SwissProt, TAIR).
CSN5A (At1g22920.1) has a splice variant (At1g22920.2) that encodes a protein of 352 aa and pI/Mw of 5.22/ 39105 Da (TAIR) and has a different version of the C-terminal region than At1g22920.1.

While searching for the gene information I encountered some confusion in the names *CSN5A* and *CSN5B* in some data bases. TAIR, until around March 2006 gave *AHJ1* gene alias as *CSN5B*, though it has since been corrected to *CSN5A*. As of April 2007, AJH1 (SwissProt Entry Q8LAZ7) was CSN5B_ARATH and AJH2 (SwissProt Entry Q9FVU9) was CSN5A_ARATH.

4.2.3 The *ppi* mutant is allelic to two independent T-DNA insertion mutant lines of *CSN5A* that have a similar phenotype to *ppi.*

The sequence data suggested that the 11 bp deletion in *CSN5A* could be responsible for the *ppi* phenotype. However, the mapping had not been of sufficiently high resolution to identify this gene on its own. Therefore we decided to identify other mutants in this gene and see if their phenotype resembled *ppi*. I searched the SIGnAL database (Salk Institute Genomic Analysis Laboratory; http://signal.salk.edu/cgi-bin/tdnaexpress) and found four T-DNA insertion lines of the gene in the Col-0 background (as available in October 2004). The lines were Salk_003442, Salk_063436, Salk_027705 and Salk_111241 See Fig 4.7 for the positions of T-DNA insertions in the gene.

The seeds for all 4 lines were obtained from the NASC (and ABRC). About 20 plants for each line were grown and visually scored for a pleiotropic phenotype similar to that of *ppi*. Five plants from Salk_027705 line and three plants from line Salk_063436 showed such phenotype (Fig 4.8a).

Plants with a *ppi*-like phenotype from the Salk_063436 line were tested for the presence and homozygosity of the insert. This was done by PCR-genotyping the DNA using the gene specific 6F and 1R primers to test for the presence of the wild-type *CSN5A* allele, and with T-DNA specific primer LBa1 and gene specific 6F or 1R, to test for the presence of the T-DNA insertion. Plants from the Salk_027705 line with a *ppi*-like phenotype were tested with gene specific primers 7F and 4R for the presence of the wild-type *CSN5A* allele and with LBa1 and 7F or 4R for the presence of the T-DNA insertion in the gene (Fig. 4.8b). Plants having a *ppi*-like phenotype in both lines were homozygous for a T-DNA insertion in the *CSN5A* gene.

The plants from the NASC seeds for Salk_003442 and Salk_111241 all had wild-type phenotype. PCR-genotyping of DNA from 10 plants of Salk_111241 with LBa1 and gene specific 5F or 5R primers for the T-DNA and primers 5F & 5R for the wild-type *CSN5A* showed that they were heterozygous for the insertion. These plants were allowed to self. PCR analysis of the progeny showed a few homozygous for a T-DNA insertion in the *CSN5A*. However, these plants did not show a *ppi*-like phenotype.

Plants from Salk_003442 line were tested with LBa1 and gene specific 1R or 6F primers and they were heterozygous for the insertion. Progeny testing as above, again, did not show the T-DNA to be segregating with a *ppi*-like phenotype. Apparently, these insertions do not disrupt the gene function, at least to be seen at the morphological level.

As we were able to obtain two insertion mutants of the gene (out of four) having a similar phenotype to *ppi* this discovery was sufficiently convincing that the *ppi* is also in *CSN5A*.

The Salk_063436 and Salk_027705 mutants that proved to be homozygous for the mutation by PCR-analysis were back-crossed to wild-type Col-0 plant and the F_1 which showed wild-type phenotype, confirming the recessive nature of the mutations in each line. The F1 plants were allowed to self and the resulting F_2 progeny were tested for segregation. All the lines showed 3:1 segregation for the wild-type: *ppi*-like phenotype (Chapter 5)

According to the SIGnAL data base, of this particular collection of T-DNA insertion lines approximately 50% of the lines are said to contain a single insert. The other 50% may have two or more inserts. For the *csn5a-1* and *csn5a-2* lines, the single insert has been confirmed by segregation analysis on Kanamycin sensitivity (Gusmaroli *et al* 2004). During our PCR genotyping, it was indicated that both the lines may contain at least two repeats of T-DNA because the T-DNA left border specific LBa1 primer gave products in combination with primers from either side of the genomic sequence flanking the inserts.

Salk_063436 and Salk_027705 have since been published (see section 4.3.1) and the names are *csn5a*-1 *csn5a*-2 respectively. I will use these names from here onwards.

The *csn5a-1* and *csn5a-2* lines that proved to be homozygous for the mutation by PCR genotyping and segregation analysis were used in allelism testing.
When *ppi* x *csn5a-1*, *ppi* x *csn5a-2* or *csn5a-1* x *csn5a-2* crosses were made, none of the mutants could rescue one another. The F_1 progeny from the crosses showed a *ppi*-like phenotype, confirming allelism between the three mutant lines (Fig. 4.8c & 4.8d). Confirmation of allelism between the three *csn5a* mutants was done by PCR-based genotyping of the double mutants (Fig 4.8e). Gene specific primer combination 6F – 1R were used to test the presence of the wild-type *CSN5A* fragment containing the first exon. The presence of the *csn5a*-1 T-DNA insertion was tested by the use of the T-DNA left border specific LBa-1 along with 6F. Similarly, gene specific primer combination 7F-4R amplifying the DNA fragment spanning the 4^{th} intron was used to test the presence of the wild-type *CSN5A* fragment. The presence of the *csn5a*-2 T-DNA insertion was tested with the primer combination LBa-1 and 7F.

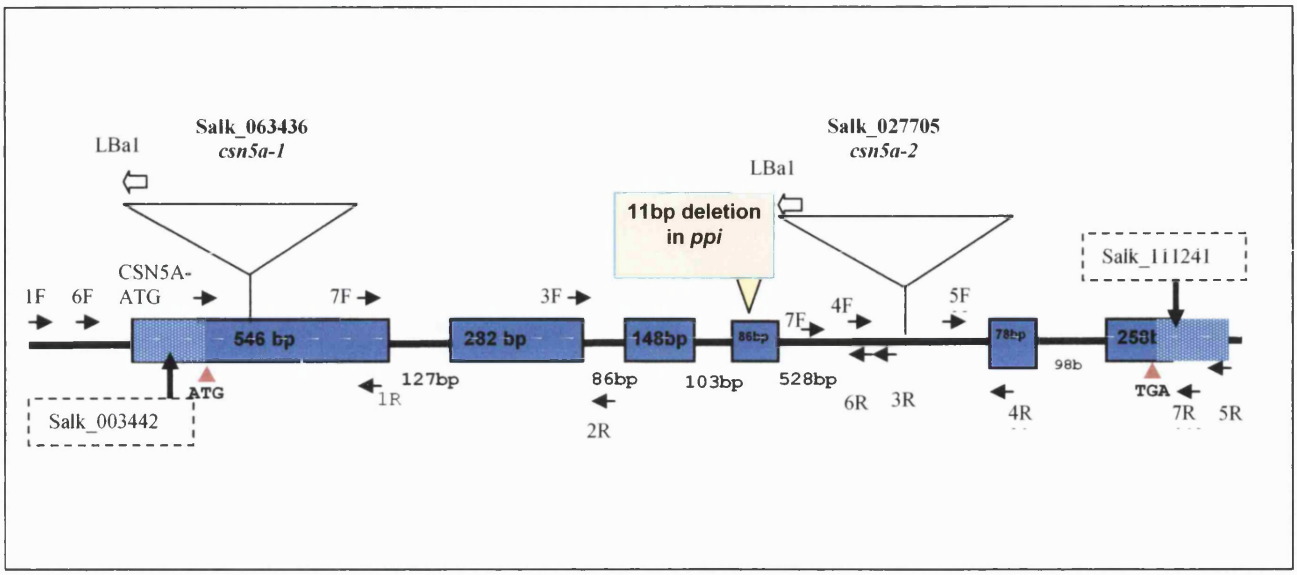

Figure 4.7 Structure of the *Arabidopsis CSN5A* gene (At1g22920.1) and graphic presentation of the *ppi* and two T-DNA insertion mutant loci.

Exons are represented by blue and dotted (untranslated regions) boxes and introns are represented by lines. An 11-basepair deletion in the 4th exon has caused the *ppi* mutation (orange box). *csn5a-1* and *csn5a-2* are T-DNA insertion loci that are confirmed to be allelic to *ppi*. Black arrows schematically represent the position and orientation of the primers used in molecular analyses and the white block arrows represent the orientation of the LBa1 T-DNA left border specific primer.

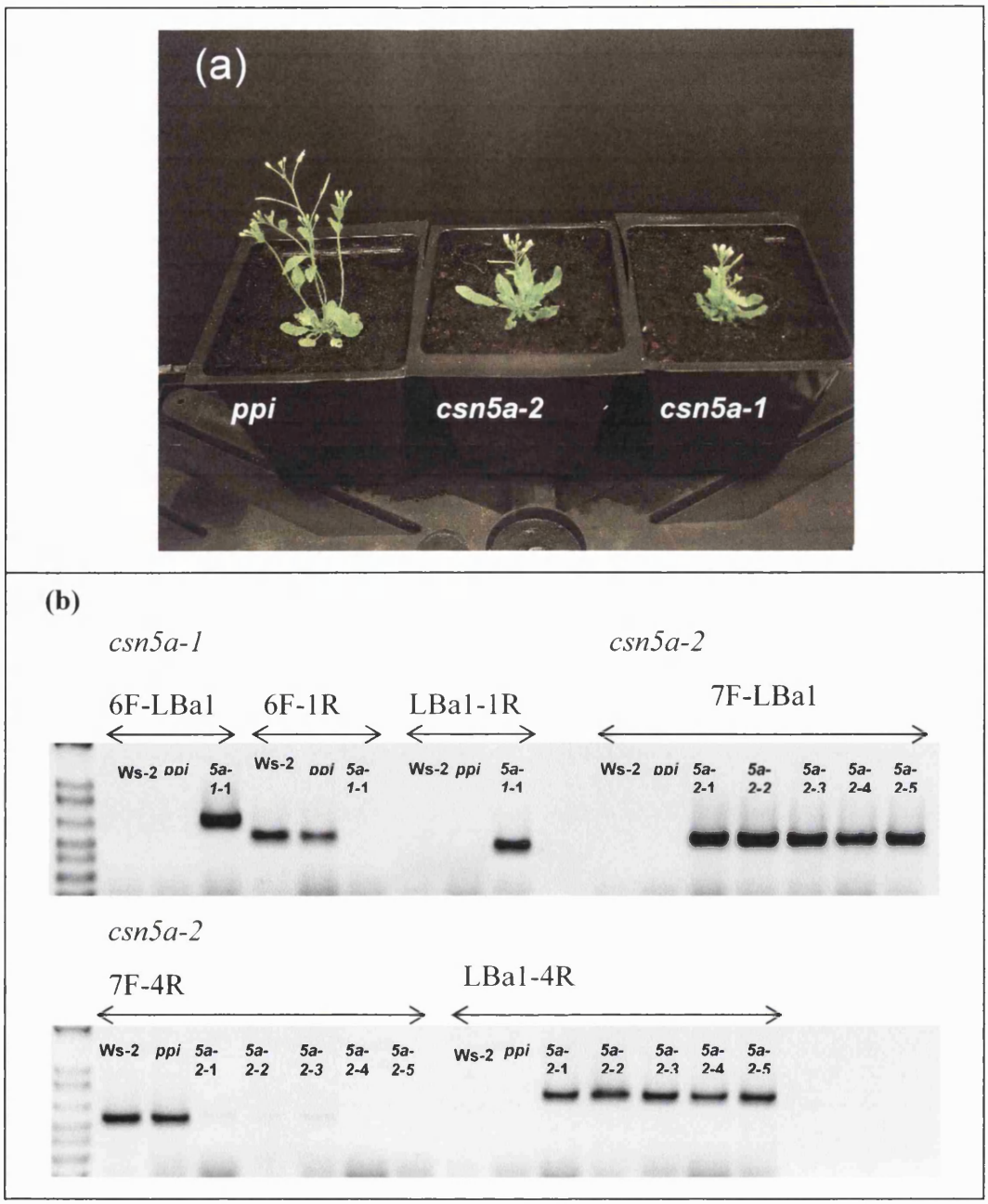

Figure 4.8: Two *CSN5A* T-DNA insertion lines from the SALK collection are allelic to *ppi*

(a) 4-week old plants of *csn5a* mutants (*ppi, csn5a*-1 & *csn5a-2*) grown under long-days (16 h light) in a controlled environment growth room.

(b) PCR-based genotyping to confirm the presence of T-DNA insertions in *csn5a*-1 (5a-1.1 in the figure) and *csn5a-2* (5a-2.1 to 5a-2.5 in the figure) mutants.
PCR-genotyping the DNA using the oligonucleotides 6F and 1R to test for the presence of the wild-type *CSN5A* allele, and with T-DNA specific primer LBa1 and the gene specific primers 6F or 1R, to test for the presence of the T-DNA insertion in *csn5a-1* . Similarly plants from the line *csn5a-2* with a *ppi*-like phenotype were tested with the oligonucleotides 7F and 4R for the presence of the WT gene and with LBa1 and 7F or 4R for the presence of the T-DNA insertion.

[Figure 4.8 continues overleaf]

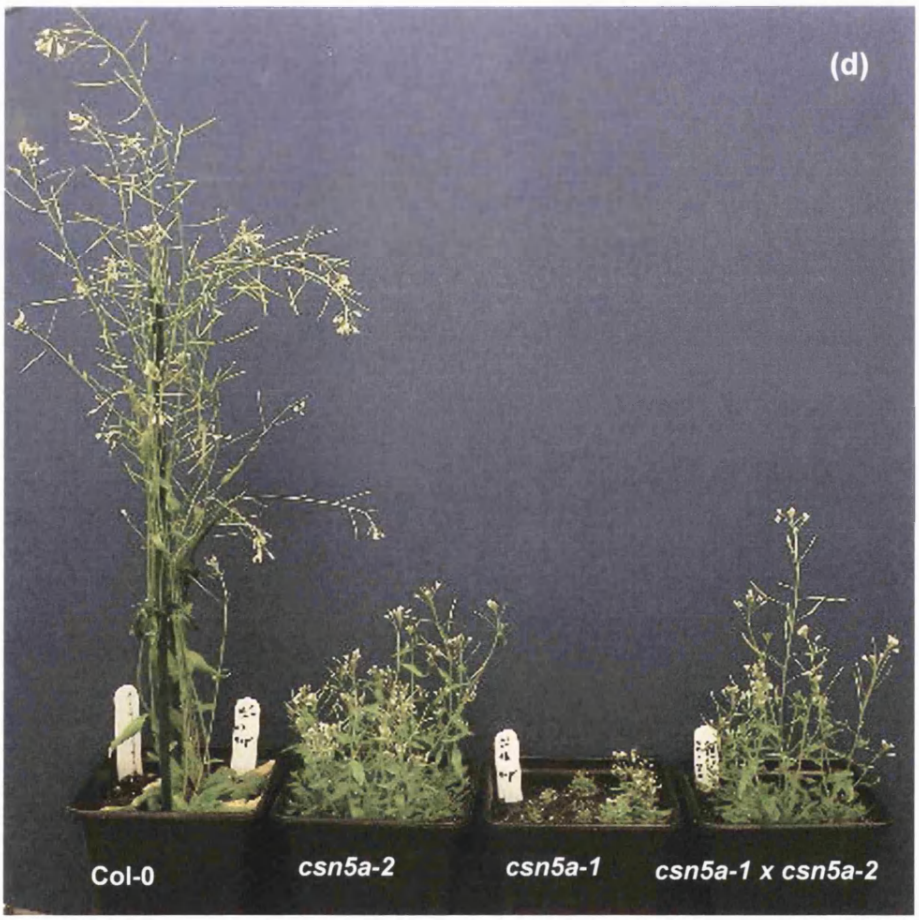

Figure 4.8 (continued): Two *CSN5A* T-DNA insertion lines from the SALK collection are allelic to *ppi*

Wild-type and F_1 progeny from crosses to test allelism.
(c) 4-week old plants and (d) 7-week old plants grown under long days in a controlled environment growth room. None of the mutants from crosses *ppi* x *csn5a-1*, *ppi* x *csn5a-2* or *csn5a-1* x *csn5a-2* could rescue each other. However, F_1 progeny from *csn5a-1* x *csn5a-2* cross show a less severe phenotype than homozygous *csn5a-1* mutants, indicating *csn5a-2* could be a partial-loss-of-function mutant.

[Figure 4.8 continues overleaf]

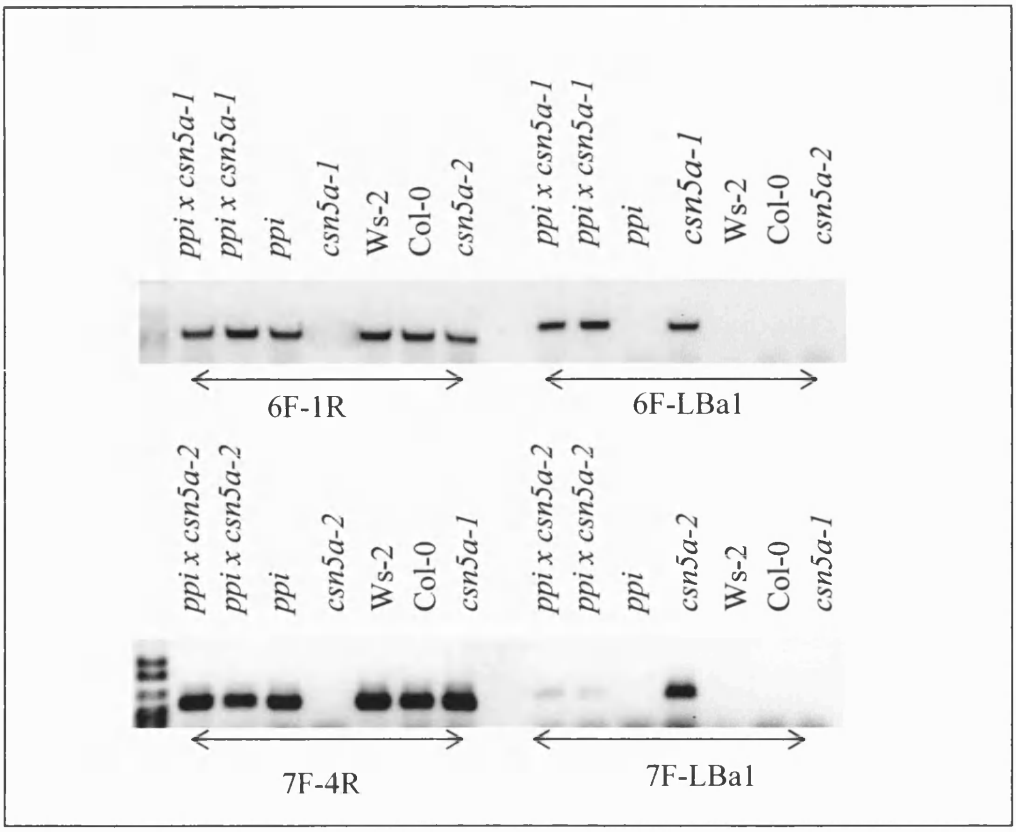

Figure 4.8 (continued): Two *CSN5A* T-DNA insertion lines from the SALK collection are allelic to *ppi*

Confirmation of allelism between *ppi* and the two T-DNA insertion mutants by PCR-based genotyping. Gene specific primer combination 6F – 1R were used to test the presence of the wild-type *CSN5A* fragment containing the first exon. The presence of the *csn5a*-1 T-DNA insertion was tested by the use of the T-DNA left border specific LBa-1 along with 6F. Similarly, gene specific primer combination 7F-4R amplifying the DNA fragment spanning the 4th intron was used to test the presence of the wild-type *CSN5A* fragment. The presence of the *csn5a*-2 T-DNA insertion was tested with the primer combination LBa-1 and 7F.

4.2.4: Low or undetectable *CSN5A* transcript levels and CSN5 protein levels in the mutants further confirm the gene locus.

RNA extracted from 2 week old seedlings grown on nutrient agar under long days (16h light) was analyzed by RT-PCR (section 2.2.10). Gene specific primers CSN5A-ATG and 7R (Table 4.4) were used to amplify the full length (1166 bp) *CSN5A* cDNA. As a positive control for the RT-PCR, gene specific primers FUS6F and FUS6R were used to amplify the *CSN1 (FUS6)* CSN sub unit 1 cDNA.
ppi showed reduced levels of *csn5a* transcript whereas it was undetectable in the two homozygous T-DNA insertion mutants (Fig. 4.9).

Total proteins extracted from 2 weeks old plants grown as above were immunoblotted with α-CSN5 antibody to detect the CSN5 protein levels (section 2.2.11). The wild-type (Ws-2 and Col-0) showed a strong band migrating around ~40 kDa (Fig 4.10a) and this could represent the wild-type protein which has a molecular weight of 39.7 kDa. The weaker band migrating slower but closer to 40 kDa could be the CSN5B protein (40.3 kDa). The α-CSN5 antibody recognizes both proteins. This presumably CSN5B was not detected in any of the mutants. In csn5a-2, the 40 kDa band was detected, but the abundance compared to the wt was very low. This band was negligible in *csn5a*-1.
The *ppi* protein sample did not show the ~40 kDa wild-type CSN5 band, but it had a prominent band migrating around 33 kDa. In fact a ~ 33 kDa band was seen for all the plants, but to a very low abundance compared to *ppi*. It is likely that there is non-specific binding at 33 kDa as faint band binds to all 5 lines and it is possible that the truncated polypeptide produced in *ppi* falls in the same molecular weight range and therefore a much intense signal seen in *ppi*. In fact, the size predicted for the *ppi* truncated protein is 33 kDa. When only the cytoplasmic, soluble protein fraction (section 2.2.12.1) was analysed by Western blotting, the 33 kDa band was more prominent in *ppi* (Figure 4.10b), where it was almost non-detectable in others.
The 40 kDa band seen in *csn5a-2* is probably the full length polypeptide where the intron has been spliced out correctly. And, probably, in *csn5a-1* there is no polypeptide.
This correlates with the phenotypic severity seen as *csn5a-1* being the most severe where the CSN5A protein is absent and therefore a null mutant. *csn5a-2,* having some amount of wild-type CSN5A, could be partially functional and therefore a less severe phenotype. In *ppi*, the CSN5A truncated protein may be partially functional.

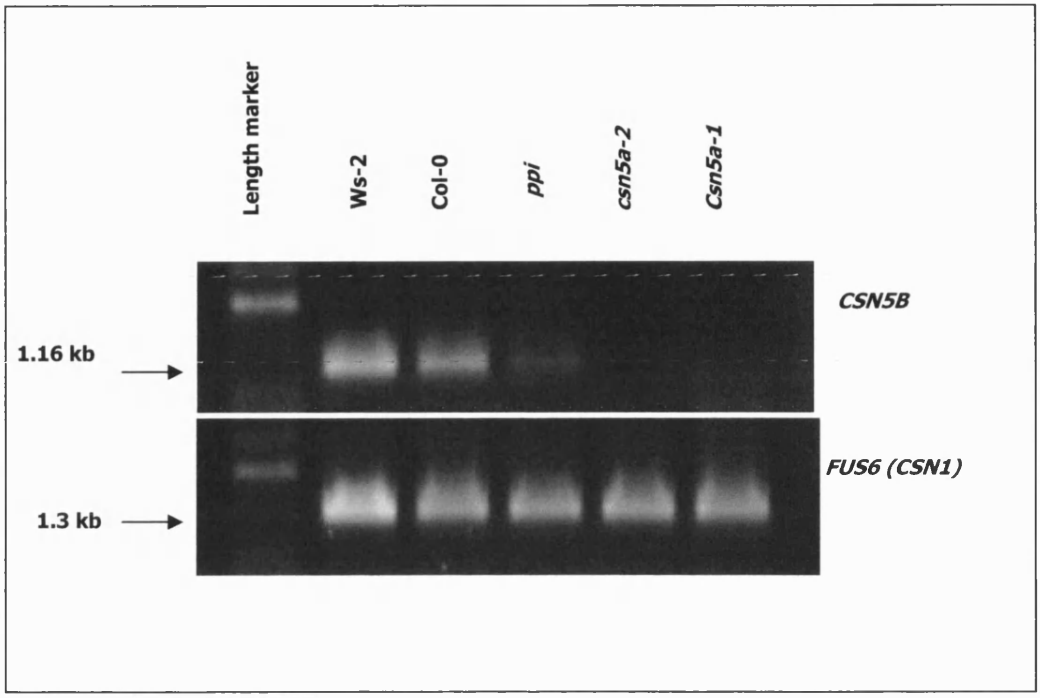

Fig 4.9 Detection of *CSN5A* transcript in 2 week-old wild-type & mutant seedlings by RT-PCR

RNA was extracted from 2 week old seedlings grown on nutrient agar under long days (16h light) was used in RT-PCR. Gene specific primers CSN5A-ATG and 7R were used to amplify the full length (1.166 kb) *CSN5B* cDNA. As a positive control for the RT-PCR, gene specific primers FUS6F and FUS6R were used to amplify the *CSN1(FUS6)* cDNA (1.3 kb).
ppi produced low levels of the mutant transcript whereas a transcript was not detectable in *csn5a*-1 or *csn5a*-2.

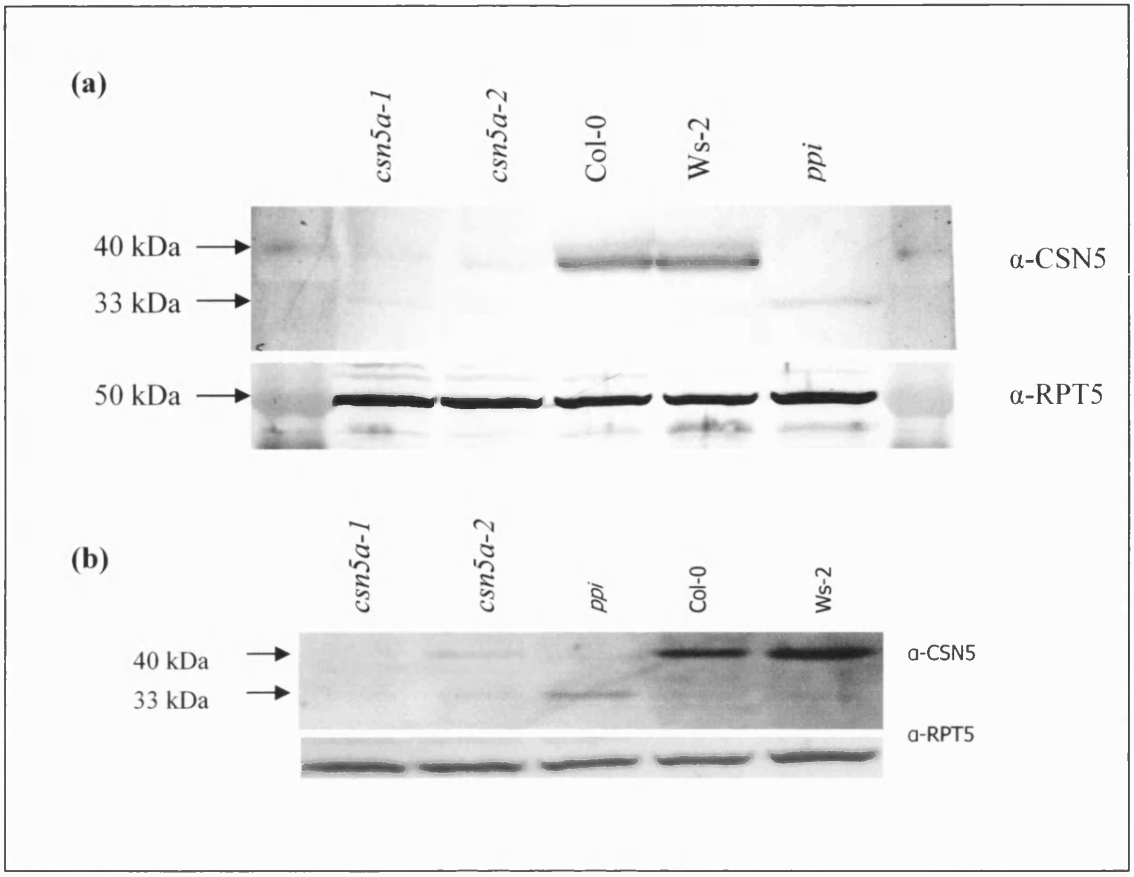

Fig. 4.10: Detection of CSN5 protein in *ppi*, *csn5a*-1, *csn5a*-2 homozygous mutants and the respective wild-types Ws-2 and Col-0 by Western Blot analysis

(a) Total proteins extracted from 2 weeks old seedlings and 20 µg sample from each plant type were subjected to SDS-PAGE and immunoblotted with α-CSN5 polyclonal antibody which recognizes both CSN5B and CSN5A isoforms. α-RPT5, (a proteasome ATPase subunit) polyclonal antibody was used to confirm equal protein loading.
A strong band migrating around ~40kDa were detected in Ws-2 and Col-0 and corresponds to the CSN5A protein. This band was detected at a very low abundance in *csn5a*-2 and was not detected in *csn5a*-1 and *ppi*. The slower migrating band around ~40 kDa seen in the wild-type could most likely be the CSN5B. This was not detectable in the mutants. *ppi* truncated protein falls within the molecular weight range ~33kDa, and the other mutants and wild-type show non-specific binding at the same molecular weight range.

(b) Cytoplasmic, soluble fractions of proteins from seedlings as above were subjected to SDS-PAGE and immunoblotted similarly. ~33kDa was much more prominent in *ppi*, was present to a lesser amount in *csn5a-2* and was barely detectable in the other mutants or the wild-type.

4. 3 Discussion

4.3.1 The *ppi* gene locus was identified within less than a year into mapping

In Chapter 3 it was shown that the *ppi* phenotype did not segregate with a T-DNA insertion and therefore I took a map-based approach in identifying the mutant locus.
With the fully sequenced *Arabidopsis* genome and a dense collection of available molecular markers, the process of mapping a novel mutation is given as approximately one year, provided that the mutant phenotype is not scored at the seed level and involves 5 cycles of plant growth, assuming 2 months/ cycle (Jander *et al*, 2002).
The second year of the my PhD research concentrated on identifying the mutant gene by map based cloning. Although map based cloning proved to be a tedious and time-taking process, it was possible to identify the locus of the *ppi* mutation within 10 months of initiating the mapping process. The typical one-year time line was reduced because it was not necessary to perform any gene complementation to find the locus. Or to very fine map the region.

The *ppi* mutant is in the Ws-2 genetic back-ground. Although the Ws-2 entire genomic sequence was not available, I found that it was possible to map the gene to a reasonable map-distance using the published markers. With the help of TAIR sequence (Col-0, CS60000 genomic sequence), polymorphisms between Ws-2 and Col-0 were identified and I used these to design new molecular markers to facilitate mapping. However, at the latter stages of fine mapping, it became extremely difficult to find polymorphic sites that could be used as markers, especially when the region was narrowed down to 167 kb between 8075 – 8242 kb on *Arabidopsis* chromosome 1. The bioinformatics search combined with the literature survey gave a good lead as to what the mutant locus might be and I could confirm it by molecular analyses.

I started my research work on *ppi* in January 2003 and completed the gene identification by October 2004. Although loss of function mutants for PCI domain sub units of the CSN had been characterized, the initial characterization of potentially loss-of-function csn5 mutants (including *csn5a*-2) in *Arabidopsis* was published only in November 2004 (Gusmaroli *et al*, 2004). By this time we had independently identified both T-DNA insertion lines from the Salk collection. The first publication on *csn5a*-1 was in July 2005 (Dohmann *et al*, 2005).

The PCI domain subunit mutants of the CSN show characteristic *cop/det/fus* phenotype and are seedling lethal (Serino and Deng, 2003). As the CSN5 and CSN6 subunits are encoded by two redundant genes, single mutants of these genes show less severe phenotype and it was only very recently using double mutants that it was shown that the loss of function of MPN subunits lead to the same *cop/det/fus* phenotype (Gusmaroli *et al*, 2007).

4.3.2 RT-PCR transcript and protein blot analyses suggest homozygous *csn5a-1* to be a null mutant whereas homozygous *csn5a-2* and *ppi* may be partial loss-of-function alleles.

Although it was true that being allelic the mutants could not rescue each other when *ppi x csn5a-1*, *ppi x csn5a-2* or *csn5a-2 x csn5a-1* crosses were made the phenotype that come out of the double mutants at the adult stage were slightly less severe compared to the homozygous individuals. This can be explained by looking at the RT-PCR and protein analyses.

In *csn5a-1*, where the T-DNA insert is in the first exon, quite close to the transcription start point, the absence of CSN5A transcript and protein demonstrates that the T-DNA insertion has given rise to a null mutation, hence the most severe phenotype. *csn5a-2* was previously reported to be a null mutant as well (Dohmann *et al*, 2005). However, we were able to detect low levels of CSN5A protein in the *csn5a-2* homozygous line, suggesting this to be a partial loss-of function allele probably still producing reduced levels of the functional protein. Less severe phenotype (compared to *csn5a-1)* of the homozygous *csn5a-2* mutants and of double mutants *csn5a-1* x *csn5a-2* could be due to this. Our data are in agreement with those reported recently by Gusmaroli *et al.*, (2007). This group has been able to detect wild-type *CSN5A* transcript using different combinations of gene specific primers, although we could not amplify the full length cDNA most likely due to the large insertion within the gene. In the *csn5a-2* homozygous line it may be possible for the intron containing the insert to be correctly spliced out, resulting in a full length *CSN5A* transcript, though at low efficiency. Removal of T-DNA in an intron has been observed previously for other T-DNA homozygous lines (Gusmaroli *et al.*, 2007).

In *ppi* low levels of *csn5a* mutant transcript (which is 11nt shorter) and a truncated polypeptide were detected. The truncated polypeptide, which is predicted from the

sequence of the mutant gene to be 299 aa, compared with the wild-type CSN5A which is 357 aa, could potentially have some partial function as all of its known functional domains are intact as judged by the sequence.

CSN5 metalloprotease JAMM motif consists of an upstream glutamate (E) followed by His-x-His-x (10)-Asp (where x indicates any residue) (Cope *et al.*, 2002). The MPN domain is 112 aa in length and span from the 57th to the 168th residue (UniProtKB 15/06/2007). The JAMM motif is from the 145th to 157th aa with the conserved glutamate at 80th position. A nuclear export (NES) signal **L** D R K **L** L E **L** L **W** in CSN5, has been shown to be important in nuclear-cytoplasmic shuttling of various proteins in a CRM1 (chromosomal region maintenance 1) dependent manner, by the CSN5 in animal cells (Tomoda *et al*, 2002). This NES is also intact in the *ppi* sequence. However, the loss of a 57 amino acid fragment from the C-terminus could be influencing the CSN5A function. Perhaps a conformational change may be affecting its nuclear localization or retention and perhaps this could be the reason that the truncated protein was seen more prominently in a cytoplasmic protein extraction. However, subcellular location of the truncated protein and its association with the CSN complex has to be investigated further.

As its molecular nature is different from the other two alleles (since it produces a truncated protein), and also as it is in a different genetic background, *ppi* could be an additional resource to gain insights into the function of the CSN. The following chapters describe detailed phenotypic characterization of the three mutants, their responses to hormone and light signalling and a comparative proteomic analysis of the mutants.

Chapter 5

Genetics analysis and phenotypic characterization of the *csn5a* mutants

5.1 Introduction

5.1.1 Informative mutants in *Arabidopsis*

Genotype is the specific allelic make-up or the genetic constitution of an individual, usually with reference to a specific character under consideration. An initial and essential step in *Arabidopsis* mutant analysis is establishing its inheritance patterns to understand the number of genetic loci involved and the dominance of the mutation relative to the wild-type (Meinke and Koornneef, 1997). Mendelian segregation analyses are performed in this respect, by crossing the mutant to the wild-type parent line and determining the phenotype distribution ratios in the F2 segregating population.

The phenotype is a measurable trait in an organism that is expressed in a subset of the individuals within the population. Epigenetic and environmental factors can affect some phenotypes; however, the primary control is by the inherited genotype. Hence, it is possible to deduce genotype by analysing easily observable phenotypes and complex phenotypes help hypothesizing about the functioning of individual genes. Thus, characterization of the phenotype of the mutant is the next essential step as it provides independent evidence as to the functional importance of the gene. *Arabidopsis* research community is in process of saturating the genome with informative mutants.

5.1.2 Phenotypes of CSN subunit mutants

Loss-of-function mutants in all the six PCI-domain subunits of CSN (CSN1 to CSN4, CSN7 and CSN8) are characterized by the *cop/det/fus* (for *constitutive photomorphogenic/ deetiolated/ fusca*) phenotype. Their pleiotropic phenotype consists of short hypocotyl, and open cotyledons in any light condition, the accumulation of anthocyanin, purple seed coat (*fusca*), the expression of light-induced genes in the dark, insensitivity to auxin and growth arrest at the seedling stage (Wei *et al,* 1994; Dohmann *et al*, 2005).

Mutants of the two MPN-domain subunits CSN5 and CSN6 do not show this severe *cop/det/fus* phenotype, nor do they arrest growth when young. Several early studies with

transgenic mutants and recent studies with T-DNA insertion alleles, describe *csn5* as a partial *cop/det* phenotype with open and enlarged cotyledons, no apical hook in the dark and reduced apical dominance with semi-dwarf stature of the adult plant (Kwok *et al,* 1998; Schwechheimer *et al*, 2001; Gusmaroli *et al*, 2004). CSN5 and CSN6 are encoded by small gene families, consisting of two genes in each. As demonstrated using null double mutants, and single mutants, the two members of each family are known to act redundantly and specifically, *CSN5A* and *CSN6A* are the predominant members as the *csn5b* and *csn6b* mutants display subtle phenotypes, under specific light conditions only (Dohmann *et al*, 2005; Gusmaroli *et al*, 2007). The double mutants of both subunits mimic the severe phenotype of previously described *cop/det/fus* mutants and up regulation of light induced genes.

5.2 Results

The *ppi* mutant was originally discovered based on its striking pleiotropic phenotype. The objective of this part of my thesis is to detail the various aspects of the pleiotropic phenotype of *csn5a* mutants. After mapping the *ppi* mutation to *CSN5A* gene, we incorporated the *csn5a-1* and *csn5a-2* alleles into the research at the beginning of the third year of my PhD (February 2005). By this time, only an initial characterization of *csn5a-2* had been published by Gusmaroli and co-workers in November 2004 (Gusmaroli *et al*, 2004). The *csn5a*-1 null mutant was first published in July 2005 (Dohmann *et al*, 2005). A detailed phenotypic characterization and genetics analysis of *ppi* were performed in the first year of my PhD. The phenotypic analysis was repeated including all three *csn5a* allelic mutants and the corresponding wt. The data for *ppi* and Ws-2 obtained for the second analysis matched the results of the previous comparative study between *ppi* and Ws-2. Results of the second analysis are reported in this chapter.

All the experiments reported in this chapter with *ppi* have been conducted with homozygous mutant plants obtained after a third back cross to the wild type Ws-2 (Chapter 4). All experiments with the *csn5a-1* and *csn5a-2* mutants were conducted with plants homozygous for the T-DNA insertion obtained after a single back-cross to the wild-type Col-0. Seeds for all five lines were harvested from plants grown simultaneously in a controlled environment growth room (SANYO) under long-day conditions (16 h light). The phenotypic differences between the mutants and the corresponding wt were analysed. Statistical tests were performed to using Minitab version 12. Difference between *ppi* (Ws-2

back-ground) and the two T-DNA mutants (Col-0 back-ground) were not analysed because the ecotype differences could obviously be influencing the comparison. However, differences between *csn5a-1* and *csn5a-2,* which are from the same ecotype, were analysed.

5.2.1 The *csn5a* mutations are recessive and monogenically inherited

The mutants were crossed to the wild-type parent lines (*ppi* with Ws-2 and the two T-DNA insertion lines with Col-0). The F1 heterozygous plants all had the wild-type phenotype indicating the mutations are recessive relative to the wild-type.

Seeds from at least three individual F1 plants for each mutant line were collected separately and grown under long-day (16 h light) conditions. The distribution ratio of wild-type to mutant phenotype was analyzed when the seedlings were 10 days old.

The segregation data were statistically analyzed using the Chi-square Goodness of Fit test, χ^2_1 (http://faculty.vassar.edu/lowry/csfit.html). The null hypothesis (H_0) being the wild-type and the mutant phenotypes segregate at 3:1 ratio, if the mutant phenotype is due to a single gene locus. H_0 was rejected at 95% confidence when the *P*-value ≤ 0.05.

Table 5.1. Segregation of *csn5a* mutant phenotype in the F2 generation.

Cross	Observed number of mutants	Observed number of wild-type	Total no. of plants	χ^2_1	*P*-value	Mutant %
ppi x Ws-2 (1)	233	631	864	1.68	0.1949	26%
ppi x Ws-2 (2)	525	1593	2118	0.05	0.8215	25%
ppi x Ws-2 (3)	514	1642	2156	1.48	0.2238	24%
ppi x Ws-2 (4)*	1051	3440	4491	6.08	0.0137	23%
csn5a-1 x Col-0 (1)	228	715	943	0.29	0.5902	23%
csn5a-1 x Col-0 (2)	401	1307	1708	2.03	0.1542	23%
csn5a-1 x Col-0 (3)	165	515	680	0.19	0.6580	24%
csn5a-2 x Col-0 (1)	511	1693	2204	3.77	0.0522	23%
csn5a-2 x Col-0 (2)	241	745	986	0.13	0.7184	24%
csn5a-2 x Col-0 (3)	183	584	767	0.47	0.4930	24%

Note: * for this particular line *P*-value < 0.05.

For all the lines analyzed, the phenotypes segregated closely to the expected ratio of 3:1 (wt: mutant) indicating that a single gene mutation is responsible for the pleiotropic phenotype (Table 5.1).

Segregation data for all crosses except one were statistically accepted. The fourth line for the *ppi* x Ws-2 cross (*) gave a *P*-value < 0.05 which is a significant result to reject H_0. However, considering the number of total individuals scored (4491), the closeness of the observation to the expected ratio (3.3: 1 wt: mutant phenotype), and the fact that all the other three lines for the cross gave statistically valid results, H_0 was not rejected. The slight deviation from the expected ratio could be due to the loss of *ppi* seedlings due to some adverse growth conditions or perhaps the proximity of the wild-type seedlings affected their establishment. The *ppi* mutant show 100% germination under normal growth conditions (Chapter 6) and therefore this could not be due to a seed-germination phenotype of the mutant.

Our data on the two T-DNA insertion mutants support the previously reported confirming the monogenic inheritance of the mutations, based on the segregation of wt to Kanamycin resistance conferred by the T-DNA insertion at 3:1 ratio (Gusmaroli *et al*, 2004). Segregation analysis experiments and the consistency of the *ppi* phenotype over more than five generations suggest that the recessive mutation, at least in *ppi*, is stable.

5.2.2 Phenotypic characterization of *csn5a* mutants

Phenotypic differences between the mutants and corresponding wt were analyzed at the seedling stage, at the onset of flowering, and at the mature reproductive stage.

Seedling data were obtained using seedlings grown vertically on nutrient agar (section 2.2.1.2) under long-day (LD) photoperiod (16 h light), or in the dark. Rosette leaf measurements were obtained from 20 or 25-d old plants at the onset of flowering, grown on compost, under LD, in a controlled environment growth room. Mature plant data were obtained from 43-d old adult flowering plants grown in the controlled environment growth room as above.

All the data sets were tested for statistical significance using Two Sample t-Test with H_0 = no significant difference in the measurements between the two data sets compared. When *P*-value ≤ 0.05, the null hypothesis was rejected with 95% confidence and the reverse applied.

5.2.2.1 The pleiotropic *csn5a* mutants display a range of defects in seedling, vegetative, and reproductive organs.

Seedlings: All three mutants, *ppi*, *csn5a*-1 and *csn5a*-2 seedlings were paler in green colour compared to the wt (Fig. 5.1a). The hypocotyl lengths of *csn5a-1* and *csn5a-2* at 5-days were significantly shorter than that of the wt although at 10-days there was no significant difference (Fig. 5.1b). Hypocotyls of *ppi* were not significantly different from wt at 5-days or 10-days. In replicate experiments with *ppi* occasionally small differences were seen in hypocotyl length compared to wt. These were not reproducible with carefully matched seed batches.

The primary root lengths of the mutants were slightly shorter than the wt at 5-days, but significantly higher than the wt at 10-days (Fig. 5.1c).

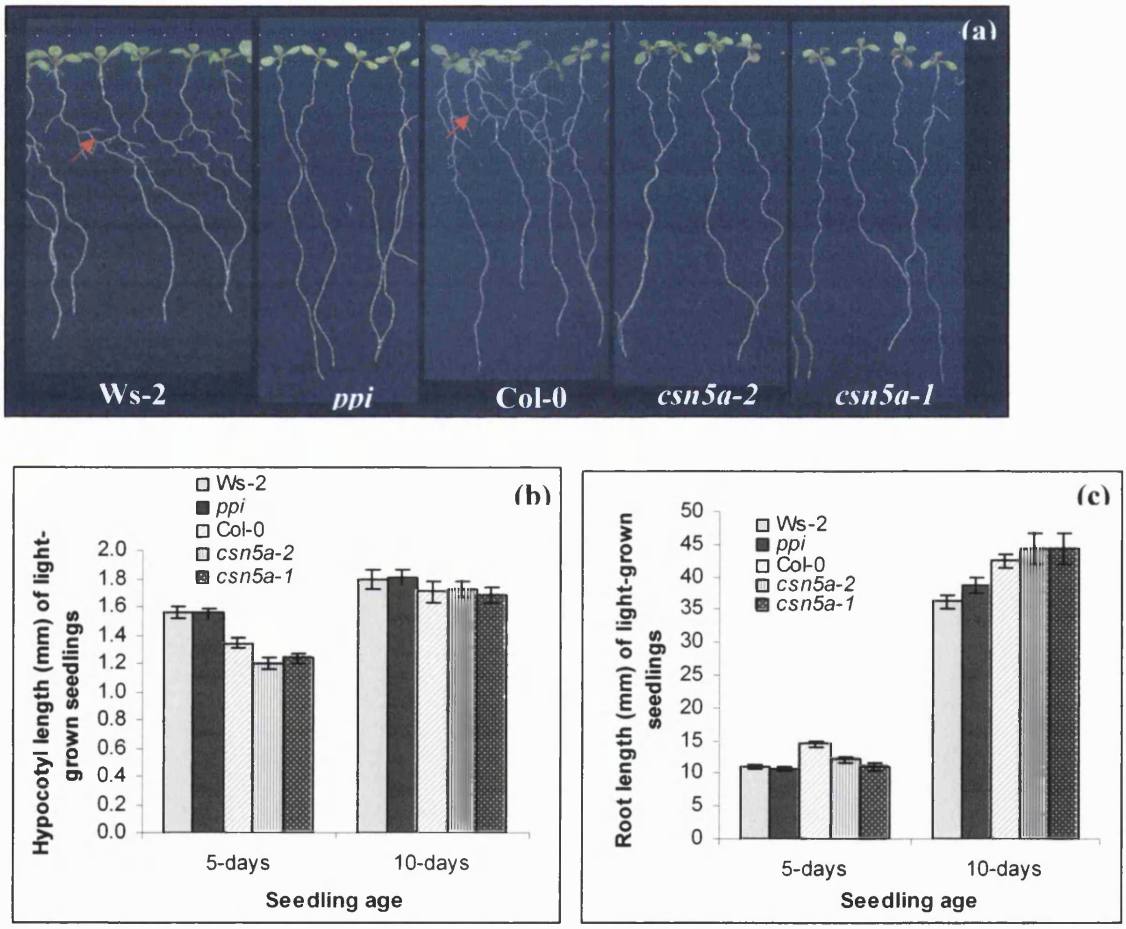

Fig. 5.1: Phenotype of seedlings under long-day (16h light) conditions. Seedlings were grown vertically on nutrient agar, and scanned at 5- and 10-days.
(a) 10-day old seedlings. Red arrows indicate the lateral roots (LR) in the wt. The mutants have reduced number of LRs.
(b) Mean hypocotyl lengths of seedlings
(c) Mean length of the primary roots. Roots of the mutants were significantly longer than the wt at 10 days.
(Error bars = SE of the mean. n= 15 – 20)

When grown in the dark, the mutant seedlings had indistinct apical hooks and partially opened and expanded cotyledons (Fig. 5.2a). The hypocotyl lengths of both 3-day old- and 5-day old mutant seedlings were significantly shorter than the wt (Fig. 5.2b).These features are consistent with the partial *cop/det* phenotypes.

The primary root lengths of the mutants were not significantly different at 3-days, though, the *csn5a-1* and *csn5a-2* apparently had slightly longer roots than Col-0. At 5-days in the dark, *ppi* primary roots were significantly longer than the wt (Fig. 5.2c). This trend was not observed for the other two mutant alleles. At 3-day and 5-day time points the seedlings were totally lacking lateral roots.

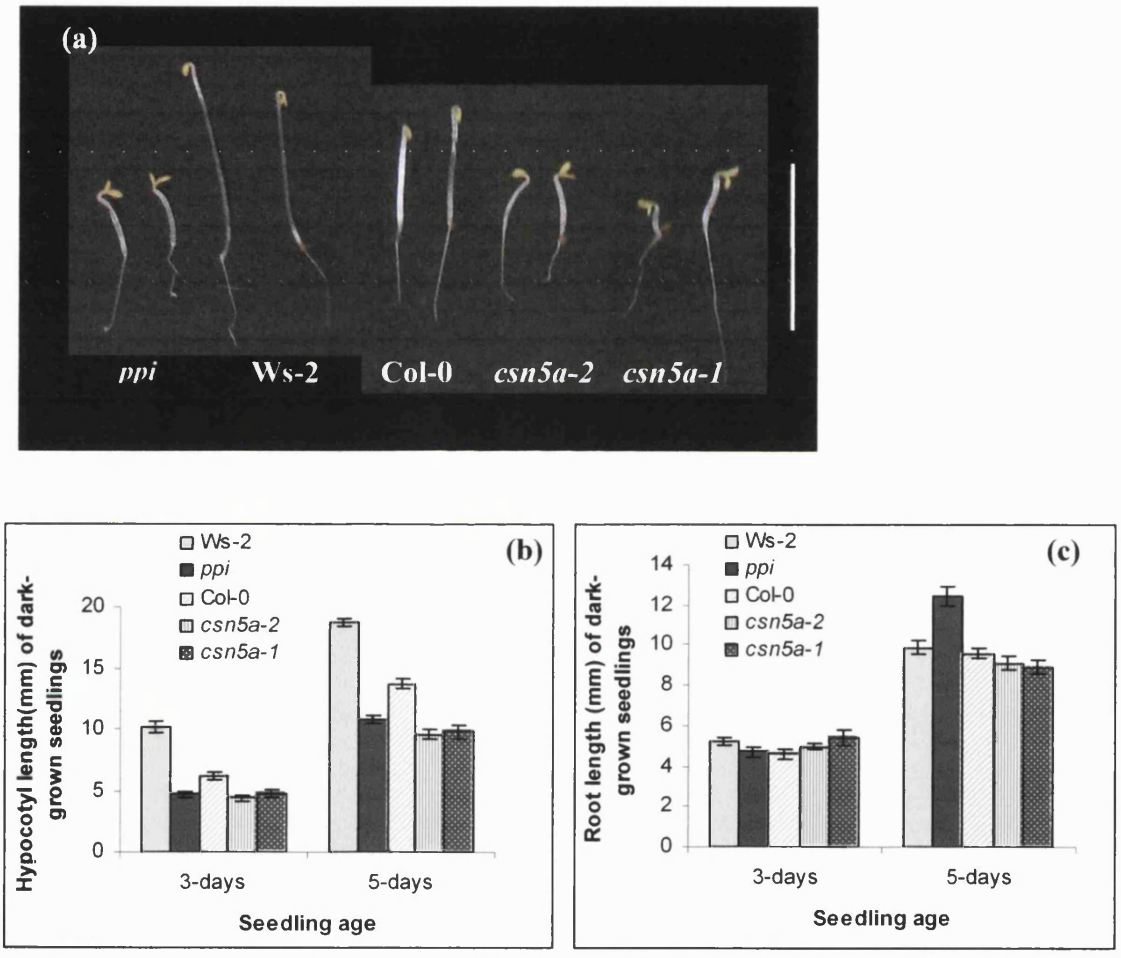

Fig. 5.2: Phenotype of seedlings grown in the dark.
Seedlings were grown vertically on agar for 3 or 5 days in the dark.
(a) Representative 3-day old seedlings.
(b) Mean hypocotyl lengths of seedlings. Mutants had significantly shorter hypocotyl lengths compared to the wt.
(c) Mean length of the primary roots. Root lengths of 5-day old ppi were significantly higher than the wt.
(two sample t-test, $p < 0.05$; n= 15 – 20; Error bars = SE)

Lateral roots and root hairs: As seen from the 10-d old light-grown seedlings (Fig. 5.1a; Fig. 5.3a) the *csn5a* mutants had substantially reduced number of lateral roots, that were shorter compared to the wt. In the 5-d old seedlings grown on nutrient agar under long-day conditions, mutants had significantly fewer root hairs compared to the wt and were generally shorter than the wt. (Fig. 5.3b; Table 5.2). The number of root hairs was significantly different between *csn5a-1* and *csn5a-2*.

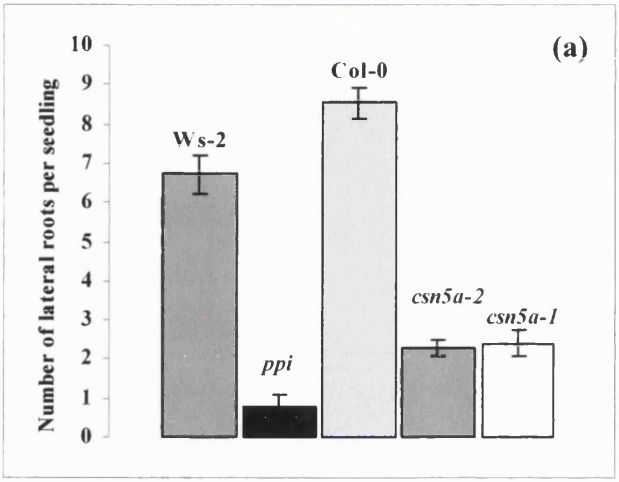

Fig. 5.3: Root phenotype of seedlings grown under long-day conditions
(a) Mean number of lateral roots per plant. (Error bars = SE of the mean; n=15)
(b) Phase contrast image of root hair containing regions of primary roots of 5-d old seedlings. Mutants have significantly reduced number of root hairs compared to the wt. Photographs were taken under the same magnification.

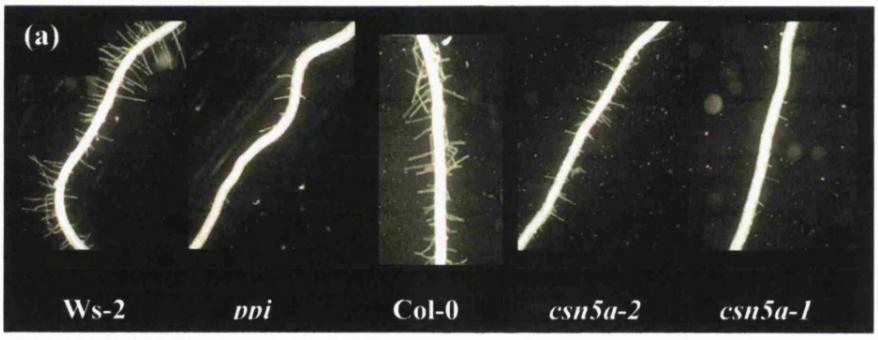

Juvenile and mature plants: At the initiation of flowering (and any other time in the life cycle), under long-day conditions the mutants had compact rosette as displayed by the reduced rosette leaf petiole- and leaf blade-lengths compared to the wt (Fig.5.4).
At the mature adult stage the mutant plants under long-day conditions were semi-dwarf, with reduced apical dominance (Fig.5. 5), pale green leaves and a reduced number of flowers in all inflorescences. The mutants had significantly reduced primary and secondary stem lengths (Fig.5.5a.). The number of secondary stems was higher in *ppi* and *csn5a-2* than the wt. It was lower in *csn5a-1* than Col-0 or *csn5a-2* (Fig. 5.5b).
The mutants had significantly reduced number of flowers in all inflorescences (Fig. 5.6a; 5.7a). All the floral organs appear normal in the mutants. However, the overall size of the flower is reduced in the mutants, with the reduction strongest in the *csn5a-1* null mutant (Fig. 5.7b & c).

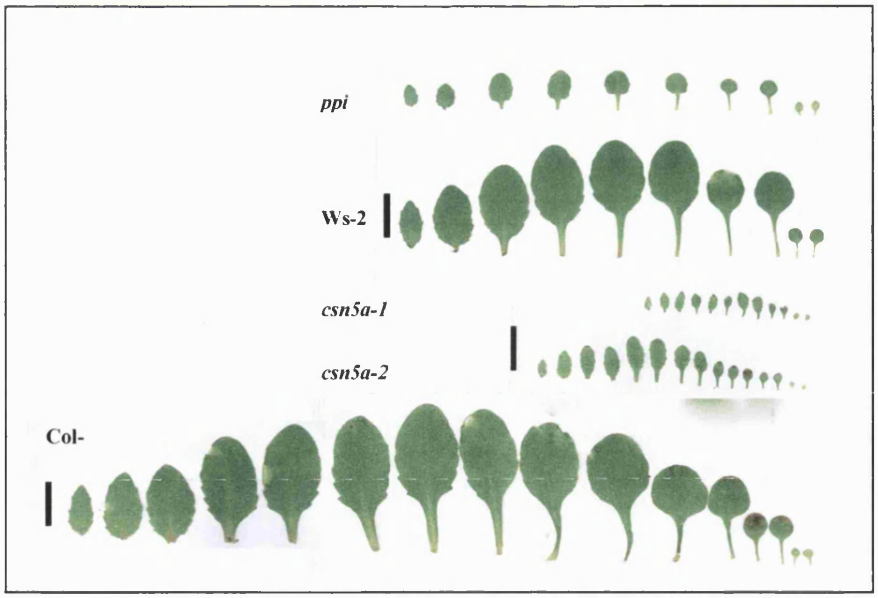

Fig. 5.4: Leaf-line-ups

Representative rosette leaves (youngest at the left end) and cotyledons (towards the right end) of 20-d (Ws-2 ecotype) and of 25-day (Col-0 ecotype) plants at the onset of flowering. Bars= 10 mm

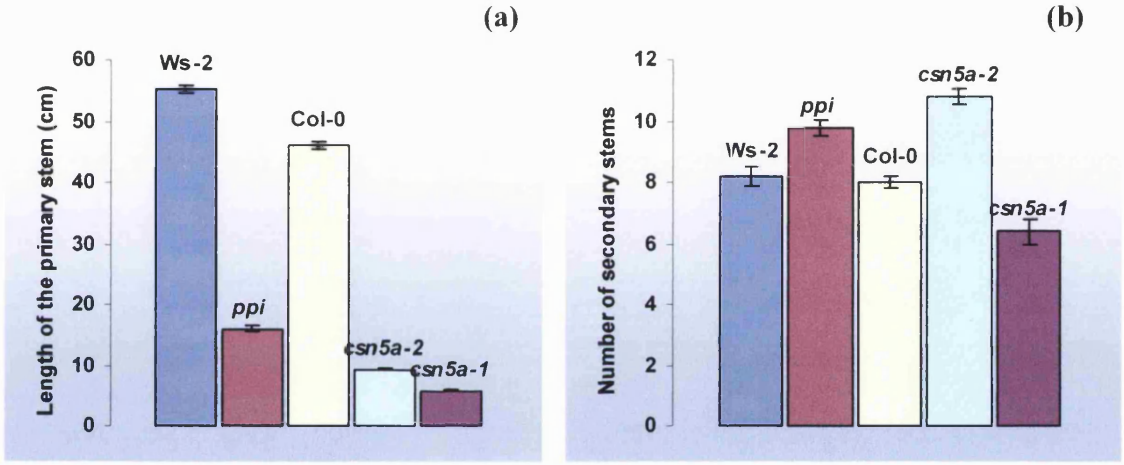

Fig. 5.5: Stem lengths and numbers of 43-d old adult plants
(a) Mean length of primary stem is significantly reduced in the mutants compared to the wt. (b) Number of secondary stems per plant are significantly higher in the mutants compared to the wt. (Two sample t-test, $p<0.05$; n=10-15); Error bars = SE

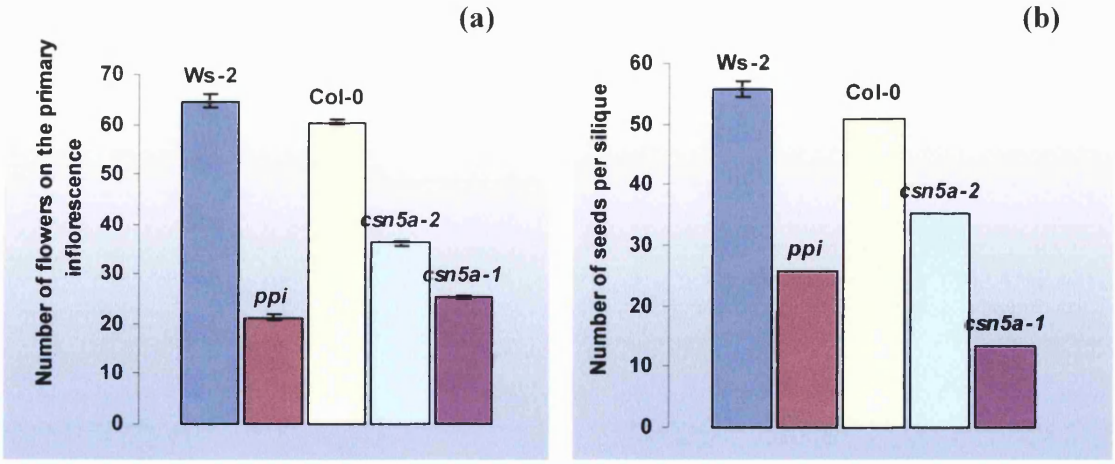

Fig. 5.6: Phenotype of flower- and seed numbers
(a) Mean number of flowers on the primary stem is significantly reduced in the mutants compared to the wt, and between *csn5a-1* and *csn5a-2*. (b) Mean number of seeds per silique is significantly reduced in the mutants compared to the wt and between *csn5a*-1 and *csn5a-2*. (Two sample t-test, $p< 0.05$; n=10-15; Error bars = SE)

The silique dimensions in the mutants are reduced as determined by the reduced pedicel and pod lengths (Table 5.2, Fig. 5.7d).

Average number of seeds per silique is reduced in the mutants (Fig. 5.6b). However, the weight per seed of *ppi* and *csn5a-1* is higher than the wt. Weight per seed in *csn5a*-2 was only slightly reduced compared to the wt (Fig. 5.7 e-i).

Table 5.2 Phenotypic characterization of *csn5a* mutants compared with wild-type

Data presented as mean ± standard error of the mean (SE). Sample number (n) is given.

	Ws-2	***ppi***	**Col-0**	***csn5a-2***	***csn5a-1***
Seedlings					
Number of root hairs in 5-d old seedlings (number per view; n=15)	76.6 ± 1.9	11.3 ± .84	60.4 ± 1.7	29.9± 1.8	9.1 ± 0.7
Plant at transition to flowering (n=10)					
Length of the largest leaf (mm)	23.6 ± 0.73	8 ± 0.33	27.2±0.66	10.8±0.61	6.7 ± 0.47
Width of the largest leaf (mm)	17 ± 0.73	7 ± 0.365	18.3± .49	6.5 ± 0.43	4 ± 0.37
Petiole length of the largest leaf (mm)	8 ± 0.66	3 ± 0.45	9 ± 0.33	5 ± 0.43	2 ± 0.47
Mature flowering plants (n=10-15)					
Primary stem length (cm)	55.3 ± 0.73	16 ± 0.54	46 ± 0.56	9.3 ± 0.2	5.84 ± 0.09
Secondary stem length (cm)	44 ± 2.35	12.3 ± 0.91	9.0 ± 0.29	6.3 ± 0.34	5.0 ± 0.25
Number of flowers on primary inflorescence	65 ± 1.32	21 ± 0.58	60 ± 0.51	36 ± 0.66	25 ± 0.51
Number of flowers on secondary inflorescences	54 ± 0.37	13 ± 0.51	45 ± 0.32	20 ± 0.37	21 ± 0.32
Length of siliques (mm)	19 ± 1.87	11 ± 1.31	18 ± 0.79	15 ± 0.21	10 ± 1.08
Length of pedicels (mm)	15.0 ± 0.49	6.0 ± 0.37	12.0±0.55	7.0 ± 0.24	4.0 ± 0.2
Number of seeds per silique	56 ± 0.37	26 ± 0.51	51 ± 0.37	36 ± 0.37	13 ± 0.4
Weight per seed (µg) (average of 100 seeds)	17.75	30.22	19.16	16.82	23.23

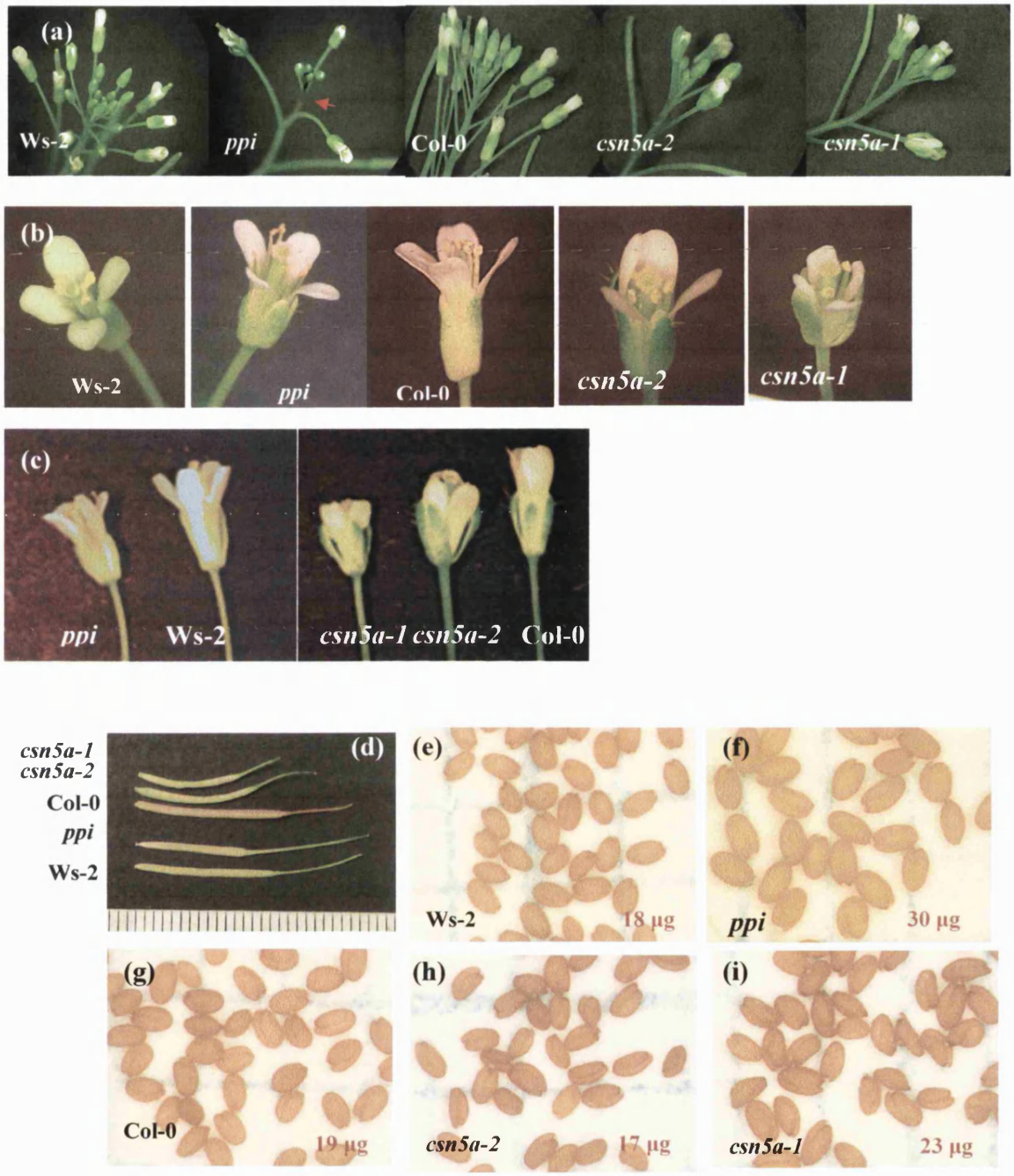

Fig. 5.7: Floral and seed phenotype.
(a) Primary inflorescences of 43-day old plants. The *csn5a* mutants have reduced number of flowers. The red arrow is pointing to the purple patch in *ppi*. The *csn5a-1* and *csn5a-2* plants do not have an equivalent pigmented zone.
(b), (c) Individual flowers. The mutant flowers are reduced in size, *csn5a-1* flowers being the smallest.
(d) Siliques from 43-day old plants
(e) – (i) Seeds. Photographed under the same magnification.

5.2.2.2 The responses of *csn5a* mutants to photoperiod.

An experiment was performed to examine the response of *csn5a* mutants to different day-lengths. Plants were simultaneously grown in controlled environment growth rooms (SANYO) with photoperiod short-day (8h day/ 16h night= 'SD'), long- day (16 h day/ 8h night = 'LD') and extra long-day (20 h day/ 4 h night = 'ELD') at 22 ± 2 °C day- and 18 ± 2 °C night temperatures. Timing of transition to flowering and also the phenotypic differences under different day-lengths were analysed.

5.2.2.2.1 Time to flowering

The number of rosette leaves at the time of flowering initiation and the number days to the transition are presented in Table 5.3.

Table 5.3 Flowering time under different photoperiods

Data presented as mean ± SE of mean; n = 7-17

	Ws-2	*ppi*	Col-0	*csn5a-2*	*csn5a-1*
Rosette leaves at flowering under SD	28.7 ± 0.27	13.1± 0.39	56.2 ±0.47	49.7± 0.91	27.3± 0.59
Days to flowering under SD	43.8± 0.86	38 ± 0.32	56 ± 0.2	63 ± 0.32	44 ± 0.32
Rosette leaves at flowering under LD	8.14 ± 0.26	7.9 ± 0.26	13.9 ±0.26	13.1± 0.26	10.1± 0.26
Days to flowering under LD	20.1 ± 0.26	20.7 ±0.29	28 ± 0.22	26 ± 0.22	27.1 ± 0.4
Rosette leaves at flowering under ELD	5.9 ± 0.14	4.1 ± 0.26	5 ± 0.22	4.8 ± 0.14	4.6 ± 0.2
Days to flowering under ELD	14.3 ± 0.18	16.7 ±0.18	16.6±0.36	17.6 ±0.29	19.7 ±0.36

Under SD the number of rosette leaves at flowering initiation in *ppi* and *csn5a*-1 were significantly less than the respective wt (Table 5.3). *csn5a*-2 was different from the wt to a lesser extent. *csn5a*-1 had fewer rosette leaves than *csn5a*-2 at flowering. The number of days to flowering initiation under SD in *ppi* was slightly less than for the wt. The number of days to flower under SD was slightly more for *csn5a*-2 than the wt and it was much less for *csn5a*-1 than the wt.

Under LD the number of rosette leaves at flowering was not different between *ppi* and *csn5a*-2 and the respective wt. *csn5a*-1 had less rosette leaves at flowering under LD than

the wt. The number of days to flowering initiation were similar in *ppi* and wt, and was only slightly different between *csn5a*-2, *csn5a*-1 and the wt.
Under ELD, the number of rosette leaves at flowering was not significantly different between the mutants and the respective wt. Under ELD, the days to flowering initiation was only slightly different between the mutants and the respective wt.
The accepted way of timing the transition to flowering is based on the number of leaves at flower initiation. With our data, no significant difference in transition to flowering under LD or ELD was observed. However, this was not the case under SD as *ppi* and *csn5a*-1, and *csn5a-2* to a lesser extent, showed significantly reduced number of rosette leaves compared to their respective wt indicating an early flowering phenotype at least under SD, although this was not as clearly reflected in the number of days to flowering. This is indicating important links between light regulation of developmental stages and the CSN.

5.2.2.2.2 Phenotypic differences of *csn5a* mutants in response to photoperiod

Under SD (Fig. 5.8a), 43-d old plants of *ppi*, *csn5a*-1 and *csn5a*-2 have quite similar phenotypes with a markedly reduced rosette size compared to their respective wild-type. Ws-2 and *ppi* are both flowering. *csn5a*-1 is smaller than *csn5a*-2.
Under LD (Fig. 5.8b), the phenotype of all three mutants are slightly different from one another. *csn5a*-1 is the smallest and is flowering. *csn5a*-2 is discernibly larger than *csn5a*-1 while *ppi* is clearly larger than the other two mutants. To an extent the phenotype of *ppi* appears to be a reflection of the earlier flowering time of Ws-2 ecotype compared to the Col-0 as can be seen by comparing the wild-type plants.
Under ELD (Fig. 5.8c & d), the phenotype of *ppi* is quite different from the other two mutant alleles. Under these conditions *ppi* has a profusion of secondary inflorescences and is significantly taller than when grown under SD or LD. To an extent this is also reflected in the wild type Ws-2. however, the *csn5a*-1 and *csn5a*-2 mutants are much more severely dwarfed under ELD conditions compared with LD or SD in spite of the fact that the wild-type Col-0 is taller and bushier under ELD compared with LD and SD. Under ELD, *ppi* had better root development than the other two alleles.

These observations suggest significant effects of the ecotype and photoperiod dependent differences between the null *csn5a*-1, reduced-expression *csn5a*-2 and the *ppi* mutant which produces a truncated CSN5A protein.

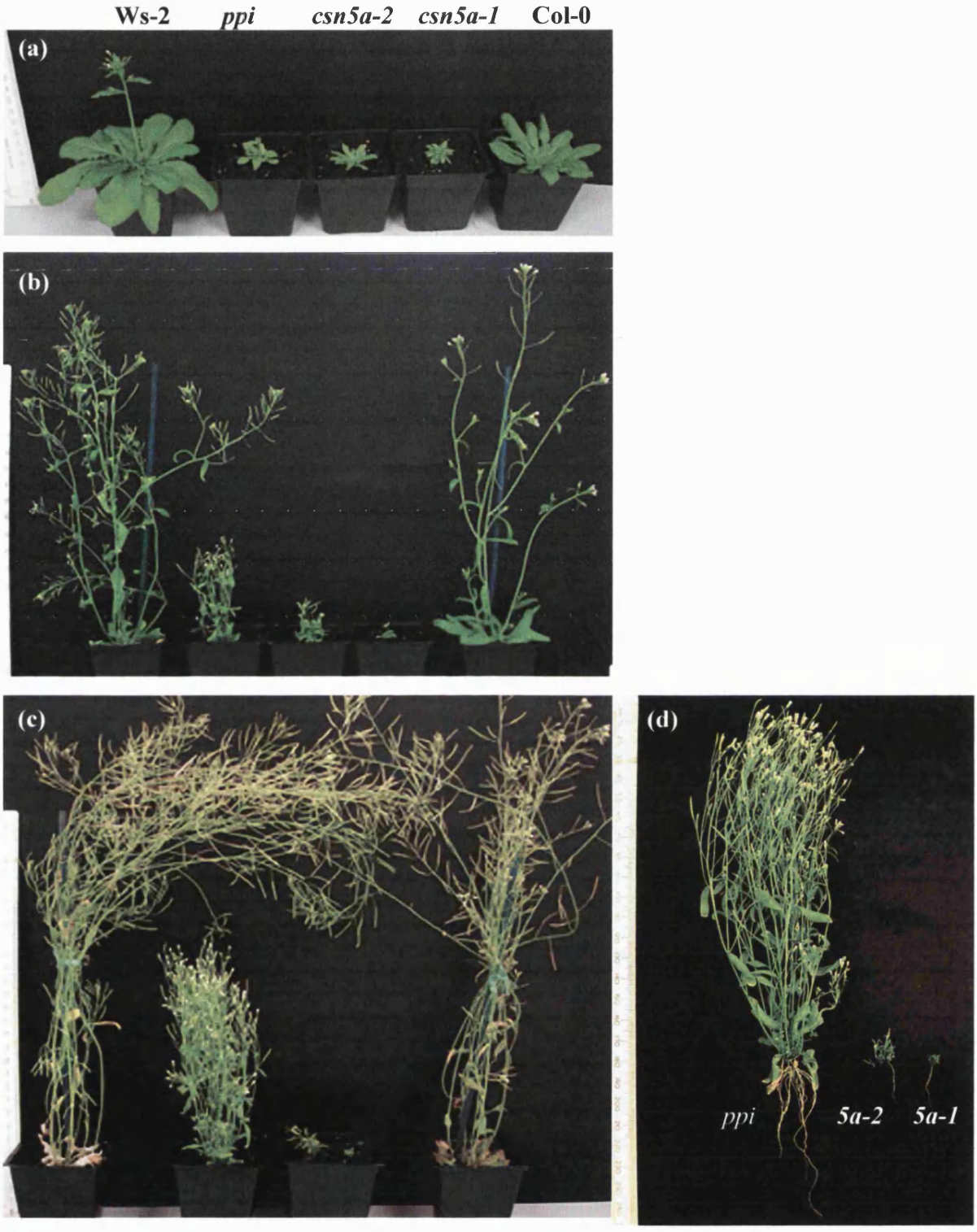

Fig. 5.8: Effect of photoperiod on phenotype
45-day old plants grown simultaneously in controlled environment growth rooms (SANYO) under different day-length regimes.
(a) Plants grown under SD (8h day/16h night)
(b) Plants grown under LD (16h day/ 8h night)
(c) Plants grown under ELD (20h day/4h night).
(d) The three *csn5a* mutants grown under ELD.

5.2.2.3 The purple patch in the *ppi* inflorescence is due to accumulation of anthocyanin.

Of the three *csn5a* mutants, the purple pigmented patch in the inflorescence is unique to *ppi*. Purple or red pigmentation in vegetative tissue is usually due to higher than basal levels of anthocyanin, and is indicative of stress response.
Undergraduate student Sharon Casey (2004) characterized the pigmented zone in *ppi*. This experiment was done before the *ppi* was mapped to *CSN5A* and before the other two mutant alleles were incorporated into our study, and those were therefore not included.

Initially, the pigment responsible for the purple patch in *ppi* was identified spectrophotometrically as being anthocyanin based on a defining UV absorbance maximum at 535nm in solvent extracted samples.
Anthocyanin accumulation in *ppi* pigmented zones and the equivalent regions of wt plants were determined by a method described by Lange *et al* (1971) and compared.
Analysis of the pattern of accumulation showed that anthocyanin concentration in *ppi* increased steadily with time, mature adult plants having the highest levels and the levels in primary inflorescences being consistently higher than in the secondary inflorescences. A comparison between anthocyanin levels in the primary inflorescence of *ppi* and that of wild-type, showed that the level in *ppi* was x30 times higher than the wt as *ppi* and Ws-2 had 37.9 and 1.1relative units of anthocyanin per μg of fresh weight of plant tissue respectively.

5.2.2.4 The anthocyanin levels in *ppi* seedlings increased in response to sucrose or ABA induced stress.

Anthocyanin induction in 3-5 day old seedlings, by different concentrations of exogenous ABA and sucrose was analysed. When treated with exogenous sucrose or ABA, *ppi* was seen contained more pronounced anthocyanin levels than the wt seedlings and this trend was consistent across the assayed concentrations. Increased ABA or sucrose levels were accompanied by an enhancement of anthocyanin accumulation in both the wt and *ppi* but *ppi* produced much more anthocyanin than the wt as seen for the 100 μM ABA or 10% sucrose concentrations (Fig.5.9).

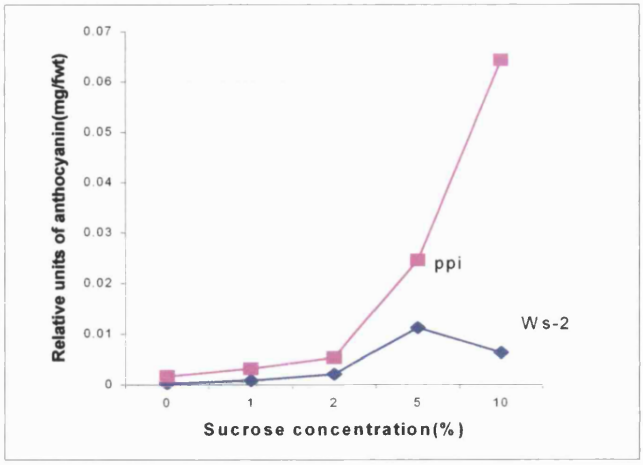

Fig. 5.9: Anthocyanin concentrations, induced through exogenous sucrose, in *ppi* and Ws-2 seedlings.

Each individual point refers to the mean concentration, obtained from 3 repeat experiments, of 14 seedlings, at different sucrose concentrations expressed as a % (w/v)
Data and figure were taken from Sharon Casey's project report (BSc 2004)

5.2.2.5 The *ppi* mutants have abnormal trichomes

The wt and the two T-DNA insertion mutant alleles have exclusively three-branched trichomes typical of *Arabidopsis*. In *ppi*, almost all the trichomes are two-branched, and smaller (Fig. 5.10). An occasional three-branched trichome is seen on ppi leaves.

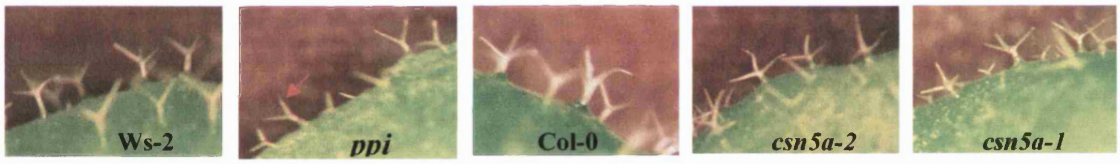

Fig. 5.10: Trichome phenotype of *ppi*
Leaf surface photographs showing trichomes. Red arrow indicates comparatively smaller trichomes with only two-branches, in *ppi*.
The others have *Arabidopsis* typical three-branched trichomes.
The photos were taken under the same magnification.

At the seedling stage, *csn5a-1* and *csn5a-2* have been reported to completely lack trichomes (Gusmaroli *et al*, 2007). We did not observe this with adult *csn5a-2* and *csn5a-1* plants, though it is possible that the number of trichomes may be less in the mutants compared to the wt. Our observations support the fact that the CSN has an important role in trichome formation and development in *Arabidopsis*. Further investigations are required to obtain a better picture of the CSN or CSN5 in regulating trichome initiation and development.

5.3 Discussion

In this chapter a detailed phenotypic characterization of the three *csn5a* mutants was reported. The phenotype of *csn5a* mutants as a whole, does not match any other *Arabidopsis* mutant phenotype. The observations reported here reflect the pleiotropic nature of the mutations in the *CSN5A* gene affecting the entire life cycle from seed germination to adult stages. This could be indicative of CSN function as a general regulator of many developmental and signalling pathways in plants.

5.3.1 The *csn5a* mutants may be showing an altered meristem determinacy leading to an overall reduction in organ size and numbers as a result of impaired CSN or CSN5 function.

One interesting feature of the phenotype is the reduction in the number of flowers in all inflorescences in the mutants. The size of the flowers as well as the numbers, in the *csn5a* mutants are reduced compared to wt, as shown by the smaller floral organs. When looking at the mutant phenotype closely, the reduced size and reduced numbers of organs are observed through out the entire plant morphology. Reduced size, particularly in aerial parts of the adult plant, is reflected in its striking semi-dwarf stature.

Organ size of a particular species is genetically determined. Inherited genetic mechanisms exist to maintain the meristematic competence or the ability to grow and divide of cells in organ primordia, in connection with developmental and environmental signals and in turn, define intrinsic organ size. In order to sustain growth, there is a steady state balance between the production of new cells in the meristems and their recruitment to form new organs/ tissues. This steady-state is persistent in *Arabidopsis* vegetative, root and inflorescence meristems in which the growth is indeterminate, and the size of these organs are primarily influenced by the environmental factors. In the case of floral meristems, which are determinate, the meristem is genetically programmed to stop producing new cells at a specific developmental stage, and such organs have predetermined size and shape (Sablowski, 2007).

The organ size is based on both the cell number and cell size. Processes such as polyploidy and endoreduplication affect the cell number. Factors influencing cell division also affect the organ size as larger organs usually have comparatively more cells. Phytohormones

such as ethylene and cytokinins influence cell expansion and therefore increase the size along the transverse axes. Gibberellins, auxins and brassinosteroids regulate expansion along the longitudinal axes and thereby greatly influence plant stature and organ size (Mizukami, 2001).

In *Arabidopsis*, *WUSCHEL* (*WUS*) and *SHOOT MERISTEMLESS* (*STM*) genes, in particularly *WUS,* are important in the establishment and maintenance of the shoot meristem (Sablowski, 2007). *CLAVATA* (*CLV*) regulates *WUS* expression and the meristem size is suggested to be stabilized by a *WUS/CLV* regulatory loop. *APETALA1/CAULIFLOWER* (*AP1/CAL*) and *LEAFY* (*LFY*) are key regulators of floral meristem identity. *LFY* also promotes determinacy. To maintain indeterminate inflorescence meristem, *AP1/CAL* and *LFY* must be activated only in the floral primordia. Expression of these in the inflorescence meristem is prevented by the *TERMINAL FLOWER1* (*TFL1*) gene. Specific combinations of MADS-domain proteins such as AP1, AP3, PISTILLATA (PI) and AGAMOUS (AG) control the target genes required for the development of a particular organ type. AG is prominent as it controls meristem determinacy probably by regulating WUS. *AINTEGUMENTA (ANT*) is another gene playing a role in maintaining meristematic competence organ primordia thereby helping to define intrinsic organ size. The molecular nature of meristematic competence is largely unknown and the signals triggering the related events are still not fully known. Localized increase in GA levels is thought to mediate meristem antagonizing by AG since AG activates GA biosynthesis. Cytokinins play a positive role in meristem maintenance. Increased GA levels and reduced sensitivity to cytokinins may contribute to termination of meristem maintenance (Sablowski 2007).

When considering the aerial features of the *csn5a* phenotype, reduction in numbers of flowers can be explained, in a way, by linking it to the reduction of the overall inflorescence length/size. Gradual termination of meristematic activity of the inflorescence meristem of mutants before the wt, would make it no longer capable of further growth, or to the extent of the wt. Supported by the observation that the *csn5a* mutants do not have any unusual organs as common for mutations in many meristem identity genes, the CSN function in regulating plant organ size could be considered as more generalized.

SCF E3 complexes regulate several aspects of floral development in *Arabidopsis* (Ni *et al* 2004). The F-box protein UFO (UNUSUAL FLORAL ORGANS) regulates multiple

aspects of floral development as a part of a SCF complex, including floral meristem identity and floral organ identity gene influencing the floral organ size and development. SCF^{UFO} E3 ubiquitin ligase complex has been shown to physically interact with the CSN (Schwechheimer, 2001). However, the *csn5a* mutants do not show the severe floral organ phenotype of *ufo* mutant, indicating other mechanisms are affected by the mutations.

There are several lines of evidence linking targeted protein degradation and organ size regulation. E3 ubiquitin ligases are more and more implicated in organ size control via meristem maintenance. Proteasome mediated degradation has been proposed to regulate organ size, by targeting negative regulators of meristem maintenance. SHA1, RHA2b and BB are non SCF-type E3 ubiquitin ligases expressed in meristematic regions, suggesting roles in meristem function (Sonada *et al,* 2007). Of these, the RING finger protein BB (BIG BROTHER) is of particular interest as it has fewer, smaller flowers, somewhat similar to those of *csn5a* mutants. It has been proposed as a plant specific central negative regulator of organ- particularly, floral organ- size (Disch *et al* 2006). BB has been demonstrated to limit organ size by "restricting the duration of the proliferative growth phase, gradually diminishing the cells' capacity for further growth and division, in dosage dependent manner". BB shows E3 ligase activity and is thought to be targeting factors that stimulate cellular growth and cell division. BB-GUS protein is produced in actively growing and proliferating regions of the plant and is itself rapidly turned over by proteasome mediated degradation. BB over expression causes reduction of overall size, and it has been shown to act independently of major phytohormones (Disch *et al*, 2006).

The CSN could be targeting yet unknown negative regulators via a SCF- or non-SCF pathway, so that in the *csn5a* mutants, the function may be impaired. On the other hand, rapid turnover of BB or another similar protein through the proteasome pathway may require CSN or CSN5, so that in the *csn5a* mutants, those proteins accumulate, leading to overall cell size and number reduction as seen with over expressed BB. In fact, the CSN has been shown to regulate the animal cell cycle inhibitor p27 (Tomoda *et al*, 2002). Impaired CSN function, particularly of CSN5 leads to accumulation of p27 resulting in cell cycle inhibition and severe growth reduction in animal systems. It is possible that similar mechanisms operate in *Arabidopsis*.

5.3.2 Some aspects of the pleiotropic *csn5a* phenotype could be due to altered light- and hormone responses

Involvement of auxin in root development has been known for a long time. In the young seedling, auxin synthesized in the primary leaves is transported to the root where it promotes the outgrowth of lateral roots (Bhalerao *et al*, 2002). Recently, involvement of shoot induced phytochrome in auxin regulation of root development was demonstrated, by demonstrating a role for phytochrome in regulating auxin distribution (Salisbury *et al*, 2007). Phytochrome affects at least a sub-set of its responses by manipulating seedling auxin distribution. Cryptochromes, too, have been implicated in modulating distribution of auxins (Canemaro *et al,* 2006). Phytochrome coordinates shoot and root development at least in part, by reciprocally regulating auxin gradients in aerial and root structures, and this may be the reason for the extensive overlap between light and auxin responses. Reduced apical dominance, reduced number and length of lateral roots, reduced number of root hairs are all related to auxin dependent responses. Exogenous auxins (IAA, NAA, 2, 4-D) promote lateral root initiation in *Arabidopsis* and the auxin transport inhibitor NPA, blocks the initiation. One critical point for auxin mediated LR initiation is the cell cycle regulation. (Fukaki *et al* 2005). Auxin inducible NAC1 transcription factor, which acts downstream of the auxin receptor TIR1, determines the number of lateral root primordia (Scheres *et al*, 2002).
Through auxin receptor F-box TIR1/AFB proteins, auxin promotes ubiquitination of AUX/IAA proteins which are repressors of auxin responsive transcription through $SCF^{TIR1/AFB1/AFB2/AFB3}$ E3 ubiquitin ligase complexes (Teale *et al*, 2006). With transgenic *csn5a* mutants, it has been demonstrated that they have reduced auxin responses due to the reduced function of SCF^{TIR1}, leading to stabilization of AUX/IAA proteins (Schwechheimer *et al*, 2001). Some aspects of the *csn5a* mutants such as the reduced apical dominance of the adult plants and reduced lateral root and root hairs of the seedlings could be at least partially due to stabilizing of AUX/IAA leading to reduced auxin responses as a result of impaired CSN function.

The *csn5a* mutants have a fewer and shorter root hairs compared to the wt. Some genes such as *WER (WEREWOLF), TTG (TRNASPARENT TESTA GLABRA), GL2 (GLABRA2)* are involved in non-root hair cell differentiation in the root epidermis. *TTG, GL2* also affect trichome formation in the shoot epidermis (Grierson and Schiefelbein, 2004). *WER/GL1, TTG, GL2* control epidermal hair formation in opposite ways in the root and in

the leaf as these are required for the formation of non-root hair cells in the root and trichome bearing cells in the leaf. Ethylene and auxin promote root hair cell differentiation. Auxin resistant *dwf*, and *axr2* (auxin, ethylene and ABA resistant) mutants show a root hairless phenotype. Deficiency of phosphate, iron, manganese and zinc, particularly, phosphates, lead to an increase in the density and length of root hairs.
Again, a link between light and root hair formation has been demonstrated by Salisbury *et al* 2007. Null *phyB* mutants have elongated root hairs suggesting enhanced aux signals mimicking the *hy5* mutant. HY5 regulates auxin signalling by targeting negative regulators of the pathway. A possibility of phyB moderating auxin signalling through the HY5 pathway has been suggested (Salisbury *et al*, 2007). The CSN is linked to HY5 function as it regulates COP1 which targets HY5 for degradation in the dark.

Altered responses of the *csn5a* mutants to photoperiod indicate the importance of CSN in light responses.
An allelic difference of *ppi* compared to the other two mutant alleles was implicated in its response to ELD. Whereas, *csn5a-2* and *csn5a-1* showed severe growth retardation, *ppi* somehow bypassed the same. The truncated CSN5A protein in *ppi* must be helping the plant to overcome the size reduction under ELD at least partially, as it could not rescue the phenotype entirely.
In adult plants red: far-red ratio and photoperiod are the two main light signals affecting growth and development of the adult *Arabidopsis* (Fankhauser & Casal, 2004). Both are detected mainly by phytochromes. phyA detects the day length to accelerate flowering. phyB active form (Pfr) is needed to limit growth in stems, petioles etc. Cryptochromes are important in photoperiod induction of flowering. Mutations leading to accumulations of phytochromes or cryptochromes will lead to altered light sensitivity.

Transition to flowering in plants is regulated by multiple signals such as day length, temperature, nutrient availability and phytohormones GA and cytokinin, through multiple pathways. The pathways converge to regulate the meristem identity genes including *AGAMOUS LIKE20 (AGL20)* and *LFY* which in turn regulates the floral homeotic genes to produce floral organs (Taiz and Zeiger, 2002). Phytochromes and cryptochromes are involved in the photoperiodic pathway of flower initiation. Red light absorbing phyB inhibits flowering while far-red light via phyA and blue light via cryptochromes in concert with circadian clock, promotes expression of the *CONSTANS* (*CO*) transcription factor that promotes flowering through other genes by increasing the expression of *LFY* (Blazquez

2000). In an autonomous pathway, *Arabidopsis* responds to an internal signal of producing a fixed number of leaves resulting in reduction of *FLOWERING LOCUS C (FLC)* gene expression that inhibits *LFY* gene expression. A GA dependent pathway is required for early flowering and for flowering under short days (Taiz and Zeiger, 2002).

In the *csn5a* mutants one or more of these pathways could be altered leading to a flowering time phenotype under SD. Altered sensitivity to different light signal perception and signalling pathways could be the reason. CSN5 is important in the transition to flowering from the juvenile stage. The effect is apparently stronger in the short-days and subtle under LD or ELD, indicating CSN5 function is more essential under SD. Based on our observations it could be hypothesized that CSN5B and not CSN5A is more important under LD or ELD with respect to flowering. On the other hand, it could be that neither CSN5A nor CSN5B are particularly important under LD/ELD, but could be affecting a pathway important only under SD.

5.3.3Two-branched trichomes and anthocyanin pigmentation in *ppi* could be indicative of CSN5 specific function.

Increased flavonoids, particularly anthocyanins, are seen in plants under environmental stress, due to their function as scavengers of Reactive Oxygen Species (ROS) produced during such conditions. In addition, anthocyanin levels increase when environmental or developmental alterations increase a plant's susceptibility to the environment (Winkel-Shirley, 2002). Light, temperature, nutrient status, wounding, pathogen attack and water deficiency regulate accumulation. Accumulation of anthocyanin is a result of transcriptional up-regulation of anthocyanin metabolic genes, primarily by blue light, via an anion-channel dependent pathway (Noh and Spalding, 1998). One well studied anthocyanin biosynthetic gene is the *TTG1* (*TRANSPARENT TESTA GLABRA1*), a WD40 repeat protein, which controls the synthesis of DFR (dihydroflavonol-4-reductase) in the anthocyanin biosynthetic pathway. The *ttg1* mutant displays pleiotropic effects in which leaves and stems are glabrous, lacking purple pigmentation, lacking mucilage in the seed coat, and with extra root hairs on atrichoblast cells (Walker *et al*, 1999).
Prolonged presence of anthocyanin in vegetative organs including petioles, veins, stems, lower layers of shade leaves and dormant seeds are linked to a lack of carbon assimilation as a primary function in tissues or inactive growth stages (Steyn *et al*, 2002). Thus,

accumulation of the pigment in selective vegetative regions in *ppi* could be indicative of defective carbon assimilation, or, more likely, inactive growth of the cells.

Trichomes, or the shoot epidermal hairs, are important in protecting the plant against insect herbivores, UV light, reduced transpiration and increasing tolerance to freezing. Trichome cells are initiated from protodermal cells at the base of the young leaf. Once the mitotic cell division is stopped, four endoreduplication cycles resulting in 32C DNA content cause the trichome cell to enlarge in size. Two consecutive branching events co-aligned with the plant's basal-distal axis results in typical three-branch trichomes of *Arabidopsis*. *GLABRA1, TRANSPARENT TESTA GLABRA1 (TTG1), GL3, ENHANCER OF GLABRA3 (EGL3), TRIPTYCHON (TRY)* and *CAPRICE (CPC)* are some genes important in trichome patterning, initiation and differentiation (Hülskamp, 2004). Factors affecting the number of endoreduplication cycles affect the number of trichomes as well as trichome branching. Plant hormones and protein degradation, among others, play important roles. GA promotes endoreduplication cycles. In the constitutive GA responsive mutant *spindly (spy)* trichome DNA content is 64C. The GA synthesis mutant *ga1-3* has no trichomes. The *KAKTUS/UPL3* gene that encodes a putative HECT-domain type E3 ubiquitin ligase involved in regulating progression of endoreduplication (Downes *et al*, 2003). *CONSTITUTIVE PATHOGEN RESPONSE5* (*CPR5*) gene is implicated in programmed cell death as well as controlling progression of endoreduplication cycles. Over expression of the cell cycle inhibitor ICK/KRP in *Arabidopsis* also leads to reduced ploidy levels and early trichome cell death (reviewed in Hülskamp, 2004).

The number of trichome branches depends on the ploidy level of the cell. The reduction in ploidy level results in reduced number of branches. One mutant of particular interest with relevance to our research data is *cpr5-2* which has abnormal trichomes "smaller than wt, with transparent 'glassy' appearance, and have only two branches- and have elevated PR gene expression (particularly PR5 and PR2) in the absence of pathogens (Clarke *et al*, 2001). In fact, *ppi* apparently mimic *cpr5-2*, in the sense it has abnormal trichomes very much resembling those of *cpr5-2*, and it has enhanced levels of PR5 and PR2 as revealed by 2-D gel electrophoresis (Chapter 7).

The other interesting relevance is the *TTG1* and possibly other related proteins involvement in both trichome initiation and anthocyanin biosynthesis. *ppi* shows accumulation of anthocyanin in selective areas of vegetative tissue.

Apparently, the *ppi* mutation in *CSN5A* could be affecting a subset of interrelated genes whose products are components of pathways including systemic acquired resistance (SAR), programmed cell death, trichome patterning/branching, endoreduplication cycles and cell division, anthocyanin biosynthesis/accumulation. Or it could be affecting one component which is a point of convergence of those pathways. CSN5 or CSN5A could itself be the point of convergence, and perhaps the truncated CSN5A in *ppi* is non-functional at least in this respect where as it could be partially functional in the CSN related functions. Careful consideration of these ideas and further molecular, biochemical studies on *ppi* would give valuable insights into CSN5 specific functions that may or may not involve the CSN holo-complex.

Chapter 6

Responses of *csn5a* mutants to phytohormones, localized nitrates and light.

6.1 Introduction

6.1.1 The CSN mediates plant responses to phytohormones by regulating the activities of cullin-RING E3 ubiquitin ligases.

As an adaptation primarily for their sedentary life style, plants have to adjust responsiveness to requirements regarding growth and development or those imposed by environmental conditions. Such adjustments are brought about by precise and specific regulation of components in biochemical and signal transduction pathways, and one method this is achieved is by ubiquitin-mediated proteolysis via the 26S proteasome (Chapter 1). In *Arabidopsis*, >1300 genes (~5% of the genome) are said to encode components of the 26S proteasome pathway (Sullivan *et al.*, 2003). The targeted protein is polyubiquitinated by enzymatic action and eventually recognized, and degraded by the 26S proteasome. Substrate specificity in the pathway is determined by the E3 ubiquitin ligases (E3 ligases). Of the types of E3 ligases found in *Arabidopsis*, SCF (Skp1, Cdc53p/Cullin, F-box protein) type E3 ligases are the best characterized. The SCF complex contains four components: a cullin subunit, usually CUL1, SKP1-like adaptor protein, and F-box domain protein that binds the target substrate and the fourth component RBX1, a small RING-finger protein that interacts with the cullin and the E2. SCF complexes are particularly important in regulating plant responses to hormones, light and pathogen resistance (Schwechheimer and Schwager, 2004; Serino and Deng, 2003).

The CSN regulates the activity of SCF E3 ligases, as derubylation of the cullin subunit is mediated by the metalloprotease activity of the CSN5 subunit in the complex. This action is required for, and enhances the substrate ubiquitination by the SCF. The CSN has been shown to physically interact with SCF^{UFO}, SCF^{TIR1} and SCF^{COI1} which are involved in mediating floral identity, auxin responses and jasmonic acid responses respectively (reviewed in Serino and Deng, 2003). Many other SCF complexes, if not all, have the potential to be regulated by the CSN. As the CSN has been shown to interact with almost all the cullins in *Arabidopsis*, it has the potential to regulate all cullin containing E3s (Gusmaroli *et al.*, 2007).

The CSN is a key regulator of many developmental pathways, and because of this it is possible that mutations in components of the CSN could result in phenotypes reflecting defects in more than one developmental pathway. In addition, there are emerging implications (Tomoda *et al.,* 2002, Kwok *et al.,*, 1998) of the functional importance of single- or subsets of CSN subunits, that may or may not be independent of the CSN complex and these contribute further to the range of phenotypes observed.
The CSN and its subunit involvement in the regulation of subcellular location of E3 ligases and other regulatory proteins has been suggested (Cope and Deshaies, 2003; Tomoda *et al.*, 2002). Nucleo-cytoplasmic partitioning is a way of controlling E3 activity. This function is of great significance, particularly with relation to COP1 (Yi and Deng, 2005; Cope and Deshaies, 2003). COP1 regulates the activity of transcription factors HY5, HYH, LAF1, HFR1 that are responsible for photomorphogenic response in light by targeting them for degradation in the dark. In order to bring about this regulation COP1 has to be nuclear localized in the dark. CSN is required for the nuclear retention or import of COP1 although the exact mechanism is not known.

Phytohormones are endogenous chemical growth regulators that have specific effects on plant growth at low concentrations (Teale *et al.,* 2006). Auxins, gibberellins (GA), cytokinins, ethylene, and abscisic acid (ABA) are the five major classes and brassinosteroids, jasmonates (JA), salicylic acid (SA) and small extra cellular signalling peptides are also considered as plant growth regulators. Plants' responses to these signals are adjusted through selective proteolysis.
Regulated proteolysis in plant growth and development has been a topic for many recent reviews including Sullivan *et al.,* (2003), Moon *et al.,* (2004), Schwechheimer and Schwager, (2004). CSN functions in relation to plant development have been reviewed by Cope and Deshaies, (2003), Serino and Deng, (2003) and Wei and Deng, (2003). An account of implications of the CSN and the 26S proteasome pathway in regulating plant responses to various phytohormones and environmental stimuli is given below.

6.1.1.1 Auxins

Auxins are the main coordinative growth regulator in plants,, and their function is thought to be indispensable as no mutant fully lacking auxins have been reported yet, probably because such mutants do not survive (Teale *et al.,* 2006). The main bioactive auxin in plants is indole-3-acetic acid (IAA) which generates the majority of the auxin responses in the plant (Taize and Zeiger, 2002). Synthetic auxin analogs include 1-naphthaleneacetic

acid (NAA) and 2,4-dichlorophenoxyacetic acid (2,4-D). Polar auxin transport is an important component of auxin reponses and this is the only plant hormone that shows polar transport. IAA requires active transport across membranes whereas NAA is freely diffusable. Polar auxin transport can be inhibited by NPA (1-*N*-naphthylphthalamic acid) by preventing auxin efflux (Ruegger *et al,*1997).

Auxin response is primarily mediated by selective protein degradation. The *AUX/IAA* genes encode proteins that negatively regulate gene expression. The ARF (AUXIN RESPONSE FACTOR) transcription factors bind to an auxin responsive element (ARE) in the promoters of auxin responsive genes. The binding of AUX/IAA proteins to ARFs at the basal auxin levels blocks the transcription of auxin responsive genes. When auxin levels are increased due to external or internal stimuli, AUX/IAA proteins are targetted for 26S proteasome mediated degradation by SCF^{TIR1} E3 ubiquitin ligase. SCF^{TIR1} has been shown to interact directly with the CSN (Schwechheimer *et al,* 2001). It is possible that other F-box proteins such as those related to the TIR1, namely ABF1 (Auxin binding F-box protein1), ABF2 and ABF3 could be parts of other SCF complexes that have roles in specific auxin responses. Impaired CSN or CSN5 function would lead to stabilization of AUX/IAA proteins and hence, reduced auxin response.

6.1.1.2 Gibberellins

Gibberellins (GAs) are a large family (about 126 known so-far) of tetracyclic diterpenoid compounds derived from the *ent*-gibberellane ring. Only a few GAs (GA_1, GA_3, GA_4 and GA_7) are biologically active (Taiz and Zeiger, 2002). GA mediated processes include stem elongation, especially in dwarf and rosette species and grasses, seed germination promoted by breaking dormancy, transition to flowering, sex determination and fruit set (Taiz and Zeiger, 2002).

GA signalling is primarily moderated by the DELLA-domain proteins (GAI, RGA, RGL1, RGL2 and RGL3 in *Arabidopsis*) which are transcriptional regulators and suppress the GA responsive gene expression at basal GA levels (Peng *et al,* 1997, Silverstone *et al,* 1997). SPY protein (SPINDLY) is a negative regulator of GA response and an activator of DELLA proteins. Binding of GA to receptors GID1 and related proteins (Nakajima *et al.*, 2006, Ueguchi-Tanaka *et al.,* 2005) triggers the degradation of DELLA proteins via the ubiquitin 26S proteasome pathway through the F-box protein SLY (SLEEPY) via the SCF^{SLY1} in *Arabidopsis* (Fleet and Sun, 2005).

DELLA proteins are a point of intersection for several hormone signalling pathways. Auxins promote GA dependent degradation of DELLAs in the root (Fu and Harberd, 2003) and ethylene inhibits DELLA degradation (Achard *et al.*, 2003).

6.1.1.3 Cytokinins

Cytokinins are N^6-substituted amino purines and the predominant plant cytokinin is zeatin. It can occur as the free base (the bioactive form) or as riboside- or ribotide-conjugates (Taiz and Zeiger, 2002). Regulation of cytokinin is mainly through irreversible degradation by cytokinin oxidases and also by interconverting among free-base and the nucleotide/nucleoside form.

Cytokinins are regulators of cell division. They also regulate morphogenesis of shoots and roots, chloroplast maturation, cell enlargement and senescence. Cytokinins promote cell expansion in leaves and cotyledons. Ratio of auxin to cytokinin is important in differentiation of cultured plant cells into either roots or buds.

Auxins and cytokinins regulate the cell cycle and are both required for cell division. Auxins and cytokinins regulate the cell cycle by controlling the activity of cyclin dependent kinases (CDKs). Cytokinins are able to stimulate cell division by enhancing CYCD3 (a D-type cyclin) function. Increased levels of endogenous cytokinins lead to enhanced expression of *KNAT1 & STM* genes which are transcription factors in the regulation of meristem function.

Over expression of cytokinin catabolic genes reduce the level of cytokinin resulting a strong retardation of shoot development due to a reduction in cell proliferation rate in the SAM.

Opposite roles of cytokinin are observed in regulation of cell proliferation in root and shoot meristems (Taiz and Zeiger, 2002). Cytokinins produced in the stem nodes have been shown to release axillary buds from apical dominance (Tanaka *et al*, 2006).

A link between ubiquitin-proteasome pathway and cytokinin has been demonstrated. Mutants of RPN12a- proteasome lid subunit, have shown reduced sensitivity to cytokinins, auxins and expression of cytokinin induced genes even in the absence of the hormone (Smalle *et a*l, 2002). Recently a new cullin1 mutant, *cul1-6*, which has impaired SCF function, was shown to have altered sensitivity to cytokinin (Moon *et al,* 2007).

6.1.1.4 Ethylene, brassinoteroids (BR), abscisic acid (ABA) and jasmonates (JA)

Plants responses to ethylene, BRs, ABA and JA are also regulated at least partially by proteolysis.

The gaseous plant hormone ethylene mediates fruit ripening, seed germination, leaf and petal abscission, organ senescence, and responses to stress. The transcription factor EIN3 promotes ethylene regulated gene expression (Guo and Ecker, 2003). Ethylene stabilizes EIN3. In the absence of the hormone, EIN3 is degraded by the proteasome via $SCF^{EBF1/EBF2}$. In mutations where EIN3 is stabilized, the plants show constitutive ethylene response or constitutive triple response.

SCFs degrade repressors of auxin, GA and ABA responses. In the case of ethylene, SCFs degrade positive regulators in the absence of ethylene.

The BRs are steroid growth regulators in plants and are recognized by the plasma membrane receptor kinase BRI1. BR biosynthetic and response mutants are defective showing dwarfism, sterility and photomorphogenesis in the dark. BZR1 is a positive regulator of BR signalling, and in the absence of BR it is phosphorylated and degraded via the 26S pathway in the cytoplasm. BRs promote accumulation of BZR1 by dephosphorylation and preventing degradation (Molnàr *et al.,* 2002).

ABA protects developing plants from drought stress. ABA induces growth arrest of seedlings under stress. This action depends on the expression of the transcription factor ABI5 which accumulates in response to ABA. ABI5 is ubiqutinated and subsequently degraded by the 26S proteasome (Sullivan *et al.,* 2003)

Jasmonates or JA [(+)-7-iso-Jasmonic acid (JA), precursor OPDA and other oxylipins] are important signals in mediating responses to stress induced by wounding, UV, ozone exposure, drought, insect/pathogen defence and they also regulate fruit ripening, root growth, pollen development and anther dehiscence (Devoto and Turner 2005).

COI1 (Coronatine Insensitive1) is related to the auxin receptor TIR1 and is required for JA mediated responses. COI1 is a part of SCF^{COI1} and CSN regulates SCF^{COI1} activity. JA have been implicated in signal cross-talk with other hormones. Ethylene and JA promote final steps of floral development. In apical hook development JA and ethylene antagonizes each other. JA signalling negatively regulates the expression of salicylic acid (SA)-responsive genes in *Arabidopsis* (Devoto and Turner, 2005).

6.1.2 Plant's responses to light

In *Arabidopsis* three types of photoreceptors, namely phytochromes, cryptochromes and phototropins are used to monitor the light environment. With the help of these photoreceptors, plants sense and respond to changes in irradiance, wavelength or the quality of light, direction and photoperiod (Fankhauser and Casal, 2004).

Phytochromes (phyA to phyE) absorb red (600-700 nm) and far-red (700-750 nm) light. Although they are considered the red/far-red photoreceptors, phytochromes also absorb over the entire visible spectrum and participate in blue light perception too.

Phytochromes exist in two photoconvertible isoforms. Pr absorbs maximally in the red region and Pfr absorbs maximally in the far-red region. Absorption of red light promotes Pr conversion to the Pfr, the active form. This process is reversed by far-red light. Activation of phytochromes results in a conformational change in the molecule that exposes nuclear localization signal and facilitates nuclear translocation (Nagatani 2004, Chen *et al.,* 2005).

phyA is responsible for the majority of the far-red light responses including inhibition of hypocotyl elongation, opening of cotyledons, accumulation of anthocyanin and far-red light pre-conditioned blocking of greening (Yang *et al.,* 2005). phyB to phyE predominantly mediate light responses under continuous red and white light.

Phytochromes are also important for triggering of seedling de-etiolation and throughout the entire plant life. They control vegetative architecture, apical dominance and timing of reproductive development (Salisbury *et al.,* 2007).

phyA is the only light labile phytochrome. phyA controls the far-red high irradiance response (FR-HIR) that brings about seedling de-etiolation in continuous far-red light. They also act in a second distinct signalling mode – responsible for the very low fluence response (VLFR) on the entire visible spectrum and this is important for seed germination and as a seedling emerges from the soil and detects light for the first time (Fankhauser and Casal, 2004). In adult plants phyA is required to detect day length to accelerate flowering.

phyB-E mediate responses to continuous red-light and are responsible for the R/FR reversible reaction (Taiz and Zeiger 2002). phyB is the major receptor in mediating de-etiolation in response to red-light- but multiple phytochromes participate in this response. phyB active Pfr form is required to limit growth in stem, petioles etc (Fankhauser and Casal, 2004).

Cryptochromes (cry1 and cry2 in *Arabidopsis*) are UVA/blue light receptors (320 – 500 nm). They play key function during de-etiolation under blue light and photoperiod controlled induction of flowering. cry1 is more important under high light intensities. cry2

is more important in low light irradiance and is light labile. Phytochromes (mostly phyA) too mediate inhibition of hypocotyl growth in blue light. Cryptochromes are important in blue light regulated gene expression, anthocyanin accumulation and day-length dependent induction of flowering (Taiz and Zeiger, 2002).
Phototropins (phot1 and phot2 in *Arabidopsis*) absorb blue light and mediate specific responses including phototropism, stomatal aperture and chloroplast movements. Phytochromes and cryptochromes are also involved in this response, but phototropins are the primary photoreceptors (Fankhauser and Casal, 2004).

Hormone and light signalling pathways interact at many points. Recent work by Salisbury *et al.,* (2007) demonstrated that phytochromes (combined phyA and phyB) to control the distribution of auxin between the shoot and the root. Subjecting *Arabidopsis* to low R:FR that reduces active Pfr, resulted in an accumulation of auxin responsive gene promoter DR5::GUS protein in the base of the hypocotyls. The plants had elongated hypocotyls and fewer lateral roots. Cytokinin and light signalling pathways are suggested to intersect with cytokinins being linked to blue light responses too. HY5 has been suggested as a point of convergence between cryptochrome and cytokinin signalling pathways in *Arabidopsis* (Vandenbussche *et al*, 2007).

Some SCFs have been implicated in light responses. F-box proteins EID1 and AFR are important in phyA mediated responses and are known to be regulated by the circadian clock. It is suggested that SCF^{AFR} degrades a repressor of light responses in preparation for light signals at dawn. SCF^{EID1} probably degrades positive regulators of phyA. (reviewed in Sullivan *et al*, 2003).
COP1, in addition to its role in degrading HY5 and functionally related transcription factors, is known to mediate degradation of phyA. Work by Yang *et al.,* (2005) has shown that the bHLH transcription factor HFR1 which is regulated via COP1 is required for both phyA mediated far-red and cryptochrome mediated blue light responses. Cryptochromes too, have been shown to directly interact with COP1 (Yang *et al*, 2001; Wang *et al*, 2001). The *hy5* mutant shows longer hypocotyls than the wt under all light qualities and HY5 is an example of a downstream component required for both the phytochrome and cryptochrome signalling pathways. *COP/DET/FUS* gene products act downstream of the phytochromes and cryptochromes proving existence of signalling elements common to both classes acting both positively and negatively (Fankhauser and Casal, 2004).

6.2 Results

Responses of the *csn5a* mutant seedlings to a range of growth regulators, localized NO_3^- and different light qualities were studied in comparison to corresponding wild-types (wt). It was already suggested that *csn5* mutants were defective in auxin responses because various aspects of the phenotype are consistent with this. The objective of this part of my project was to identify any alterations in responses to a wide range of stimuli. I chose to do this with seedlings because it is far more practical to do this with seedlings than with mature plants.

As in the case for the phenotype characterization (Chapter 5), ecotype differences were expected between *ppi* and the two T-DNA insertion alleles. These were noted but not pursued unless a drastic change was observed. I focussed attention on analysing the differences between the mutants and the corresponding wt, and between mutants from the same ecotype.

Typically, seedlings were grown in nutrient agar, as described in Section 2.2.1.2 Growth response assays were conducted as described in section 2.2.2. The root and hypocotyl lengths are presented as a % of the untreated control unless otherwise stated, for convenience of interpretation of results. The differences mentioned here, were statistically significant (Two Sample t-Test; P-value < 0.05; n > 15).

The growth response assays with auxins, NPA and localized nitrates were performed by Katherine Downes working under my day to day supervision for her BSc final year research project (2006).

6.2.1 The *csn5a* mutants display altered responses to auxins

IAA is rapidly degraded in *Arabidopsis* agar medium, but has been shown to be stabilized by an antioxidant such as butylated hydroxyl toluene (BHT) (Paciorek *et al.*, 2005). Therefore, the growth medium contained 10 mg/ml BHT.

Low concentrations of IAA (0.01 & 0.1 μM) promote hypocotyl elongation in Ws-2 (Fig.6.1a). In contrast, *ppi* hypocotyls were significantly shorter than the untreated control at 0.1uM IAA and above. Concentrations of IAA that were growth enhancing for wt were inhibitory to *ppi* and there was greater inhibition of hypocotyl elongation by IAA in *ppi* than in the wt at higher IAA concentrations. Col-0 hypocotyl growth was inhibited at all the concentrations tested. The *csn5a*-1 and *csn5a*-2 mutants behave differently to each other. Hypocotyls of *csn5a*-1 were significantly longer than the untreated control at the two lowest concentrations of IAA, and while there was some inhibition of hypocotyl elongation

at the two highest concentrations it was not as great as in the wild type. In contrast, *csn5a*-2 showed slightly greater IAA inhibition of hypocotyl elongation than the wt.
Roots of *ppi* and the T-DNA mutant alleles respond to IAA in different ways compared with their respective wild types (Fig.6.1b). *ppi* showed greater inhibition of root elongation growth by IAA at all concentrations tested, whereas the other two alleles showed less inhibition of root elongation.

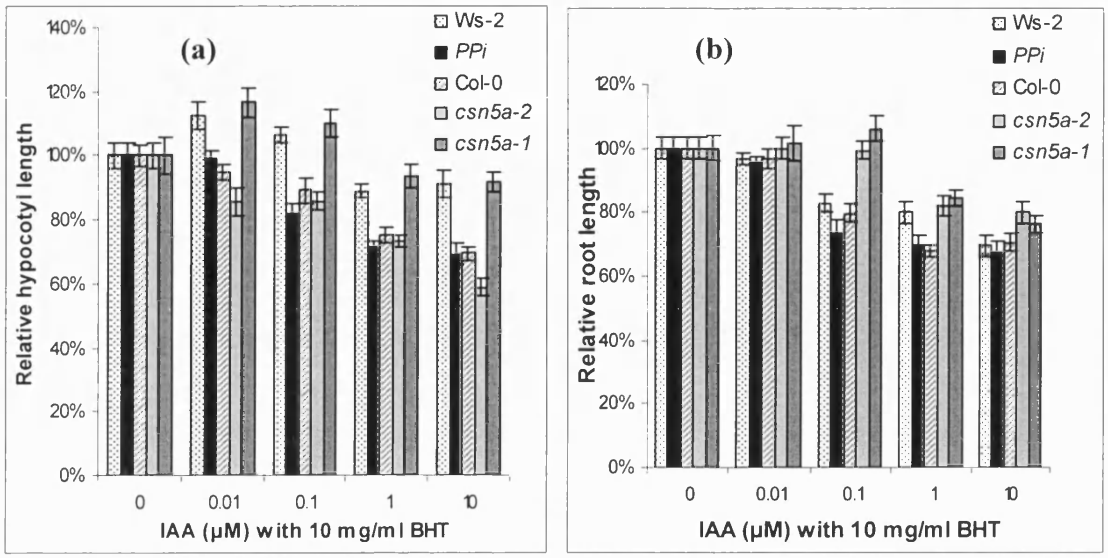

Fig.6.1: Response of seedlings to IAA
The mutant and wt seedlings were grown under long-day conditions for 5 days on agar plates containing either no hormone or a range of IAA concentrations. The medium contained 10 mg/ml BHT to prevent rapid degradation of IAA.
The mean hypocotyl or root lengths are presented here as a percentage of the untreated control.
(a) Mean hypocotyl length as % untreated
(b) Mean root length as % untreated
Error bars represent the SE; n > 15

Hypocotyl elongation of *ppi* was enhanced at 2, 4-D concentration of 0.01 µM and 0.2 µM, whereas for the wt 2, 4-D was inhibitory at these concentrations (Fig.6.2a). For *csn5a*-1 and *csn5a*-2, 0.01 µM 2, 4-D did not enhance growth as it did for Col-0. At the highest concentration tested (1 µM), all three mutants showed less inhibition of elongation growth than their corresponding wt.
2, 4-D strongly inhibited root elongation growth of the wt and mutants at 0.2uM and 1.0uM (Fig.6.2b). At 0.01uM roots of *ppi* did not show the same extent of growth inhibition as the wt while *csn5a*-1 and *csn5a*-2 were more sensitive than the wt at this point. No significant difference was observed between the mutants and wt at any other data point.

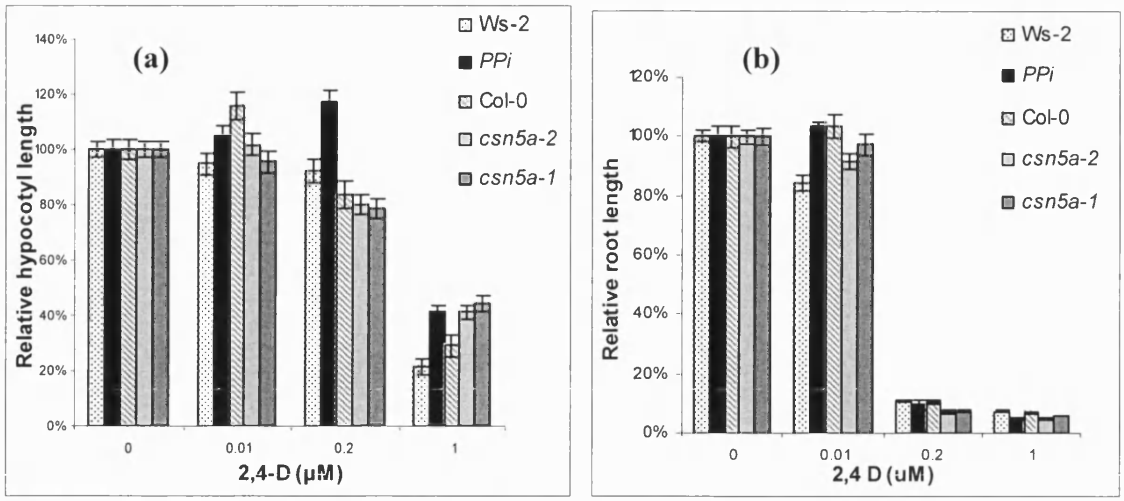

Fig. 6.2: Response of seedlings to 2, 4-D

The mutant and wt seedlings were grown under long-day conditions for 5 days on agar plates containing either no hormone or a range of 2,4-D concentrations.
The mean hypocotyl or root lengths are presented here as a percentage of the untreated control.
(a) Mean hypocotyl length as % untreated
(b) Mean root length as % untreated
Error bars represent the SE. n > 15

Both Ws-2 and *ppi* had slightly enhanced root growth at low NAA concentration (0.01 µM) and the rest of the concentrations were inhibitory (Fig. 6.3). *ppi* showed a slightly reduced response compared to the wt at 0.2 µM. Col-0 root growth was inhibited at all concentrations tested. Both, *csn5a*-1 and *csn5a*-2 had reduced sensitivity at 0.01 µM and 0.2 µM.

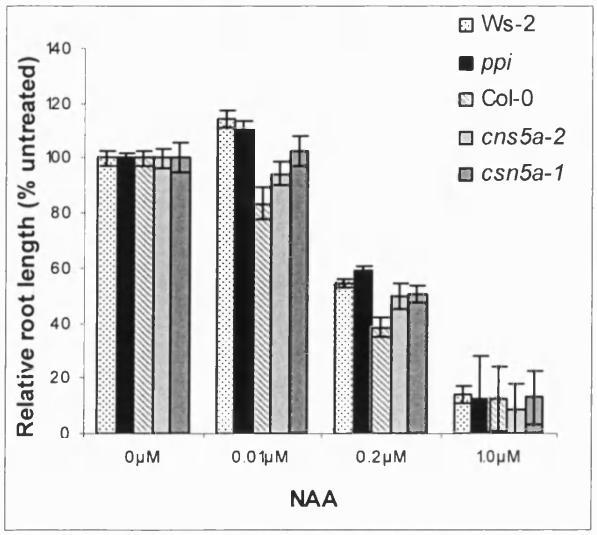

Fig. 6.3: Root response of seedlings to NAA

The mutant and wt seedlings were grown under long-day conditions for 5 days on agar plates containing either no hormone or a range of NAA concentrations.
The mean root lengths are presented here as a percentage of the untreated control.
Error bars represent the SE. n > 15

The polar auxin transport inhibitor NPA inhibits auxin efflux and that this alters auxin distribution. NPA is known to inhibit root elongation. *ppi* root growth was more severely inhibited that that of the wt at 10 μM and 20 μM NPA (Fig. 6.4). *csn5a*-1 was more strongly inhibited than the wt at all concentrations tested and *csn5a*-2 was more strongly inhibited than the wt at 5 μM and 10 μM NPA.

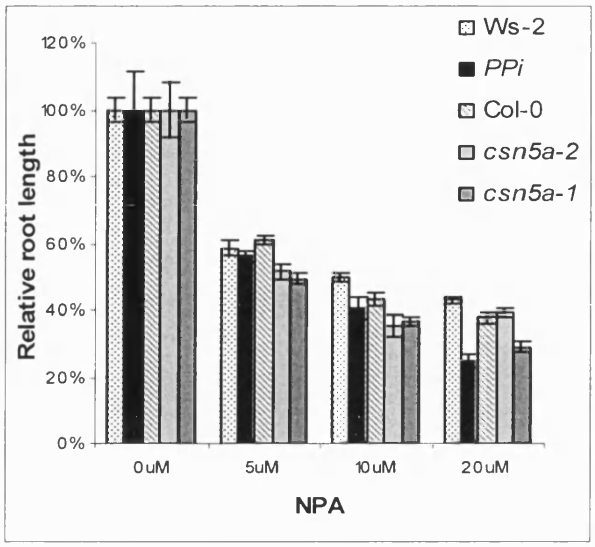

Fig.6.4: Root response of seedlings to NPA

The seedlings were germinated on nutrient agar without NPA and transferred to NPA +/- media after 3 days and the amount of root length after transfer were measured when the seedlings were 7 days old.
The mean root lengths are presented here as a percentage of the untreated control.
Error bars represent the SE; n > 15

6.2.2 The *csn5a* mutants show altered and varied responses to cytokinins, ACC and EBR

The *ppi* mutant showed slightly more hypocotyl elongation by 2iP (N^6-[2-isopentenyl adenine]) than the wt at low concentrations (0.1 μM and 1 μM), and showed substantially less hypocotyl elongation at 10 μM (Fig. 6.5a). *csn5a*-2 showed reduced hypocotyl lengths between 0.01- 1 μM than the wt. *csn5a*-1 showed less hypocotyl elongation at 1 and 10 μM than the wt.
Root growth was inhibited at all concentrations tested (Fig. 6.5b). *ppi* was inhibited more than wt at 0.01 μM and 0.1 μM. *csn5a*-1 and *csn5a*-2 were inhibited more than wt at all concentrations. *csn5a*-1 showed slightly greater root growth inhibition than *csn5a*-2.

The ethylene precursor ACC (1-aminocyclopropane-1-carboxylic acid) enhanced the hypocotyl elongation of the wt (Fig. 6.6a). *ppi* showed less hypocotyl elongation growth enhancement than the wt at 1uM and 10uM ACC. *csn5a*-1 showed reduced hypocotyl lengths than the wt at all concentrations tested. *csn5a*-2 at 0.1 μM showed longer hypocotyls than the wt, but showed less elongation than the wt at other concentrations.

Root growth inhibition of *ppi* was the same as for the wt (Fig. 6.6b). *csn5a*-2 was less inhibited than the wt at 0.1 µM and 1 µM, and more inhibited than the wt at 10 µM. *csn5a*-1 was more inhibited than the wt at all concentrations.

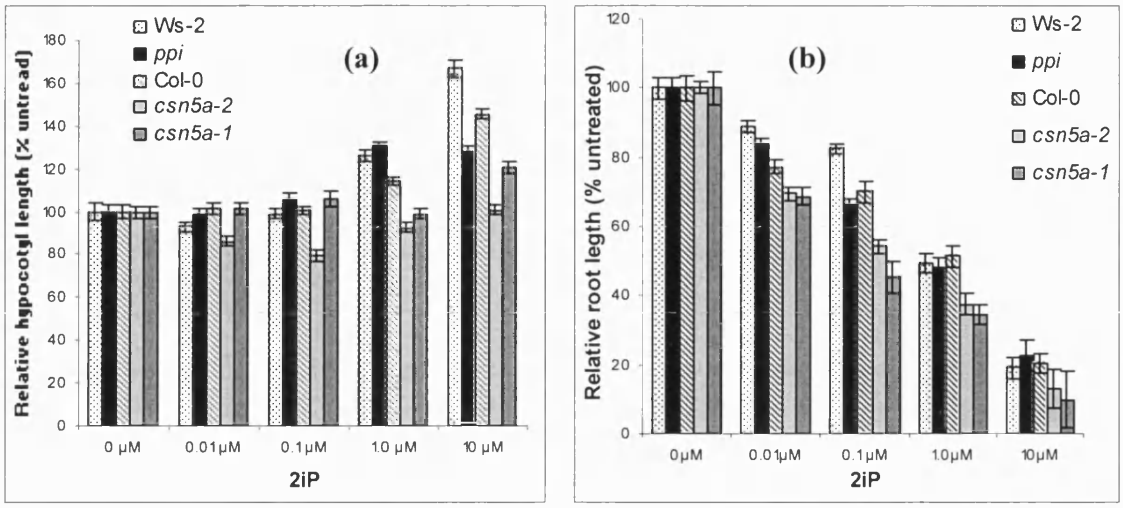

Fig.6.5: Response of seedlings to 2iP
The mutant and wt seedlings were grown under long-day conditions for 5 days on agar plates containing either no hormone or a range of 2iPconcentrations.
The mean hypocotyl or root lengths are presented here as a percentage of the untreated control.
(a) Mean hypocotyl length as % untreated
(b)Mean root length as % untreated
Error bars represent the SE. n > 15

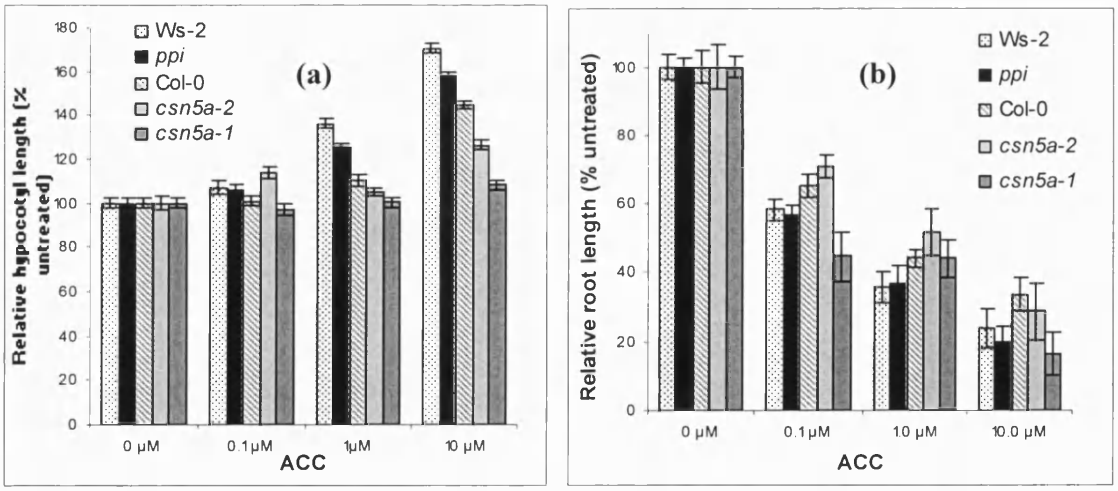

Fig. 6.6: Response of seedlings to ACC
The mutant and wt seedlings were grown under long-day conditions for 5 days on agar plates containing either no hormone or a range of ACC concentrations.
The mean hypocotyl or root lengths are presented here as a percentage of the untreated control.
(a) Mean hypocotyl length as % untreated
(b)Mean root length as % untreated
Error bars represent the SE. n > 15

ppi hypocotyls were longer than wt in the presence of 0.1uM EBR but otherwise there was little difference between the mutant and wt (Fig. 6.7a). *csn5a*-1 and *csn5a*-2 hypocotyls were longer than wt at 1 μM and 10 μM EBR.

Root growth was inhibited at all concentrations (Fig. 6.7b). *ppi* was less inhibited than the wt at 0.01 μM EBR and more inhibited at high concentrations. Roots of the *csn5a*-1 and *csn5a*-2 were more inhibited at 0.01 μM and less at 0.1-10 μM than the wt.

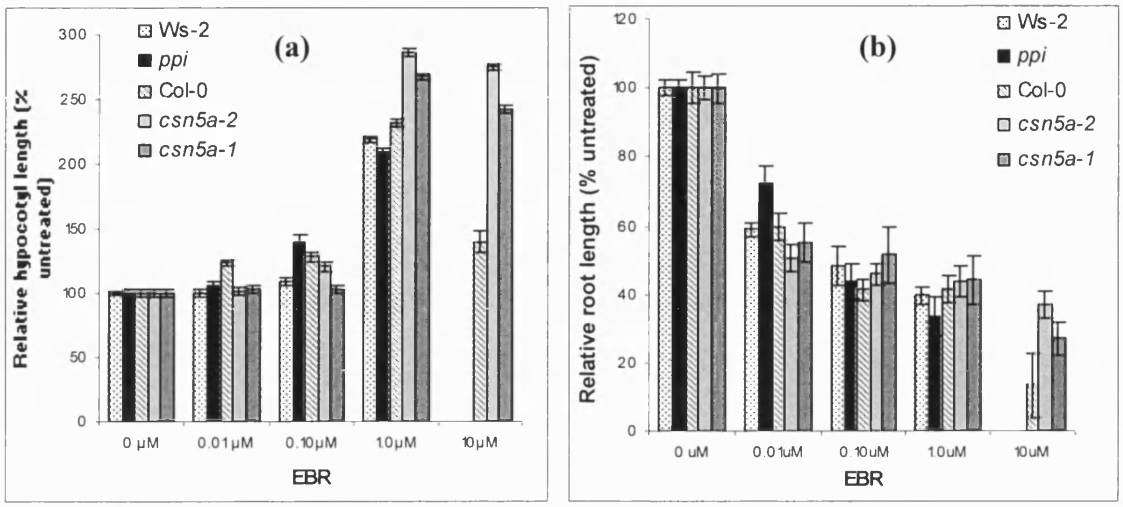

Fig.6.7: Response of seedlings to EBR
The mutant and wt seedlings were grown under long-day conditions for 5 days on agar plates containing either no hormone or a range of EBR concentrations.
The mean hypocotyl or root lengths are presented here as a percentage of the untreated control. The *ppi* and Ws-2 did not germinate at the highest EBR level tested.
(a) Mean hypocotyl length as % untreated
(b)Mean root length as % untreated
Error bars represent the SE. n > 15

6.2.3 The *csn5a* mutants show altered responses to GA and ABA

All the three mutants showed less hypocotyl elongation growth compared to the wt at 1- 10 μM GA_3 (Fig. 6.8).

Ws-2 and Col-0 both showed root elongation at 0.1 μM ABA (Fig. 6.9). The root length of the mutants at 0.1 μM ABA was not different from that of the untreated. Ws-2 roots were elongated at 1.0 μM ABA. In contrast, *ppi* roots were inhibited at the same concentration. The inhibition of root elongation was more for *ppi* at 10, & 100 μM ABA, compared to the wt.

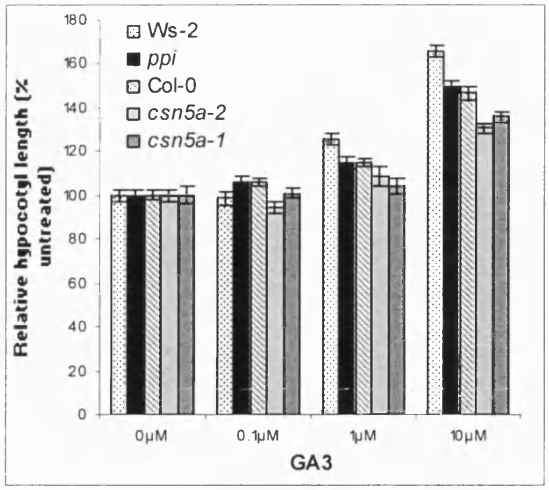

Fig. 6.8: Hypocotyl response of seedlings to GA3

The mutant and wt seedlings were grown under long-day conditions for 5 days on agar plates containing either no hormone or a range of GA3 concentrations.
The mean hypocotyl lengths are presented here as a percentage of the untreated control.
Error bars represent the SE. n > 15

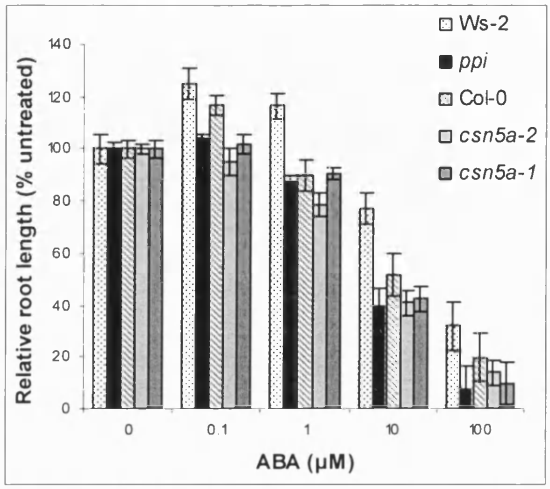

Fig. 6.9: Root response of seedlings to ABA

The mutant and wt seedlings were germinated and grown on agar without ABA for 3 days and transferred to ABA+/- plates. The amount of root length after the transfer were measured when the seedlings were 7 days old.
The mean root lengths are presented here as a percentage of the untreated control.
Error bars represent the SE. n > 15

6.2.4 The *csn5a* mutants were more sensitive to inhibition of seed germination by Paclobutrazol and ABA.

The Effect of the GA biosynthesis inhibitor paclobutrazol on seed germination was tested. Ecotype differences were significant in this test as the completely inhibitory concentration of paclobutrazol for the Ws-2 ecotype was 3 µM whereas for the Col-0 ecotype it was > 50 µM, a >10-fold difference. Therefore the results are presented in two separate graphs for the two ecotypes.

A significant difference was brought out by subtle changes in paclobutrazol concentration. Inhibition of seed germination of *ppi* by paclobutrazol was more compared to the wt (Fig. 6.10a). the germination was reduced to 50% in *ppi* between 0.5 and 0.7 µM paclobutrazol whereas for Ws-2 it was between 1.5 and 2 µM, at least two-fold difference than that for *ppi*. Similarly, *csn5a*-2 and *csn5a*-1 were more sensitive to paclobutrazol inhibition of germination as their germination reduction to 50% was around 5 µM whereas for the wt it was between 7-10 µM. *csn5a*-2 was more sensitive than *csn5a*-1 for 1-20 µM paclobutrazol. Above 10 µM, *csn5a*-1 response was similar to the wt (Fig. 6.10b).

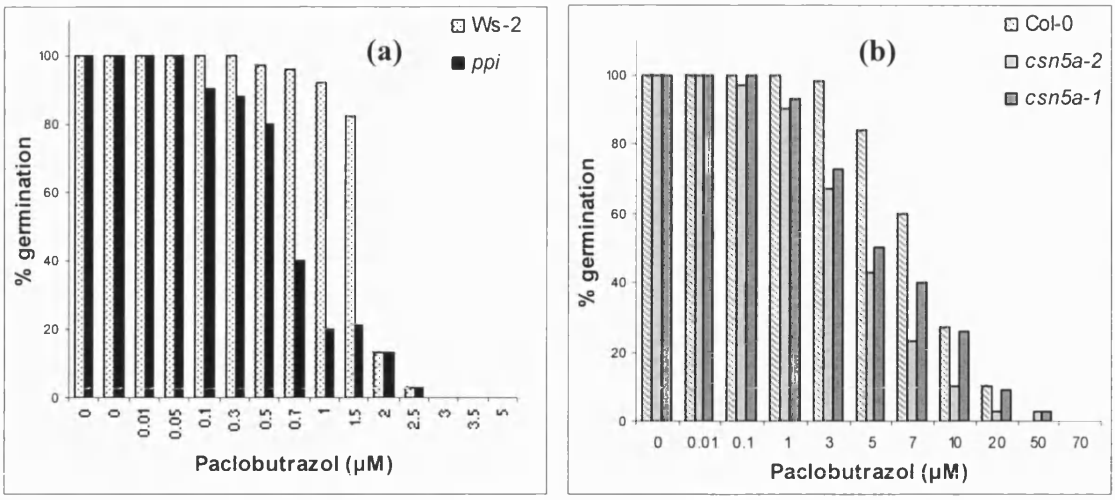

Fig. 6.10: Inhibition of seed germination by paclobutrazol
The mutant and wt seeds were germinated in the absence or presence of a range of paclobutrazol concentrations.
Data presented are means of 100 seeds per treatment.
(a) % germination of Ws-2 and *ppi* seeds
(b) % germination of Col-0, *csn5a*-1 and *csn5a*-2

Inhibition of seed germination by ABA as for *ppi* was more than that for the wt, as *ppi* seeds were 100% inhibited by 4 μM ABA, whereas, for the wt 100% inhibition of germination was not reached until 10 μM ABA (Fig. 6.11a). Both *csn5a*-1 and *csn5a*-2 were more sensitive than the wt. *csn5a*-1 reached 50% decrease at 4 μM and *csn5a*-2 reached 50% decrease at 6 μM ABA (Fig. 6.11b). Both the wt and the *csn5a*-1, *csn5a*-2 mutants were 100% inhibited at 8 μM ABA.

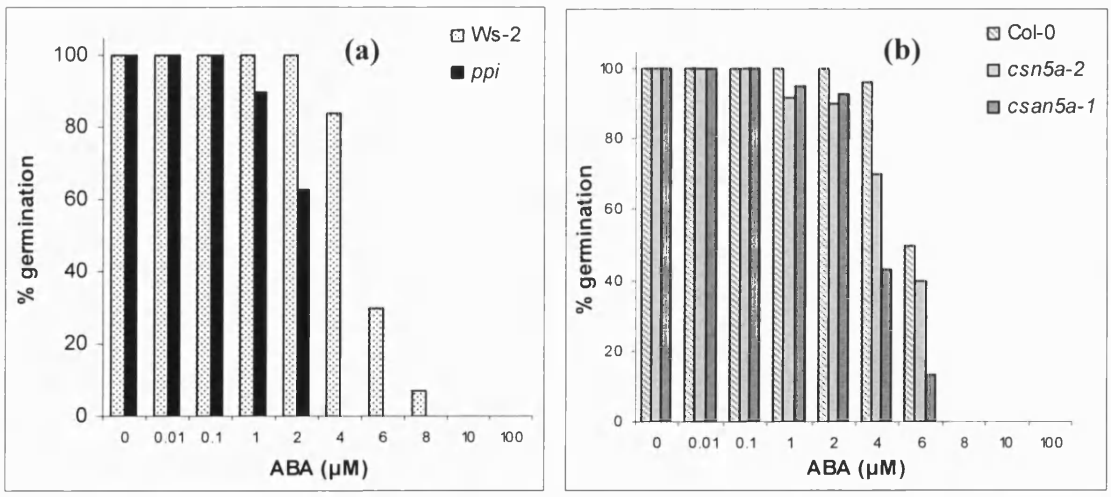

Fig. 6.11: Inhibition of seed germination by ABA
The mutant and wt seeds were germinated in the absence or presence of a range of ABA concentrations.
Data presented are means of 100 seeds per treatment.
(c) % germination of Ws-2 and *ppi* seeds
(d) % germination of Col-0, *csn5a*-1 and *csn5a*-2

6.2.5 Localized NO_3^- treatment could partially rescue the lateral root phenotype of the *csn5a* mutants.

If roots of plants grown under low NO_3^- conditions are exposed to a localized region of high NO_3^- the outgrowth of lateral roots is stimulated specifically in that region of the root. This increased elongation due to enhanced meristematic activity in the lateral root tips, has been linked with the auxin response induced by nitrates (Forde, 2002; Zhang and Forde, 2000). In view of the reduced response shown by the *csn5a* mutants to auxin (section 6.2.1), we decided to investigate their response to localised nitrate.

Seeds germinated and grown on medium containing 0.5% (w/v) sucrose, 23mM MES buffer (pH 5.7), 1% plant agar and Gamborg's B5 salts in which KNO_3 and $(NH_4)_2SO_4$ were replaced with 1mM KCl and 10μM NH_4NO_3 (Zhang and Forde, 1998) (section 2.2.2.3). After about 3-4 days, when the primary roots reached ~2 cm, the seedlings were transferred to segmented agar plates in which the middle segments were supplemented with either KNO_3 or KCl (designated 'control'), with the root tip just touching the middle section. After 12 days growth, the plates containing the seedlings were scanned and the lateral root lengths of the plants in the middle section were measured and number of lateral roots per plant in the middle agar segment was noted.

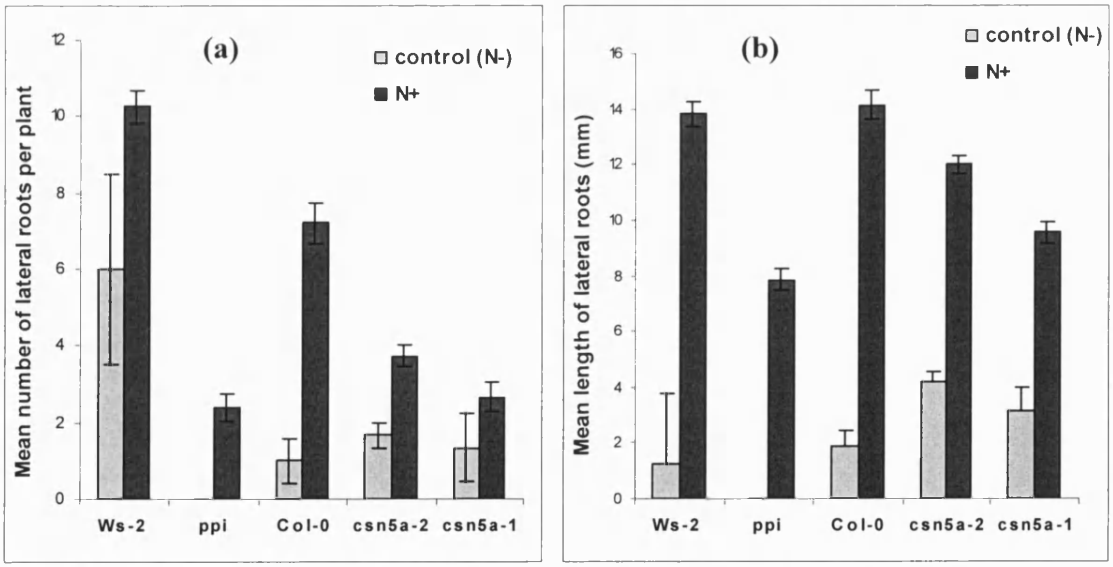

Fig. 6.12: Effect of localized nitrate treatment on lateral root (LR) development of seedlings

Wt and mutant seedlings were germinated and grown for 3-4 days on a low nitrate medium, and then transferred to segmented agar plates (Zhang and Forde, 2000) with the middle section treated with either KNO_3 (N+) or KCl (Control N-). After 12 days, the LR numbers and lengths in the middle sections were measured.
(a) The mean number of LRs per plant ($n > 15$; $p < 0.05$, two-sample t-test)
(b) The mean LR length ($n = 10\text{-}50$; $p < 0.05$, two sample t-test)
Error bars represent the SE.

Localized nitrate treatment increased the number of lateral roots in the mutants but not to the same extent as the wt (Fig. 6.12a). The difference was most prominent between Ws-2 and *ppi*, but it was very clearly shown by both *csn5a*-1 and *csn5a*-2 compared with Col-0. The *csn5a*-1 mutant responded less than *csn5a*-2.
Lateral roots were significantly longer in *ppi* treated with localized nitrates compared to the untreated (control), but again, not to the same extent as the wt. *csn5a*-1 and *csn5a*-2 gave similar results (Fig. 6.12b).

6.2.6 The *csn5a* mutants show altered responses to Red-, Far-Red- and Blue-light

To investigate the defects of the *csn5a* mutants in light signalling, fluence-rate experiments were performed at the University if Tuebingen, Germany, by Dr. Virtudes Mira-Rodado at Professor Klaus Harter's lab. The results of those experiments are presented here with the permission of Dr. Mira-Rodado. The experimental procedure is given in section 2.2.2.4.

The hypocotyl lengths of seedlings grown for 3 days under a range of fluence rates of red, far-red or blue light were measured.
In blue light, *ppi* did not respond at all as the hypocotyl lengths were not different from those in the dark (Fig. 6.13a).
In far-red light, the three mutants showed hyposensitivity, as slight enhancement of the hypocotyl lengths were seen at fluence rates which were inhibitory to the wt. At the highest fluence rate tested hypocotyl elongation in all three mutants was inhibited similarly as the wt (Fig. 6.13b).
Red light stimulated hypocotyl elongation in all three mutants, whereas it was inhibitory to the wt. At the highest fluence rate the hypocotyls of the mutants were longer than their respective wild types (Fig. 6.13c-d) The growth enhancement is highest in *ppi* and then in *csn5a*-1 and *csn5a*-2 respectively (Fig. 6.13d).
The data suggest that the three *csn5a* mutants have altered responses to red light, particularly under the low fluence rates tested. They show slightly altered response to far-red light under low fluence rates, but were not different from the wt response at high fluence rates. The *ppi* mutant did not respond to blue light, for the range of fluence rates tested.

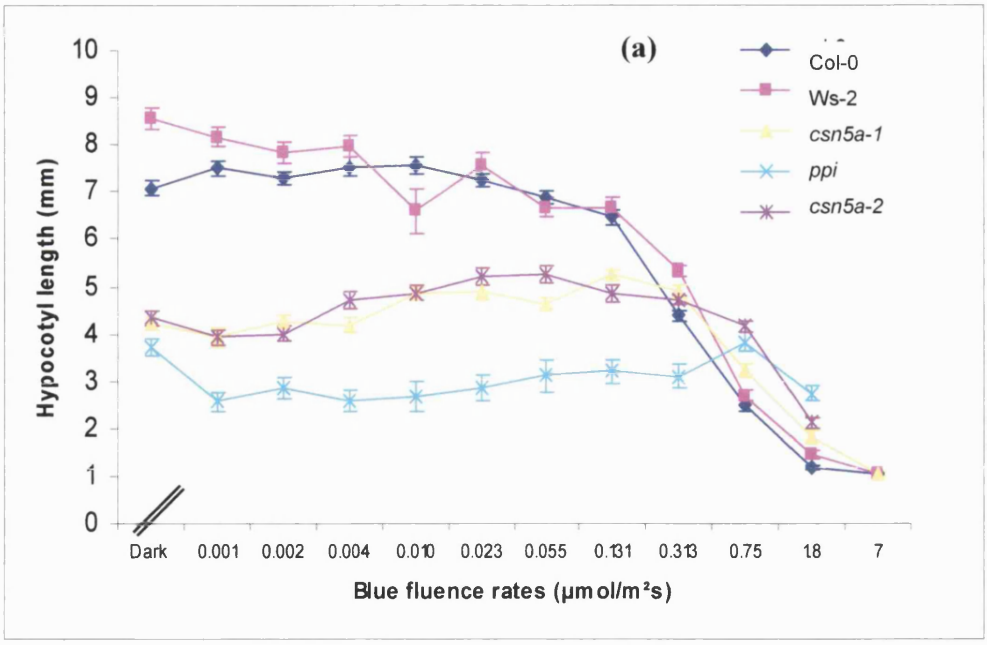

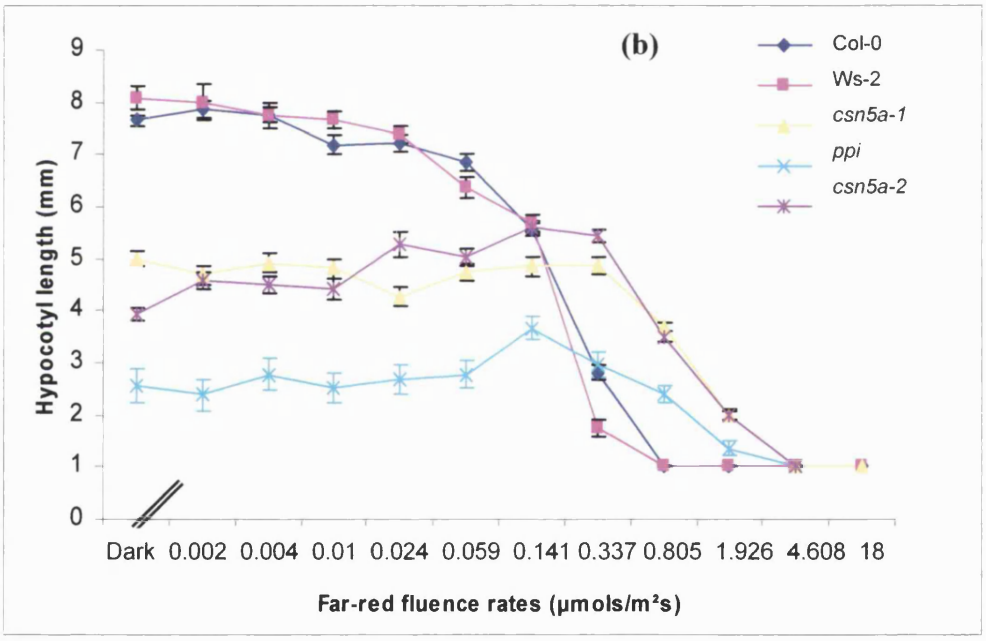

Fig. 6.13: Fluence-rate dependence of hypocotyl length

Seedlings were grown for 3 days under continuous Red, Far-Red and Blue light at the indicated light intensities or in darkness.
The initial data point is the length in the dark. The values represent the mean hypocotyl length and the error bars represent SE (n>30).
(a) Response of seedlings to Blue light
(b) Response of seedlings to Far-Red light

[Fig.6.13 continues over leaf]

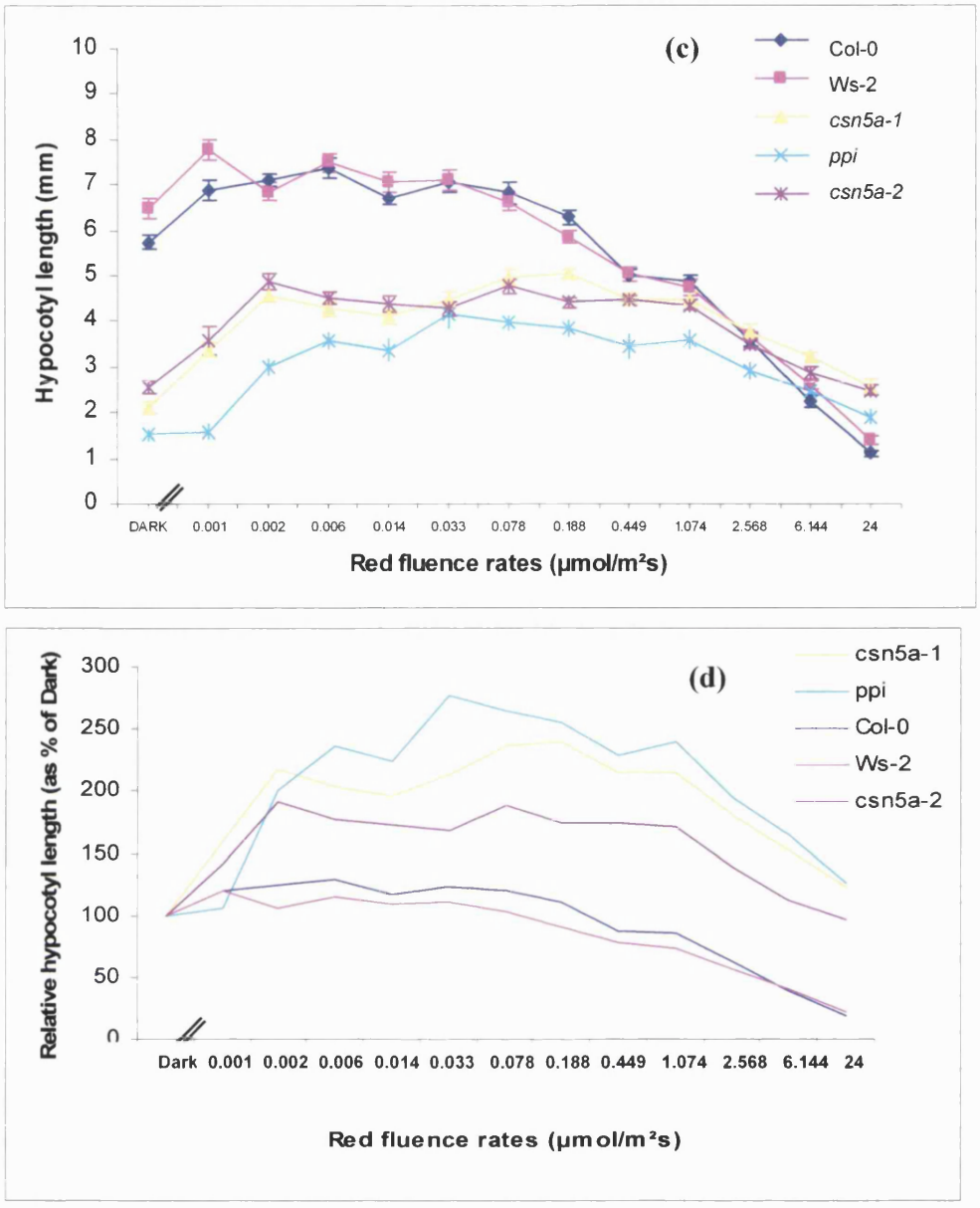

Fig. 6.13: Fluence-rate dependence of hypocotyl length

(Continued from previous page)

Seedlings were grown for 3 days under continuous Red light at the indicated light intensities or in darkness.

The initial data point is the length in the dark.

(c) Response of seedlings to Red light
The values represent the mean hypocotyl length and the error bars represent SE (n>30).

(d) Response of seedlings to Red light
The values represent the mean hypocotyl length (Fig6.13c) presented as a % of the mean hypocotyl lengths of the dark-grown seedlings.

6.3 Discussion

6.3.1 Localized NO_3^- treatment could partially rescue the lateral root phenotype of the *csn5a* mutants

The localized nitrate treatment promotes lateral root elongation by enhanced root meristem cell division rate in lateral root primordia through auxin signalling (reviewed in Forde, 2002).

The localized nitrates could only partially rescue the lateral root phenotype of the *csn5a* mutants. One possibility is that the poor response to nitrate was caused by insensitivity to auxin although we cannot eliminate the possibility that CSN is required for different components of the response to both of these signals. The observed increased number and length of lateral roots after nitrate treatment could be due to either the enhanced activity of root primordia or induction of new primordia or both. It is more likely that the *csn5a* mutants could be unable to trigger cell division in the primordia they already possess (*ppi* in particular, which had no lateral roots without the treatment).

Further analysis of number of primordia per plant was required to confirm this and a preliminary analysis was performed by Amy Percival for her BSc final year project (2006). It was observed that the localized nitrate treatment could increase the number of lateral root primordia, especially in *ppi*. However, the treatment could enhance the activity of the primordia only partially, as many did not grow to form lateral roots (data not shown). In animals, the cell cycle inhibitor p27 is down regulated at least partially by the action of the CSN and CSN5 (Tomoda *et al.*, 2002). Accumulation of p27 leads to cell cycle arrest. It is possible that *Arabidopsis* may also have similar factors affecting the rate of cell division, that are regulated by the CSN and in the *csn5a* mutants this function of CSN is impaired.

6.3.2 The *csn5a* mutants show altered light responses

When dark grown seedlings are exposed to light (UV-A/blue, red and far-red), de-etiolation is initiated and the rapid hypocotyl elongation is stopped, cotyledons are unfolded and expanded, pigmentation is increased and the photosynthetic apparatus is organized. Hypocotyl responses to different light conditions give an idea of the functioning of light signalling pathways in a plant.

For *csn5a*-1 and *csn5a*-2 it has been recently reported that the seedlings grown for 6-days under constant white (121 μmol), far-red (0.2 μmol), red (40 μmol) and blue (6.8 μmol),

had shown reduced hypocotyl lengths compared to the wt under all light conditions tested (Gusmaroli *et al*, 2007). Our experimental conditions were different from those and using different fluence rates we have observed the mutant responses were not the same particularly for low fluence rates.
In our experimental conditions, the three *csn5a* mutants were markedly less sensitive to red light induced inhibition of hypocotyl elongation as they showed enhanced hypocotyl lengths instead of being inhibited. They were slightly less responsive to far-red light.
The *csn5a-1* and *csn5a-2* responses to blue light were not markedly different from the wt. However, *ppi* did not respond to blue light in any way as the hypocotyl lengths were not different from that of the dark-grown seedlings indicating *ppi* could be defective in blue light signalling at least under our experimental conditions. Since this was not observed with the other two alleles, it may be a unique feature of *ppi*.

Mutants selectively impaired for de-etiolation in far-red light are considered phyA signalling mutants as phyA is the only receptor active in those conditions (Fankhauser and Casal, 2004). Mutants with selective impairment of de-etiolation in red light could be generally considered as defective in phyB signalling as phyB is the major photoreceptor but since in *Arabidopsis* all 5 phytochromes are involved in this response such a result cannot be simply explained. Moreover, mutants affecting the circadian clock selectively affect red light sensitivity (Fankhauser and Casal, 2004).
Blue light perception defective responses (in suppression of hypocotyl elongation) of mutants is again difficult to interpret simply with regard to which light signalling pathways is affected as cry1, cry2, phyA and to a lesser extent phyB and phot1 are playing roles during de-etiolation in the blue light.
From what we have observed on the responses of the *csn5a* mutants to light, it can be said that the mutations in *CSN5A* affect not only phyA response as can be explained by a defective COP1 function (due to defective CSN) in relation to degrading phyA, but possibly involves other phytochrome and cryptochrome signalling pathways as well. The CSN or CSN5 is possibly a downstream regulating point in phytochrome and cryptochrome signalling and probably linking the circadian clock too.
To see the affect of the mutant on individual photoreceptor pathways, more investigations are required. These can be possibly done with double mutants of the *csn5a* and relevant photoreceptor mutants.

6.3.3 The *csn5a* seed germination was more inhibited by the exogenous application of GA biosynthesis inhibitor paclobutrazol and by ABA

ABA and GA play antagonistic roles to each other in seed germination in *Arabidopsis*. ABA establishes dormancy during embryo maturation and GA is required to break this ABA induced dormancy (Koornneef and Karsen 1994). Seed germination is a point in development where hormone cross-talk plays a major influence. For example, BRs act in a similar way to GA, helping to break the ABA induced seed dormancy and stimulate germination, though it is not essential (Steber and McCourt, 2001), as shown by its ability to stimulate germination and hypocotyl elongation of *sly1* GA response mutant and GA biosynthetic mutants. BR biosynthetic mutants are more susceptible to ABA inhibition of germination.

GA antagonizes the dormancy promoting effects of ABA and germination inhibition effects of DELLA proteins (particularly, RGL2) in *Arabidopsis*, which are rapidly degraded by the proteasome pathway in response to GA. Light also, believed to affect the GA signal transduction to promote seed germination, probably related to a manner in which DELLA proteins are degraded (Zhao *et al.*, 2007). As the reduced CSN function could be stabilizing the DELLA proteins in the *csn5a* mutants they can be more inhibited by the action of paclobutrazol which reduces the endogenous GA levels. As GA and ABA act antagonistically to each other, especially during seed germination, an already deficient GA signalling as in the *csn5a* mutants may result in a higher sensitivity to inhibitory effects of ABA.

6.3.4 The *csn5a* mutants show altered responses to a range of phytohormones, possibly via signalling cross-talk.

The mutants showed alterations in their responses to a range of hormones and light signals and this is consistent with the *csn5a* component of the CSN playing a role in the numerous functions of the CSN. A number of cellular pathways are regulated by the CSN and these pathways could be intersecting at various points, and there may be much cross-talk between components of different pathways. How the networks of signalling pathways operated in time and space is not completely understood and much research is being done on this respect. Although the functional significance and diversity of the roles of the CSN is emerging, our observations suggest a role for *csn5a* in response to a range of hormones and light.

The mutants chosen for the study were in different ecotypes in which their responses may differ for a particular stimulus. The fact that the ecotypes are different makes it difficult to draw direct comparisons between the three mutants. The allelic differences also play a significant role. In Chapter 4, it was shown that *ppi* is producing a truncated CSN5A protein whose influence on the functions of CSN complex or the possible CSN-independent functions are yet to be determined. Our work and other recent reports (Gusmaroli *et al.,* 2007) indicate the *csn5a-2* to be partially functional, and the *csn5a-1* to be a null mutant. In view of the fact that we have established reasonably well how the mutants differ from one another with respect to the production of CSN5A protein it is nevertheless useful to make comparisons between them in trying to deduce the function of CSN5 and the CSN complex.

The *csn5a* mutants showed reduced responses to exogenous auxins. Our data on the effect of various auxins and the auxin transport inhibitor NPA suggest that the *csn5a* mutants to show reduced auxin responses compared to the respective wild-type. One way this could be possible is via the impaired SCF^{TIR1} action in down regulating AUX/IAA proteins as a result of reduced CSN functioning in the mutants. The differences between the mutants' and the wt responses to auxins were not very large, implying the role of CSN5A in mediating auxin response is not critical.

The *csn5a* mutants showed enhanced responses to cytokinin induced inhibition of root elongation and showed reduced response to hypocotyl elongation by the same hormone. Exogenous cytokinin is known to inhibit cell elongation in stems and roots (Cary *et al.,* 1995). In our experimental conditions, the wt hypocotyl growth was enhanced at low cytokinin levels and the root growth was inhibited. The null *csn5a-1* showed reduced sensitivity to hypocotyl elongation and increased sensitivity to root growth inhibition. Hypocotyl elongation could be an indirect effect by cytokinin induced ethylene production. Cytokinin is known to inhibit root growth in the dark by stabilizing ACC synthase. Smalle *et al,* (1997), using nutrient starved *Arabidopsis* seedlings, demonstrated that hypocotyl elongation could be stimulated by ACC or ethylene in the light as a result of cell expansion rather than cell division.

The *csn5a* mutants showed enhanced responses to the ethylene precursor ACC.
The SCF^{EIB3} targets positive regulators of ethylene response for degradation via the proteasome pathway in the absence of the hormone. Impaired SCF could result in

hypersensitivity to ethylene. Our results indicate that the loss or reduction of *csn5a* function could result in a hypersensitive response to ACC, as shown by the increased response of the null *csn5a-1* mutant for ACC induced root inhibition.
The *csn5a* mutants, however, do not show the constitutive ethylene response of the *eib3* mutant, indicating other pathways independent of CSN and CSN5 in mediating ethylene response. The mutants show small differences in ACC response so CSN5A cannot be considered to be essential for ethylene action. However there was clearly some modulation of the response in the *csn5a-1* null mutant. It would be better to have been able to alter ethylene levels directly but we did not have the facilities for this.

The *csn5a* mutants showed enhanced response to EBR induced hypocotyl elongation and reduced response to root inhibition by EBR. BRs, like auxins, often inhibit primary root elongation but stimulate shoot growth and BR stimulation of seed germination and hypocotyl elongation has been observed in GA responsive and GA biosynthetic mutants (Steber amd McCourt, 2001). As the *csn5a* mutants were defective in GA response , the exogenous BR could be helping to overcome this deficiency in GA response, thereby increase hypocotyl length. BRs are known to inhibit root growth by induction of ethylene. Since the *csn5a* mutants were somewhat hypersensitive to ethylene, it can be speculated that such induction of ethylene by BR might lead to an increased hypersensitivity to root inhibition as seen for *csn5a-1* and *csn5a-2* mutants. It is possible that BR could be inducing ethylene in the hypocotyl as well; hence the largely increased hypocotyl length of the mutant compared to the wt could be due to additive effects of both GA and ethylene.

The *csn5a* mutants showed reduced response to GA induced hypocotyl elongation that could at least partially be due to stabilization of GA response repressing DELLA proteins as result of reduced SCF function in the *csn5a* mutants.
The *csn5a* mutants were hypersensitive to inhibitory effects of ABA on root growth. Low levels of ABA are known to stimulate *Arabidopsis* root growth whereas higher concentrations are inhibitory (Ghassemian *et al.,* 2000) and this was seen with the wt. However, the *csn5a* mutants did not respond to the growth enhancing effects of ABA, instead their growth was inhibited.

Altered responses of the *csn5a* mutants to plant hormones and other stimuli can be considered as cross-talk between hormone and light signalling pathways, and not only because of impaired proteolysis of components in each pathway. In bringing about the

phenotypic plasticity of plants in adapting to environmental and developmental changes, there is a tight interaction between hormone and light signalling pathways. A balanced response is generated through the interaction of many pathways and there is much cross-talk between components of various pathways (Weiss and Ori, 2007, Gazzarrini and McCourt, 2003) One example of hormone cross talk is the maintenance of apical hook in *Arabidopsis* seedlings. Although the precise mechanisms are not fully understood yet, ethylene, BR, GA and auxins all have functions in this and it is suggested that DELLA proteins play a major role (Vandenbussche and Van Der Straeten, 2004). Plant hormone cross talk involves diverse mechanisms, which act at both the hormone response and biosynthesis levels, creating a delicate response network. For example endogenous active GA levels are governed by feed back regulation, where active GA suppresses the expression of GA biosynthetic genes and promotes GA catabolic genes (Weiss and Ori, 2007).

Our observations provide further support for a role for the CSN in the responses to plant hormones although understanding the precise mechanisms of its involvement would require further research.

Chapter 7

Comparative proteomic analysis of soluble proteins from the *csn5a* mutant and wild-type *Arabidopsis* shoots by Two Dimensional Gel Electrophoresis (2DE).

7.1 Introduction

7.1.1 Comparative proteomics in *Arabidopsis*

Having genetically characterized a mutant, the next essential step is to functionally characterize it in order to understand the role of the gene. This is usually done by analysing the gene expression at the transcriptome and/or proteome level (Rose *et al*, 2004). Nowadays, an immense amount of information is gathered from high-through-put transcriptomics. Microarray studies are particularly useful in understanding the expression dynamics of genes.

The mRNAs are molecular intermediates and the next molecular link from the gene to its function or the phenotype is the protein. The proteome more directly influences the cellular biochemistry and therefore may produce a more accurate representation of the cellular status than mRNAs. Proteomics analyses are especially useful in studying post-translational modifications that lead to dramatic increases in protein complexity without altering the level of gene expression. Recent advancements in techniques to isolate subcellular protein fractions and to isolate multi-subunit complexes are making the proteomics approaches attractive. The expansion of genomic, cDNA, EST and protein data bases provide better opportunities for protein identification. Comparative proteomics are increasingly used to study complex biological questions.

The highly heterogeneous nature of the proteins combined with structural complexity, presents the major challenge in proteomics as they complicate the extraction, solubilization, handling, separation and identification of proteins. There is no single extraction and separation technique that could be used for all proteins. Certain subsets, for example membrane proteins, are extremely difficult to extract, solubilize and resolve by electrophoresis. It has been reported that even under optimal conditions, and after combining a range of separation and identification strategies, only ~25% of the expected proteome could be observed at best (Patterson, 2004). The *Arabidopsis* genome encodes

approximately 11,000 gene families, yet on a good quality single dimension IEF gel, or 2-D gel at best only a few hundred polypeptides can be resolved. Not surprisingly therefore these are found to encode major abundant house keeping proteins. There are difficulties in detecting low abundance proteins and because these include many important regulatory proteins it limits the depth of insight that is possible with the current proteomic technology. The inability of proteomic techniques to capture the dynamic nature of the protein networks is an additional drawback in the approach. Despite these limitations, proteomic analysis can give valuable insight into gene function.

7.1.2 Two-Dimensional Gel Electrophoresis (2-DE) of proteins as a tool for comparative proteomics

The most widely used approach for comparative proteomic analyses is 2-DE. It has been applied in proteomic analyses to monitor developmental changes or the effect environmental stimuli have on protein patterns (Gallardo *et al*, 2001). It is often used in assessing genetic variability at the proteome level (Canovas *et al*, 2004 and references therein). Detailed description of the 2-DE technique is provided by Berkelman & Stenstedt (2002).

In 2-DE, proteins in a mixture are sorted on the basis of two independent properties in two separate steps. Firstly, the proteins are sorted according to their isoelectric points or the pIs ('first dimension iso-electric focusing' or IEF). Secondly, SDS-PAGE separates proteins according to their relative molecular weights (M_r). The result is a two-dimensional array of spots in which each spot corresponds to a single protein in the sample. A large number of proteins can be separated and identified by this method and information such as protein pI, apparent M_r, and the amount of protein present can be obtained.

Basic steps involved in a proteomic analysis by 2-DE are, protein extraction and sample preparation, first dimension IEF, second dimension SDS-PAGE, staining of polypeptides, image detection and analysis, spot identification and database searches. All these steps must be performed carefully to obtain accurate results.

Protein extraction and sample preparation is the most critical step in any proteomic study since it should ideally be able to capture and solubilize the full complement of proteins in a given sample in a reproducible manner and should minimize the post-extraction artefacts

and non-proteinaceous contaminants (Giavalisco *et al*, 2003). The optimal procedure for a sample type may be determined based mainly on the research objectives (Rabilloud,1996).

In the first dimension IEF, the proteins are electrophoretically separated according to their isoelectric points (pI). Proteins, being amphoteric molecules, carry either positive or negative or zero net charge, depending on the pH of their surroundings. The net charge is the sum of all the negative and positive charges of its amino acid side chains and amino acid carboxyl termini. The pI is the pH at which the net charge is zero. If the pH is less than pI, the protein is positively charged. If the pH is higher than pI the protein is negatively charged. When an electric field is applied in the presence of a pH gradient, a protein will migrate to the position in the gradient where its net charge is zero. Positive net charged proteins migrate towards the cathode, becoming less positive until it reaches the pI. Similarly, negatively charged proteins will migrate toward the anode. If a protein should diffuse away from its pI, it immediately gains charge and migrates back. This is called the 'focusing effect' of IEF, which concentrates proteins at their pIs and separates on the basis of very small charge differences (Berkelman & Stenstedt, 2002). The resolution depends on the slope of the pH gradient and the electric field strength. Therefore, IEF is performed at very high voltages, typically above 1000V. When the proteins have reached their final positions in the pH gradient, there is very little ionic movement in the system, resulting in a very low final current, below 1mA. The carrier-ampholyte generated pH gradients in polyacrylamide gel-rods in the original method have been replaced with immobilized pH gradients (IPG) (Görg *et al*, 1988, Görg *et al,* 2000). An immobilized pH gradient is created by covalently incorporating a gradient of acidic and basic buffering groups into a polyacrylamide gel at the time it is cast. IPG gel is cast onto a plastic backing for improved performance and simplified handling and also improved gel to gel reproducibility. Now pre-cast IPG strips are commercially available in dry form as 3mm wide strips in various pH ranges, and varying strip lengths.

In the second dimension SDS-PAGE, the polypeptides already separated in the first dimension by IEF are separated further electrophoretically according to their M_r.
SDS is an anionic detergent and when in aqueous solution, forms micelles. SDS masks the charge of the proteins and the formed anionic complexes between the protein and SDS have a roughly constant net negative charge per unit mass. When treated with both SDS and reducing agent such as DTT (breaks any –S-S- linkages in proteins), the degree of electrophoresis separation depends largely on the molecular weight M_r of the protein.

In the next step, imaging and visualization of 2-D gels, the detection method should be highly sensitive, have a wide linear range for quantification, and be compatible with mass-spectrometry (MS) and of low toxicity to the environment. Autoradiography and fluorography are the most sensitive methods (down to 200 fg proteins per spot (Görg *et al.*, 2000). Silver staining is the most sensitive non-radioactive method (down to less than 1 ng). Coomassie staining is relatively simple, although it is less sensitive than silver staining it is more quantitative. Colloidal staining methods provide highest sensitivity down to 100 ng per protein spot. More recently, sensitive fluorescent stains such as SYPRO Ruby and SYPRO Orange have been developed with similar sensitivity to silver stain, but are easier to use and with good compatibility to MS. SYPRO Ruby, a ruthenium metal chelate which binds to the basic amino acids in proteins directly by electrostatic mechanism (Nishihara & Champion 2002), is now used routinely in 2DE. After staining, gel imaging is usually performed with a laser scanner or a CCD-based system.

Image analysis is usually done by using a software package such as ImageMaster 2D Platinum version5 (http://www.amershambiosciences.com). Manual intervention is required for spot editing, quantification, annotation, comparisons and generation of web-framed data sets and therefore represents the major bottle neck in a proteomic study. Introduction of the fluorescent 2-D Difference-in-gel electrophoresis (DIGE), which involves covalent labelling of two different protein extracts with one of two fluorescent cyanine (Cy) dyes, has made image analysis easier (Unlu *et al.*, 1997). The two labelled protein samples are mixed, separated on the same 2-D gel and scanned on a variable wavelength laser imaging system (Rose *et al.*, 2004). The two dyes, Cy3 and Cy5 show different excitation and emission spectra and since the two protein samples have been separated on the same gel, it is far more easy to compare protein expressions in the two original samples.

Once a set of differentially expressed spots has been identified from a series of 2-D gels, the next step is to identify the cognate proteins and genes. MS is now the most commonly used method for protein identification and also for characterisation of post-translational modifications. In protein identification, 2-D gel plugs containing the protein spots of interest are excised, and are in-gel digested with a site-specific protease such as trypsin, and then MS analysis of the resultant eluted peptides. Two MS approaches are being commonly used in proteomic research. The first one, Matrix assisted laser desorption/ionization time-of-flight (MALDI-ToF) MS is typically used to measure the

masses of the peptides derived from the tryptinized parent protein spot, generating a peptide mass finger print (PMF). Several software packages are then available (MASCOT, Matrix Science; SwissProt) that can compare the peptide mass list with a predicted 'theoretical' list of tryptic peptide fragments of every protein in the public data bases, together with equivalent translated genomic and EST data bases.
The alternative to the PMF approach is sequencing by electro spray ionization tandem mass spectrometry (ESI MS/MS), which yields amino acid sequences of selected tryptic peptides (Rose *et al*, 2004).

7.1.3 Objectives and experimental approach

We identified the gene responsible for the *ppi* mutation to be At1g22920, *CSN5A* that encodes the fifth subunit of the COP9 signalosome. Two other mutant alleles of the gene (*csn5a-1* and *csn5a-2)* that have a similar pleiotropic phenotype were obtained from the SALK collection.
From Western blot analysis, *ppi* was shown to produce a truncated protein that may be more abundant in the cytoplasmic soluble fraction. The *csn5a-2* produced a reduced amount of the wild-type CSN5A suggesting it is partially functional. The *csn5a-1* did not produce a detectable amount of the CSN5A protein, therefore could be a loss-of-function mutant. The responses of the mutants to phytohormones and light were in many cases different from one another and this is consistent with the allelic differences.

The CSN is a key regulator of many processes, the best known being its involvement in derubylation of cullin components of the SCF E3 ligases. This is known to be catalyzed by the CSN5 subunit and is essential for substrate ubiquitilation by the SCF and subsequent recognition and degradation via the 26S proteasome. Since the *csn5a* mutants are known to be defective in a gene encoding a subunit of CSN that has been implicated in protein degradation, we hypothesized that the reduction of CSN5A function could be affecting the protein complement of *Arabidopsis*. Therefore, a comparative proteomic analysis of the mutant and wt protein samples was performed using 2-DE. Because of time limitations it was only possible to analyse the cytosolic protein fractions. Because targets of the CSN are known to be present in both the cytoplasm and nucleus our strategy is valid however further analysis of total or nuclear proteins would be worthwhile. A parallel microarray analysis would have given additional valuable information, but was not possible due to both time- and financial limitations.

The experimental procedure used in this proteomic analysis was the one that is used successfully for *Arabidopsis* proteins at the proteomic facility at Centre for Research in Plant Science (CRIPS), The University of the West of England (UWE) and the 2-DE of the protein samples were carried out at the CRIPS, UWE, under the guidance of Dr. Richard Amey.

7.2 Results

In an initial pilot study 2-DE was performed for *ppi* and its wt Ws-2 to optimise conditions. Following the successful pilot study protein samples were prepared freshly from all 5 genotypes. The results of the second experiment matched those of the first round for *ppi* and Ws-2.
Cytosolic protein samples from shoot tissue (all 'above ground' tissue) from 20-d old plants were prepared and the 2DE was performed as described in section 2.2.12 .
Triplicate 2-D gels were run for each individual genotype. When an 'interesting' spot based on the presence/absence and relative abundance of the protein in the gels, was seen, gel plug containing the spot was excised from at least three gels and each individual spots processed separately for MS. Protein identification by data base searches using the MALDI-ToF-MS peptide mass fingerprints and confirmation of the identities were performed as described section 2.2.12.6.

As expected due to the size difference between the *csn5a* mutants and wild-type, the number of mutant plants required to obtain 300 mg fresh shoot tissue for protein extraction were 2- to 3-fold higher compared with the wild type (Table 7.1). Consequently, the total soluble protein yield obtained per mg of fresh plant tissue for mutants was higher, though the amount of total soluble proteins obtained per plant was less in mutants compared to the wild-type.

Table 7.1: Protein amount after extraction and sample preparation prior to first dimension IEF

Genotype	Number of plants required to obtain 300mg fresh shoot tissue	Amount of cytosolic proteins extracted per weight of fresh shoot tissue [µg /mg]	Amount of cytosolic proteins extracted per plant [µg /plant]
Ws-2	5	3.5	210
ppi	15	7.0	140
Col-0	8	5.0	188
csn5a-2	16	6.5	121
csn5a-1	18	6.0	108

7.2.1 Five proteins that were differentially expressed among the genotypes could be identified using the MALDI-ToF-MS peptide mass finger prints

Good quality 2-D gels were obtained after staining with SYPRO Ruby fluorescent dye. Typically ~ 400 spots were resolved against a clear background. The overall protein pattern was very similar in all genotypes (Fig.7.1) and was reproducible for all replicate samples and for both rounds of 2-DE, in the case of Ws-2 and *ppi*.
In the non-linear gradient of pH 3-10, the majority of the spots were dispersed more or less evenly between pH 4 - 7. Although many high molecular weight (> 100 kDa) protein spots were distinguishable in the gels, low molecular weight (<10 kDa) spots were not very clear.

Out of the ~ 400 spots distinguishable in a gel, 33 displayed differences in abundance or presence/ absence among the five different genotypes studied, and were selected for MALDI-ToF MS (some are presented in Table 7.2). Once the PMF data are generated, the software associated with MALDI-ToF-MS searches the SwissProt data base for protein identity by comparing with the theoretical PMF patterns for annotated proteins. Later, a second database search was performed using the Mascot search engine to extend the search to hypothetical proteins as well. In this study, the results obtained by both means were similar.
Location of the selected spots in the 2D gel and comparison of expression for each identified protein in 2D gels are shown in Fig.7.2 and Fig.7.3 respectively. The steps involved in identifying a protein based on MALDI – ToF MS/ PMF data are shown in Fig.7.4.

With the SwissProt/ Mascot database searches 11 protein spots were identified with good matches for the PMF data. Of these, only 6 identities were confirmed as those were having close theoretical and observed M_r & pI values. The results are summarized in Table 7.3. Spot numbers 1 & 2 which are very closely located in the 2-D gels turned out to be the same protein PR5. Therefore, altogether five proteins were identified from the 2-D gels. Of the five, the RuBisCO Activase (RCA), Catalase2 (CAT2) and GSTF2 were more abundant in 2-D gels of the three *csn5a* mutants compared to the wts. The Pathogenesis Related protein2 (PR2) was more abundant in *ppi* 2-D gels compared to all other genotypes. The PR5 protein spot was present and highly expressed only in *ppi* 2-D gels .

It should be noted here that in this report I am considering the protein spots that were confidently identified based on all three criteria (peptide fragment matches and close values for theoretical and observed M_r, pIs). However, it does not mean the matches came up for the other 5 spots should be eliminated. Post translational modifications could influence the charge of a protein and in turn, the pI. Post-translational processing, proteolytic damage etc would change the M_r. As the observed pI for the gels was determined using a standard calibration curve provided by the manufacture for the IPG-strips (section 2.2.12.6) and observed M_rs are based on the standard molecular markers that were run on the gel, both could therefore be slightly deviated from the actual values. The theoretical values are based on the amino acid sequence and do not consider any posttranslational modifications that could alter the charge or the molecular weight, and therefore could be slightly different from the actual values. For examples the *PYRB* (At3g20330) aspartate carbamoyl transferase (spot # 10 in our 2-D gels) is a protein that contains a transit peptide (http://au.expasy.org/uniprot/P49077) that would eventually be cleaved off when the protein enters the Chloroplast. The databases give the M_r for the unprocessed precursor as 70 kDa. Another interesting protein was EOL1 (Ethylne overproducer 1-like1) as it was more abundant in all three *csn5*a mutants, but its identity could not be confirmed as the observed and theoretical isoelectric points and molecular weights differed greatly. Further investigations including Blastn sequence similarity searches on the peptide fragments for those proteins are required before they can be eliminated as incorrectly identified.

Table 7.2: Protein abundance or presence/absence in 2-D gels for some spots selected for MALDI ToF

The number of '+' marks the increasing strength of the signal which is indicative of the relative abundance of the protein in gels from each genotype

Spot number	Ws-2	*ppi*	Col-0	*csn5a-2*	*csn5a-1*	Presence / absence of spots and protein abundance in 2-D gels
1	-	++++	-	-	-	Present only in *ppi*
2	-	++	-	-	-	Present only in *ppi*
3	+	++	+	++	++	More abundant in all three mutants compared to the wt
4	+	+++	+	+	+	More abundant in *ppi* compared to other two mutant alleles and wt
5	++	++++	++	++++	++++	More abundant in all three mutants compared to the wt
6	+	+++	+	++	++	More abundant in all three mutants compared to the wt
7	++	++	++	++	+	Less abundant in *csn5a-1* compared to other genotypes
8	++	+++	++	+++	+++	More abundant in all three mutants compared to the wt
9	+	++	+	++	++	More abundant in all three mutants compared to the wt
10	-	-	-	+++	-	Present only in *csn5a-2*
11	++	+++	-	-	-	Present only in Ws-2 ecotype
12	+	-	+	+	+	Absent in *ppi*

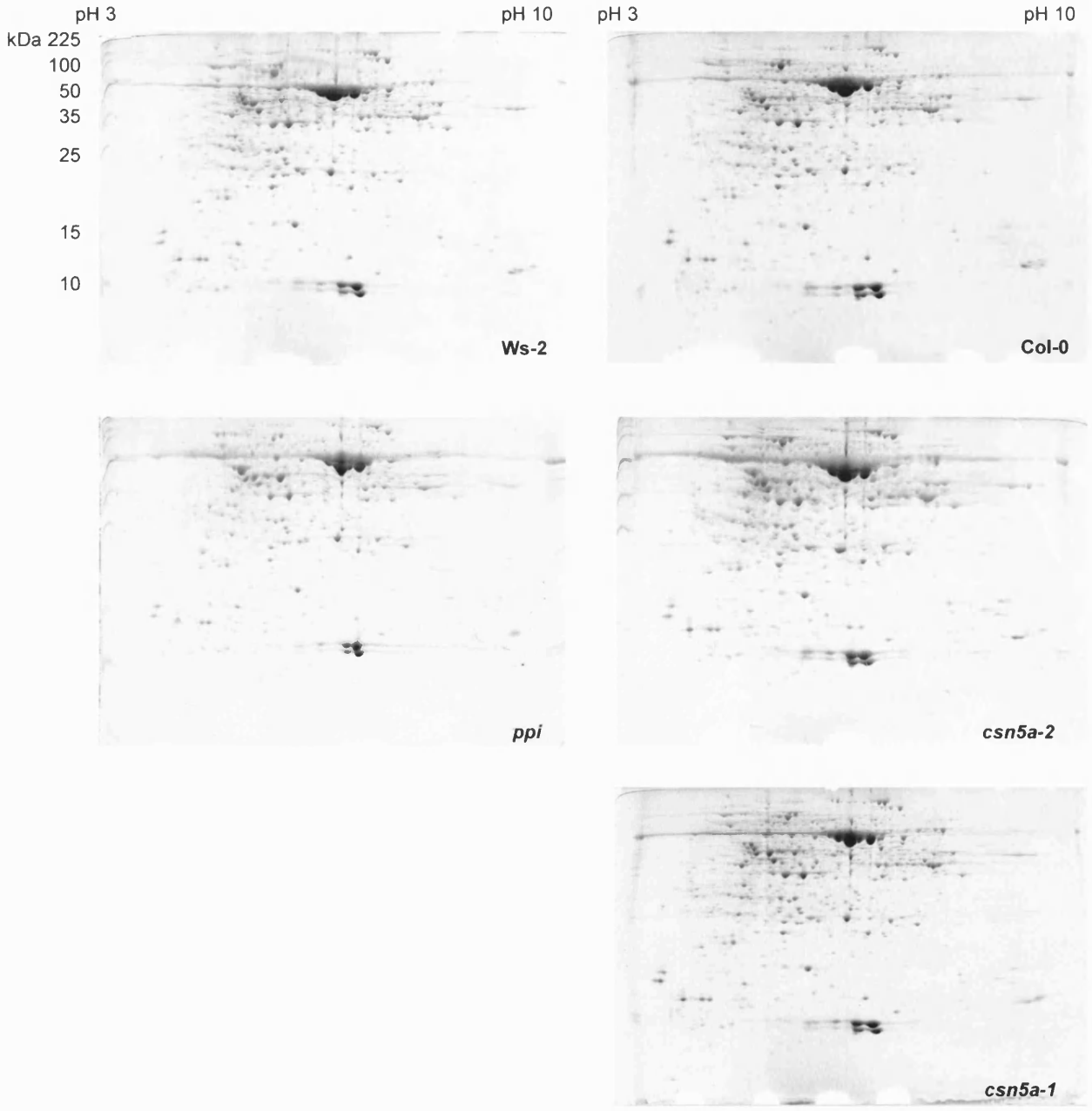

Fig. 7.1. Comparative 2-DE analysis of cytosolic proteins extracted from shoots of *csn5a* mutants and the respective wild-types

Soluble cytosolic proteins were extracted from 21-d old Ws-2, *ppi, csn5a-2* , *csn5a-1* and Col-0 plants grown on M&S medium under long day conditions. A protein sample of 200 µg from each genotype was focussed on 24 cm IPG strips with non-linear pH 3-10 gradient, then separated by SDS-PAGE on 12.5 % gels. Gel images were obtained by Typhoon laser scanner after staining the gels with SYPRO™ Ruby fluorescent dye.

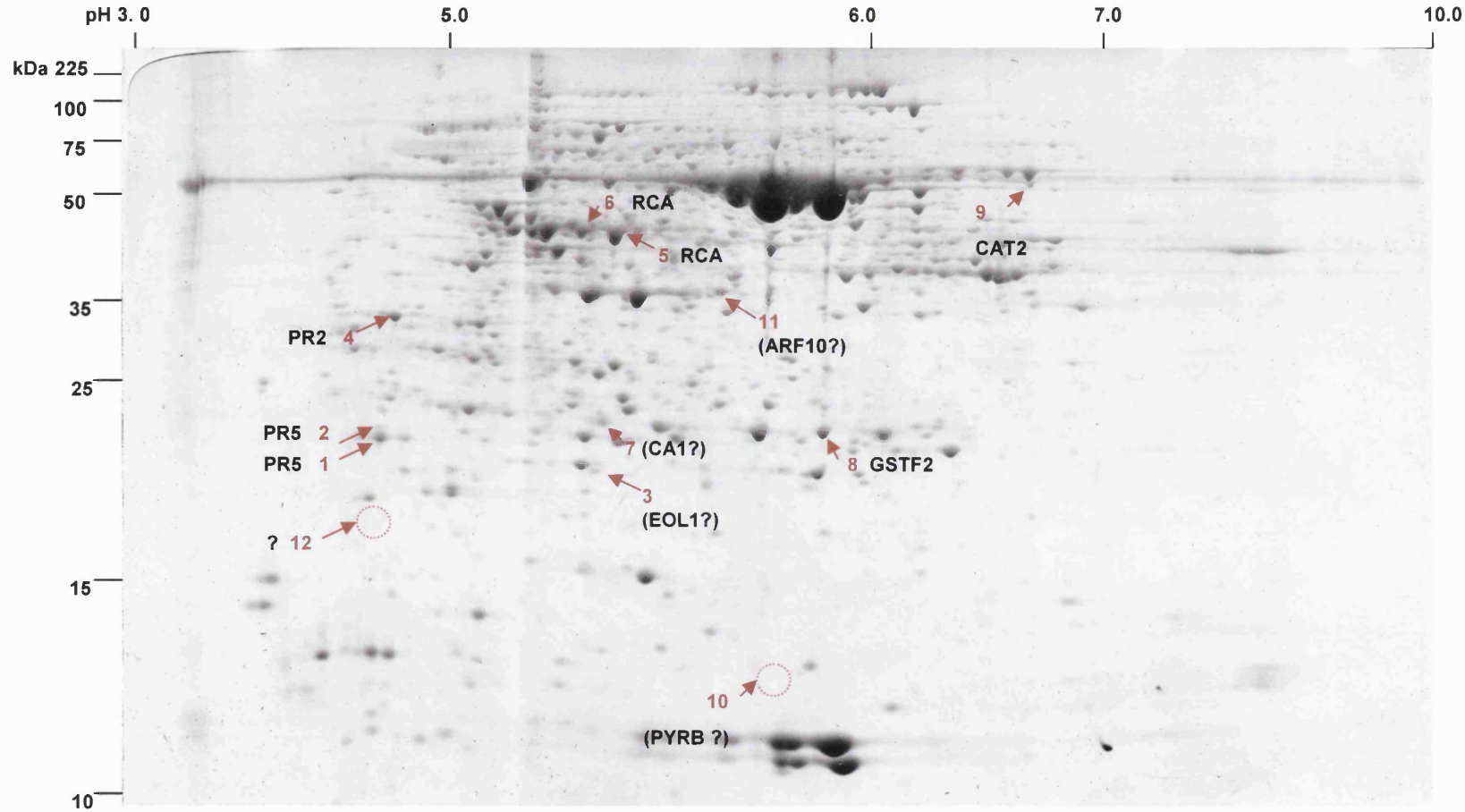

Fig.7.2 Protein spots that differ in abundance among the studied samples

The 2-gel image of cytosolic proteins extracted from shoot tissue of 21-d old ppi plants grown on M&S medium under long-days. A protein sample of 200 µg was focussed on 24 cm IPG strips with a non-linear pH gradient 3-10, then separated by SDS-PAGE on a 12.5 % gel and stained with SYPRO™ Ruby fluorescent dye.

Arrowed numbers indicate the location of spots that differ in abundance between the genotypes studied. The dotted circles represent spots that did not appear on gels for this particular genotype, but appeared in gels for another genotype/s. The name of the proteins for those that were identified are given along with the spot number. The proteins whose PMF data found a match in the databases but could not be confirmed due to their theoretical and observed Mr/pI differences are given with brackets with a question mark.

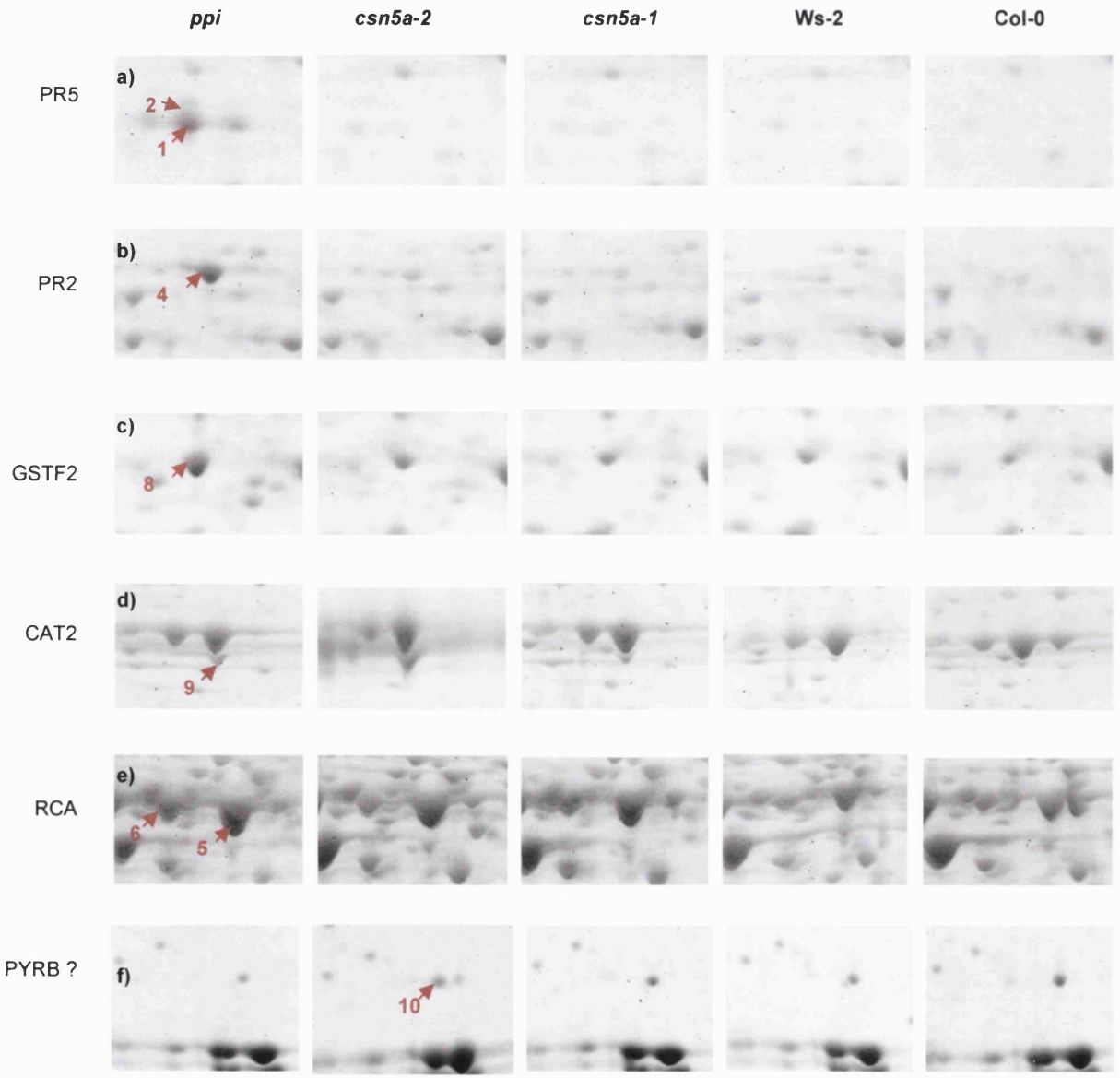

Fig. 7.3 Relative abundance of identified spots in the five genotypes

a) PR5 (spot # 1 & 2) was present only in the 2-D gels derived for *ppi* protein samples.

b) PR2 (spot # 4) was more abundant in *ppi*

c) GSTF2 (spot # 8) was more abundant in all three mutant lines compared to their respective wild types

d) CAT2 (spot # 9) was more abundant in all three mutant lines compared to their respective wild-types

e) Spot # 5 & 6 were identified as the same protein RCA and were more abundant in all three mutants compared to the wild-types

f) Spot # 10 was present only in the gels of csn5a-2. PMF data gave a match for PYRB, but was disregarded as the observed M_r did not match with the theoretical value.

(a)

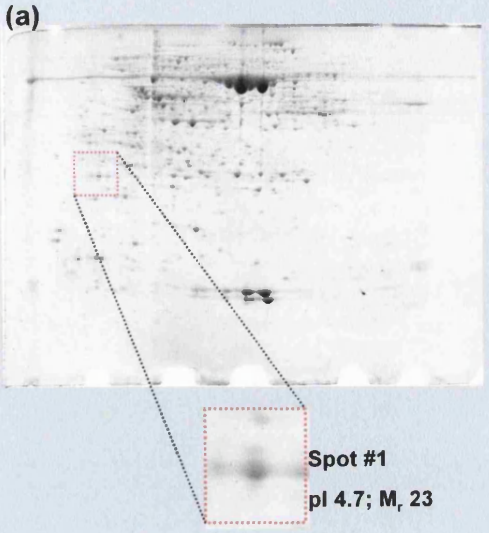

(b)

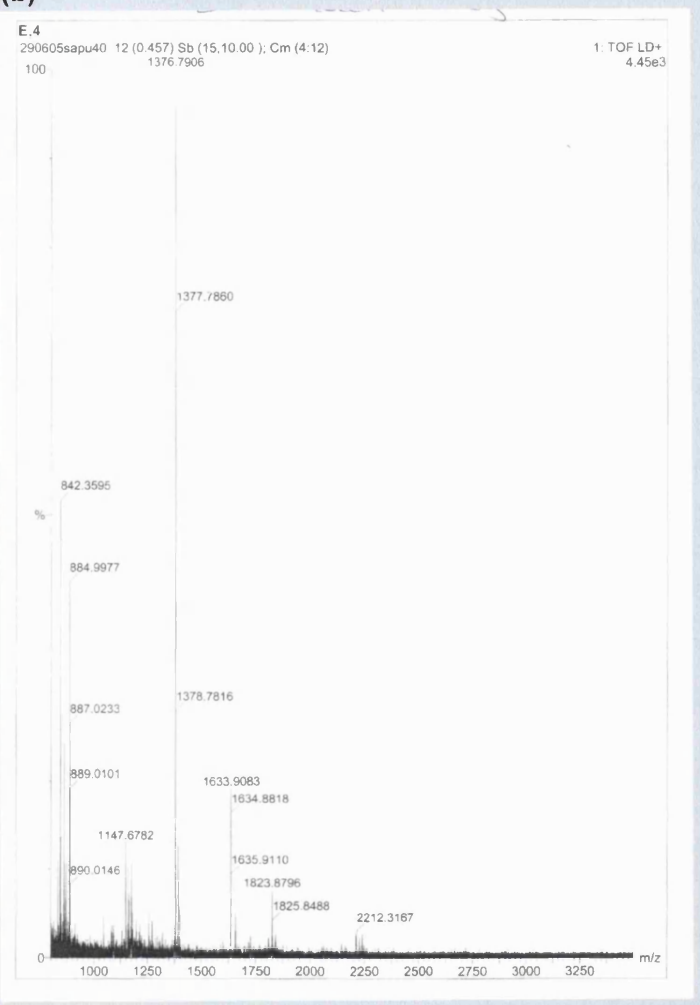

Fig.7.4 Steps involved in identifying a protein spot in a 2D analysis based on MALDI-ToF-MS/PMF data

(a) 2-D gel image (SYPRO Ruby) of cytosolic proteins from ppi. Spot # 1 (enlarged) was selected for MS.

(b) MALDI-ToF- Mass spectrum derived for spot #1 digested with trypsin

(c) Swiss-Prot result for PMF data for spot #1. Of the several matches, only the most appropriate one with the closest pI and M_r (circled red) values is presented.

(Figure 7.4 continued over leaf)

(c)

1. P28493 (Pathogenesis related protein 5 precursor PR 5)

Proteins

Accession Number	Name	Description	MW	pI	Score	Coverage	Matches
P28493	PR5_ARATH	Pathogenesis related protein 5 precursor PR 5	25235.672	4.736	12.0	16.7	3

Peptides

Sequence	Submitted Mass	Submitted Charge	Experimental Mass	Retention Time	MW	Delta (Da)	Delta (PPM)	Modifications	Start	End	Score	Ladder Score
CVTGDCGGLR	1094.581	1.0	1093.573	0.0	1093.464	-0.109	-99.838	Carbamidomethyl C(1) Carbamidomethyl C(6)	89	98	4.3	
DFYDVSLVDGYNVK	1633.925	1.0	1632.917	0.0	1632.767	-0.150	-91.970		121	134	3.2	
GANDKPETCPPTDYSR	1807.959	1.0	1806.951	0.0	1806.784	-0.167	-92.520	Carbamidomethyl C(9)	190	205	4.5	

(d)

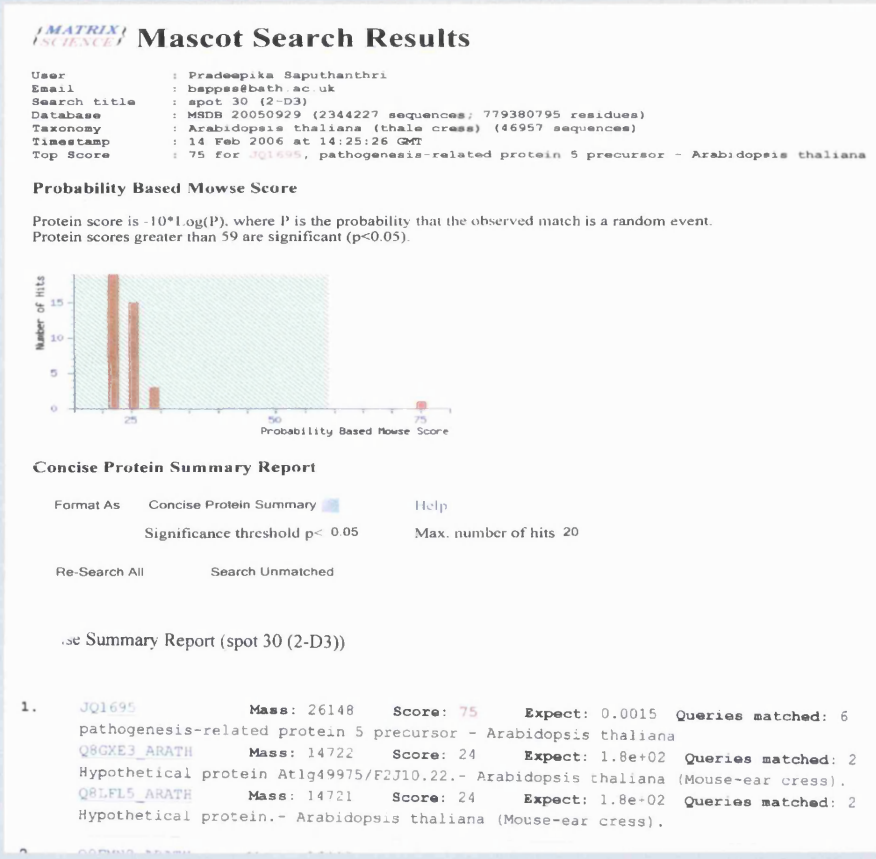

MATRIX SCIENCE Mascot Search Results

User : Pradeepika Saputhanthri
Email : bspps@bath.ac.uk
Search title : spot 30 (2-D3)
Database : MSDB 20050929 (2344227 sequences; 779380795 residues)
Taxonomy : Arabidopsis thaliana (thale cress) (46957 sequences)
Timestamp : 14 Feb 2006 at 14:25:26 GMT
Top Score : 75 for JQ1695, pathogenesis-related protein 5 precursor - Arabidopsis thaliana

Probability Based Mowse Score

Protein score is -10*Log(P), where P is the probability that the observed match is a random event.
Protein scores greater than 59 are significant (p<0.05).

Concise Protein Summary Report

Format As Concise Protein Summary Help

Significance threshold p< 0.05 Max. number of hits 20

Re-Search All Search Unmatched

se Summary Report (spot 30 (2-D3))

1. JQ1695 Mass: 26148 Score: 75 Expect: 0.0015 Queries matched: 6
pathogenesis-related protein 5 precursor - Arabidopsis thaliana
Q8GXE3_ARATH Mass: 14722 Score: 24 Expect: 1.8e+02 Queries matched: 2
Hypothetical protein At1g49975/F2J10.22.- Arabidopsis thaliana (Mouse-ear cress).
Q8LFL5_ARATH Mass: 14721 Score: 24 Expect: 1.8e+02 Queries matched: 2
Hypothetical protein.- Arabidopsis thaliana (Mouse-ear cress).

(e)

Mascot Search Results: Protein View

MATRIX SCIENCE Mascot Search Results

Protein View

Match to: JQ1695 Score: 75 Expect: 0.0015
pathogenesis-related protein 5 precursor - Arabidopsis thaliana

Nominal mass (M_r): 26148; Calculated pI value: 4.75
NCBI BLAST search of JQ1695 against nr
Unformatted sequence string for pasting into other applications

Taxonomy: Arabidopsis thaliana
Links to retrieve other entries containing this sequence from NCBI Entrez:
AAF21072 from Arabidopsis thaliana
AAA32865 from Arabidopsis thaliana
AAB68336 from Arabidopsis thaliana
AAK59672 from Arabidopsis thaliana
AAL15220 from Arabidopsis thaliana
AAG51023 from Arabidopsis thaliana
PR5_ARATH from Arabidopsis thaliana

Fixed modifications: Carbamidomethyl (C)
Variable modifications: Oxidation (M)
Cleavage by Trypsin: cuts C-term side of KR unless next residue is P
Number of mass values searched: 37
Number of mass values matched: 6
Sequence Coverage: 31%

Matched peptides shown in Bold Red

1 MANISSIHIL FLVFITSGIA VMATDFTLRN NCPTTVWAGT LAGQGPKLGD
51 GGFELTPGAS RQLTAPAGWS GRFWARTGCN FDASGNGRCV TGDGGGLRCN
101 GGGVPPVTLA EFTLVGDGGK DFYDVSLVDG YNVKLGIRPS GGSGDCKYAG
151 CVSDLNAACP DMLKVMDQNN VVACKSACER FNTDQYCCRG ANDKPETCPP
201 TDYSRIFKNA CPDAYSYAYD DETSTFTCTG ANYEITFCP

Show predicted peptides also

Sort Peptides By Residue Number Increasing Mass Decreasing Mass

http://www.matrixscience.com/cgi/protein_view.pl?file=../data/20060214/FAgpCbTO.dat&hit=1

Fig.7.4 (contd.) Steps involved in identifying a protein spot in a 2D analysis based on MALDI-ToF-MS/PMF data

(d) Screen capture of MASCOT search results showing the predicted identification of PR5 (spot #1)

(e) Screen capture of MASCOT search results showing the matched peptide fragments (in red)

Table 7.3: List of proteins identified using MALDI-ToF-MS/PMFs and SwissProt/ MASCOT data base searches

Protein identifications that were confirmed by matching experimental M_r and pI values with those of theoretical ones are given in bold.

Spot No.	Observed from 2-D gels		UniProtKB/Mascot data base search results				
	M_r (kDa)	pI	UniProt Accession Number	Protein Name/ Synonyms	Gene locus & name	Theoretical	
						M_r (kDa)	pI
1	**23**	**4.7**	**P28493**	**Pathogenesis-related protein 5 [Precursor] / PR5**	**At1g75040**	**25.2**	**4.73**
2	**23.2**	**4.7**	**P28493**	**Pathogenesis-related protein 5 [Precursor] / PR5**	**At1g75040**	**25.2**	**4.73**
3	22	5.4	Q9ZQX6	ETO1-like protein 1 / Ethylene over producer 1-like protein 1	At4g02680 EOL1	100	5.75
4	35	4.8	P33157	Glucan endo-1,3-beta-glucosidase, acidic isoforms [Precursor]/ Beta-1,3 glucanase 2/ Pathogenesis-related protein 2 precursor / PR2 /EC3.2.1.39	At3g57260 BG2/ BGL2	37.3	4.88
5	**43**	**5.4**	**P10896**	**Ribulose bisphosphate carboxylase/oxygenase activase, chloroplast [Precursor]/ RuBisCO activase / RCA**	**At2g39730 RCA**	**43**	**5.9**
6	**43**	**5.3**	**P10896**	**RuBisCO activase / RCA**	**At2g39730 RCA**	**46**	**5.89**
7	22	5.5	P27140	Carbonic anhydrase, chloroplast [Precursor] / EC 4.2.1.1 /Carbonate dehydratase	At3g01500 CA1	37	5.9
8	**23**	**5.9**	**P46422**	**Glutathione S transferase PM24/ AtGSTF2/ 24kDa Auxin binding protein**	**At4g02520**	**23.9**	**6.45**
9	**57**	**7.0**	**P25819**	**Catalase 2**	**At4g35090 CAT2**	**56.8**	**7.04**
10	14	5.8	P49077	Aspartate carbamoyl transferase, chloroplast[Precursor]/ EC 2.1.3.2	At3g20330 PYRB	43	6.5
11	37	5.7	Q9SKN5	Auxin response factor 10	At2g28350 ARF10	70	7.9

Compared to the Ws-2 and Col-0 wild-types, all the three *cns5a* mutants showed enhanced accumulation of RCA, CAT2 and GSTF2 proteins in the 2-D gels.

RCA / RuBisCO Activase/ At2g39730/ P10896 :

RCA, a nuclear encoded chloroplast protein, functions in activation of RuBisCO (ribulose-1,5-bisphosphate carboxylase/oxygenase and involves the ATP-dependent carboxylation of the epsilon-amino group of lysine leading to a carbamate structure (http://au.expasy.org/uniprot/P10896). Two isoforms are produced by alternative splicing and the light activation of RuBisCO requires the 46kDa larger isoform and redox regulation of RCA is required for the down regulation of RuBisCO in low light (Zhong *et al*, 1994). RCA mRNA is highly expressed in almost all vegetative tissue of *Arabidopsis,* including immature siliques, immature seeds and to a lower extent in shoot apex, but not expressed in roots, mature pollen, mature-, dry or imbibed seeds (Schmidt *et al*, 2005).

The presence of this chloroplast protein in the cytoplasmic fraction of proteins used for 2-DE could be most likely because chloroplast degradation had occurred to some extent in the sample preparation which is not unusual. Similarly, proteins that can be only loosely associated with the membranes may be found in the cytoplasmic protein extracts. However, we cannot rule out a possible effect of the *csn5*a mutations that influences its distribution and probably its upregulated expression in the mutant lines compared to the wt. As the plant material for this experiment was obtained from light-grown plants, the loss of COP1 activity leading to increased HY5 accumulation and subsequent miss-expression of light induced genes in the dark cannot be applied to explain increased RCA accumulation in the mutants. However, the *csn5* mutants (*csn5*a-2 *csn5*b-1 double mutant), as well as other *csn* subunit mutants have been shown to upregulate light induced genes compared to the wt, not only in the dark, but also in the light. This has been demonstrated by RT-PCR analysis of two light induced genes *RBCS1* (encodes small subunit of RuBisCO) and *PSBA* (encodes 32 kDa protein of the Photo system II). Particularly, *PSBA* transcript levels were up regulated compared to the wt in the double mutant and another csn subunit mutant (Dohmann *et al*, 2005). To confirm whether the *csn5*a mutant show upregulated RCA, further experiments such as 2DE with protein samples from dark-grown plants or RT-PCR with light- and dark-grown plant material are required.

CAT2/ Catalase2/ At4g35090/ P25819 :

CAT2 is a peroxisomal catalase involved in the H_2O_2 catabolic process and is involved in protecting cells from the toxic effects of H_2O_2. The protein occurs in almost all aerobically respiring organisms and at least 6 -7 isozymes are produced from 3 gene products (http://au.expasy.org/uniprot/P28493).

CAT2 mRNA is usually abundant in root tissue, highly expressed in bolts and leaves. It is not induced by plant hormones, but is highly induced by cold treatment (Schmidt *et al*, 2005) . The mRNA expression patterns showed circadian regulation and seedling mRNA abundance is regulated by light and is not seen in etiolated seedlings. CAT2 mRNA accumulation is induced by exposure to high fluence blue or far-red light, but not by red light, suggesting phytochrome involvement (Zhong *et al*,1994).

GSTF2 /Glutathione S transferase/ 24 kDa Auxin binding protein/At4g02520/ P46422:

The GSTF2 protein catalyzes the conjugation of reduced glutathione to a wide number of exogenous and endogenous hydrophobic electrophiles and is known to be located in microsomes and plasma membrane vesicles (http://au.expasy.org/uniprot/P46422). Finding this protein in the cytoplasmic fraction could again be indicative of the quality of the protein sample as mentioned in the case for RCA.

GSTF2 mRNA levels are very high in young leaves, moderately high in rosette leaves- and high in the cauline leaves after transition to flower. The mRNA is highly induced by abiotic stress including osmotic stress and UV-B and to a lesser extent by wounding (Schmidt *et al*, 2005). GSTF2 is expressed during normal plant development and in response to phytohormones such as auxin, ethylene and a variety of stress conditions or stress inducing substances such as SA, GSH, pathogen attack, copper, herbicides and herbicide safeners (Smith *et al.*, 2003 and references therein).

Arabidopsis GSTF2 shows glutathione peroxidase activity in addition to glutathione transferase activity and also has been identified as an auxin binding protein (Zettle *et al* 1994, Murphy *et al* 2002). AtGSTF2 was identified while screening for ethylene induced genes (Zhou and Goldsbrough, 1993 in Smith *et al* 2003). AtGSTF2 mRNA expression in both shoots and roots of seedlings is induced by ethylene and a link between ethylene, GSTF2 and root hair development has been suggested (Smith *et al*, 2003, Mang *et al.*, 2004).

The *ppi* mutant displayed high accumulation of PR5. This protein spot was absent in the 2-D gels from any other genotype. The PR2 protein was more abundant in *ppi* 2-D gels compared to all the other genotypes.

PR5/ Pathogenesis related protein5/ At1g75040/P28493:

The PR5 protein is partially responsible for systemic acquired pathogen resistance (SAR), and belongs to the thaumatin family. It is a secreted protein and accumulates in the apoplast before secretion into the extra cellular space (http://au.expasy.org/uniprot/P28493). The protein is strongly induced by pathogen infection, by 2,6-dichloroisonicotinic acid (INA) and salicylic acid indicating it may be a possible endogenous signal for acquired resistance (SAR) (Uknes *et al*, 1992).
The PR5 mRNA is not expressed in seeds, siliques, shoot apices, unopened flower buds, pollen or vegetative rosette plants however, at transition to flowering it is expressed in entire rosette, cauline leaves, and in flowers and sepals (Schmidt *et al*, 2005). The mRNA expression is very high in senescent leaf tissue. The mRNA was induced highly by pathogens and to a lesser extent by abiotic stress (osmotic stress, UV-B). The hormones or hormone precursors ACC, zeatin, IAA, ABA, GA_3, MeJA and brassinosteroids enhanced the mRNA expression slightly. Li and Strid (2005) demonstrated that PR5 induction in *Arabidopsis* is paralleled by increased secondary metabolism, as shown by enhanced chalcone synthase (CHS) gene expression and anthocyanin accumulation in leaves after decapitation of inflorescence stem and a possibility of PR5 gene expression in regulating anthocyanin accumulation has been proposed.

PR2/ β-1,3-glucanase/BGL2/ At3g57260/P33157:

PR2 catalyses the hydrolysis of 1,3-beta-D-glucosidic linkages in 1,3-beta-D-glucans and is implicated in the defence of plants against pathogens (http://au.expasy.org/uniprot/P33157; Uknes *et al*, 1992). Its subcellular location and induction by pathogens, INA and SA and its mRNA expressions are more or less similar to PR5 (Schmidt *et al*, 2005) .

7.3 Discussion

7.3.1 The *csn5a* mutants may have activated mechanisms to combat toxic effects of excess reactive oxygen species (ROS).

The features associated with the *csn5a* mutants such as altered hormone and light responses, possible miss-expression of light-induced genes are indicative of altered or imbalanced cellular metabolic processes. The phenotypic aspects of the mutants such as production of fewer root hairs could place the mutants under stress as the water and nutrient uptake must be impaired in the mutants. Production of excess reactive oxygen species (ROS) is a common feature when a plant is under environmental stress or under conditions where the cellular homeostasis is imbalanced.

ROS are the partially reduced-, or activated derivatives of oxygen (superoxide $O_2^{\cdot-}$ singlet oxygen $^1O_2$, hydrogen peroxide H_2O_2 and the hydroxyl radical $HO\cdot$) and are normally produced as a result of electron flow to molecular oxygen from multiple sites in the photosynthetic and respiratory chains (Foyer and Noctor, 2005). Production of ROS is enhanced in plants by conditions limiting CO_2 fixation, such as drought, salt and temperature stress as well as by the combination of these conditions with high-light stress (Mittler *et al.*, 2004). ROS are highly reactive and toxic, and can lead to oxidative destruction of cells mainly by oxidative damage to proteins, DNA and lipids (Buchanan *et al.*, 2000). Thus, a tight regulation of steady state levels of ROS in plant cells is required and plants have mechanisms to combat excess ROS produced in abiotic stress conditions or in any other disturbance to the cellular homeostasis, particularly during environmental stress conditions. The anti-oxidative system, consisting of Superoxide dismutase (SOD), ascorbate peroxidase (APX), catalase (CAT), glutathione peroxidase (GPX) and peroxiredoxins (PrxR) and the non-enzymatic antioxidants in plants and ascorbate (Vitamin C), reduced glutathione (GSH), α-tocopherol (Vitamin E) and carotenoids determines primarily the extent to which ROS accumulates in a cell (Foyer and Noctor, 2005; Mittler *et al*, 2004, Amme *et al* 2006).

Increased levels of CAT2 in *csn5a* mutants could be directly linked to a possible requirement of detoxification of excess ROS produced in these plants as the mutations have placed them under stress. AtGSTF2, too has been implicated in detoxification of ROS by its glutathione peroxidase activity and could be scavenging ROS among its many other roles. A closely related protein, AtGSTF6 (or Auxin binding protein1,ABP1) is considered as a marker gene for plant stress, particularly oxidative stress and it has been suggested that

reactive oxygen species might be a common secondary stress factor responsible for the induction of GST genes (Marrs 1996). It would be interesting therefore in future research to determine the levels of ROS in *csn5a* mutants.

7.3.2 Certain redox signalling pathways could be activated or altered in *ppi.*

Production of ROS may also substantially alter the redox balance in the responding cells. Redox signal transduction or ROS-mediated signaling has been implicated in regulation of many mammalian transcription factors such as AP-1, Nf-κB. Binding of the transcription factors to DNA is favoured by a reducing environment and is inhibited by GSSG or oxidized thioredoxins (Drög 2002). It is possible that the activity of specific plant transcription factors may also be regulated by changes in the redox status of cells.

The ROS signalling in plants has been particularly implicated in responses to stress, including pathogen defence, programmed cell death (PCD), stomatal behaviour and regulation of development (Apel and Hirt, 2004). Any stimulus that disturbs the cellular redox balance (such as low levels of ascorbate or changes to cellular glutathione levels) may induce these signal transduction pathways and may induce a number of defence genes including PR proteins (Foyer and Noctor, 2005).

H_2O_2 is known to induce genes for proteins involved in certain cell protection mechanisms, for example, glutathione S-transferase and it induces benzoic acid 2-hydroxylase (BA 2-H) enzyme activity, which is required for biosynthesis of SA (Buchanan *et al,* 2000). SA has been implicated in the regulation of PCD and also in regulating PR proteins in association with SAR. Both ROS and anti-oxidants have been linked to SA signalling. This is likely related to redox modulation of NPR1 (non-expressor of PR1), a protein necessary for SA signalling. NPR1 exists as an oligomer formed by intermolecular disulfide bonds and induction of SAR leads to a change in cellular reduction potential that reduces NPR1 to its monomeric form, which accumulates in the nucleus and activates target gene expression (Chern *et al.*, 2005; Mou *et al.*, 2003). *Arabidopsis npr1* mutants cannot induce *PR* genes as NPR1 nuclear localization is essential for its function in promoting *PR* gene expression.

From this proteomic analysis it appears that the mutation in *ppi* particularly seems to affect a pathway leading to the accumulation of PR proteins. The difference between the other two alleles and *ppi* is that *ppi* has been shown to produce a truncated CSN5A protein that could be more abundant in the cytoplasmic fraction of protein extracts. It is possible that this truncated protein could be affecting *ppi* gene expression or protein regulation in a

manner different to that of the other two alleles and leading to enhanced accumulation of these two PR proteins in *ppi*.

7.3.3 The CSN/ CSN5 is involved in *Arabidopsis* stress signalling

CSN seems to be a point of convergence for several protein degradation pathways as it interacts with cullin containing E3 Ub-ligases including SCFs, CUL3/BTB1 and COP1 (Moon *et al* 2004). The SCF type E3 ubiquitin ligases are important, particularly in stress signalling pathways in plants. One example is the jasmonate mediated responses to stress such as wounding and elicitor molecules, UV light and ozone exposure, drought, defences against insects and pathogens (reviewed in Devoto and Turner 2005). These responses are mediated through SCF^{COI1}, which has been demonstrated to interact physically with and regulated by the CSN. As for many other stimuli such as plant hormones, plant's responses to stress are modulated by signalling cross-talk and the CSN and its subunits could possibly be mediating such networks by regulating other E3 ligases.

As detailed in Chapter 1, the CSN is involved in stress response pathways in mammalian cells, as has been shown by its interactions with various transcription factors regulating AP-1 activity and phosphorylation of proteins such p53, c-Jun, IκBα by CSN-associated kinase. CSN5/JAB1 plays a major role in some stress responses as its binding has been shown to stabilize or destabilize components of pathways, particularly those associated with AP-1 activation (Wei & Deng, 2003).
The link between the CSN or CSN subunits and *Arabidopsis* stress responses has not been demonstrated though the CSN has been implicated in *Arabidopsis* pathogen response in relation to *R*-gene mediated pathogen response (Sullivan *et al*, 2003).

Our studies reported here indicate that the CSN/ CSN5 could be involved in stress responses in *Arabidopsis*. The *ppi* mutant seems to present a useful system to study related aspects, especially how CSN5 or CSN links to SAR. The results presented here suggest that it would be interesting to assess the response of the *csn5a* mutants to a range of stress conditions.

Chapter 8

General Discussion

8.1 New insights into the role of CSN in *Arabidopsis*.

In this thesis I have reported the isolation and characterization of a novel mutant allele of *AtCSN5A, purple patch inflorescence* in *Arabidopsis thaliana* ecotype Ws-2, with a pleiotropic phenotype. With this study we have gained new insights into the contribution of *CSN5A* and the CSN^{CSN5A} in plant development and responses to endogenous and environmental signals.

The *ppi* mutation mapped to the *CSN5A* (At1g222920) gene that encodes the fifth subunit of the COP9 Signalosome. The best known function of the CSN is its ability to derubylate cullin-RING E3 complexes, regulating the ubiquitination of their substrate proteins and subsequent degradation via the 26S proteasome. The CSN in plants is also known for its role as a repressor of photomorphogenesis in the dark, primarily by mediating the activity of COP1.

Sequence analysis of the *ppi* DNA revealed an 11-bp deletion in the 4^{th} exon of *CSN5A*, leading to a predicted truncated protein in which the last 58 amino acids are lost leaving 1-299 amino acids. The *ppi* mutant was found to be allelic to *csn5a-1* and *csn5a-2*, two T-DNA insertion mutants from the Salk collection in the Col-0 back ground.
RT-PCR and Western blot analyses indicated that *ppi* produces reduced levels of the truncated CSN5A protein suggesting a partially functional CSN. The *csn5a-2* mutant showed residual levels of the wild-type CSN5A protein, and therefore it, too, could be partially functional. The *csn5a-1* mutant did not produce any detectable levels of the transcript or the protein and therefore is a null mutant. These results on the T-DNA insertion alleles are in agreement with the observations reported recently by Gusmaroli *et al* (2007).
The overall phenotype of the three mutants were similar under long-day photoperiod, but they also reflected allelic differences to some extent as the *csn5a-1* null mutant displayed a more severe phenotype compared to the other two mutant lines.

We have shown that although the phenotypes of the three alleles are not very different from each other under long-day conditions, they could vary drastically under different or extreme conditions as demonstrated by the responses to extra-long day length.

The *csn5a*-1 and *csn5a-2* mutants have previously been reported to show reduced auxin responses and reduced cytokinin responses (Schwechheimer *et al*, 2001, Dohmann *et al*, 2005, Gusmaroli *et al*, 2007). We confirmed these observations and in addition have demonstrated all three *csn5a* mutants to show altered responses to other hormones and hormone precursors including ACC, EBR, GA and ABA. The differences in the responses to hormones were most pronounced for the inhibition of seed germination by the GA biosynthesis inhibitor paclobutrazol and for ABA. The three mutants showed reduced response to lateral root elongation under treatment with localized nitrate, as it could only partially rescue the lateral root phenotype.
Light fluence rate experiments showed that all the three mutants behave opposite to the wt under a range of red-light intensities as their hypocotyl elongation was enhanced and not inhibited as in the wt. In contrast to the other two mutant lines and the wt, *ppi* did not respond to blue light under our experimental conditions. Our results were different from the previously reported hypocotyl inhibition for the *csn5a-1* and *csn5a-2* mutants under constant blue, red, or far-red light (Gusmaroli *et al*, 2007), but obviously, our experimental conditions were not the same as those reported, and have given additional information on the response of *csn5a* mutants to different light qualities at different intensities.
A comparative proteomic analysis by 2-DE of the shoot protein samples revealed that the ROS scavenging enzymes Catalase2 and GSTF2, and also the photosynthesis related RuBisCO Activase were more abundant in the mutants compared to the wt, suggesting that the *csn5a* mutations lead to the plants becoming stressed, possibly similar to high-light intensity. From microarray analysis of other *csn* and *cop/det/fus* mutants it has been shown that in light they mimic gene profiles similar to wt plants grown under high light intensity stress (Ma *et al*, 2003). The CSN has been implicated in animal stress response pathways and it is involved in *Arabidopsis* stress response via the regulation of JA responses through SCF^{COI1}. Our data support the role of the CSN, and specifically the CSN5 subunit in *Arabidopsis* stress responses.

The 2-DE of *ppi* protein samples displayed a unique feature by accumulating two pathogenesis related proteins PR5 and PR2, in the absence of pathogens. A connection between the CSN and the *R*-gene mediated pathogen response pathway in *Arabidopsis* has

been implicated (reviewed in Sullivan *et al*, 2003). We have demonstrated that there is a link between the CSN or CSN5 and expression of *PR* genes, probably through redox signalling pathways.

In view of the levels of CSN5 in the mutants we can reasonably speculate that the level of the CSN present in plants could affect its functions and this is supported by the previous observations that a reduction in the level of one sub unit leads to a reduction in the overall amount of the CSN and thereby its function (Serino and Deng, 2003).

We have shown that it is important to study the behaviour of mutants under different growth conditions and a range of growth stimuli to obtain a more complete picture of the gene function. We observed distinct phenotypic differences and timing of flowering of the *csn5a* mutants only under extreme light regimes. Under long-day photoperiod, there were only subtle differences among the three alleles in their phenotypes, but under the extra-day length, *ppi* behaved opposite to the other two alleles as the truncated protein produced in the *ppi* apparently was able to release the mutant from the severely dwarfed phenotype of the *csn5a-1* and *csn5a-2* alleles. If not for the sophisticated controlled environment growth facilities, we would not be able to capture those allelic differences.
Similarly, by using a range of intensities we were able to observe altered light responses of the *csn5a* mutants that had not been reported previously. The *csn5a-1* and *csn5a-2* mutants have been described as hyperphotomorphogenic under any light condition as their hypocotyls were shorter compared to the wt under constant blue, red, far-red or white light (Gusmaroli *et al*, 2007). Looking at the fluence rate graphs it is clear that at certain fluence rates you observed the same i.e. that mutant hypocotyls were shorter than wt, however, our data demonstrates greater complexity as all the three *csn5a* mutants show hypocotyl elongation at low red-fluence rates, before starting to be inhibited, whereas for the wt, it was inhibitory through out the range of red fluence rates used. Under our experimental conditions, the *ppi* did not respond to blue light at all.

It is emphasized here that by utilizing three mutant alleles, we were able to gain greater insight into the function of the gene which would have been difficult or not possible at all, using any one of the mutants alone. The common practice of using a knock-out line to elucidate the gene function is of limited value especially when the gene product is involved in a range of cellular processes as in the case of CSN. Even in a single sub unit, the functions are affected by the availability of various functional domains/ motifs. A mutation

in a specific part of a gene could give significantly altered responses from other alleles. So at this point it would be logical to consider what the *ppi* mutant tells us about the possible function of the C-terminal region of the protein as the truncated CSN5A protein in ppi lacks a part of the C-terminal region.

8.2 The *ppi* is a unique *csn5a* mutant allele with alterations in possible CSN5 specific functions.

Most of the aspects of the pleiotropic phenotype and altered hormone/light responses of the *cns5* mutants could be linked to the CSN function in regulating cullin-RING E3 ubiquitin ligases.

The *ppi* mutants, in general, gave results more or less similar to the other two alleles or other csn subunit mutants. However, it showed some unique features of its own and not observed in other two alleles. Those were, the anthocyanin accumulation in localized areas on the inflorescence, blue-light non-responsiveness of the hypocotyls, extremely bushy but tall stature under extra-day length, abnormal two-branched trichomes, and accumulation of two pathogenesis related proteins PR5 and PR2 in the absence of pathogens. At least some of these processes are regulated by interconnected and overlapping pathways.

Systemic acquired resistance (SAR) in plants is the immune response that is induced in the uninfected parts of the plant after pathogen attack (Clarke *et al*, 2001). SAR is characterized by an increase of endogenous SA levels, expression of a subset of PR proteins and enhanced resistance to a broad spectrum of virulent pathogens. Exogenous application of salicylic acid (SA) and its chemical analogue INA can induce SAR and activate *PR* gene expression.

Local response to pathogen attack is the hypersensitive response (HR). In this, commonly an interaction between plant *R* gene products and a pathogen *avr* gene product in the cells, leads to rapid ion flux, oxidative burst giving rise to ROS accumulation, generation of SA, nitric oxide and local/systemic activation of defence related genes. Often necrosis in the form of localized cell death is associated with the HR and a balance between the levels of ROS, SA, nitric oxide are believed to be important in bringing about the HR (Clarke *et al*, 2001). Plant hormones JA and ethylene play a role as important mediators of local and systemic disease resistance pathways independent of SA.

There is a complex interplay of signalling molecules determining the plant's response to pathogens and components of SAR and HR pathways overlap at various points. One

component is the NPR1 (Non-expresser of PR genes 1) that functions downstream of SA. In the *Arabidopsis npr1* mutants the induction of SAR and SA responsive PR gene expression is severely impaired (reviewed in Devoto and Turner, 2005). On the other hand, the mutants of the *CPR* (Constitutive Activator of PR genes) genes express PR genes constitutively. As mentioned in Chapter 5, the *ppi* mutant mimics at least partly the *cpr5-2* mutant that has two branched trichomes, shows spontaneous necrotic lesions and constitutively express *PR5* and *PR2* (Jens *et al*, 1998; Boch *et al*, 1998).

In animal cells, the cyclin dependent kinase (CDK) inhibitor p27 regulates the cell cycle and induces apoptosis. The CSN and CSN5/Jab1 regulate p27 (detailed in Chapter 1) in a number of ways.
ICK (Inhibitor of CDK), the *Arabidopsis* homolog of the animal p27, when over-expressed ubiquitously via *35S:ICK* leads to severe growth reduction with reduced organ size and cell numbers in transgenic *Arabidopsis* plants (Mizukami, 2001). When it was expressed specifically in trichomes, the endoreduplication cycle progression was stopped and the trichome cells eventually died prematurely (Hülskamp, 2004).
The *Arabidopsis cpr5* mutant shows a trichome phenotype similar to ICK/KRP over expressing lines where endoreduplication cycle stops and with a ploidy level of 8C, trichome cells undergo unscheduled cell death (Hülskamp, 2004; Clarke *et al*, 2001).

Considering our data on the *ppi*, it could be suggested that the CSN / CSN5 functions at least partially at a point of intersection upstream of pathways regulating cell cycle/ endoreduplication progression, programmed cell death, HR and SAR in *Arabidopsis* .

The next obvious question to answer is why only *ppi* and not the other two allelic mutants. The difference between the *ppi* and the other two alleles is that it produces a truncated CSN5A whereas the other two produce either very low levels of the wt CSN5A (*csn5a-2* mutant) or none at all in the case of the null *csn5a-1* mutant. It could be reasoned that the truncated protein has acquired a novel function as the aspects of the phenotype were exclusive to *ppi*. This possibility has to be eliminated because the mutation is recessive.

In the *ppi* truncated protein, the amino acid region 300 - 357 is lost and the 1-299 region is intact. Somehow, absence of a part of the C-terminal region in the truncated *csn5a* protein of *ppi* had led to the activation of pathways that lead to the above observations.

Much research has been done on the regulation of p27 because of its significance in cell cycle regulation and human cancers. A link between the CSN5/Jab1 functional domains and regulation of p27 has been demonstrated using mammalian cell cultures (Tomoda *et al*, 2002). It has been suggested that CSN5/Jab1 functions as an adaptor between p27 and the nuclear transport receptor CRM1 to induce nuclear export and subsequent degradation of the p27 in the cytoplasm. CRM1 binds specifically to the nuclear export signal (NES) in the CSN5/ Jab1, and mediates nuclear export of p27. The NES has been shown to be conserved among CSN5 in various species and is found in the 233-242 amino acid region in AtCSN5 and is intact in the *ppi* mutant.

Although it was not possible for them to find another typical NES, the research work by Tomoda *et al* (2002) had indicated an additional putative NES in the C-terminal 242-334 region of the CSN5/Jab1 because deletion of the region lead to complete loss of the CRM1 binding to the NES and down regulation of p27. The possibility of functional domains other than NES has been emphasized for the C-terminus. Kwok *et al* (1998) reported a putative coiled-coil domain in the 264-290 region of AtCSN5A but this region too, should be intact in the *ppi* protein. However, the mutation in *ppi* could be affecting the overall conformation of the protein which may affect its specific interactions with other molecules. The functional importance of the CSN5A C-terminus is also reflected in the existence of two splice variants At1g22920.1 and At1g22920.2 that have two different versions of the C-terminal region. Taking into account the homologous gene *CSN5B*, the CSN5 has three versions of C-terminus that could be used in specific functions of the protein.

An important matter that needs addressing is how the functions of the truncated protein in *ppi* relate to the CSN complex and other CSN subunits.

In proliferating mouse fibroblast cells CSN5/ Jab1 was shown to exist in at least two forms (Tomoda *et al*, 2002): one ~ 100kDa, in association with a subset of other CSN subunits and had an accessible C-terminal region; the other ~450 kDa corresponding to the CSN-holo complex associated form, and had both the N- and C-termini blocked, as judged by the binding of CSN5/ Jab1 region specific anti bodies. In *Arabidopsis*, CSN5 monomer (~40 kDa) has been reported (Kwok *et al*, 1998). It has been suggested the p27 nuclear-cytoplasmic transport to be associated with the CSN and not by the CSN5 monomer (Tomoda *et al*, 2002). Chamovitz and Segal (2001) suggest that the CSN may be acting like a scaffolding complex for CSN5 and its nuclear substrates. The specific functions of the monomer or of the 'mini-CSN' complexes have not been established.

Two important questions to be addressed with *ppi* future work are whether the truncated protein is assembled into the CSN complex and its subcellular distribution relative to the wild-type CSN5. The CSN holo-complex is mainly nuclear and it has been reported that only the N-terminal region of the CSN5 is sufficient for its assembly into the complex (Tomoda *et al*, 2002). Our observations indicated a pronounced presence of the truncated CSN5A of ppi to be in a cytoplasmic protein extraction. The significance of this observation with respect to the CSN5 functions needs to be investigated further.

Many *Arabidopsis* mutants with truncated proteins have given valuable insights into various aspects of plant growth and development. One such example is the GA insensitive *gai* mutant. The DELLA proteins GAI/RGA are negative regulator of GA response in *Arabidopsis*. GA regulates stem elongation via GAI and RGA and seed germination via RGL2. The GAI/RGA genes were originally defined by the cloning of the mutant *gai* allele (Peng *et al*, 1997). The *gai* gene encodes a mutant protein that lacks a region of 17 amino acids close to the N-terminus. The mutation confers a dominant dwarf phenotype with a reduced GA response (Lee *et al*, 2002).

As mentioned in Chapter 1, the significance of the CSN is immense as it is highly conserved in eukaryotes and is key regulators of many cellular and developmental pathways. The understanding of the functions of the CSN and its subunits is far from complete. Our work on the *ppi* mutant suggests that it could provide an excellent system to further study the functions of the complex and also CSN5 specific functions in plants.

References

Achard P, Vriezen WH, Van Der Straeten D, Harberd NP. 2003. Ethylene regulates *Arabidopsis* development via the modulation of DELLA protein growth repressor function. *Plant Cell* **15**: 2816-2825.

AGI: *Arabidopsis* Genome Initiative. 2000. Analysis of the genome sequence of the flowering plant *Arabidopsis thaliana*. *Nature* **408**: 796-815.

Amme S, Matros A, Schlesier B, and Mock H. 2006. Proteome analysis of cold stress response in *Arabidopsis thaliana* using DIGE-technology. *Journal of Experimental Botany* **57**(7): 1537-1546.

Apel K, and Hirt H. 2004. Reactive oxygen species: Metabolism, Oxidative Stress, and Signal Transduction. *Annu. Rev. Plant Biol.* **55**: 373-399.

Azpiroz-Leehan R , and Feldmann K. 1997. T-DNA insertion mutagenesis in Arabidopsis: going back and forth. *Trends in Genetics.* **13:** 152-156.

Bauer J, Chen K, Hiltbrunner A, Wehrli E, Eugster M, Schnell D. and Kessler F. 2000. The major protein import receptor of plastids is essential for chloroplast biogenesis. *Nature* **403**: 203-207.

Bech-Otschir D, Seeger M, Dubiel W. 2002. The COP9 signalosome: at the interface between signal transduction and ubiquitin-dependent proteolysis. *J. Cell Sci.* **115**: 467-73.

Bell CJ, and Ecker JR. 1994. Assignment of 30 microsatellite loci to the linkage map of *Arabidopsis*. *Genomics* **19**: 137-144.

Bendahmane A, Kanyuka KV, and Baulcombe DC. 1997. High-resolution genetical and physical mapping of the Rx gene for extreme resistance to potato virus X in tetraploid potato.*TAG Theoretical and Applied Genetics* **95**: 1-2.

Berkelman T, and Stenstedt T. 2002. *2-D Electrophoresis using immobilized pH gradients: Principles and Methods*. Uppsala, Sweden : Amersham Biosciences.

Bhalerao RP, Eklof J, Ljung K, Marchant A, Bennett M, and Sandberg G. 2002. Shoot-derived auxin is essential for early lateral root emergence in *Arabidopsis* seedlings. *Plant J.* **29**: 325-332.

Blazquez MA. 2000. Flower development pathways. *J. Cell. Sci*. **113**: 3547-3548.

Buchanan BB, Gruissem W, Jones RL. (eds). 2000.*Biochemistry and Molecular Biology of Plants*. Rockville, Maryland: American Society of Plant Physilogists.

Canamero RC, Bakrim N, Bouly JP, Garay A, Dudkin EE, Habricot Y, and Ahmad M. 2006. Cryptochrome photoreceptors cry1 and cry2 antagonistically regulate primary root elongation in *Arabidopsis thaliana*. *Planta* **224**: 995-1003.

Canovas FM, Dumas-Gaudot E, Recorbet G, Jorrin J, Mock HP, and Rossignol M. 2004. Plant proteome analysis. *Proteomics* **4**: 285-298.

Cary AJ, Liu W , and Howell SH. 1995. Cytokinin action is coupled to ethylene in its effects on the inhibition of root and hypocotyl elongation in *Arabidopsis thaliana s* eedlings. *Plant Physiology,* **107**: 1075-1082.

Chamovitz DA, and Segal D. 2001. JAB1/CSN5 and the COP9 signalosome, a complex situation. *EMBO Rep.* **2**: 96-101.

Chamovitz DA, Wei N, Osterlund MT, von Arnim AG, Staub JM, et al. 1996. The COP9 complex, a novel multisubunit nuclear regulator involved in light control of a plant developmental switch. *Cell* **86**: 115-21.

Chen M, Tao Y, Lim J, Shaw A , and Chory J. 2005. Regulation of phytochromeB nuclear localization through light-dependent unmasking of nuclear-localization signals. *Curr. Biol.* **15**: 637-642.

Chen Z, Hagler J, Palombella VJ, Melandri F, Scherer D, Ballard D, and Maniatis T. 1995. Signal-induced site-specific phosphorylation targets IκBα to the ubiquitin-proteasome pathway. *Genes Dev.* **9**: 1586-1597.

Chern M, Fitzgerald HA, Canlas PE, Navarre DA, and Ronald PC. 2005. Overexpression of a Rice NPR1 Homolog Leads to Constitutive Activation of Defense Response and Hypersensitivity to Light. *Molecular Plant-Microbe Interactions* **18**(6): 511-520.

Claret FX, Hibi M, Dhut S, Toda T, Karin M. 1996. A new group of conserved coactivators that increase the specificity of AP-1 transcription factors. *Nature* **383**: 453-57.

Clarke JD, Aarts N, Feys BJ, Dong X , and Parker JE. 2001. Constitutive disease resistance requires EDS1 in the *Arabidopsis* mutants *cpr1* and *cpr6* and is partially EDS1-dependent in *cpr5* . *The Plant Journal* **26**(4): 409-420.

Cope GA, and Deshaies RJ. 2003. COP9 signalosome: A multifunctional regulator of SCF and other cullin-based ubiquitin ligases. *Cell* **114:** 663-671.

Cope GA, Suh GS, Aravind L, Schwarz SE, Zipursky SL, et al. 2002. Role of predicted metalloprotease motif of Jab1/Csn5 in cleavage of Nedd8 from Cul1. *Science* **298**: 608-11.

Delp G, and Palva ET. 1999. A novel flower-specific *Arabidopsis* gene related to both pathogen-induced and developmentally regulated plant β-1,3-glucanase genes. *Plant Molecular Biology* **39**: 565-575.

Deng XW, Dubiel W, Wei N, Hofmann K, Mundt K, et al. 2000. Unified nomenclature for the COP9 signalosome and its subunits: an essential regulator of development. *Trends Genet.* **16**: 202-203.

Devoto A, and Turner JG. 2005. Jasmonate-regulated *Arabidopsis* stress signalling network. *Physiologia Plantarum* **123**: 161-172.

Disch S, Anastasiou E, Sharma VK, Laux T, Fletcher JC, and Lenhard M. 2006. The E3 ubiquitin ligase BIG BROTHER Controls *Arabidopsis* organ size in a dosage-dependent manner. *Current Biology* **16**: 272-279.

Dohmann EM., Kuhnle C, and Schwechheimer C. 2005. Loss of the constitutive photomorphogenic9 signalosome subunit 5 is sufficient to cause the *cop/det/fus* mutant phenotype in *Arabidopsis. Plant Cell* **17:** 1967-1978.

Downes BP, Stuper RM, Gingerich DJ, and Vierstra D. 2003. The HECT ubiquitin-protein ligase (UPL) family in Arabidopsis: ULP3 has a specific role in trichome development. *The Plant Journal*. **35**(6): 729-742.

Drög W. 2002. Free radicals in the physiological control of cell function. *Phyiol. Rev.* **82**: 47-95

Edwards K, Johnstone C , and Thompson C. 1991. A simple and rapid method for the preparation of plant genomic DNA for PCR analysis. *Nucleic Acids Research* **19**(6): 1349.

Fankhauser C , and Casal JJ. 2004. Phenotypic characterization of a photomorphogenic mutant. *The Plant Journal* **39:** 747-760.

Feng S, Ma L, Wang X, Xie D, Dinesh-Kumar SP, et al. 2003. The COP9 signalosome physically interacts with SCFCOI1 and modulates jasmonate responses. *Plant Cell* **15**: 1083-94.

Fleet CM, and Sun T. 2005. A DELLAcate balance: the role of gibberellin in plant morphogenesis. *Current Opinion in Plant Biology* **8**: 77-85.

Forde BG. 2002. Local and long-range signalling pathways regulating plant responses to nitrate. *Annu. Rev. Plant Biol.* **53**: 203-24.

Foyer CH, and Noctor FG. 2005. Redox Homeostasis and Antioxidant Signaling: A metabolic Interface between Stress Perception and Physiological Responses. *The Plant Cell.* **17**: 1866-1875.

Fu X, and Harberd NP. 2003. Auxin promotes *Arabidopsis* root growth by modulating gibberellin response. *Nature* **421**: 740-743.

Gallardo K, Job C, Groot SPC, Puype M, Demol H, Vandekerckhove J, and Job D. 2001. Proteomic analysis of *Arabidopsis* seed germination and priming. *Plant Physiol.* **126**: 835-848.

Gazzarrini S , and McCourt P. 2003. Cross-talk in plant hormone signalling: what *Arabidopsis* mutants are telling us. *Annals of Botany* **91**: 605-612.

Ghassemian M, Nambara E, Cutler S, Kawaide H, Kamiya Y , and McCourt P. 2000. Regulation of abscisic acid signalling by the ethylene response pathway in Arabidopsis. *Plant Cell* **12:** 1117-1126.

Giavalisco P, Nordhoff E, Lehrach H, Gobom J, Klose J. 2003. Extraction of proteins from plant tissues for two-dimensional electrophoresis analysis. *Electrophoresis* **24**: 207-216.

Giraudat J, Beaudoin N, and Serizet C. 1999. EMBO COURSE- Practical Course on Genetic and Molecular Analysis of Arabidopsis- Module 2 : Mapping mutations using molecular markers. [WWW] http://www.isv.cnrs-gif.fr/embo99/manuals/pdf/ch2.pdf. (July 2003)

Glickman MH, Rubin DM, Coux O, Wefes I, Pfeifer G, et al. 1998. A subcomplex of the proteasome regulatory particle required for ubiquitin-conjugate degradation and related to the COP9-signalosome and eIF3. *Cell* **94**: 615-23.

Görg A, Boguth G, Obermaier C, Harder A, WeissW. 1998. 2-D electrophoresis with immobilized pH gradients using IPGphor isoelectric focusing system. *Life Science News* **1**: 4-6.

Görg A, Obermaier C, Boguth G, Harder A, Scheibe B, Wildgruner R, and Weiss W. 2000. The current state of electrophoresis with immobilized pH gradients. *Electrophoresis* **12**: 531-546.

Grierson C, and Schiefelbein J. 2002. Root Hairs. *The Arabidopsis Book*; doi: 10.1199/tab.0060 [WWW]http://www.bioone.org/archive/1543-8120/41/1/pdf/i1543 8120-41-1-1.pdf (August 2007)

Guo H, and Ecker JR. 2003. Plant responses to ethylene gas are mediated by SCF (EBF1/EBF2)-dependent proteolysis of EIN3 transcription factor. *Cell* **115**: 667-677.

Gusmaroli G, Figueroa P, Serino G and Xing Wang Deng XW. 2007. Role of the MPN Subunits in COP9 Signalosome Assembly and Activity, and Their Regulatory Interaction with *Arabidopsis* Cullin3-Based E3 Ligases. *The Plant Cell* **19**: 564-581.

Gusmaroli G, Feng S, and Deng XW. 2004. *Arabidopsis* CSN5A and CSN5B subunits are present in distinct COP9 signalosome complexes, and mutations in their JAMM domains exhibit differential dominant negative effects on development. *Plant Cell* **16:** 2984-3001.

Hayashi H, Czaja I, Lubenow H, Shell J , and Walden R. 1992. Activation of a plant gene by T-DNA tagging: auxin-independent growth in vitro. *Science* **258**: 1350-1353.

Hershko A, and Ciechanover A. 1998. The ubiquitin system. *Annu. Rev. Biochem.* **67**: 425-79.

Hess J, Angel P, and Schorpp-Kistner M. 2004. AP-1 subunits: quarrel and harmony among siblings. *Journal of Cell Science* **117**: 5965-5973.

Huang X, Hetfeld BKJ, Seifert U, Kähne T, Kloetzel P.-M., Naumann M, Bech-Otschir D and Dubiel W. 2005. Consequences of COP9 signalosome and 26S proteasome interaction. *FEBS Jl.* **272**: 3909-3917.

Hülskamp M. 2004. Plant Trichomes: A model for cell differentiation. *Nature Reviews –Molecular Cell Biology* **5**: 471-480.

Jander G, Norris SR, Rounsley SD, Bush DF, Levin IM, and Last RL. 2002. *Arabidopsis* Map-Based Cloning in the Post-Genome Era. *Plant Physiol.* **129**: 440-450.

Jander G, Norris SR, Rounsley SD, Bush DF, Levin IM, and Last RL. 2002. *Arabidopsis* Map-Based Cloning in the Post-Genome Era. *Plant Physiology*, **129:** 440-450.

Jens B, Verbsky ML, Robertson TL, Larkin JC , and Kunkel BN. 1998. Analysis of Resistance Gene-Mediated Defense Responses in *Arabidopsis thaliana* Plants Carrying a Mutation in *CPR5* . *MPMI* **11**(12): 1196-1206.

Johnson CS, Kolevski B , and Smyth DR. 2002. Transparent testa glabra2: a Trichome and Seed Coat Development Gene of Arabidopsis, Encodes a WRKY Transcription Factor. *The Plant Cell* **14**: 1359-1375.

Kanyuka K, Praekelt U, Franklin KA, Billingham OE, Hooley R, Whitelam GC, Halliday KJ. 2003. Mutations in the huge Arabidopsis gene *BIG* affect a range of hormone and light responses. *The Plant Journal* **35**(1): 57-70.

Kapelari B, Bech-Otschir D, Hegerl R, Schade R, Dumdey R, Dubiel W. 2000. Electron microscopy and subunit-subunit interaction studies reveal a first architecture of COP9 signalosome. *J. Mol. Biol.* **300**: 1169-78.

Karniol B, Yahalom A, Kwok S, Tsuge T, Matsui M, et al. 1998. The *Arabidopsis* homologue of an eIF3 complex subunit associates with the COP9 complex. *FEBS Lett.* **439**: 173-79.

Kim B-C, Lee H-J, Park SH, Lee SR, Karpova TS, McNally JG, Felici A, Lee DK, and Kim S-J. 2004. Jab1/CSN5, a Component of the COP9 Signalosome Regulates Transforming Growth Factor ß Signaling by Binding to Smad7 and Promoting Its Degradation. *Molecular and Cellular Biology* **24**(6): 2251-2262.

Kim T, Hofmann K, von Arnim AG, Chamovitz DA. 2001. PCI complexes: pretty complex interactions in diverse signaling pathways. *Trends Plant Sci.* **6**: 379-86.

Kircher S, Kozma-Bognar L, Kim L, Adam E, Harter K, Scha¨fer E, Nagy F. 1999. Light quality-dependent nuclear import of the plant photoreceptors phytochrome A and B. *The Plant Cell* **11**: 1445-1456

Kleemann R, Hausser A, Geiger G, Mischke R, Burger-Kentischer A, et al. 2000. Intracellular action of the cytokine MIF to modulate AP-1 activity and the cell cycle through Jab1. *Nature* **408**: 211-16.

Klose J. 1975. Protein mapping by combined isoelectric focusing and electrophoresis of mouse tissues. A novel approach to testing for induced point mutation in mammals. *Humangenetik* **26:** 231-243.

Knox K, Grierson CS , and Leyser O. 2003. AXR3 and SHY2interact to regulate root hair development. *Development* **130**: 5769-5777.

Kosambi DD. 1944. The estimation of map distances from recombination values. *Ann. Eugen.* **12**: 172-175

Krysan PJ, Young, JC , and Sussman MR. 1999. T-DNA as an Insertional Mutagen in Arabidopsis. *The Plant Cell* **11:** 2283-2290.

Kwok SF, Solano R, Tsuge T, Chamovitz DA, Ecker JR, et al. 1998. *Arabidopsis* homologs of a c-Jun coactivator are present both in monomeric form and in the COP9 complex, and their abundance is differentially affected by the pleiotropic *cop/det/fus* mutations. *The Plant Cell* **10**: 1779-90.

Laemmli UK. 1970. Cleavage of structural proteins during the assembly of the head of bacteriophage T4. *Nature* **227**: 680–685.

Lange H, Shropshimr W , and Mohr H. 1971. An Analysis of Phytochrome-mediated Anthocyanin Synthesis. *Plant Physiol.* **47:** 649-655.

Lee S, Cheng H, King KE, Wang W, He Y, Hussain A, Lo J, Harberd NP , and Peng J. 2002. Gibberellin regulates Arabidopsis seed germination via RGL2, a GAI/RGA-like gene whose expressionis up-regulated following imbibition. *Genes Dev*. **16:** 646-658.

Li S, and Strid A. 2005. Anthocyanin accumulation and changes in CHS and PR-5 gene expression in Arabidopsis thaliana after removal of the inflorescence stem (decapitation). *Plant Physiology and Biochemistry* **43**(6): 521-525.

Lister C, and Dean C. 1993. Recombinant inbred line for mapping RFLP and phenotypic markers in *Arabidopsis thaliana*. *The Plant Journal*. **4**: 745-750.

Liu Y-G, Mitsukawa N, Oosumi T , and Whittier RF. 1995. Efficient isolation and mapping of Arabidopsis thaliana T-DNA insert junctions by thermal asymmetric interlaced PCR. *The Plant Journal* **8**(3): 457-463.

Lukowitz W, Gillmor CS, Scheible WR. 2000. Positional cloning in Arabidopsis: why it feels good to have a genome initiative working for you. *Plant Physiol* **123**: 795-805.

Ma L, Zhao H, Deng X. 2003. Analysis of the mutational effects of the *COP/DET/FUS* loci on genome expression profiles reveals their overlapping yet not identical roles in regulating *Arabidopsis* seedling development. *Development* **130**: 969-81.

Mang HG, Kang EO, Shim JH, Kim S, Park KY, Kim YS, Bahk YY, Kim WT. 2004. A proteomic analysis identifies glutathione S-transferase isoforms whose abundance is differentially regulated by ethylene during the formation of early root epidermis in Arabidopsis seedlings. *Biochimica et Biophysica Acta* **1676**: 231-239.

Marrs KA. 1996. The functions and regulation of glutathione S-transferases in plants. *Annu. Rev. Plant Physiol. Plant Mol. Biol.* **47**: 127-158.

McElver J, Patton D, Rumbaugh M, Liu C, Yang LY , and Meinke D. 2000. TheTITAN5 gene of Arabidopisis encodes a protein related to the ADP ribosylation factor family of GTP binding proteins. *The Plant Cell* **12**: 1379-1392.

Meinke D, and Koornneef M. 1997. Community standards for Arabidopsis genetics. *The Plant Journal* **12**(2): 247-253.

Meinke DW, Meinke LK, Showalter TC, Schissel AM, Mueller LA, and Tzafrir I . 2003. A Sequence-Based Map of Arabidopsis Genes with Mutant Phenotypes. *Plant Physiol*. **131**: 409-418.

Meinke DW, Cherry JM, Dean C, Rounsley SD, Koornneef M (1998) *Arabidopsis thaliana*: a model plant for genome analysis. *Science* **282**: 662-682.

Millar AH, and Heazlewood JL. 2003. Genomic and proteomic analysis of mitochondrial carrier proteins in *Arabidopsis*. *Plant Physiol.* **131:** 443-453.

Misera S, Muller AJ, Weiland-Heidecker U, Jurgens G. 1994. The FUSCA genes of *Arabidopsis:* negative regulators of light responses. *Mol. Gen. Genet.* **244**: 242-52.

Mittler R, Vaderauwera S, Gollery M and Van Breusegem F. 2004. Reactive oxygen gene netwrok of plants. *Trends in Plant Science* **9**(10): 490-498.

Mizukami Y. 2001. A matter of size: developmental control of organ size in plants. *Current Opinion in Plant Biology* **4**:533-539

Molnàr G, Bancoş S, Nagy F , and Szekeres M .2002. Characterization of BRH1, a brassinosteroid-responsive RING-H2 gene from Arabidopsis thaliana. *Planta* **215**: 127-133.

Moon J, Parry G, and Estelle M. 2004. The ubiquitin-proteasome pathway and plant development. *The Plant Cell* **16**: 3181-3195.

Moon J, Zhao Y, Dai X, Zhang W, Gray WM, Huq E , and Estelle M. 2007. A New CULLIN 1 Mutant Has Altered Responses to Hormones and Light in Arabidopsis. *Plant Physiology* **143**: 684-696.

Mou Z. Fan W, and Dong X. 2003. Inducers of plant systemic acquired resistance regulate NPR1 function through redox changes. *Cell* **113**: 1-10.

Murphy A, and Taiz L. 1999. Naphthlylphthalamic acid is enzymatically hydrolyzed at the hypocotyl-root transition zone and other root tissues of *Arabidopsi* s thaliana seedlings. *Plant Physiol. Biochem.* **37**: 413-430.

Nacry P, Camilleri C, Courtial B, Caboche M , and Bouchez D. 1998. Major chromosomal rearrangements induced by T-DNA transformation in Arabidopsis. *Genetics* **149**: 641-650.

Nagatani A. 2004. Light-regulated nuclear localization of phytochromes. Curr. Opin. *Plant Biology* **7**: 708-711.

Nakajima M, Shimada A, Takashi Y, Kim YC, Park SH, et al. 2006. Identification and characterization of *Arabidopsis* gibberellin receptors. *Plant J*. **46**: 880-889.

Naumann M, Bech-Otschir D, Huang X, Ferrell K, Dubiel W. 1999. COP9 signalosome-directed c-Jun activation/stabilization is independent of JNK. *J. Biol. Chem.* **274**: 35297-35300.

Ni W, Xie D, Hobbie L, Feng B, Zhao D, Akkara J, and Ma H. 2004. Regulation of Flower Development in Arabidopsis by SCF Complexes. *Plant Physiology* **134**: 1574-1585

Noh B, and Spalding EP. 1998. Anion Channels and the Stimulation of Anthocyanin Accumulation by Blue Light in Arabidopsis Seedlings. *Plant Physiol.* **116**: 503-509.

O'Farrell PH. 1975. High resolution two-dimensional electrophoresis of proteins. *J. Biol. Chem.* **250**: 4007-4021.

Osterlund MT, Ang LH, Deng XW. 1999. The role of COP1 in repression of *Arabidopsis* photomorphogenic development. *Trends Cell Biol.* **9**: 113– 18.

Osterlund MT, Hardtke CS, Wei N, Deng XW. 2000. Targeted destabilization of HY5 during light-regulated development of *Arabidopsis* . *Nature* **405**: 462-466.

Paciorek T, Zažímalová E, Ruthardt N, Petrášek J, Stierhof Y-D, Kleine-Vehn J, Morris DA, Emans N, Jűrgens G, Geldner N , and Friml J. 2005. Auxin inhibits endocytosis and promotes its own efflux from cells. *Plant Biology* **435**: 1251-1256.

Parinov S , and Sundaresan V. 2000. Functional genomics in Arabidopsis: large-scale insertional mutagensis complements the genome sequencing project. *Current Opinion in Biotechnology* **11:** 157-161.

Patterson SD. 2004. How much of the proteome do we see with discovery-based proteomic methods and how much do we need to see? *Curr. Proteomics* **1**: 3-12.

Peng J, Carol P, Richards DE, King KE, Cowling RJ, et al. 1997. The *Arabidopsis GAI* gene defines a signaling pathway that negatively regulates gibberellin responses. *Genes Dev.* **11**: 3194-3205.

Peng Z, Serino G, Deng XW. 2001. Molecular characterization of subunit 6 of the COP9 signalosome and its role in multifaceted developmental processes in *Arabidopsis* . *Plant Cell* **13**: 2393-2407.

Rabilloud T. 1996. Solubilization of proteins for Electrophoretic analyses. *Electrophoresis* **17**: 813-829.

Rabilloud T. 2002. Two-dimensional gel electrophoresis in proteomics: old, old fashioned, but it still climbs up the mountains. *Proteomics* **2**: 3-10.

Rose JKC, Bashir S, Giovannoni JJ, Jahn MM, and Saravanan RS. 2004. Tackling the plant proteome: practical approaches, hurdles and experimental tools. *The Plant Journal* **39**: 715-733.

Ruegger M, Dewey E, Hobbie L, Brown D, Bernasconi P, Turner J, Muday G, Estelle M. 1997. Reduced naphthylphthalamic acid binding in the *tir3* mutant of *Arabidopsis* is associated with a reduction in polar auxin transport and diverse morphological defects. *Plant Cell* **9**: 745–757.

Sablowski R. 2007. Flowering and determinacy in Arabidopsis. *Journal of Experimental Botany* **58**(5): 899-907

Salisbury FJ, Hall A, Grierson CS , and Halliday KJ. 2007. Phytochrome coordinates Arabidopsis shoot and root development. *The Plant Journal* **50**(3): 429-438.

Sanders PM, Lee PY, Biesgen C, Boone JD, Beals TP, Weiler EW , and Goldberg RB. 2000. The Arabidopsis *DELAYED DEHISCENCE1* gene encodes as enzyme in the jasmonic acid synthesis pathway. *The Plant Cell* **12:** 1041-1061.

Scheres B, Benfey P, and Dolan L. 2002. Root Development. The *Arabidopsis* Book; doi: 10.1199/tab.0101 [WWW] http://www.bioone.org/archive/1543-8120/40/1/pdf/i1543-8120-40-1-1.pdf (online accessed July 2007)

Schmidt M, Davison TS, Henz SR, Pape UJ, Demar M, et al. 2005. A gene expression map of Arabidopsis thaliana development. *Nature Genetics* **37**: 501-506. *Arabidopsis . Plant J.* **42**: 111-123.

Schwechheimer C, and Deng XW. 2001. COP9 signalosome revisited: a novel mediator of protein degradation. *Trends Cell Biol.* **11**: 420– 26.

Schwechheimer C, Serino G, Callis J, Crosby WL, Lyapina S, et al. 2001. Interactions of the COP9 signalosome with the E3 ubiquitin ligase SCFTIRI in mediating auxin response. *Science* **292**: 1379– 82.

Schwechheimer C, Serino G, Deng XW. 2002. Multiple ubiquitin ligase-mediated processes require COP9 signalosome and AXR1 function. *Plant Cell* **14**: 2553-63.

Seeger M, Kraft R, Ferrell K, Bech-Otschir D, Dumdey R, et al. 1998. A novel protein complex involved in signal transduction possessing similarities to 26S proteasome subunits. *FASEB J.* **12**: 469-78.

Serino G, and Deng XW. 2003. The COP9 signalosome: regulating plant development through the control of proteolysis. *Annu. Rev. Plant Biol.* **54**: 165-182.

Sheehan D, Meade G, Foley VM, and Dowd CA. 2001. Structure, function and evolution of glutathione transferases : implications for classification of non-mammalian membersof an ancient enzyme superfamily. *Biochem. J.* **360**: 1-16.

Silverstone AL, Mak PY, Martýnez EC , and Sun T. 1997. The new RGA locus encodes a negative regulator of gibberellin response in Arabidopsis thaliana. *Genetics* **146**: 1087-1099.

Smalle J, Haegman M, Kurepa J, Van Montagu M , and Van Der Straeten D. 1997. Ethylene can stimulate Arabidopsis hypocotyl elongation in the light. *Proc. Natl. Acad. Sci.* **94:** 2756-2761.

Smalle J, Kurepa J, Yang P, Babiychuk E, Kushnir S, Durski A, and Vierstra RD. 2002. Cytokinin growth responses in *Arabidopsis* involve the 26S proteasome subunit RPN12. *Plant Cell* **14**: 17-32.

Smalle, J., and Vierstra, R.D. (2004). The ubiquitin 26S proteasome proteolytic pathway. *Annu. Rev. Plant Biol.* **55**: 555-590.

Smith A, Nourizadeh SD, Peer WA, Xu J, Bandyopadhyay A, Murphy AA, and Goldsbrough PB. 2003. *Arabidopsis AtGSTF2* is regulated by ethylene and auxin, and encodes a glutathione S-transferase that interacts with flavonoids. *The Plant Journal* **36**: 433-442.

Sonoda Y, Yao SG, Sako K, Sato T, Kato W, Ohto M, Ichikawa T, Matsui M, Yamaguchi J, and Ikeda A. 2007. SHA1, a novel RING finger protein, functions in shoot apical meristem maintenance in Arabidopsis, *The Plant Journal* **50**(4): 586-596.

Steber CM , and McCourt P. 2001. A role for brassinosteroids in germination in Arabidopsis. *Plant Physiology* **125**: 763-769.

Steyn WJ, Wand SJE, Holcroft DM, Jacobs G. 2002. Anthocyanins in vegetative tissues: a proposed unified function in photoprotection . *New Phytologist* **155**(3): 349-361.

Stintzi A , and Browse J. 2000. The Arabidopsis male-sterile mutant, opr3, lacks the 12-oxophytodienoic acid reductase required for jasmonate synthesis. *PNAS* **97**(19): 10625-10630.

Stintzi A, Heitz T, Prasad V, Wiedemann-Merdinoglu S, Kauffmann S, Geoffroy P, Legrand M, and Fritig B. 1993. Plant pathogenesis-related proteins and their role in defense against pathogens. *Biochimie* **75**: 687-706.

Sullivan JA, Shirasu K and Deng XW. 2003. The diverse roles of ubiquitin and the 26S proteasome in the life of plants. *Nature Rviews Genetics* **4**: 948-958.

Sun T, and Gubler F. 2004. Molecular mechanism of gibberellin signaling in plants. *Annu. Rev. Plant Biol*. **55**: 197–223.

Sweere U, Eichenberg K, Lohrmann J, Mira-Rodado V, Ba¨urle I, Kudla J, Nagy F, Scha¨fer E, Harter K. 2001. Interaction of the response regulator ARR4 with phytochrome B in modulating red light signaling. *Science* **294**: 1108-1111.

Taiz L , and Zeiger E. 2002. *Plant Phsyiology* . 3rd ed. Massachusetts: Sinauer Associates Inc. Publishers.

Tanaka M, Takei K, Kojima M, Sakakibara H , and Mori H. 2006. Auxin controls local cytokinin biosynthesis in the nodal stem in apical dominance. *The Plant Journal* **45**: 1028-1036.

Teale WD, Paponov IA , and Palme K. 2006. Auxin in action: signalling, transport and the control of plant growth and development. *Nature Reviews-Molecular Cell Biology* **7**: 847-859.

Tomoda K, Kubota Y, Arata Y, Mori S, Maeda M, et al. 2002. The cytoplasmic shuttling and subsequent degradation of p27Kip1 mediated by Jab1/CSN5 and the COP9 signalosome complex. *J. Biol. Chem.* **277**: 2302-2310.

Tomoda K, Kubota Y, Kato J. 1999. Degradation of the cyclin-dependent-kinase inhibitor p27Kip1 is instigated by Jab1. *Nature* **398**: 160-165.

Townend J. 2002. *Practical statistics for environmental and Biological Scientists*. England: John Wiley & Sons Ltd.

Ueguchi-Tanaka M, Ashikari M, Nakajima M, Itoh H, Katoh E, Kobayashi M, Chow TY, Hsing YI, Kitano H, Yamaguchi I, Matsuoka M. 2005. Gibberellin insensitive dwarf1 encodes a soluble receptor for gibberellin. *Nature* **437**: 693-698.

Uknes S, Mauch-Mani B, Moyer M, Potter S, Williams S, Dincher S, Chandler D, Slusarenko A, Ward E, and Ryals J. 1992. Acquired resistance in Arabidopsis.*The Plant Cell*. **4**. 645-656.

Unlu M, Morgan ME, and Minden JS. 1997. Difference gel electrophoresis: a single gel method for detecting changes in protein extracts. *Electrophoresis* **18**: 2071-2077.

Vandenbussche F , and Van Der Straeten D. 2004. Shaping the shoot: a circuitry that integrates multiple signals. *Trends in Plant Science* **9**(10): 499-506.

Vandenbussche F, Habricot Y, Condiff AS, Maldiney R, Van Der Straeten D , and Ahmad M. 2007. HY5 is a point of convergence between cryptochrome and cytokinin signalling pathways in Arabidopsis thaliana. *The Plant Journal* **49**(3): 428-441.

Vierstra RD. 2003. The ubiquitin/26S proteasome pathway, the complex last chapter in the life of many plant proteins. *Trends in Plant Science* **8**: 135-142.

von Arnim AG, Deng XW. 1994. Light inactivation of *Arabidopsis* photomorphogenic repressor COP1 involves a cell-specific regulation of its nucleocytoplasmic partitioning. *Cell* **79**: 1035-1045.

Walker AR, Davison PA, Bolognesi-Winfield AC, James CM, Srinivasan N, Blundell TL, Eschc JJ, Marks MD, and Gray JC. 1999. The *TRANSPARENT TESTA GLABRA1* Locus, Which Regulates Trichome Differentiation and Anthocyanin Biosynthesis in *Arabidopsis* , Encodes a WD40 Repeat Protein. *Plant Cell* **11:** 1337-1350.

Wang H, Ma LG, Li JM, Zhao HY, and Deng XW. 2001. Direct interaction of *Arabidopsis* cryptochromes with COP1 in light control development. *Science* **294**: 154-158.

Wang X, Feng S, Nakayama N, Crosby WL, Irish V, et al. 2003. Regulation of SCFUFO by the COP9 signalosome during *Arabidopsis* flower development. *Plant Cell* **15**: 1071-1082.

Wei N, Chamovitz DA, and Deng XW. 1994. *Arabidopsis* COP9 is a component of a novel signaling complex mediating light control of development. *Cell* **78**: 117-124.

Wei N, and Deng XW. 1992. COP9: a new genetic locus involved in light-regulated development and gene expression in *Arabidopsis* . *Plant Cell* **4**: 1507-1518.

Wei N, Deng XW. 1998. Characterization and purification of the mammalian COP9 complex, a conserved nuclear regulator initially identified as a repressor of photomorphogenesis in higher plants. *Photochem. Photobiol.* **68**: 237-241.

Wei N. and Deng XW. 2003. The COP9 Signalosome. *Annual Review of Cell and Developmental Biology* **19**: 261-286.

Weigel D, Ahn JH, Blazquez MA, Borevitz JO, Christensen SK, Fankhauser C, Ferrandiz C, Kardailsky I, Malancharuvil EJ, Neff MM, Nguyen JT, Sato S, Wang Z, Xia Y, Dixon RA, Harrison MJ, Lamb CJ, Yanofsky MF , and Chory J. 2000. Activation Tagging in Arabidopsis. *Plant Physiology* **122**: 1003-1013.

Weiss D , and Ori N. 2007. Mechanisms of Cross Talk between Gibberellin and other hormones. *Plant Physiology* **14:** 1240-1246.

Wilson ZA. 2000. *Arabidopsis* : *A Practical Approach* . Oxford, UK: Oxford University Press.

Xirodimas D, Saville M, Bourdon J, Hay R, Lane D. 2004 . Mdm2-Mediated NEDD8 Conjugation of p53 Inhibits Its Transcriptional Activity. *Cell* **118**(1): 83-97.

Yang HQ, Tang RH, and Cashmore AR. 2001. The signalling mechanism of *Arabidopsis* CRY1 involves direct interaction with COP1. *Plant Cell* **13**: 2573-2587.

Yang J, Lin R, Sullivan J, Hoecker U, Liu B, Xu L, Deng XW , and Wang H. 2005. Light regulates COP1-mediated degradation of HFR1, a transcription factor essential for light signaling in Arabidopsis. *Plant Cell* **17**: 804-821.

Yang X, Menon S, Lykke-Andersen K, Tsuge T, Di X, et al. 2002. The COP9 signalosome inhibits p27(kip1) degradation and impedes G1-S phase progression via de-neddylation of SCF Cul1. *Curr. Biol.* **12**: 667-672.

Yi C , and Deng XW. 2005. COP1-from plant photomorphogenesis to mammalian tumorigenesis. *Trends in Cell Biology* **15**(11): 618- 625.

Zhang H , and Forde BG. 1998. An Arabidopsis MADS box gene that controls nutrient-induced changes in root architecture. *Science* **279**: 407-409.

Zhang H , and Forde BG. 2000. Regulation of Arabidopsis root development by nitrate availability. *Journal of Experimental Botany* **51**(342): 51-59.

Zhang N, Kallis RP, Ewy RG, and Portis AR Jr. 2002. Light modulation of Rubisco in *Arabidopsis* requires a capacity for redox regulation of the larger Rubisco activase isoform. *PNAS* **99**(5): 3330-3334.

Zhao X-Y, Yu X-H, Liu, X-M , and Lin C-T. 2007. Light Regulation of Gibberellins Metabolism in Seedling Development. *Journal of Integrative Plant Biology* **49**(1): 21-27.

Zhong HH, Painter JE, Salome PA, Straume M, and McClung CR. 1998. The circadian clock gates the light-responsiveness of the *CAT2* catalase gene in etiolated *Arabidopsis* seedlings. In: 9th International conference on *Arabidopsis* research.

Zhou J, and Goldsbrough PB. 1993. An Arabidopsis gene with homology to glutathione S-transferase is regulated by ethylene. *Plant Mol. Biol.* **22:** 517- 523.